# 4-DIMETHYLAMINO PYRIDINE (DMAP) CATALYST WITH FLUXIONAL CHIRALITY: SYNTHESIS AND APPLICATIONS

A Dissertation
Submitted to the Graduate Faculty
of the
North Dakota State University
of Agriculture and Applied Science

By

Gaoyuan Ma

In Partial Fulfillment of the Requirements
for the Degree of
DOCTOR OF PHILOSOPHY

Major Department:
Chemistry and Biochemistry

November 2015

Fargo, North Dakota

# North Dakota State University
Graduate School

**Title**

4-Dimethylamino Pyridine (DMAP) Catalyst with Fluxional Chirality: Synthesis and Applications

**By**

Gaoyuan Ma

The Supervisory Committee certifies that this ***disquisition*** complies with North Dakota State University's regulations and meets the accepted standards for the degree of

**DOCTOR OF PHILOSOPHY**

SUPERVISORY COMMITTEE:

Prof. Mukund P. Sibi
Chair

Prof. Gregory R. Cook

Prof. Pinjing Zhao

Prof. Dean C. Webster

Approved:

| 11/30/2015 | Prof. Gregory R. Cook |
|---|---|
| Date | Department Chair |

## ABSTRACT

Organocatalysis using small organic molecules to catalyze organic transformations, has emerged as a powerful synthetic tool that is complementary to metal-catalyzed transformations and remarkably promote stereoselective synthesis. Our group has designed useful templates, ligands, and additives that use fluxional groups to control and/or enhance stereoselectivity in a variety of asymmetric transformations. A key feature of this strategy is that the size of the fluxional substituent can be varied readily. As an extension of this strategy we became interested in developing efficient and broadly applicable and adjustable 4-dimethylaminopyridine (DMAP) organocatalysts. In our design, we surmised that a fluxional group would be effective in relaying stereochemical information from the fixed chiral center to the catalytic center of DMAP. Presented herein the synthesis of novel fluxionally chiral DMAP catalysts and their application in the acylative kinetic resolution of secondary alcohols and axially chiral biaryls, dynamic kinetic resolution of chiral biaryls with low rotation barriers and allylic substitution reactions.

In the beginning, a comprehensive study of the chiral relay concept in enantioselective transformations was reviewed and the historic and current story of the chiral relay concept is covered.

The design and synthesis of fluxionally chiral 4-dimethylaminopyridine catalysts was introduced. The key issues addressed in this chapter include the design concept regarding a stereoselective fluxionally 4-dimethylaminopyridine catalyst and muti-step synthesis strategies developed for catalyst synthesis.

The development of fluxionally chiral 4-dimethylaminopyridine catalysts in the acylative kinetic resolution studies of secondary alcohols as well as axially chiral biaryls is investigated.

Six different secondary alcohols are resolved with good selectivity factors (6-37) and ten biaryl substrates are resolved with moderate to high selectivity factors (10-51).

Dynamic kinetic resolution has more practical applications to organic synthesis than simple kinetic resolution. The dynamic kinetic resolution of atropisomeric biaryls using the novel fluxionally chiral 4-dimethylaminopyridine catalysts was explored and the corresponding acylated products were obtained with 11-80 %ee.

The newly designed DMAP catalysts containing fluxional groups as a stereocontrol unit could also be effectively applied as a nucleophilic catalyst in asymmetric allylic aminations. A range of α-methylene-β-amino esters were obtained with good yields and selectivities (up to 72 %ee).

## ACKNOWLEDGEMENTS

I would like to express the deepest gratitude to my advisor, Dr. Mukund Sibi, for his full support, expert guidance, understanding and encouragement throughout my study and research in NDSU. Without his guidance and persistent help, my thesis work would have been a frustrating pursuit. He always provided me with scientific advice and knowledge and valuable insightful discussions and suggestions about the research, and then I can go through the rough road to finish my thesis. I hope that I could be as lively, enthusiastic, and energetic as Dr. Sibi in the future scientific studies. I thank him wholeheartedly and consider it as a great opportunity to do my doctoral study under his guidance and to learn from his research expertise. Thank you, Dr. Sibi, for everything you have done for me during these years!

I am very thankful to Dr. Gregory Cook, Dr. Pinjing Zhao and Dr. Dean Webster for having served on my committee. Their thoughtful questions and comments on my research were valued greatly. Great thanks for helping me with my coursework and academic research during my graduate years.

I want to give very special thanks to Dr. Jun Deng, who not only taught me to set up experiments when I began my research, but also laid a foundation for me to carry out my graduate study. In addition, I want to thank Kyle Anderson, Daniel Weisz and Hae Ju Choi for their research assistance and friendship when we worked together.

I am also appreciative to Dr. Angel Ugrinov for solving X-ray crystal structures, especially for sharing his crystal software expertise so willingly and being patient with my questions. I want to thank Dr. Ganesh Bala for analytical assistance, Daniel Wanner and Dr. John Bagu for assistance with NMR techniques.

I also thank the former members of the Sibi group: Dr. Selvakumar Sermadurai, Dr. Shinya Adachi, Dr. Yonghua Yang, Dr. Nicolas Zimmerman, Dr. Saravanakumar Rajendran, Dr. Chao Deng. They are very helpful and knowledgeable and I appreciate their help and discussions during my graduate years!

I thank all the present members of the Sibi group: Dr. Retheesh Krishnan, Dr. Itaru Suzuki, Dr. Karthikeyan Iyanar, Dr. Ramkumar Moorthy, Hari Subramanian, Eric Serum, Jesse Joyce, Catherine Sutton, Krystal Kalliokoski. Thank you all!

Thanks also go to my fellow graduate students at the Chemistry and Biochemistry Department. Special thanks go to my dear friends who helped me throughout my academic exploration.

I also thank the wonderful staffs in the Chemistry and Biochemistry Department for always being so helpful and friendly. They are very nice. I thank stockroom persons for all their help these years with bringing our needed chemicals and supplies.

I also thank my friends for providing support and being my side throughout my time here. I would like to extend my sincere thanks to all of them.

Last, I am deeply thankful to my parents. Words can't express how grateful I am to my mother and father for their love, support, and sacrifices that they have made for me. I want to let them know: "You raise me up to more than I can be."

## DEDICATION

I dedicate this thesis to

my family for their constant support and unconditional love.

I love you all.

## TABLE OF CONTENTS

## LIST OF TABLES

## LIST OF FIGURES

## LIST OF SCHEMES

## LIST OF ABBREVIATIONS

Å ..... Angstrom

α ..... Alfa

Ac ..... Acetyl

$Ac_2O$ ..... Acetic anhydride

Ar ..... Aryl

aza-MBH ..... aza-Morita-Baylis-Hillman

β ..... Beta

BINAM ..... 1,1'-binaphthyl-2,2'-diamine

BINAP ..... 2,2'-bis(diphenylphosphino)-1,1'-binaphthyl

BINIM ..... Binaphthyldiimine

BINOL ..... 1,1'-Bi-2-naphthol

Bn ..... Benzyl

Boc ..... *tert*-Butyloxycarbonyl

$Boc_2O$ ..... Di-*tert*-butyl Dicarbonate

*n*BuLi ..... *n*-Butyl lithium

Bz ..... Benzoyl

Cat* ..... Chiral catalyst

$CDCl_3$ ..... Deuterated chloroform

$CH_2Cl_2$ ..... Dichloromethane

$CHCl_3$ ..... Chloroform

$CH_3CN$ ..... Acetonitrile

CN ..... Cyano

Conv. ..... Conversion

$Cs_2CO_3$ ..... Caesium carbonate

| | |
|---|---|
| CsF | Caesium fluoride |
| $CuCl_2$ | Copper chloride |
| $Cu(OTf)_2$ | Copper triflate |
| d | Days |
| DA | Diels-Alder |
| DABCO | 1,4-Diazabicyclo[2.2.2]octane |
| Davphos | 2-Dicyclohexylphosphino-2′-(N,N-dimethylamino)biphenyl |
| DBU | 1,8-Diazabicyclo[5.4.0]undec-7-ene |
| de | Diastereomeric excess |
| $(DHQD)_2PHAL$ | Hydroquinidine 1,4-phthalazinediyl diether |
| $(DHQD)_2PYR$ | Hydroquinidine-2,5-diphenyl-4,6-pyrimidinediyl diether |
| $(DHQD)_2AQN$ | Hydroquinidine (anthraquinone-1,4-diyl) diether |
| DIPEA | Diispropyl ethylamine |
| DKR | Dynamic kinetic resolution |
| DMAP | 4-Dimethylamino pyridine |
| DMF | Dimethylformamide |
| DNA | Deoxyribonucleic acid |
| dr | Diastereomeric excess |
| DYKAT | Dynamic kinetic asymmetric transformations |
| ee | Enantiomeric excess |
| Equiv. | Equivalent |
| er | Enantiomeric ratio |
| $Er(OTf)_3$ | Erbium triflate |
| ESI | Electrospray ionization |

Et ..... Ethyl

$Et_2AlCl$ ..... Diethylaluminium chloride

$Et_2O$ ..... Diethyl ether

EtOAc ..... Ethyl acetate

EWG ..... Electron-withdrawing group

$Fe(NTf_2)_2$ ..... Iron triflimide

h ..... Hours

HBTM ..... Homobenzotetramisole

HCl ..... Hydrochloric acid

$H_2NNH_2$ ..... Hydrazine

HPLC ..... High pressure liquid chromatography

HRMS ..... High resolution mass spectroscopy

Hz ..... Hertz

IR ..... Infrared

*J* ..... Coupling constants (in NMR)

k ..... Rate constant

$K_2CO_3$ ..... Potassium carbonate

KHMDS ..... Potassium bis(trimethylsilyl)amide

$K_3PO_4$ ..... Tripotassium phosphate

KR ..... Kinetic resolution

L ..... Ligand

L* ..... Chiral ligand

LA ..... Lewis acid

$LiAlH_4$ ..... Lithium aluminum hydride

$Li_2CO_3$ ..... Lithium carbonate

*m* ..... meta

M ..... Molar

MBH ..... Morita-Baylis-Hillman

Me ..... Methyl

MeCN ..... Acetonitrile

MeLi ..... Methyllithium

MeO ..... Methoxy

MeOH ..... Methanol

$MgBr_2$ ..... Magnesium bromide

$Mg(ClO_4)_2$ ..... Magnesium perchlorate

$MgI_2$ ..... Magnesium iodide

$Mg(NTf_2)_2$ ..... Magnesium triflimide

$MgSO_4$ ..... Magnesium sulfate

min ..... Minute(s)

mL ..... Milliliter

mol ..... Moles

Mol. Wt. ..... Molecular weight

MS ..... Molecular sieves

$NaBH_4$ ..... Sodium borohydride

NADH ..... Nicotinamide adenine dinucleotide(reduced)

$NaHCO_3$ ..... Sodium bicarbonate

$NaHSO_4$ ..... Sodium bisulfate

NaOAc ..... Sodium acetate

NaOH ..... Sodium hydroxide

NaOMe ..... Sodium methoxide

Naph ..... Naphthyl

$Na_2SO_4$ ..... Sodium Sulfate

NaI..... Sodium Iodide

NBS ..... N-Bromosuccinimide

$NEt_3$..... Triethylamine

NHC ..... N-heterocyclic carbene

NMR ..... Nuclear magnetic resonance

$NO_2$ ..... Nitro

NOBIN..... 2-Amino-2'-hydroxy-1,1'-binaphthyl

Nu..... Nucleophile

*o*..... ortho

*O*..... Oxygen

OTf..... Triflate

Ox..... Oxazolidinone

*p*..... para

*t*-$Bu_3P$..... Tri-tert-butylphosphine

$Pd_2(dba)_3$ ..... Tris(dibenzylideneacetone)dipalladium

$Pd(OAc)_2$..... Palladium acetate

$Pd(PPh_3)_4$..... Tetrakis(triphenylphosphine)palladium

Ph ..... Phenyl

PhMe..... Toluene

PPL..... Porcine pancreatic lipase

ppm ..... Parts per million

*i*-Pr..... Isopropyl

*i*$Pr_2NEt$..... Diisopropyl ethylamine

Proton sponge..... 1,8-Bis(dimethylamino)naphthalene

PMB ..... *p*-methoxybenzyl

Pybox ..... Pyridine 2,6-bis(oxazoline)

R..... Substituents or stereogenic center

*rac* ..... Racemic

RCM..... Ring Closing Metathesis

$[RhCl(coe)_2]_2$..... Chlorobis(cyclooctene)rhodium dimer

RNA ..... Ribonucleic acid

rt ..... Room temperature

RX ..... Alkyl halide

*s* ..... Selectivity factor

$Sc(OTf)_3$ ..... Scandium triflate

$S_N1$ ..... Unimolecular nucleophilic substitution

$S_N2$ ..... Bimolecular nucleophilic substitution

TADDOL ..... α,α,α,α-tetraaryl-1,3-dioxolane-4,5-dimethanol

Temp ..... Temperature

Tert..... Tertiary

TFA ..... Trifluoroacetic acid

THF ..... Tetrahydrofuran

TLC ..... Thin layer chromatography

TMS ..... Trimethylsilyl

$(TMS)_3SiH$ ..... Tris(trimethylsilyl)silane

Tol ..... Tolyl

$t_R$..... Retention time

$TsNH_2$ ..... *p*-Toluenesulfonamide

UV ..... Ultraviolet

VANOL ..... 3,3’-Diphenyl-2,2’-bi-1-naphthol

Xantphos ..... 4,5-Bis(diphenylphosphino)-9,9-dimethylxanthene

Y ..... Relay group

$Y(OTf)_3$ ..... Yttrium triflate

$Yb(OTf)_3$ ..... Ytterbium triflate

$Zn(OTf)_2$ ..... Zinc triflate

# CHAPTER 1. CHIRAL RELAY IN ENANTIOSELECTIVE TRANSFORMATIONS

## 1.1. Introduction

Chirality plays a fundamental role in our life. An object or a system is chiral if it is distinguishable from its mirror image that is said to be chiral. The simple example is our hands. Right hand and left hand are mirror image pairs but one hand couldn't be superposed onto the other, so they are distinguishable. Much like our right and left hands, chiral molecules exist as one of two possible structures that are chemically identical but arranged such that they are mirror images of each other. Many important molecules required for life, exist in two forms called enantiomers. Biological and pharmaceutical activity of many molecules is often directly related to their chirality or to a single enantiomer.[1]

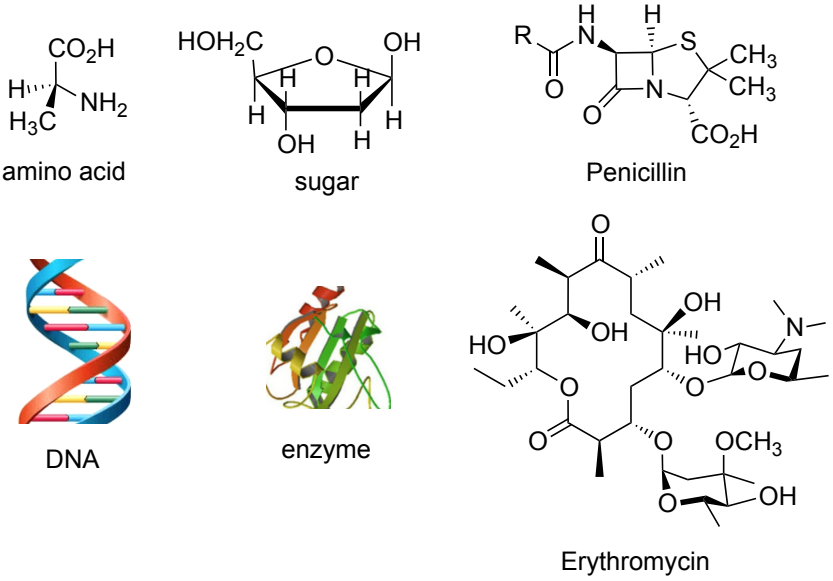


Figure 1.1. Examples of Chiral Molecules

Nearly all biological macromolecules are homochiral.[2] Most amino acids in proteins are left-handed. While all sugars that make up the helical backbone of DNA, RNA, and in the metabolic pathways are right-handed (Figure 1.1). More dramatic and crucially important is chirality in many pharmacologically active natural products[3] and drug molecules.[4] The impact of

chirality on biological activity of many theraoeutic agents has been demonstrated in many instances. In many of these cases, one may be helpful while the other may be inactive or even toxic. One example is thalidomide (Figure 1.2),[5] a sedative or antinauseat agent for pregnant women with morning sickness. Some women who took the drug with the racemic form had delievered off-springs with severe birth defects. A later study revealed that one enantiomer of thalidomide has the desired sedative activity, while the other form could cause birth defects. The enantiomers of thalidomide interacted differently with the chiral biomolecules in the body such as enzymes.

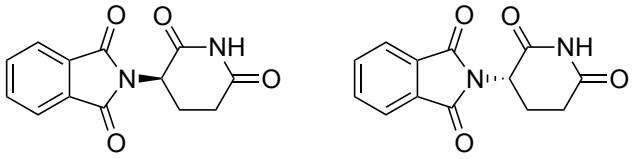


(*R*)-thalidomide (*S*)-thalidomide

Figure 1.2. Enantiomers of Thalidomide

Since the majority of therapeutics and natural products are single enantiomers, scientists have developed a number of asymmetric strategies. Chiral compounds synthesized from achiral starting materials and reagents are racemic. Separation of racemates into their enantiometic from is a process called resolution. The resolution of racemic mixtures by crystallization in the presence of a molecule from the chiral pool that is capable of forming a pair of diastereomeric salts has been used with great success.[6] The separation of racemic mixtures using chiral stationary phases has also become more practical.[7] At times, these methods are sometimes not flexible enough depending on the complexity of chiral compounds.

Asymmetric synthesis,[8] that is the precise control of chirality in a chemical transformation, offers the potential to eliminate disadvantages in the resolution of racemic

mixtures. In asymmetric synthesis, one of the identical groups is preferentially modified or replaced, so that the product is a mixture of two dissymmetric compounds, one of which predominates. Several ways[9] have been developed to realize asymmetric synthesis, such as chiral substrates, chiral auxiliaries, chiral catalysts and ligands, chiral reagents, *etc*.

### 1.2. Chiral Relay Substrates and Auxiliaries

Chiral substrates mediated synthesis is one of the oldest approaches to realize asymmetric synthesis. A readily available naturally derived chiral starting material is manipulated through sequential reactions, often using achiral reagents, to obtain the desired target chiral molecule. The stereogenic centers on the chiral substrate are from the enantiomerically pure natural products. Most commonly used materials are amino acids and carbohydrates. Another way to realize asymmetric synthesis is by the use of chiral auxiliaries, which have found wide applications in a variety of reactions over the last three decades for the synthesis of enantiomerically pure compounds.[10] A chiral auxiliary is an enantiomerically pure compound, which connects to the substrate through convalent bond(s) to form a new compound and can influence the configuration of stereogenic centers in the reaction. In most cases, at the end of the reaction, the auxiliary is cleaved under conditions that will not cause racemization of the product, and recovered for future use (Scheme 1.1).[11] The use of chiral auxiliaries allows the enrichment of diastereoselectivity in the reaction process and hence the enantioselectivity of the product after removal of the auxiliary.

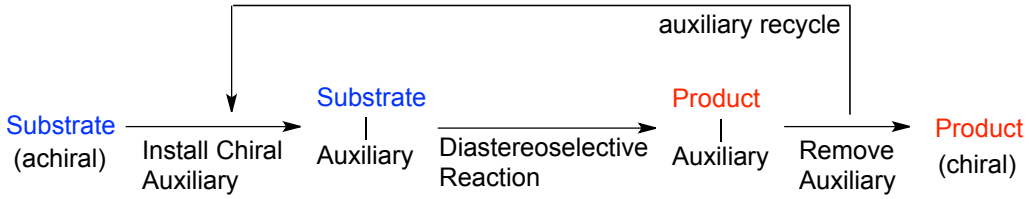


Scheme 1.1. Diastereoselective Synthesis using Chiral Auxiliaries

To impact the diastereoselectivity, the stereogenic center of the auxiliary should be close to the prochiral reactive site in the substrate. However this close orientation is not always attained and some examples that rely on relatively remote stereogenic centers to control diastereoselectivity were investigated.[12] An example of stereochemical control from a remote stereocenter in a diastereoselective asymmetric transformation is illustrated in Scheme 1.2. Schöllkopf and coworkers developed **1.1**, derived from *O*-methylation of diketopiperazine, which had been used in the synthesis of non-proteinogenic α-amino acids.[13] This strategy relied on the alkylation of a masked glycine enolate where diastereofacial selectivity is controlled by a remote chiral *iso*-propyl group (Scheme 1.2). But this remote control exhibited moderate diastereoselectivities in the enolate alkylation with linear or branched electrophiles.

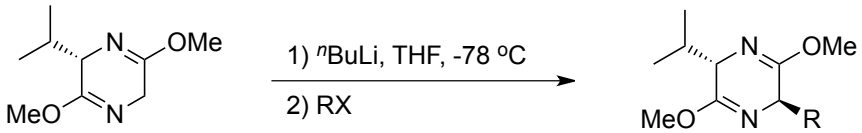


**1.1** **1.2**

| Electrophile RX | Yield% | de% |
|---|---|---|
| Methyl iodide | 54 | 50 |
| Benzyl bromide | 81 | 91 |
| Allyl bromide | 83 | 74 |
| Prop-2-ynyl bromide | 70 | 52 |

Scheme 1.2. 1,4-Asymmetric Induction in Bis-Lactim Ether Auxiliary

In 1998, Davies introduced the concept of chiral relay,[14] that involves relaying stereochemical information from a static chiral center to a fluxional center, which is inserted between the stereogenic center and the prochiral reactive center. Due to steric interactions with the stereogenic center, the fluxional group adopts a defined conformation that shields efficiently one face of the reaction center. During this process, the stereochemical information can be relayed and amplified from the existing stereogenic centers via a relay network to the reaction center. Unlike the conventional remote asymmetric induction in Scheme 1.3 (left), in chiral relay auxiliary design (Scheme 1.3-right),[14] steric interactions between the stereogenic center **R** and the relay group **Y** make them to organize in an antiperiplanar arrangement, thus the attacking group will approach the prochiral reactive center from an *anti* orientation to the relay group **Y**.

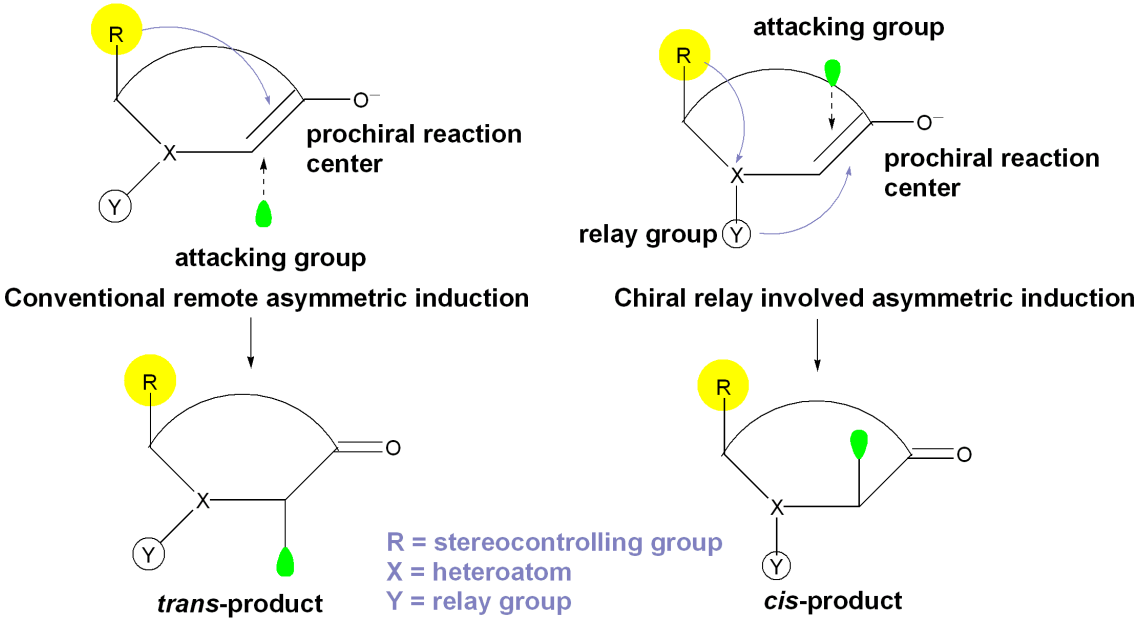


Scheme 1.3. Chiral Relay Design

Numerous studies have reported such a strategy for the control of enantioselectivity in a variety of transformations.[15] Davies and coworkers designed a new chiral template, which

employed a chiral relay network based on the non-stereogenic N-benzyl protecting groups to enhance diastereocontrol during enolate alkylation (Scheme 1.4).[16]

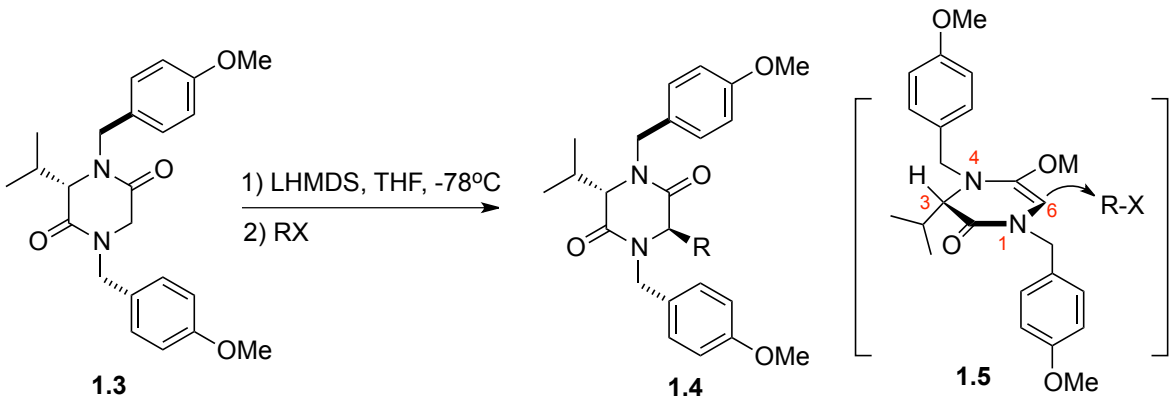


| Electrophile RX | Yield% | de% |
|---|---|---|
| Methyl iodide | 72 | 93 |
| Benzyl bromide | 88 | 98 |
| Allyl bromide | 63 | 94 |
| Prop-2-ynyl bromide | 74 | 89 |

Scheme 1.4. Chiral Relay Network in Davies' s Auxiliary

In Davies' s design, the enolate **1.5** derived by deprotonation of **1.3** adopts a conformation that the stereochemical information of the (3*S*)-isopropyl group will be relayed through space *via* non-stereogenic benzyl protecting groups. The isopropyl group controls the conformation of the proximal N4 benzyl *anti*, which in turn directs the N1 benzyl group *syn* to the isopropyl group. This fixed geometry can effectively block the *Si* face of enolate **1.5** towards incoming electrophile at C6 (Scheme 1.4). Alkylation of **1.3** with a range of electrophiles afforded products **1.4** in much higher de (>90%) and yield than **1.1**. They also obtained more evidence by conducting the alkylation of *N*,*N'*-dimethylated piperazine-2,5-dione, where the methyl group couldn't enhance the stereoselectivity via the proposed relay mechanism, and the diastereoselectivity was reduced to 33% de. The different results suggested that the proximity of

the N1 benzyl group to C6 results in significantly higher alkylation diastereoselectivities compared to Schöllkopf's case where the stereofacial control is only provided by the C3 isopropyl group. *Trans*-alkylated auxiliary **1.4** can be deprotected to α-amino acid via oxidative removal of the *p*-methoxybenzyl groups using ceric ammonium nitrate in $CH_3CN$-$H_2O$ and followed by acid hydrolysis to obtain the mixture of (*S*)-valine and (*R*)-alanine.[16]

Santarsiero and coworkers found a morpholin-2-one based chiral substrate shows a similar relay effect (Scheme 1.5). The enolate of *N*-Boc morpholinone **1.6** was benzylated and **1.7** was obtained in 99% de with *trans*-selectivity, while the enolate of the *N*-benzyl morpholinone **1.8** was benzylated to give a major product **1.10** with 94% de with a *cis*-relationship.[17]

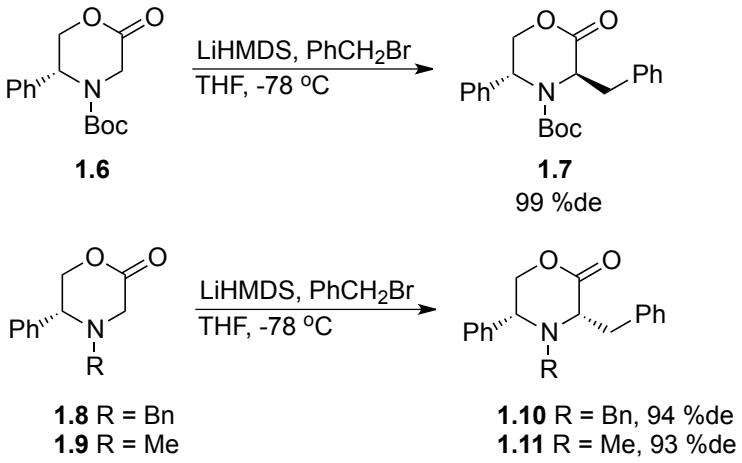


Scheme 1.5. Chiral Relay in Morpholin-2-one Based Chiral Auxiliary

Further studies showed the enolate of corresponding *N*-methyl morpholinone **1.9** produced *cis*-product **1.11** with 93 %de. This result is consistent with the selectivity observed in **1.10**. Thus the reversed selectivity observed in **1.10** and **1.11** was explained by stereoelectronic as well as chiral relay effect, where the fluxional *N*-benzyl group is fixed *anti* to the C5-phenyl

group results in the incoming electrophile to approach the *Si* face of the enolate and lead to *cis*-enolate alkylation. While the *trans*-selectivity observed for **1.7** was explained by the conventional 1,3-asymmetric induction and the *N*-Boc protecting group didn't affect the face selectivity induced by C5-phenyl chiral group (Scheme 1.6).[14,18]

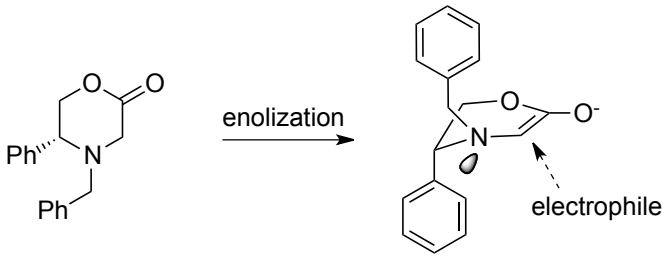


Scheme 1.6. Conventional 1,3-Asymmetric Induction *vs* Chiral Relay Induction

Craig and coworkers reported a stereoselective alkylation of conjugated iminium species, which was derived from the Lewis acid mediated ionization of chiral substrate **1.12**. The reaction proceeded via an $S_N1'$ mechanism and gave the allylation products exclusively as 2,6-*syn* diastereomers, regardless of the configuration at C4 in **1.12**. They presumed that the initial Lewis acid-assisted ionization of **1.12** generated the conjugated iminium species **1.14** and the incoming nucleophiles preferred to approach exclusively from the bottom face to give 2,6-*syn* products. The conjugated cyclic iminium would take more chair-like transition-state as a consequence of stereoelectronic reasons and the tosyl group might block the top face of the cyclic iminium species, thus affording the *cis*-substituted product (Scheme 1.7).[19]

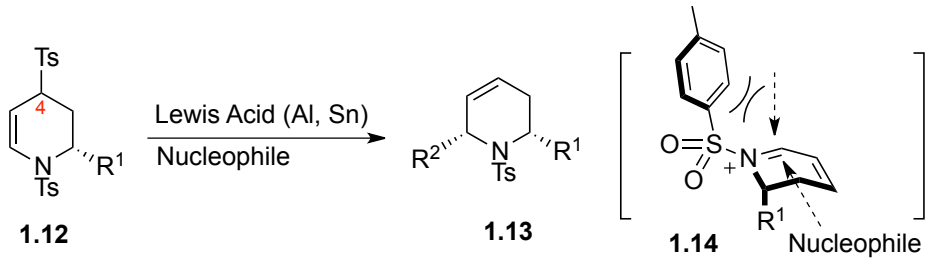


Scheme 1.7. Chiral Relay Effect in Tetrahydropyridine

Clayden and coworkers found that the conformation of a tertiary amide substituent on an aromatic ring could relay the stereochemical information to the nearby stereogenic center. They first demonstrated this discovery by adding single *ortho*-lithiated 1-naphthamide **1.15** to aldehyde, in which the two atropisomeric diastereoisomers of the product **1.16** are formed in ratios of up to 85:15 (Scheme 1.8).[20]

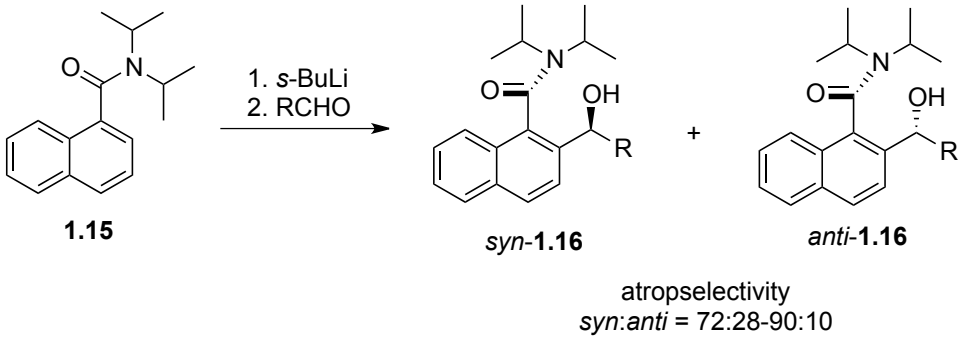


Scheme 1.8. Atropisomeric Addition of Lithiated *N,N*-Dialkyl-1-Naphthamides to Aldehydes

Later, they developed a bis-amide aryl based system, which uses two tertiary amides to realize remote 1,6-stereocontrol control (Scheme 1.9). The conformation of the first axis in **1.17** is relayed around the ring and the stereochemical information of the C1 position fixed the adjacent C2 position diisopropyl *anti* to the group at C1 due to steric hindrance. After introduction of a second tertiary amide substituent into **1.18**, the stereochemical information is relayed to the *meta*-position of the phenyl ring through the first axis. When the second

stereocenter at C4 in **1.20** is installed, it is *anti* to the diisopropyl group at C3 and under the ultimate control from the *para*-position of the ring through this relay network. Additionally, this two relay units can retain the stereochemical information by two inversions.[21]

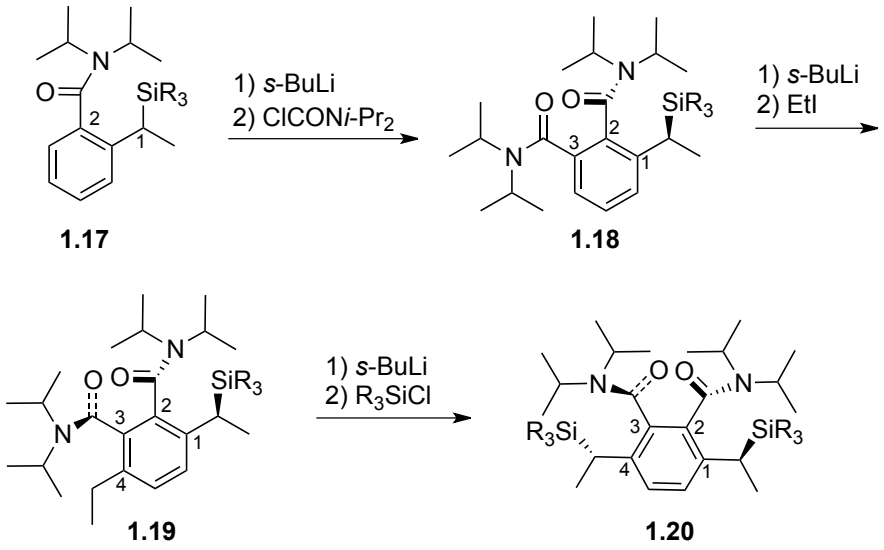


Scheme 1.9. Chiral Relay through a Benzene-1,2-Dicarboxamide

Hitchcock and coworkers utilized (1*R*, 2*S*)-ephedrine-based oxadiazinone derived chiral auxiliary for the asymmetric aldol reaction by treatment with titanium tetrachloride, triethyamine and aldehydes. When N4 of oxadiazinone was substituted with a methyl group, the *syn*-products were obtained with 3:1 to 99:1 diastereoselectivities, while substituted with isopropyl group, the aldol adducts were found to have diastereoselectivities ranging from 8:1 to 99:1 favoring *syn*-substitution.[22] The diastereoselectivities observed in **1.23** with more bulky isopropyl group at N4 enhanced the observed diastereoselectivities of the aldol addition compared to methyl substituted oxadiazinone **1.21**, which suggested the stereochemical impact of the ephedrine fragment (C5-substituent and C6-phenyl of the oxadiazinone) is transmitted to the appended N3-enolate by way of intramolecular chiral relay via the stereogenic N4-nitrogen.[23] Additionally, their X-ray

crystal structure showed the proximity of the N4-methyl group to the N3-substituent is the dominant factor for asymmetric induction. A proposed transition state for the process is shown in Scheme 1.10. The C5-methyl and C6-phenyl fixed the N4-alkyl group at the bottom and the aldehyde will approach from the less hindered top face in the proposed transition state.

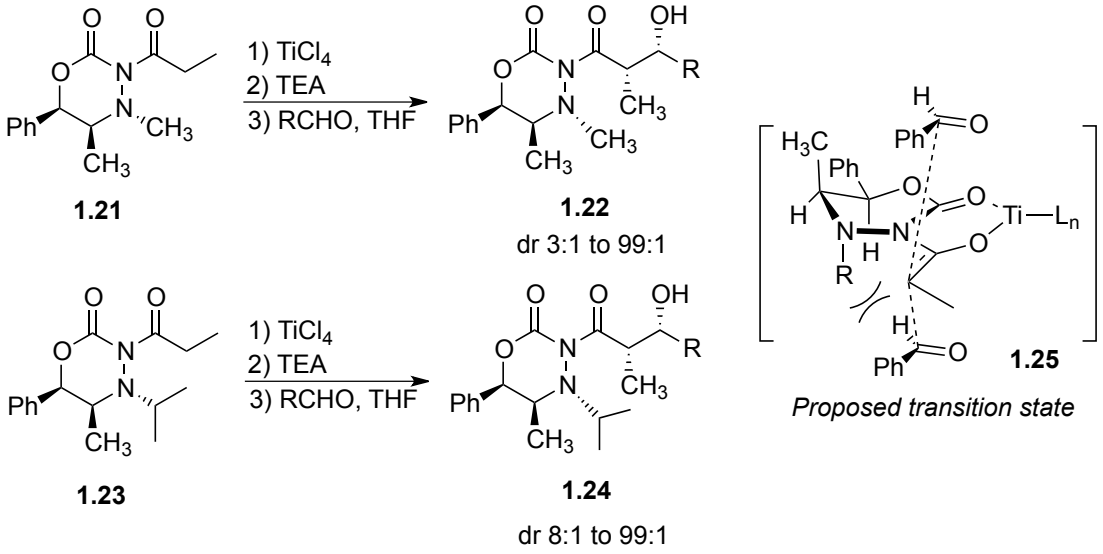


Scheme 1.10. Asymmetric Aldol Reaction using Oxadiazinone Template

Levacher and coworkers designed a chiral NADH reagent that relies on a chiral axis control through a chiral relay installed on the cyclic structure. This reagent was applied in the reduction of methyl benzoylformate and afforded (*R*)-methyl mandelate in up to 84 %ee (Scheme 1.11). The deuterated **1.26** afforded the reduction product **1.27** with no deuterium incorporation and the quinolinium salt **1.28** was recovered with high deuterium content. More experimental evidence suggested that the *syn* orientated hydrogen in **1.26** was preferentially transferred in the reduction and this preference may arise due to the conformational control of C=O lactam in **1.26**.[24]

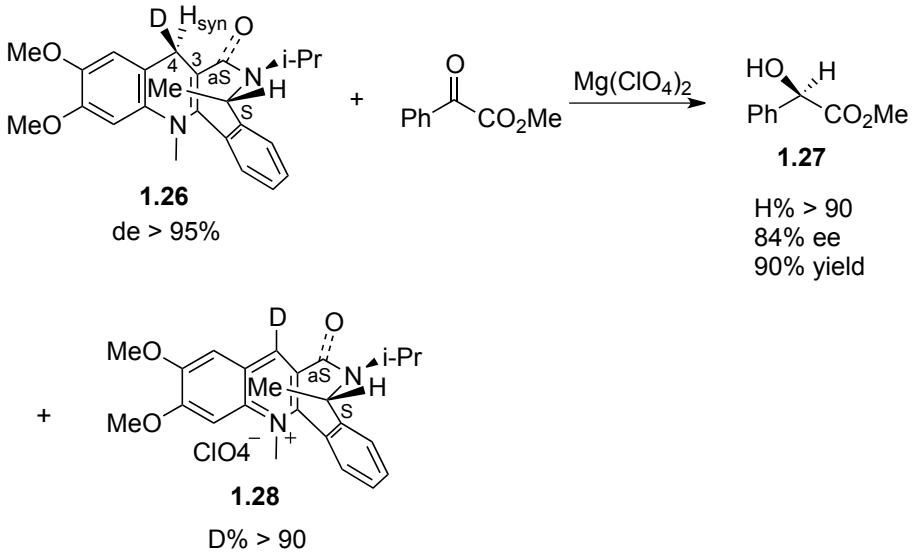


Scheme 1.11. Asymmetric Reduction of Methyl Benzoformate with Chiral NADH

The chiral element (methyl group) on the lactam ring in **1.26** takes on an *anti*-periplanar orientation with *N*-isopropyl group because of steric interaction, which leads to the staggered conformation and also a C3-C=O chiral axis was formed in this process. This chiral axis enables to differentiate the two diastereotopic hydrogens at C4 and the two enantiotopic faces of methyl benzoylformate.

Davies and coworkers also developed *N*-1-(1'-naphthyl)ethyl-*O*-*tert*-butylhydroxylamine chiral auxiliary, which can act as chiral Weinreb amide equivalents (Scheme 1.12). This achiral auxiliary was synthesized in four steps and followed by chiral resolution with (+)-camphorsulfonic acid to obtain the chiral form. A range of enantiopure acyl derivatives **1.29** were prepared. Reacting **1.29** with KHMDS followed by an alkyl halide gave the corresponding α-substituted derivatives **1.30** in good yield and high diastereoselectivity (>95:1). Reductive cleavage of **1.30** with $LiAlH_4$ gave chiral aldehydes **1.31** with high selectivities (>=94 %ee) and with MeLi to afford the corresponding chiral methyl ketones **1.32** in high yields and excellent

enantioselectivity (>97 %ee). The auxiliary was recovered from cleavage reactions in >98 %ee and recycled.[25]

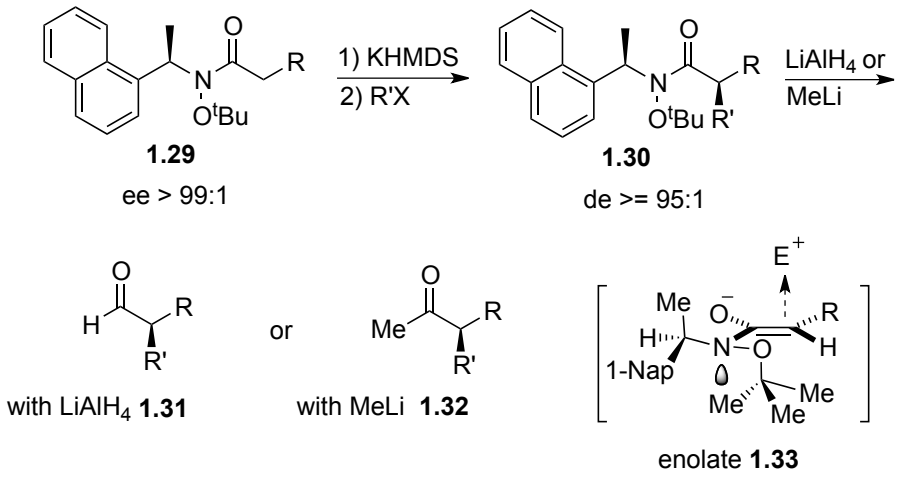


Scheme 1.12. Diastereoselective Enolate Alkylations of *N*-Acyl Derivatives of *N*-1-(1'-Naphthyl)ethyl-*O*-*tert*-Butylhydroxylamine

They proposed a mechanism to rationalize the observed stereochemical outcome based on chiral relay effect. Deprotonation of **1.29** would form (*Z*)-enolate **1.33** with two oxygen atoms taking an *anti*-periplanar orientation to minimize electrostatic repulsions.[26] The stereochemical information will transfer from the asymmetric carbon center to the bulky *tert*-butyl group and the adjacent nitrogen center. The sterically demanding asymmetric *C*-methyl and *O*-*tert*-butyl groups will be in the opposite conformation due to steric interaction, thus in the subsequent enolate alkylation, the incoming electrophile is expected to approach from the *Re* face, opposite to both the nitrogen lone pair and the bulky *tert*-butyl group.

### 1.3. Chiral Lewis Acid Mediated Chiral Relay

Although the use of chiral substrates and auxiliaries provides good results in many cases, it required the use of a stoichiometric quantity of the initial chiral source. Therefore, methods that employ catalytic quantities of the initial source of chirality have been and continue to be the

subject of intense investigations. As an alternative approach to increase selectivity, our group hypothesized a new achiral auxiliary, which may allow amplifying and relaying stereochemical information when cooperating with when coupled with a catalytic amount of chiral source. The template of interest to our study is the pyrazolidinone auxiliary **1.34** (Figure 1.3). Pyrazolidinones are attractive because they don't have permanent chirality but have a fluxional *N*-1 center, which may work with an external chiral source together and be able to provide strong steric shielding. Additionally, **1.34** is easily prepared and the fluxional R group can be readily varied to provide tunability. The pyrazolidinone auxiliaries also offer the advantage that they need not to be synthesized from chiral pool precursors.

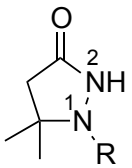


**1.34**

Figure 1.3. Pyrazolidinone Templates

Chiral Lewis acid catalysis has been widely used in enantioselective transformations.[27] Many efforts in this area have focused on the design and development of chiral ligands that are able to selectively shield one face of a reaction center when complexed with a Lewis acid.[28] Ligand design continues to play a major role in Lewis acid catalysis, but to access new ligand architectures is not easy due to the inherent synthetic challenges. In the process of searching for chiral activators that could work cooperatively with the achiral pyrazolidinone template, we envisioned that a Lewis acid with simple (potentially commercially available) chiral ligands providing minimal steric shielding, would be an optimal choice. In this situation, the Lewis basic sites in the pyrazolidinone-derived substrate are suitable for coordination with the chiral Lewis

acid and the fluxional pseudo-chiral nitrogen center would be in a consonance or dissonance relationship with the static chirality present in the ligand. In this scenario, consonant chiral relay would be an attractive approach to amplify selectivity (Scheme 1.13). The coordination between a pyrazolidinone and a Lewis acid leads to equilibrium conformations such as **1.35** and **1.36** which are diastereomeric. When an incoming attacking group approaches the chiral Lewis acid coordinated substrate, the reaction might proceed preferentially through one of the two fluxional conformations during a dynamic process. If the pyrazolidinone R group were to act in a consonant fashion with a chiral Lewis acid, the chirality at the fluxional nitrogen may function in a similar manner like a chiral auxiliary such as **1.37**.

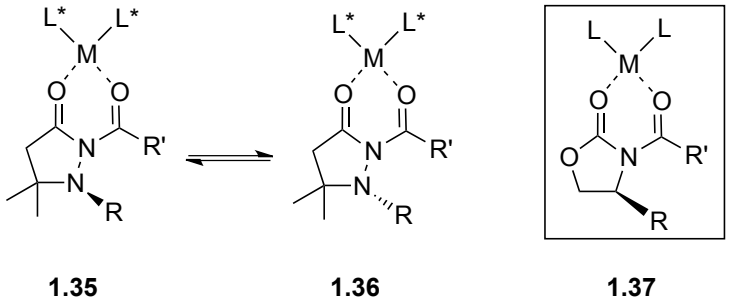


**1.35** **1.36** **1.37**

Scheme 1.13. Coordination Between Pyrazolidinone and Chiral Lewis Acid

Chiral oxazolidinone auxiliary **1.37** has been utilized in Lewis acid catalyzed asymmetric transformations, for example a Diels-Alder cycloaddition, and provides the cycloadduct with high level of stereoselectivity. The Evans group has carried out a large amount work using **1.37** in asymmetric synthesis.[29] They reported that chiral oxazolidinone **1.38** could provide high level of asymmetric induction in a diastereoselective Diels-Alder reaction in the presence of achiral $Et_2AlCl$ (Scheme 1.14).

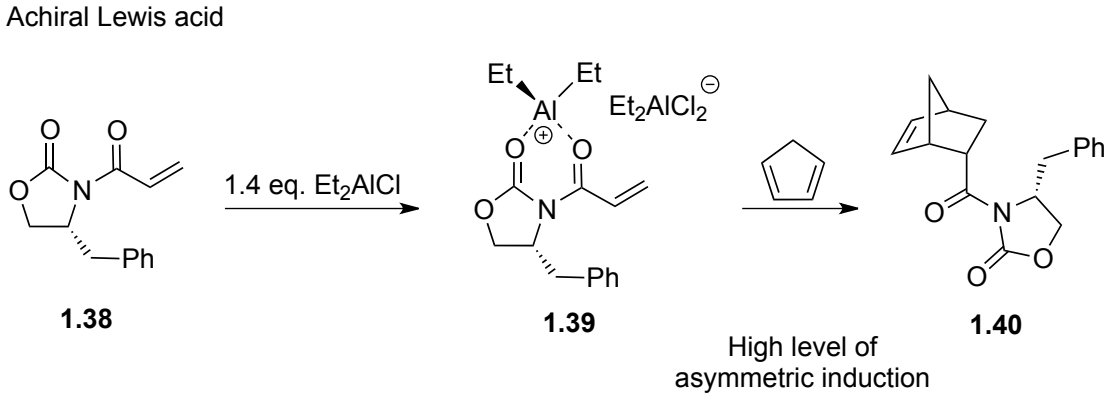


Scheme 1.14. Chiral Oxazolidinone Auxiliary in Diastereoselective Diels-Alder Reaction

Furthermore, they demonstrated that the level of asymmetric induction could be improved substantially by using a matched chiral Lewis acid in cooperation with the chiral oxazolidinone **1.38**. It is notable that this reaction was performed using a catalytic amount of the chiral Lewis acid (Scheme 1.15). In contrast, in the matched case with ligand and auxiliary shielding opposite faces, both selectivity and reactivity are low.

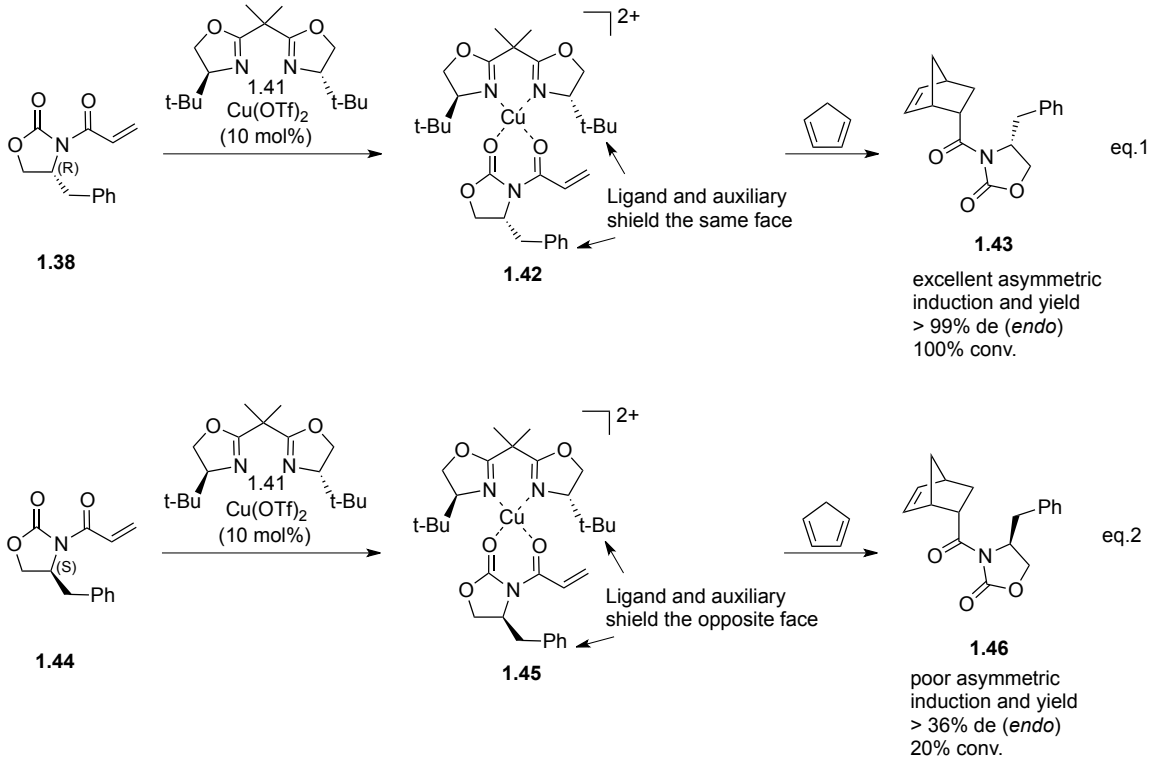


Scheme 1.15. Asymmetric Induction Between Chiral Lewis Acid and Chiral Oxazolidinone Derivative

In the achiral pyrazolidinone case, if the fluxional character of the N atom takes a certain pyramidalized conformation consonant with the permanent chirality of the chiral Lewis acid in the reaction process, we can expect an amplification of selectivity, which is similar to the Evans' matched case, would be possible (Scheme 1.16). Thus, a relay of stereochemical information was established where the chiral Lewis acid would bias the fluxional nitrogen making the pyrazolidinone a chiral auxiliary with the fluxional R group shielding one face of the reaction center. In the ideal case, the static chirality of the chiral ligand and the chirality of the fluxional nitrogen would work in a matched conformation to amplify enantioselectivity (complex **1.49**).

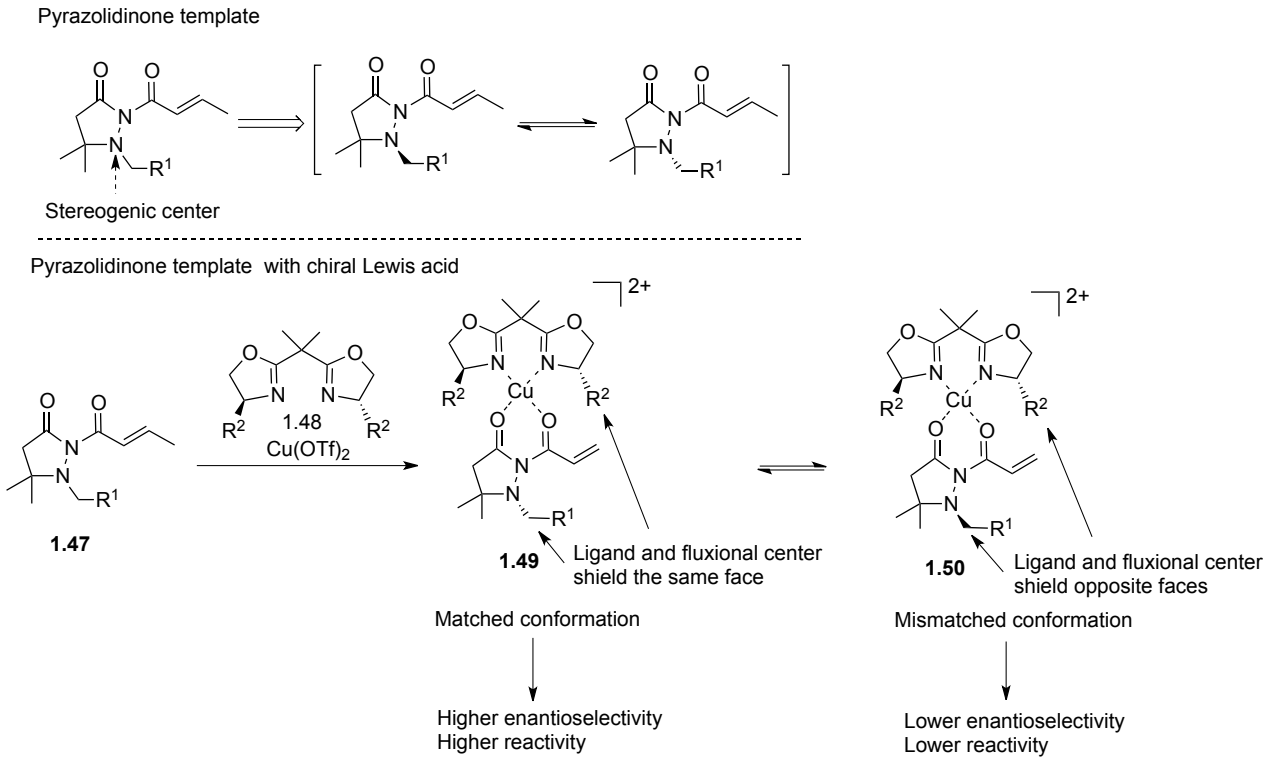


Scheme 1.16. Asymmetric Induction Between Chiral Lewis Acid and Achiral Pyrazolidinone Derivative

Notably, unlike in Davies' s chiral auxiliary relay strategy, our approach is not inherent to the substrate but the chirality in the external source (chiral Lewis acid), working synergistically with the template influences reaction outcome. Additionally, this new strategy also allows for the use of permanent chirality in a catalytic amount. The pyrazolidinone templates were prepared in a straightforward manner from β,β-disubstituted enolates **1.51** (Scheme 1.17).

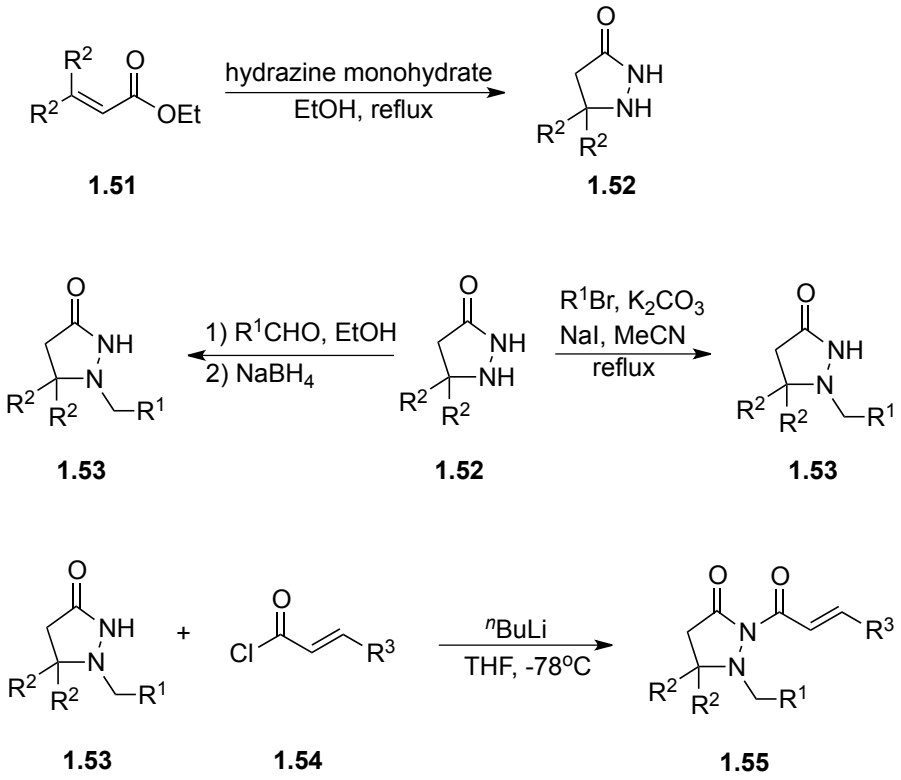


Scheme 1.17. Synthesis of β-Substituted α,β-Unsubstituted Pyrazolidinone Imides

Condensation of **1.51** with hydrazine hydrate gave N1 unsubstituted pyrazolidinones **1.52**. N1 substitution was installed by either alkylation of the more basic N1 nitrogen or by reductive amination with an aldehyde. Acylation of **1.53** at N2 occurs upon deprotonation with *n*-BuLi and subsequent addition of the appropriate α,β-unsaturated acid chloride generated pyrazolidinone imide **1.55**. When $R^2$ = methyl or cyclohexyl, LiHMDS was used as the base to deprotonate **1.53**. Our group has utilized α,β-unsaturated pyrazolidinone imide templates in a variety of Lewis acids catalyzed enantioselective transformations and these transformations are described in the next section.

### 1.3.1. Achiral Pyrazolidinone Template and Other Achiral Templates in Enantioselective Diels-Alder Reactions

A large number of templates have been utilized to carry out enantioselective Diels-Alder reactions catalyzed by a variety of activators. Diels-Alder (DA) cycloaddition of cyclopentadiene to pyrazolidinone derived crotonates was undertaken to examine the effectiveness of the chiral relay template in providing efficient stereocontrol in the presence of a chiral Lewis acid activator.[30] The DA reactions were carried out at room temperature with substrates **1.57a-d** featured with different *N*-substituents (Table 1.1). In an initial experiment, bisoxazoline **1.58** with a small C4 methyl group was chosen. The authors surmised that since the methyl substituent is small, it may not provide effective steric shielding without amplification from the pyrazolidione auxiliary. As seen from the data in Table 1.1, the selectivity is very low when oxazolidinone **1.56** was used (38 %ee, entry 1). However, when pyrazolidinone auxiliaries with different size of *N*-substituents were investigated as substrates, the enantioselectivity showed a dependence on the size of the fluxional group. As the size of R group increases (Me < Ph < 2-naphthyl, 1-naphthyl), so does the enantioselectivity of the cycloadduct (entry 2-5). Interestingly, the use of the bulky 1-naphthyl fluxional group furnished the adduct in 86 %ee (entry 6). These results suggested that the enantioselectivity for the major *endo* adduct correlates directly with the size of the *N*-substituents in pyrazolidinone templates. Furthermore, it also suggested that the size of *N*-substituent in pyrazolidinone templates may play a major role in enantiocontrol.

The use of ligand **1.59** and **1.60** with medium-size C4 substituents in the Diels-Alder reaction showed similar trends as ligand **1.58**, **1.57d** still gave the best enantioselectivities for the DA adduct. Compared to the low enantioselection observed using oxazolidinone **1.56**, the result

(entries 2-5) also suggested that pyrazolidinone templates are able to amplify enantioselectivity by tuning the size of *N*-substituents using the medium steric bulkyl chiral ligand.

When applying a sterically bulky ligand **1.61**, a similar trend as described above was also observed. The pyrazolidinone templates amplified enantioselectivity relative to oxazolidinone and the enantioselectivity increased with the size of the *N1*-substituent. The high selectivities obtained when R = Ph, 2-naphthyl, and 1-naphthyl indicated that the medium sized pyrazolidinone R group in conjunction with the sterically demanding chiral ligand was able to provide nearly complete face-shielding in the cycloaddition.

Employing bisoxazoline ligand **1.62** derived from amino indanol, the enantioselectivities for the Diels-Alder adduct were uniformly high (95-96 %ee) regardless of the size of the pyrazolidinone R group. The high enantioselectivity observed for all pyrazolidinone-derived substrates versus oxazolidinone substrate again shows the strong amplification of steric information although reactions with ligand **1.62** suggested that it is the major controller of the stereoinduction in the cycloaddition.

All the above results suggested that in combination with an appropriate chiral ligand, a pyrazolidinone auxiliary could amplify enantioselectivity to a large extent and produce *endo*-selective Diels-Alder product with high stereoselectivity.[31]

Table 1.1. Diels-Alder Reactions with Pyrazolidinone Templates using Chiral Bisoxazolines

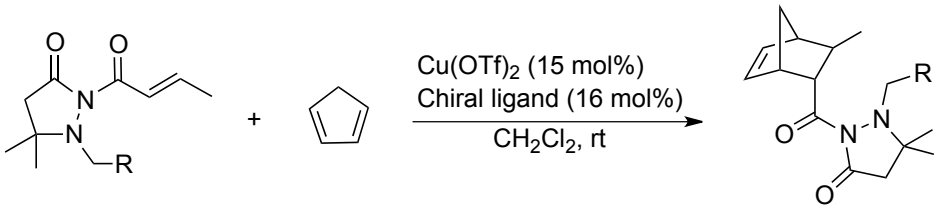


**1.57a-d** **1.63** *endo*-adduct

| | 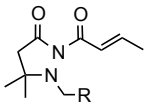 | 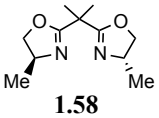 **1.58** | 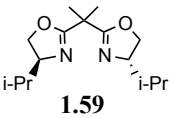 **1.59** | 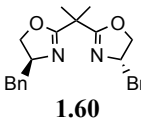 **1.60** | 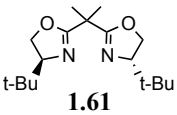 **1.61** | 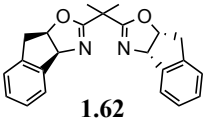 **1.62** |
|---|---|---|---|---|---|---|
| Entry | Substrate | %ee (*endo*/*exo*) | %ee (*endo*/*exo*) | %ee (*endo*/*exo*) | %ee (*endo*/*exo*) | %ee (*endo*/*exo*) |
| 1 | 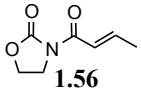 **1.56** | 38 (88:12) | 23 (87:13) | 17 (86:14) | 54 (81:19) | 83 (89:11) |
| 2 | R = Me **1.57a** | 64 (91:9) | 56 (96:4) | 55 (88:12) | 77 (93:7) | 96 (92:8) |
| 3 | R = Ph **1.57b** | 71 (93:7) | 84 (92:8) | 71 (91:9) | 97 (92:8) | 95 (91:9) |
| 4 | R = 2-Naphthyl **1.57c** | 79 (93:7) | 65 (91:9) | 69 (90:10) | 99 (93:7) | 96 (93:7) |
| 5 | R = 1-Naphthyl **1.57d** | 86 (90:10) | 95 (93:7) | 85 (87:13) | 99 (90:10) | 96 (90:10) |

Generally, for stereoelectronic reasons, normal DA cycloadditions show *endo* selectivity. Thus development of methods for the formation of the *exo* adducts by overriding the normal stereoelectronic preference for *endo* adduct is noteworthy. The selective formation of *exo*-DA adduct has been investigated (Table 1.2). It was hypothesized that by choosing the appropriate combination of pyrazolidinone auxiliary with a chiral Lewis acid, the *endo* approach of the diene may be blocked. A range of chiral Lewis acids was screened for *exo*-selective DA reactions. When Cu (II), Mg (II) and Zn (II) salts combined with bis(oxazoline) ligands, *endo*-selective

products were obtained as the major diastereomer. In contrast, using $Yb(OTf)_3$ or $Y(OTf)_3$ as a Lewis acid with a Pybox ligand, the ratio of the *exo* product increased. The effect of the ligand on selectivity was tested and the result showed that 2-amino-1,2-diphenyl ethanol-derived pybox ligand **1.66** led to the much more improved *exo* selectivity than other ligands. Later, the impact of pyrazolidinone N1 substituent on *exo*/*endo* selectivity was investigated. The reaction of pyrazolidinone **1.64a** with cyclopentadiene under $Yb(OTf)_3$/**1.66** produced that *endo* adducts as the major product (entry 1). A small increase in the *exo*/*endo* ratio was observed when pyrazolidinone **1.64b** was used as the dienophile (entry 2).

Table 1.2. Effect of Pyrazolidinone N1 Substitution on *exo*/*endo* Selectivity

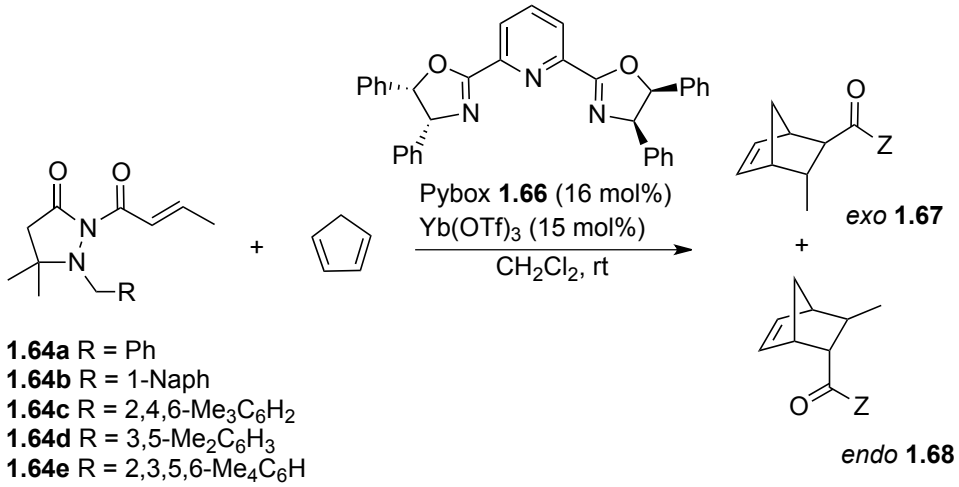


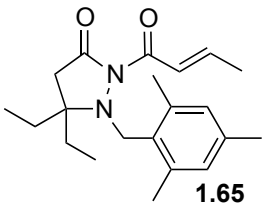

**1.65**

| entry | Substrate | Yield% | *exo*/*endo* | ee% (*exo*) |
|---|---|---|---|---|
| 1 | **1.64a** | 80 | 37:63 | 88 |
| 2 | **1.64b** | 84 | 45:55 | 95 |
| 3 | **1.64c** | 91 | 74:26 | 93 |
| 4 | **1.64d** | 78 | 40:60 | 81 |
| 5 | **1.64e** | 71 | 71:29 | 90 |
| 6 | **1.65** | 62 | 84:16 | 93 |

Further increase in *exo* selectivity was observed when **1.64c** was employed (entry 3). Notably, high enantioselectivities for *exo* adduct were obtained with dienophiles **1.64b** and **1.64c**. Reaction with dienophile **1.64d** with 3,5-dimethyl substituted phenyl fluxional group was *endo*-selective (entry 4). When comparing data from entry 3 and entry 4, it seems that 2,6-substitution may be necessary for the optimal *exo* selectivity and this notion was confirmed by using **1.64e** as the dienophile, which produced a higher proportion of the *exo* adduct **1.64c** (entry 5). Modifying C5 substituent on pyrazolidinone ring showed the pyrazolidinone crotonate **1.65** bearing C5 ethyl substituents as the dienophile efficiently improved *exo* selectivity in the product and high enantioselectivity was also obtained (entry 6). Additional increase in the size of the C5 substituent decreased the selectivity.[32]

The Sibi group also studied chiral Lewis acid catalyzed Diels-Alder cycloaddition between β-substituted pyrazolidinone propiolimides and cyclic dienes. Acetylenic dienophiles possess two orthogonal sets of $\pi$-orbitals and each of them can participate in the cycloaddition, which brings a challenge for enantiomeric control.[33] The Diels-Alder reaction between more reactive β-silyl, β-halo, β-stannyl or β-unsubstituted α,β-acetylenic dienophiles and cyclic dienes to generate Diels-Alder product in good yields and enantioselectivities have been reported.[34] The challenge of using β-alkyl α,β-acetylenic substrate in the Diels-Alder reaction is that alkyl acetylenic substrate is a less reactive dienophile. Besides, after coordination with chiral Lewis acid, the reaction center is prone to be far away from the stereocontrol of chiral ligand, which is different with α,β-alkenyl carbonyl compounds that can have better stereocontrol in the presence of a chiral Lewis acid.

In this study, β-alkyl α,β-acetylenic substrate containing achiral pyrazolidinone auxiliaries were designed and this template derived acetylenic dienophile was hypothesized to

provide a solution for solving challenges discussed above.[35] After optimizing reaction conditions, the effect of pyrazolidinone N1 substitution on the enantioselectivity of the Diels-Alder adduct was studied. The results showed that the size of N1 substituent R had slight effect on enantioselectivity (Table 1.3). Dienophile **1.69b** was less selective than other substrates and the selectivity for **1.69a**, **1.69c** and **1.69d** were similar.

Table 1.3. Diels-Alder Cycloaddition with β-Substituted Pyrazolidinone Propiolimides

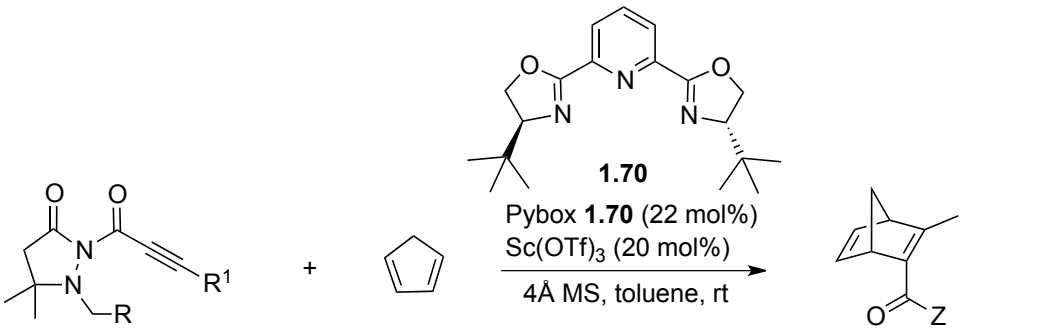


**1.69a** R = Ph, $R^1$ = Me
**1.69b** R = Mes, $R^1$ = Me
**1.69c** R = 1-naphthyl, $R^1$ = Me
**1.69d** R = 2-naphthyl, $R^1$ = Me
**1.69e** R = Ph, $R^1$ = TMS

| entry | Substrate | Yield% | ee% |
|---|---|---|---|
| 1 | **1.69a** | 74 | 52 |
| 2 | **1.69b** | 70 | 34 |
| 3 | **1.69c** | 60 | 50 |
| 4 | **1.69d** | 68 | 48 |
| 5 | **1.69e** | 82 | 50 |

These results suggested that the pyrazolidinone N1 substituent is not positioned properly to positively impact the facial selectivity of the cycloaddition or the bias for *endo* or *exo* approach of the diene. Substrate with β-trimethylsilyl substituent was also a suitable dienophile for producing enantioenriched cycloadduct in high yield (entry 5).

Renaud and coworkers designed achiral templates, 4-substituted 1,3-benzoxazol-2-(3H)-ones, for enantioselective Diels-Alder reactions (Figure 1.4). They proposed that two diastereomeric conformations A and B should form after the acrylamide **1.72** coordinated with chiral Lewis acid, thus the achiral auxiliary can adopt chiral conformations and relay the chiral information from the chiral Lewis acid to the reaction center at the same time. These two diastereomers result from the chiral axis in the substrate and should exist in unequal amounts and react with dienes in different rates and with different stereoselectivity.[36]

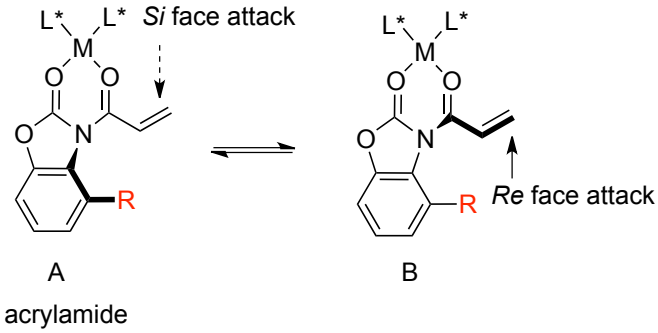


Figure 1.4. Diastereomeric Complexes A and B

In the presence of $MgBr_2/Et_2O$ and bisoxazoline ligand **1.73**, the size of R group in the achiral template of *N*-acryloyl derivatives was examined (Table 1.4). The nonsubstituted substrate **1.72a** generated the *endo* product with low enantioselectivity (entry 1). As the effective size of the relay group increases, so does enantioselectivity for the product. The methyl substituted substrate **1.72b** showed significant improvement in enantioselectivity (entry 2) and the ethyl substituted substrate showed a slight increase in enantioselectivity (entry 3). When R was replaced by benzyl or PMB (*p*-methoxybenzyl), high enantioselectivity was obtained for both substrates (entries 4-5). More bulky substituents lowered the enantioselectivity (entries 6-8) and can be attributed to inefficient chelation to the metal ion. Further study suggested that the stereochemical outcome correlates well with an increase of twist angle around the C(O)-N bond.

Larger twist angles impact the chelation in substrates with large substituents resulting in lower enantioselectivities.

Table 1.4. Diels-Alder Reaction with Achiral 4-Substituted 1,3-Benzoxazol-2-(3H)-Ones Templates

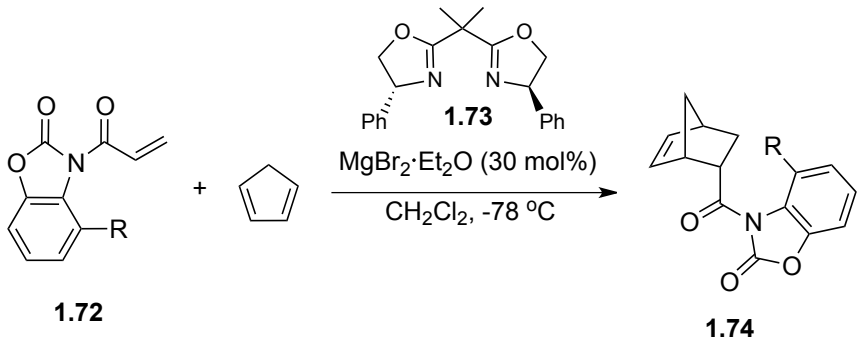


**1.72** **1.74**

| entry | Substrate | R | Yield% (*endo*/*exo*) | ee% (*endo*-*S*) |
|---|---|---|---|---|
| 1 | **1.72a** | H | 98 (22:1) | 14 |
| 2 | **1.72b** | Me | 97 (32:1) | 74 |
| 3 | **1.72c** | Et | 97 (33:1) | 76 |
| 4 | **1.72d** | Bn | 97 (11:1) | 86 |
| 5 | **1.72e** | PMB | 98 (16:1) | 88 |
| 6 | **1.72f** | $CH_2{}^tBu$ | 98 (20:1) | 10 |
| 7 | **1.72g** | $CH(Ph)_2$ | 97 (17:1) | 72 |
| 8 | **1.72h** | $SiMe_3$ | 95 (40:1) | 40 |

### 1.3.2. Achiral Template in Enantioselective 1,3-Dipolar Cycloadditions

Pyrazolidinone templates have also been investigated in the 1,3-dipolar cycloaddition with nitrones. Chiral Lewis acid catalyzed enantioselective and regioselective dipolar cycloadditions of nitrones to alkenes have been reported by several research groups,[37] but in most cases, *endo* diastereomers **1.77** are generated preferentially. The Sibi group described the

first examples of highly *exo* selective 1,3-dipolar cycloaddition of nitrones and dipolarophiles derived from using pyrazolidinone templates (Table 1.5).[38]

The 1,3-dipolar cycloaddition of nitrones with pyrazolidinone-derived alkenes were conducted using catalytic amounts of a Lewis acid and bisoxazoline ligands (Table 1.5). Reaction with $Cu(OTf)_2$ and ligand **1.58** afforded high yield of the *exo* isomer in good enantioselectivity (entry 1). Exploring much bulker ligands like **1.59** and **1.61** didn't improve the enantioselectivity and showed negative effects on diastereoselectivity. When applying aminoindanol-derived ligand **1.62**, the *exo* isomer was obtained with high yield, enantioselectivity as well as diastereoselectivity (entry 4). The effect of molecular sieves (MS) was evaluated. Addition of MS 4Å didn't affect the enantioselectivity of the *exo* product compared to same reactions without MS, but it led to a dramatic reversal (entry 1 *vs* entry 5) or reduction (entry 4 *vs* entry 6) in *exo*/*endo* ratios. Other Lewis acids with different coordination geometries were also examined using ligand **1.58** and the results are shown in entries 7-9. Zinc triflate preferred to produce exo product with modest diastereoselectivity, and the *exo* isomer was obtained with low ee. Magnesium and iron Lewis acids gave nearly the same amount of both *exo* and *endo* isomers with magnesium Lewis acid produced more *exo* product than the iron Lewis acid. The Lewis acids study revealed that a square planar metal complex is appropriate for providing high *exo* selectivity.

Table 1.5. Exo Selective Enantioselective Nitrone Cycloadditions

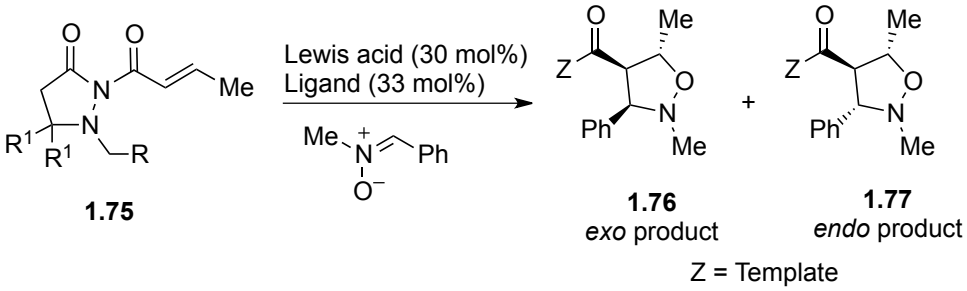


**1.75** **1.76** *exo* product **1.77** *endo* product

Z = Template

| entry | Lewis acid | Ligand | R | $R^1$ | Yield% | *exo*/ *endo* | *exo* ee% |
|---|---|---|---|---|---|---|---|
| 1 | $Cu(OTf)_2$ | **1.58** | Ph | Me | 96 | 90:10 | 75 |
| 2 | $Cu(OTf)_2$ | **1.59** | Ph | Me | 91 | 79:21 | 71 |
| 3 | $Cu(OTf)_2$ | **1.61** | Ph | Me | 24 | 83:17 | 73 |
| 4 | $Cu(OTf)_2$ | **1.62** | Ph | Me | 94 | 96:4 | 98 |
| 5 | $Cu(OTf)_2$[a] | **1.58** | Ph | Me | 88 | 19:81 | 72 |
| 6 | $Cu(OTf)_2$[a] | **1.62** | Ph | Me | 92 | 63:37 | 98 |
| 7 | $Zn(OTf)_2$ | **1.58** | Ph | Me | 90 | 86:14 | 47 |
| 8 | $Mg(OTf)_2$ | **1.58** | Ph | Me | 82 | 57:43 | 27 |
| 9 | $Fe(NTf_2)_2$ | **1.58** | Ph | Me | 44 | 45:55 | -17 |
| 10 | $Cu(OTf)_2$ | **1.58** | Me | Me | 96 | 92:8 | 78 |
| 11 | $Cu(OTf)_2$ | **1.58** | phenyl | Me | 96 | 90:10 | 75 |
| 12 | $Cu(OTf)_2$ | **1.58** | 1-naphthyl | Me | 93 | 89:11 | 86 |
| 13 | $Cu(OTf)_2$ | **1.58** | phenyl | cyclohexyl | 93 | 95:5 | 79 |
| 14 | $Cu(OTf)_2$ | **1.58** | phenyl | benzyl | 94 | 91:9 | 83 |

a. MS 4Å was added.

A template evaluation was conducted to see whether the enantioselectivity in 1,3-dipolar cycloaddition could be amplified by tuning the size of the fluxional substituents. Initially, keeping $R^1$ as a methyl group, the effect of N1-substituents in substrate **1.75** was evaluated.

Similar to the previous chiral Lewis acid catalyzed Diels-Alder reaction results, the enantioselectivity for the major *exo* isomer correlated with the steric bulk of the N1-substituent. The enantioselectivities were enhanced by increasing the size of the R from methyl to 1-naphthyl (entries 10-11). The size of C5 substituents ($R^1$ on **1.75**) also affected the ee of the major *exo* product. Varying $R^1$ from methyl to cyclohexyl to benzyl also led to the gradually increase in ee in the *exo* isomer (entries 11, 13, 14). These observations suggested that by tuning the size of N1-substituents and C5 substituents of the pyrazolidinone templates, optimal levels of selectivity for the cycloadduct could be obtained. A simple oxazolidinone template was also tested in the same reaction condition and the *exo* isomer was also obtained as the major product but with low enantioselectivity.

The substrate scope was studied by changing the enoyl substrates as well as nitrones and high enantioselectivity was observed in most cases. After evaluating all parameters, the results showed the observed *exo* selectivity in this study may be attributed to the square planar complexes formed after the coordination between chiral Lewis acid and the template. This study again showed pyrazolidinone relay networks could amplify enantioselectivity.

Later, Sibi and coworkers investigated the 1,3-dipolar cycloaddition of nitrile oxides with pyrazolidinone derived enolates. Cycloaddition of nitrile oxide and olefin produces isoxazoline derivatives, which have played an important role for the construction of five-membered heterocycles.[39] In this study, the highly regio- and enantioselective nitrile oxide cycloadditions to alkenes catalyzed by substoichiometric amount of chiral Lewis acid was developed[40] (Table 1.6).

Template screening showed that using oxazolidinone crotonate as the template, the reaction proceeded with low regioselectivity and inconsistent enantioselectivity (entries 1-3). In contrast, 3,5-dimethyl pyrazole template reversed the regioselectivity (entry 4). When achiral

pyrazolidinone template was examined, the reaction proceeded with high regio- and enantioselectivity and *C*-adducts were produced exclusively (entries 5-7). Compared to the other reactions with pyrazolidinone templates, it seems the size of *N*-substituents didn't impact the selectivity in this study. Among all ligands screened, ligand **1.62** showed the best performance. Reactions using $MgI_2$ and ligand **1.58**, **1.59** or **1.61** only gave poor regioselectivity and diminished enantioselectivity.[40]

Table 1.6. Evaluation of Templates in Nitrone Oxide Cycloadditions

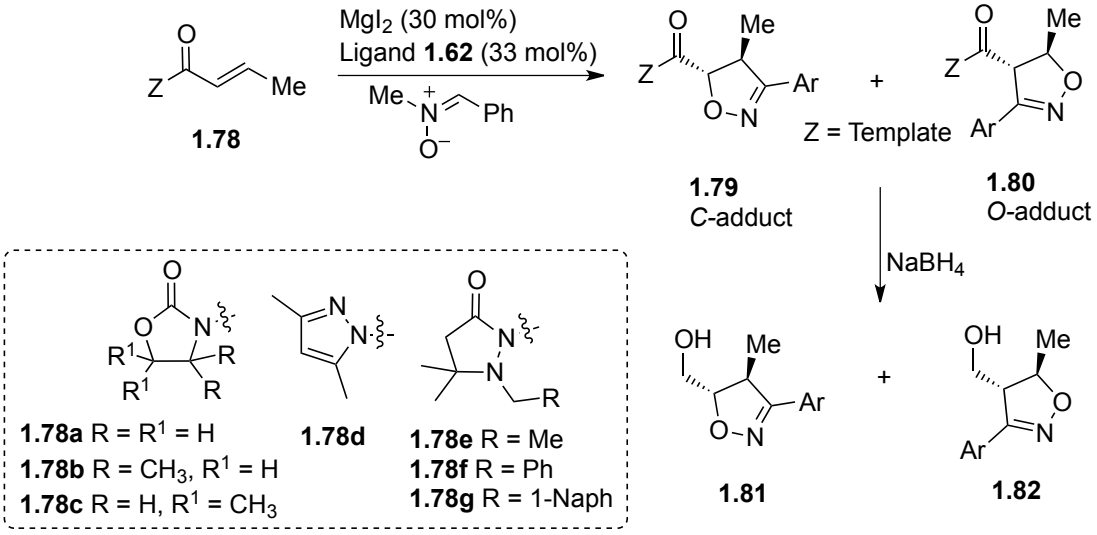


| entry | Substrate | Yield% | **1.81** /**1.82** | **1.81** ee% | **1.82** ee% |
|---|---|---|---|---|---|
| 1 | **1.78a** | 67 | 2.2:1 | 82 | 14 |
| 2 | **1.78b** | 41 | 1.6:1 | 28 | 0 |
| 3 | **1.78c** | 69 | 3:1 | 86 | 8 |
| 4 | **1.78d** | 61 | 1:5 | 37 | 3 |
| 5 | **1.78e** | 88 | 99:1 | 95 | - |
| 6 | **1.78f** | 84 | 99:1 | 99 | - |
| 7 | **1.78g** | 98 | 99:1 | 99 | - |

The generality of the reaction was investigated by changing the enoyl portion of the substrate and the nitrile oxides. These reactions led to products with good yields, high regioselectivities and enantioselectivities. A possible model was proposed as shown in Figure 1.5. The magnesium is bound to the ligand and substrate in an *s-cis* conformation. The ligand shielded the bottom face of the alkene, so the carbon end of the dipole prefers approach from the top face. Additionally, in this case, the pyrazolidinone templates again showed much higher selectivity than reaction with the oxazolidinone templates.

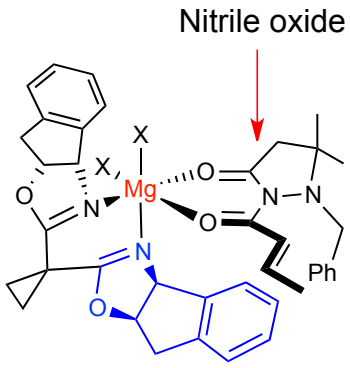


Figure 1.5. Model for Nitrile Oxide Cycloadditions

Nitrile imines as dipoles were also investigated in the 1,3-dipolar cycloaddition with achiral pyrazolidinone templates supported α-substituted or α,β-disubstituted alkenes.[41] In this case, the enantioselective synthesis of dihydropyrazole bearing a chiral quaternary center at the 5-position was developed. Using a chiral Lewis acid/template combination gave the cycloadducts in moderate to high yields (up to 97 %) and excellent enantioselectivity (up to 99 %ee).

A template screening showed substrates with 3,5-dimethylpyrazole and oxazolidinone templates didn't provide effective face shielding when catalyzed by $Mg(NTf_2)_2$ / **1.62** (Table 1.7). No enantioselectivity was observed for the 3,5-dimethylpyrazole-derived substrate (entry 1) and low enantioselectivity was obtained when oxazolidinone was used as the achiral template (entry

2). In contrast, employing the substrate bearing a pyrazolidinone template led to a significant improvement of enantioselectivity (entry 3).

Table 1.7. Template and Temperature Optimization for 1,3-Dicycloaddition of Hydrazonoyl Bromide with Methacrylate Substrates

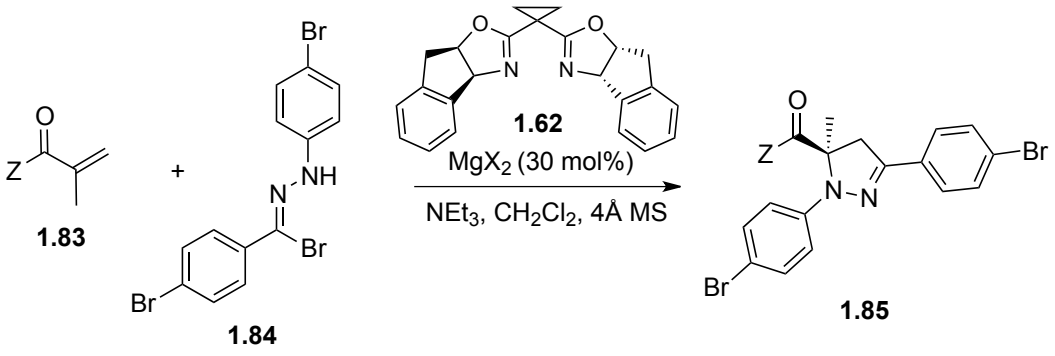


Z =

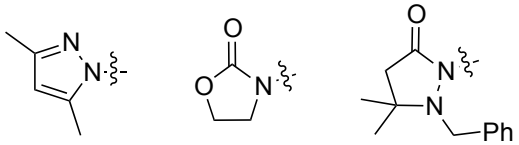

1.83a 1.83b 1.83c

| entry | Substrate | Lewis acid | Temp ($^{o}$C) | Yield% | ee% |
|---|---|---|---|---|---|
| 1 | **1.83a** | $Mg(NTf_2)_2$ | rt | 88 | 0 |
| 2 | **1.83b** | $Mg(NTf_2)_2$ | rt | 78 | 22 |
| 3 | **1.83c** | $Mg(NTf_2)_2$ | rt | 67 | 70 |
| 4 | **1.83c** | $Mg(NTf_2)_2$ | -78 | 97 | 77 |
| 5 | **1.83c** | $MgI_2$ | rt | 79 | 74 |
| 6 | **1.83c** | $MgI_2$ | -78 | 82 | 98 |

Decreasing the temperature to -78 °C, the enantioselectivity exhibited a significant increase, especially when using $MgI_2$ instead of $Mg(NTf_2)_2$ (entries 5, 6). A breadth and scope study showed that when applying α,β-disubstituted α,β-unsaturated carbonyl derived compounds as dipolarophiles, the reaction with nitrile imines also proceeded efficiently. The size of the β-substituent, catalyst loading and temperature could be adjusted to get optimal results for each

substrate. When replacing hydrazonoyl bromide with hydrazonoyl chloride, after optimizing the bases, comparable results were obtained.

The Sibi group has also developed a highly enantioselective 1,3-dipolar cycloaddition of diazoesters to β-substituted, α-substituted, and α,β-disubstituted α,β-unsaturated pyrazolidinone imides.[42] A Lewis acid screening showed that a combination of $Mg(NTf_2)_2$ and ligand **1.87** gave optimal results with respect to reactivity and enantioselectivity. Addition of 4Å Molecular sieves led to improvement in the enantiopurity of the cycloadduct. The substrate scope study for enantioselective 1,3-dipolar cycloaddition of ethyl diazoacetate was shown in Table 1.8. Substrates with β-Me, β-H and β-$CO_2{}^t$Bu proceeded in high yields and excellent enantioselectivities at -20 °C (entries 1-3). Notably, the less reactive β-aryl substituted dipolarophile can provide the adduct with good yield as well as good enantioselectivity at 40 °C (entry 4). For the α-substituted α,β-unsaturated pyrazolidinone imide, the cycloaddition with ethyl diazoacetate gave the cooresponding product in 99 %yield with 97 %ee in the presence of 30 mol% $Mg(NTf_2)_2$ (entry 5). The more challenging α,β-unsaturated pyrazolidinone imide substrates with α,β-disubstitution also showed good chemical efficiency and high selectivity when the cycloaddition was performed at elevated temperature (50 °C) with 30 mol% catalyst loading (entries 6-7). Especially, α-substituted and α,β-disubstituted substrates could produce the pyrazolines **1.88** bearing quaternary *tert*-alkyl amino stereoisomers at the 5-position of the pyrazoline.

Table 1.8. Selected Examples of Dipolar Cycloaddition with α,β-Unsaturated Pyrazolidinone Imides

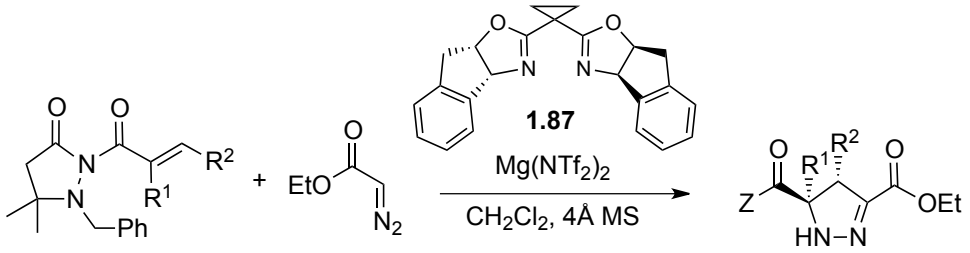


**1.86** **1.88**

| entry | Substrate | Catalyst loading (mol%) | Temp (°C) | Yield% | ee% |
|---|---|---|---|---|---|
| 1 | $R^1$ = H, $R^2$ =Me | 10 | -20 | 72 | 99 |
| 2 | $R^1$ = H, $R^2$ =H | 10 | -20 | 75 | 97 |
| 3 | $R^1$ = H, $R^2$ =$CO_2{}^t$Bu | 10 | -20 | 91 | 99 |
| 4 | $R^1$ = H, $R^2$ =Ph | 10 | 40 | 76 | 88 |
| 5 | $R^1$ = Me, $R^2$ = H | 30 | -20 | 99 | 97 |
| 6 | $R^1$ = Me, $R^2$ = Me | 30 | 50 | 52 | 98 |
| 7 | $R^1$, $R^2$ = -$(CH_2)_3$- | 30 | 50 | 62 | 99 |

A variety of azomethine ylide cycloadditions with olefins have been reported to synthesize enantioenriched pyrrolidine derivatives.[43] The strategy for cycloaddition of nitrones with α,β-unsaturated pyrazolidinone imides was also applied in the azomethine cycloadditions.[44] Similar to previous *exo*-selective nitrone cycloadditions, $Cu(OTf)_2$/bisoxazoline **1.87** also produced *exo*-adduct as major product in the azomethine imine cycloadditions and other Lewis acids like Mg(II), Zn(II), or Ni(II) salts led to *endo*-selective products. The difference in the *endo*/*exo* selectivity for chiral Lewis acids may result from the metal geometry diversity of the chiral Lewis acid complex.

Differing with the previous study of Cu(II)-catalyzed Diels-Alder and nitrone cycloaddition, the size of the fluxional N1 substituent in the pyrazolidinone auxiliary in this case didn't show a clear impact on the diastereoselectivity (Table 1.9). Compared to *N*-phenyl substituted template, smaller (Me) and larger (1-naphthyl) substituents both led to slight improvement in enantioselectivities. This result is likely because the sterically bulky ligands override any participation by the fluxional R group in face shielding of the dipolarophile.[31]

Table 1.9. Effect of Pyrazolidinone N1 Substitution in Cycloaddition with Azomethine Imines

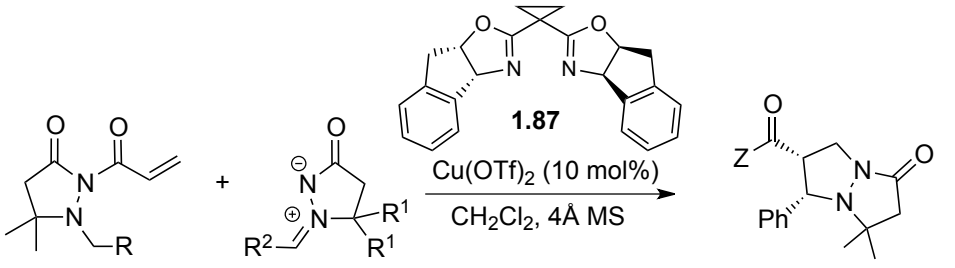


| entry | R | Temp (°C) | Yield% | *exo*/ *endo* | ee% |
|---|---|---|---|---|---|
| 1 | Ph | rt | 90 | 88:12 | 94 |
| 2 | Me | 40 | 86 | 92:8 | 98 |
| 3 | 1-Naphthyl | rt | 79 | 95:5 | 98 |

A breadth and scope study for azomethine imines indicated that electron-rich aromatic aldehydes produced the cycloadduct with high *exo* and enantioselectivities. Cycloaddition with azomethine imine derived from an aldehyde with an electron-withdrawing group led to slightly lower enantioselectivity. The substrate scope for the pyrazolidinone template was limited. Specifically, the cycloaddition of β-methyl α,β-unsaturated pyrazolidinone imide with C5-

dimethyl substituted azomethine imine didn't proceed even in the presence of 100% of Cu(II)/**1.87**. By switching to C5-unsubstituted azomethine imine, good yield, high diastereoselectivity and moderate enantioselectivity were achieved.

Suga and coworkers reported the 1,3-dipolar cycloaddition between nitrile oxides and electron-deficient olefins catalyzed by chiral binaphthyldiimine-Ni(II) (BINIM-Ni (II)) complexes (Scheme 1.18). Substituted and unsubstituted benzonitrile oxides and aliphatic nitrile oxides could be generated from the corresponding hydroximoyl chloride in the presence of MS 4Å. In contrast to the bent structure of nitrones, the challenge for nitrile oxides cycloaddition is the linear structures that might lead to a different asymmetric induction. They used achiral template derived alkenes in combination with chiral BINIM-Ni (II) complexes to induce the stereoselectivity for asymmetric cycloadditions of nitrile oxides. It was found that the regio- and enantioselectivities for the cycloadducts for reactions with different nitrile oxides with 1-benzyl-2-crotonoyl-5,5-dimethyl-3-pyrazolidinone **1.92c** were higher than using an oxazolidinone template. Especially, using 1-benzyl-2-acryloyl-5,5-dimethyl-3-pyrazolidinone **1.92d** as the dienophile in the presence of (*R*)-BINIM-4(3,5-xylyl)-2QN-Ni(II) complex (10 mol%) resulted in enantioselectivities (79-91 %ee) that exceed those of previously reported enantioselective cycloadditions of acrylic acid derivatives. A stereochemical model for the complex between the chiral Lewis acid and pyrazolidinone substrate was proposed as shown in Figure 1.6. The high enantioselectivity of the cycloaddition reactions of nitrile oxide with crotonylpyrazolidinone might be attributed to the selective *si*-face approach of the nitrile oxide to the proposed hexa-coordinated Ni (II) complex. The *re*-face is effectively shielded by the 4-(3,5-xylyl)quinoline moiety and the *N*-benzyl group on the pyrazolidinone template.[45]

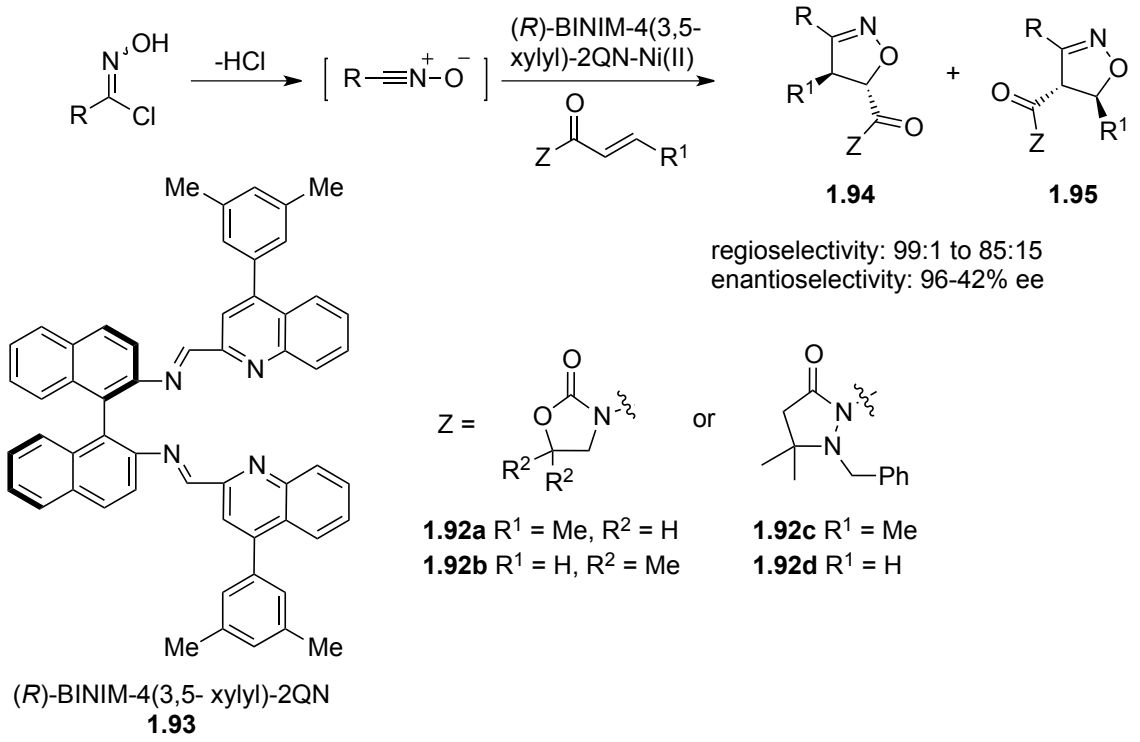


Scheme 1.18. 1,3-Dipolar Cycloaddition of Nitrile Oxides Catalyzed by Chiral Binaphthyldiimine-Ni(II) Complexes

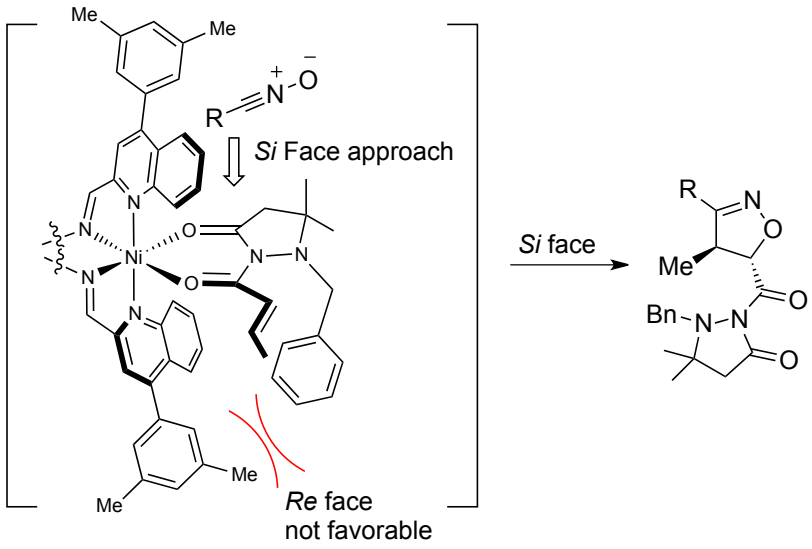


Figure 1.6. Proposed Stereochemical Model for BINIM-Ni (II) Catalyzd Asymmetric Cycloadditions of Nitrile Oxides

### 1.3.3. Achiral Templates in Enantioselective Conjugate Additions

Chiral relay templates have been successfully used in Diels-Alder reactions and dipolar cycloadditions. This strategy of using fluxional achiral templates can also be extended to the enantioselective conjugate additions. The Sibi group investigated the conjugate addition of *N*-benzylhydroxylamine to pyrazolidinone template derived crotonates.[46] The effect of N1-substituent was tested separately under two chiral Lewis acid complexes (Table 1.10).

Table 1.10. Effects of Relay Substituents on Enantioselectivity

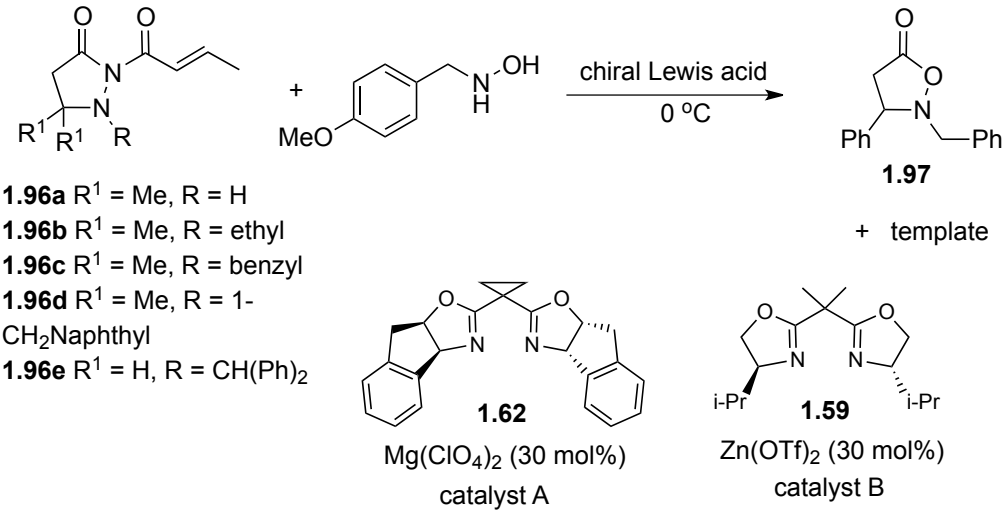


**1.96a** $R^1$ = Me, R = H
**1.96b** $R^1$ = Me, R = ethyl
**1.96c** $R^1$ = Me, R = benzyl
**1.96d** $R^1$ = Me, R = 1-$CH_2$Naphthyl
**1.96e** $R^1$ = H, R = $CH(Ph)_2$

| | | catalyst A | | catalyst B | |
|---|---|---|---|---|---|
| entry | Substrate | Yield% | ee% (*R*) | Yield% | ee% (*S*) |
| 1 | **1.96a** | 75 | 76 | 74 | 28 |
| 2 | **1.96b** | 70 | 52 | 74 | 49 |
| 3 | **1.96c** | 67 | 78 | 71 | 68 |
| 4 | **1.96d** | 77 | 81 | 75 | 75 |
| 5 | **1.96e** | 71 | 84 | 72 | 57 |

For the substrate with C5-*gem*-dimethyls, when the size of the relay group increased, there was a gradual increase in the enantioselectivity of the product using either of the two

catalysts (entries 1-5), suggesting that the pyrazolidinone templates with different size relay groups did amplify the stereochemical information. The template with a bulky diphenylmethyl substituent at the N1 but without *gem*-dimethyl group at C5 showed higher enantioselectivity under catalyst A than catalyst B (entry 6). Interestingly, the absolute stereochemistry of the product obtained using catalyst A is opposite to that obtained with catalyst B, although the ligand **1.62** and **1.59** have the same configuration at C4, so a simple change of Lewis acid can provide enantiomeric products with good selectivities. The formation of enantiomeric products using catalyst A and B suggested different geometries in chiral Lewis acid-substrate coordination.

The conjugate addition of carbon nucleophiles to enoates derived from achiral templates with fluxional substituents was investigated.[47] Different from the previous studies, a Brønsted basic site was incorporated into the fluxional substituent in some substrates (Table 1.11). The conjugate addition was performed by adding malononitrile to pyrazolidinone-derived enoate using different chiral Lewis acids. An initial screening showed that $MgBr_2 \cdot Et_2O$ and chiral ligand **1.87** can promote the conjugate addition with better selectivity than other combinations. Remarkably, the addition of molecular sieves (MS 4Å) led to significant improvement in enantioselectivity in most cases. When substrates with fluxional group either containing basic nitrogen atom or without it were examined (Table 1.11). Reaction with **1.98a** or **1.98c** showed similar trend and significant improvement for enantioselectivity was observed in the presence of MS 4Å (entries 1 and 2, entries 5 and 6). Substrate **1.98b** and **1.98d** behaved similarly in that adding MS 4Å not only improved selectivity, but also reversed the sense of asymmetric induction (entries 3 and 4, entries 7 and 8). Notably, **1.98d** containing a bigger fluxional group gave the conjugate product with higher enantioselectivity than **1.98b** with or without adding MS

4Å. These observations suggested that Brønsted base derived fluxional group was able to impact the enantioselectivity and efficient stereocontrol was obtained after adding molecular sieves.

The reaction with fluxional group without Brønsted basic sites also showed strong additive effect. Specifically, pyridine was added to mimic the substrate with Brønsted basic sites. Interestingly, reaction with **1.98e** or **1.98f** showed similar additive effects. In the absence of both MS 4Å and pyridine, both substrates gave the product in good yield and modest selectivity (entries 9 and 13). With pyridine, both selectivity decreased and reversed (entries 10 and 14). The optimal results were obtained by adding MS 4Å exclusively (entries 11 and entry 15), while slight decrease in selectivity was observed in the presence of MS both 4Å and pyridine (entries 12 and 16). The highest enantioselectivity was obtained with **1.98f** containing a bulky naphthyl fluxional unit. These results show that the efficiency of this conjugate addition is highly dependent on both the size of the fluxional group and molecular sieves as an additive. In addition, incorporating a basic unit may help to reorganize the chelation and impact the selectivities.

Table 1.11. Effect of Fluxional Groups in Conjugate Addition of Malononitrile to Pyrazolidinone-derived Enoates

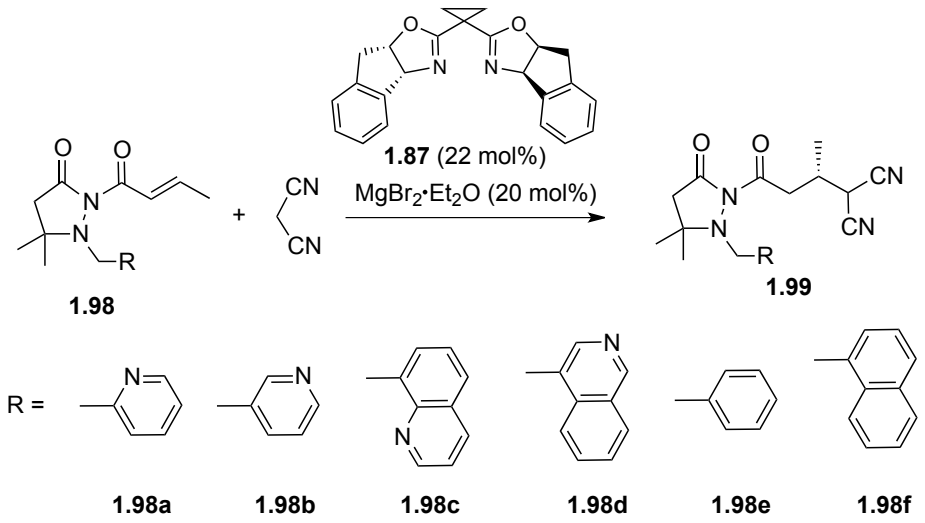


| entry | Substrate | MS 4Å | Pyridine | Yield% | ee% |
|---|---|---|---|---|---|
| 1 | **1.98a** | N | N | 88 | (+) 36 |
| 2 | **1.98a** | Y | N | 92 | (+) 78 |
| 3 | **1.98b** | N | N | 73 | (-) 27 |
| 4 | **1.98b** | Y | N | 73 | (+) 76 |
| 5 | **1.98c** | N | N | 83 | (+) 39 |
| 6 | **1.98c** | Y | N | 76 | (+) 79 |
| 7 | **1.98d** | N | N | 82 | (-) 59 |
| 8 | **1.98d** | Y | N | 87 | (+) 88 |
| 9 | **1.98e** | N | N | 69 | (+) 44 |
| 10 | **1.98e** | N | Y | 87 | (-) 2 |
| 11 | **1.98e** | Y | N | 75 | (+) 90 |
| 12 | **1.98e** | Y | Y | 84 | (+) 80 |
| 13 | **1.98f** | N | N | 22 | (+) 36 |
| 14 | **1.98f** | N | Y | 61 | (-) 15 |
| 15 | **1.98f** | Y | N | 83 | (+) 96 |
| 16 | **1.98f** | Y | Y | 85 | (+) 94 |

Lewis acids have been employed effectively to control the conformations of either the radical intermediate or the radical trap and also to enhance the reactivity of certain substrates for radical reactions.[48] The Sibi group carried out an investigation on the effectiveness of pyrazolidinone template with fluxional group to control reactivity and selectivity in chiral Lewis acid mediated conjugate radical additions (Table 1.12).[49] The reaction was conducted by adding isopropyl radical to pyrazolidinone template derived olefins using 30 mol% chiral Lewis acid derived from copper triflate and bisoxazoline ligand. Four templates containing fluxional group of varied size were evaluated. Similar to the previous observation in other enantioselective transformations using pyrazolidinone templates, the larger fluxional group in the template led to higher enantioselectivity in the radical addition process (Table 1.2, entries 1-4). Furthermore, isopropyl radical addition showed high reactivity with all four substrates. Different Lewis acids and chiral ligands were also evaluated using substrate **1.100c**. Not surprisingly, the chiral ligand **1.59** containing bulkier isopropyl substituents further improved the enantioselectivity (entry 5). Surprisingly, the metal geometry also impacted the selectivity and furnished a product with reversed absolute stereochemistry. Copper salt preferred to generate the (*S*)-isomer as the major product, while magnesium salt and some other Lewis acids (not shown) gave the (*R*)-isomer (entry 3 *vs* 6 and entry 4 *vs* 7). The reversal of stereochemical outcome might result from the chelation geometry differences around the metal. Copper Lewis acid would take on a square planar geometry, but magnesium and other Lewis acids probably take on either tetrahedral or octahedral geometries and thus lead to enantiomeric products.

Table 1.12. Chiral Lewis Acids Screening in Enantioselective Conjugate Radical Additions

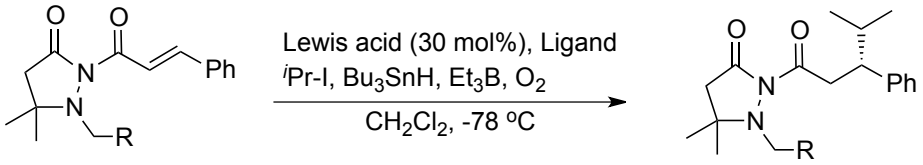


**1.100a** R = *n*-Propyl
**1.100b** R = i-Propyl
**1.100c** R = Phenyl
**1.100d** R = 1-Naphthyl

**1.101**

Ligand =

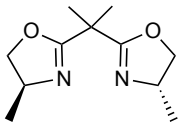

**1.58**

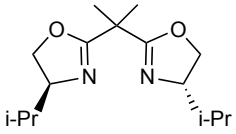


**1.59**

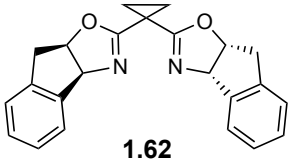

**1.62**

| entry | Substrate | Lewis acid | Ligand | Yield% | ee% |
|---|---|---|---|---|---|
| 1 | **1.100a** | $Cu(OTf)_2$ | **1.58** | 95 | 52 |
| 2 | **1.100b** | $Cu(OTf)_2$ | **1.58** | 95 | 58 |
| 3 | **1.100c** | $Cu(OTf)_2$ | **1.58** | 92 | 82 |
| 4 | **1.100d** | $Cu(OTf)_2$ | **1.58** | 91 | 90 |
| 5 | **1.100c** | $Cu(OTf)_2$ | **1.59** | 94 | 98 |
| 6 | **1.100c** | $Mg(NTf_2)_2$ | **1.58** | 87 | -42 |
| 7 | **1.100c** | $Mg(NTf_2)_2$ | **1.59** | 90 | -62 |
| 8 | **1.100c** | $Mg(NTf_2)_2$ | **1.60** | 95 | -99 |

In general, when reactions are carried out with a chiral Lewis acid that has a square planar geometry, the fluxional group in the template is more efficient in amplifying stereochemical information. Later, the tin-free enantioselective radical reactions were also studied by replacing the tributyltin hydride with the less toxic silane as a H-atom donor in the same set of reactions.[50] Unfortunately, using $(TMS)_3SiH$ or hexyl silane the reactions were less effective with respect to both chemical efficiency or selectivity compared to tributyltin hydride.

Sulfone, sulfonamide and sulfide have also been developed as an achiral template for Lewis acid catalyzed radical additions and these kinds of templates could provide two enantiotopic coordination sites in the presence of chiral Lewis acid. Selective complexation of enantiotopic groups on the sulfur serves to relay stereochemistry from the chiral Lewis acid to a reaction center. The application of sulfonamides as chiral auxiliaries has been well established by Oppolzer.[51] The two sulfonyl oxygen atoms are enantiotopic when they are substituted differentially. The prochiral sulfur becomes a new asymmetric center when chiral Lewis acid selectively coordinates one of the two enantiotopic oxygen atoms. Several examples on the use of sulfur compounds as templates in enantioselective transformations have been reported.[52]

Toru used this principle for enantioselective radical addition-trapping reactions of vinyl sulfones.[53] Substrate **1.102** gave the best result. The corresponding product **1.103** was obtained in good yield and enantioselectivity (Scheme 1.19). It was proposed that after complexation of one of the two oxygens in the sulfone, a new sulfur chiral center was generated. If the Lewis acid is chiral, it gives the diastereomeric complexes A and B. In this case the chelation with a Zinc / **1.60** complex selectively shielded the *Re* face but allowed the *Si* face open for a conjugate radical addition/ allylation sequence (Figure 1.7).

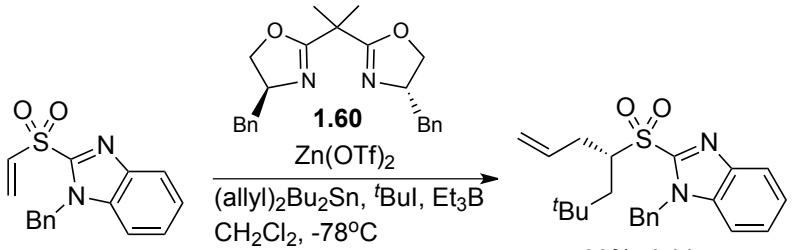


Scheme 1.19. Enantioselective Conjugate Addition/Allylation of α-Sulfonyl Radicals

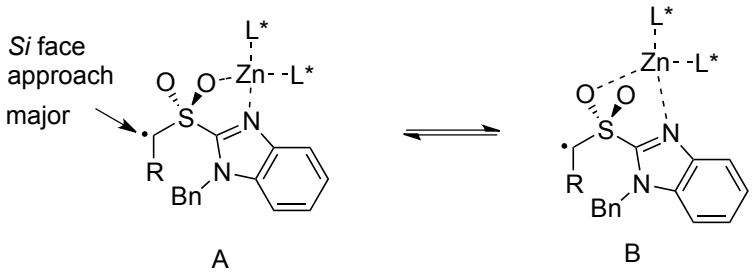


Figure 1.7. Model for Chiral Lewis Acid-Sulfone Complexes

Sibi and coworkers investigated 1,8-naphthosultam as an achiral template for nucleophilic radical addition.[54] The addition of nucleophilic radicals to sultam derived enoate using $MgBr_2$ / **1.62** followed by enantioselective H-atom transfer produced the addition product with good yields and high enantioselectivities (Table 1.13). The best results were achieved by adding methoxymethyl radical. Replacing the tetrahedral $SO_2$ group with a trigonal CO group led to a large decrease in selectivity. These results suggested that the tetrahedral nature of the sulfone allows for selective coordination with Lewis acids, thus leading to better rotamer control of the α-substituted acrylate.

Table 1.13. Enantioselective H-Atom Transfer using Sultam Templates

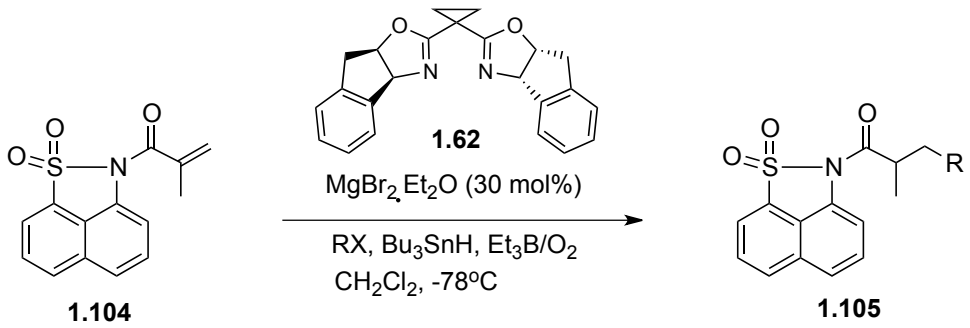


| entry | Substrate | R | Yield% | ee% |
|---|---|---|---|---|
| 1 | **1.104a** | isopropyl | 80 | 80 |
| 2 | **1.104b** | tert-butyl | 84 | 89 |
| 3 | **1.104c** | cyclohexyl | 71 | 82 |
| 4 | **1.104d** | $CH_2OMe$ | 89 | 90 |

## 1.4. Fluxional Additives in Enantioselective Catalysis

Chiral ligand optimization is usually a predominant approach to improve the selectivity in asymmetric catalysis. Optimization of additives in enantioselective transformations is also an alternative and is a relatively easier approach than chiral ligand modification.[55] The drawback within ligand modification is that a new chiral source was required in the synthesis to be used as a catalyst or a substrate, and most of time more complicated synthesis are required. In contrast, additives are much easier to be prepared. The Sibi group designed a new type of achiral additive, by incorporating fluxional blocking groups, which can dramatically amplify enantioselectivity with a variety of chiral Lewis acids[56] (Figure 1.8).

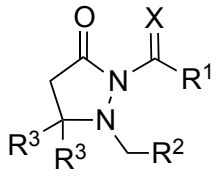


**1.106**

Figure 1.8. Fluxional Additives

Additives **1.106** were designed by connecting a pyrazolidinone unit with a Lewis basic functionality. Substituents like $R^1$, $R^2$, $R^3$ and X (heteroatom) can be modified easily. Modifying $R^1$ and X could tune the steric conformation and the Lewis basicity, while $R^2$ and $R^3$ can offer steric tunability. The hypothesis was that the chiral information from the ligand could be transferred to the fluxional additive. If the permanent chirality in the ligand and the induced chirality in the additive work in concert, this combination would lead to the stereocontrol enhancement of the catalyst system. The optimization of asymmetric reactions could be achieved through the screening of additives rather than through modifications of the chiral ligands.

The Diels-Alder reactions of *N*-acryloyl oxazolidinone **1.107** in the presence of a range of Lewis acids and bisoxazoline ligand **1.108** were examined by adding fluxional additives (Table 1.14). A large increase of enantioselectivity was observed after adding fluxional additive **1.111** compared to the reaction without additive (entries 1 and 3). The enantioselectivity remains the same after adding *N*-benzoyl oxazolidinone **1.110** as an additive suggesting that the amplifying effect observed in entry 3 originated from the fluxional group in additive **1.111**. Other Lewis acids, like Ni(II), showed similar enantioselectivity enhancement after adding **1.111**. Further studies showed molecular sieves 4Å was required to ensure the large increase in selectivity.

Table 1.14. Fluxional Additives in Diels-Alder Reactions

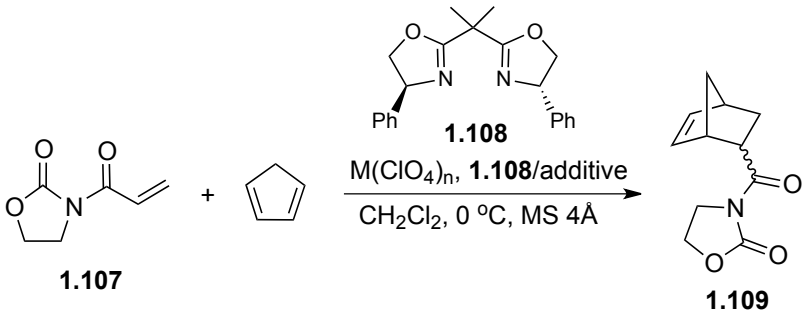


Additives

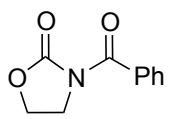

1.110

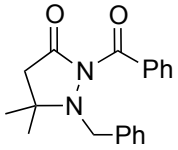

1.111

| entry | $M(ClO_4)_n$ | Additive | *endo*/*exo* | ee% |
|---|---|---|---|---|
| 1 | $Mg(ClO_4)_2$ | - | 5 | 56 |
| 2 | $Mg(ClO_4)_2$ | **1.110** | 5 | 56 |
| 3 | $Mg(ClO_4)_2$ | **1.111** | 7 | 84 |
| 4 | $Ni(ClO_4)_2$ | - | 5 | 66 |
| 5 | $Ni(ClO_4)_2$ | **1.110** | 6 | 66 |
| 6 | $Ni(ClO_4)_2$ | **1.111** | 13 | 92 |

The effects of substituent $R^1$, $R^2$ and $R^3$ in the fluxional additive on enantioselectivity were evaluated (Table 1.15). It was found that the size of fluxional group $R^2$ correlates clearly with the enantioselectivity of the Diels-Alder product. Increasing the size of $R^2$ improved the enantioselectivity (entries 1-3). Increasing the size of $R^1$ from Me to $^t$Bu to 2-naphthyl decreases the enantioselectivity of the product (entries 4-6). The effect of C5 substituents $R^3$ was also evaluated. An increase in enantioselectivity was observed by changing the C5 substituent from methyl to a larger ethyl group (entries 4 and 7), but a cyclopentyl group at C5 leads to lower enantioselectivity (entry 8).

Table 1.15. Evaluation of Additives with Fluxional Substituents in Diels-Alder Reactions

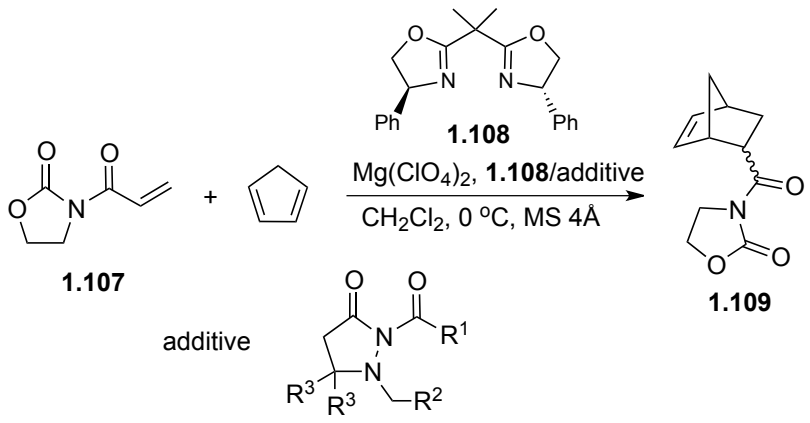


| entry | $R^1$ | $R^2$ | $R^3$ | *endo*/*exo* | ee% |
|---|---|---|---|---|---|
| 1 | Ph | Me | Me | 7 | 75 |
| 2 | Ph | Ph | Me | 7 | 84 |
| 3 | Ph | 1-Np | Me | 9 | 86 |
| 4 | Me | Ph | Me | 8 | 81 |
| 5 | *t*-Bu | Ph | Me | 7 | 78 |
| 6 | 2-Np | Ph | Me | 7 | 76 |
| 7 | Ph | Ph | Et | 4 | 87 |
| 8 | Ph | Ph | *c*-pentyl | 7 | 82 |

## 1.5. Chiral Ligands with Fluxional Groups

Rational design and synthesis of chiral ligands is always a big challenge in asymmetric catalysis. Efficient stereocontrol and high tunability in the ligand are the major consideration, which means the design should be reasonable to create an efficient chiral environment and also allow the easy modification of substituents in ligand synthesis. Previous reports from Sibi group showed fluxional blocking groups were highly effective in stereocontrol and also easy to be modified. Inspired by those achievements, Sibi group became interested in designing a new type

of modular ligands that incorporate fluxional groups, which can work with Lewis acids to control face selectivity in asymmetric transformations (Figure 1.9).

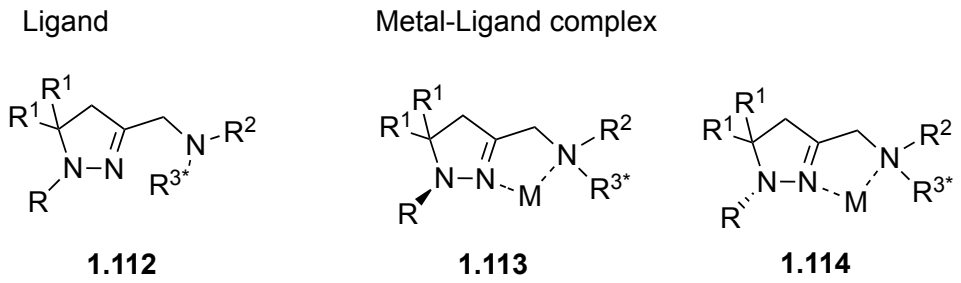


Figure 1.9. Design of Modular Chiral Ligands with Fluxional Groups

Chiral ligands with fluxional substituents were designed as shown in **1.112**. It contained a dihydropyrazole moiety with chiral group $R^3$ installed remotely to the fluxional substituent R. The hypothesis was that the permanent chirality ($R^3$) indirectly controls the orientation of the fluxional N1 substituent in a metal complex like structure **1.113** and **1.114** and the fluxional N1 substituent R provides face shielding, whereas the permanent chiral center need not necessarily do so. The shielding efficiency of the ligand in asymmetric transformations could be tuned by modifying R, $R^1$, $R^2$ and $R^3$ easily.[57]

The efficiency of chiral Lewis acids prepared from ligands **1.112** was examined in the Diels-Alder reaction between acrylate and cyclopentadiene using copper or zinc triflate as the Lewis acid (Table 1.16). For the proline ligand **1.117**, it was found the size of the substituent $R^1$ on the remote proline ring could impact the selectivity. The larger phenyl group led to higher *ee* for *endo* product using both Cu or Zn Lewis acid (entry entry 6 *vs* entry 8). In contrast, the size of the fluxional group exhibited inverse relationship with selectivity (entries 2-4). As the size increases, the selectivity of *endo* product decreases. Replacing the proline moiety with a pseudoephedrine unit **1.117e-f**, gave enhanced enantioselectivity with both $Cu(OTf)_2$ and $Zn(OTf)_2$. Surprisingly, as the size of the blocking group increases, both *endo* and *exo* adduct

were obtained with high enantioselectivities. These results demonstrated that the size of fluxional group is the prime factor in face shielding. Using ligand **1.117h** led to almost racemic products indicating that a hydroxyl group was required for obtaining high selectivity and an octahedral environment might be appropriate metal geometry. By using this strategy, the acrylate reacted with a range of dienophiles and gave the Diels-Alder products with high enantioselectivities.

Table 1.16. Chiral Ligands with Fluxional Groups in Diels-Alder Reactions

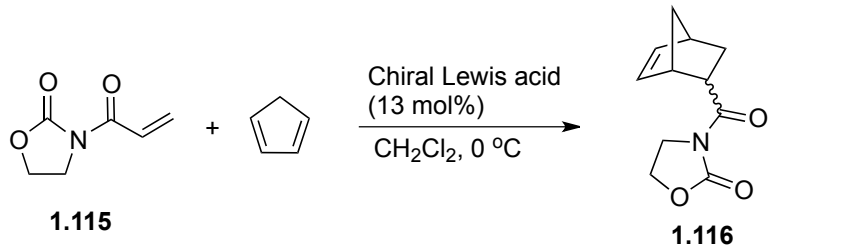


**1.115** **1.116**

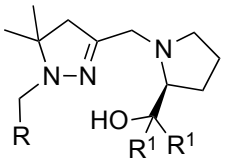

**1.117a** R = Ph, $R^1$ = $CH_3$
**1.117b** R = Me, $R^1$ = Ph
**1.117c** R = Ph, $R^1$ = Ph
**1.117d** R = 1-Naph, $R^1$ = Ph

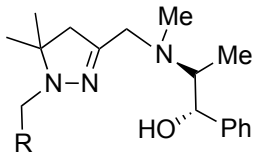

**1.117e** R = $CH_3$
**1.117f** R = Ph
**1.117g** R = 1-Naph

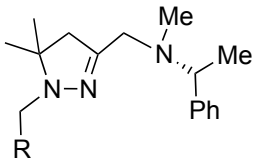

**1.117h**

| | | $Cu(OTf)_2$ | | | $Zn(OTf)_2$ | | |
|---|---|---|---|---|---|---|---|
| entry | Ligand | Yield% | *endo*/ *exo* | ee% *endo* (*exo*) | Yield% | *endo*/ *exo* | ee% *endo* (*exo*) |
| 1 | **1.117a** | 93 | 4.6 | 51 (46) | 87 | 2.8 | 23 (19) |
| 2 | **1.117b** | 87 | 5.8 | 78 (61) | 92 | 4.9 | 32 (12) |
| 3 | **1.117c** | 96 | 4.5 | 76 (71) | 90 | 4.0 | 41 (02) |
| 4 | **1.117d** | 77 | 3.7 | 62 (75) | 94 | 3.0 | 18 (14) |
| 5 | **1.117e** | 83 | 4.6 | 59 (60) | 95 | 3.9 | 54 (41) |
| 6 | **1.117f** | 90 | 3.2 | 82 (92) | 85 | 3.4 | 89 (87) |
| 7 | **1.117g** | 90 | 2.4 | 92 (97) | 83 | 3.8 | 96 (95) |
| 8 | **1.117h** | 77 | 5.2 | 08 (04) | 77 | 18.5 | 0 (0) |

Malkov and Kočovsy developed a new type of PN-ligand derived from valinol and prolinol, which were incorporated with chiral relay networks, for the asymmetric copper (I)-catalyzed conjugate addition of diethylzinc to unsaturated ketones.[58] The initial experiment showed that using the PN-ligand **1.120a** in the copper-catalyzed conjugate addition of diethylzinc to chalcone gave the product with low enantioselectivity (Table 1.17, entry 1), which was in agreement with Morimoto' s report.[59] They hypothesized that introduction of an additional alkyl group at the amide nitrogen might lead to the chiral group be away from the *N*-alkyl group and add more static element for the chelation. Thus the chiral axis at the carbonyl-pyridine bond may form and the stereochemical information would be relayed to the metal.

Applying ligand **1.120b** in the conjugate addition of diethylzinc to chalcone showed remarkable improvement in enantioselectivity with reversal selectivity (entry 2). The enantioselectivity could be further improved by tuning the 2-substituent on the pyridine moiety. Replacing 2-H of pyridine with methyl group led to the highest improvement in all cases (**1.120c**). The effect of the size of the *N*-alkyl group on enantioselectivity was investigated. An *N*-methyl group gave optimal results compared to ligand **1.120f** with an isopropyl group which showed loss of enantioselectivity (compare entry 6 with entry 2). It seems that *N*-methyl group was sufficient to induce the conformational bias, whereas isopropyl group may overcrowd the system. The conformational twist induced by *N*-methyl is also crucial for the stereocontrol, which can be further illustrated by using ligand **1.120g** containing proline ring without twist effect inside. Applying ligand **1.120g** exhibited dramatic decrease in enantioselectivity. Additionally, ligand **1.120h** lacking pyridine unit gave the product with low yield and selectivity indicating that the pyridine nitrogen was required for both reactivity and enantioselectivity of the catalyst system.

Table 1.17. Amino Acid Derived N,P-Ligands in Conjugate Addition

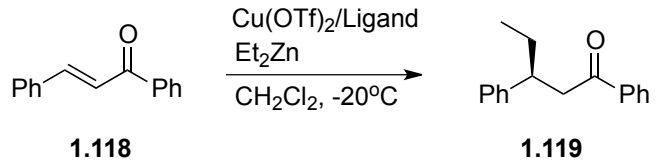


**1.118** **1.119**

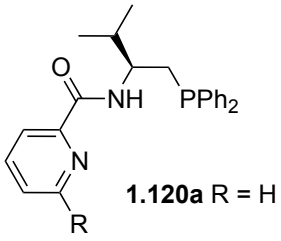


**1.120a** R = H

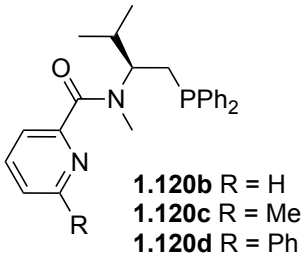


**1.120b** R = H
**1.120c** R = Me
**1.120d** R = Ph

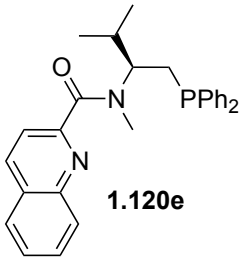


**1.120e**

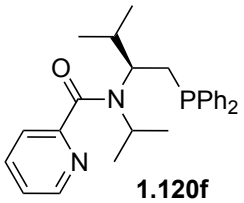


**1.120f**

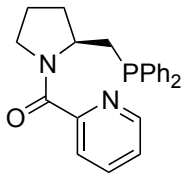


**1.120g**

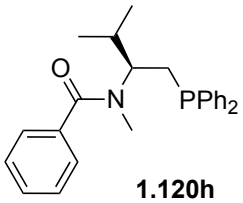


**1.120h**

| entry | Ligand | Yield% | ee% |
|---|---|---|---|
| 1 | **1.120a** | 82 | 30 |
| 2 | **1.120b** | 78 | -71 |
| 3 | **1.120c** | 86 | -81 |
| 4 | **1.120d** | 84 | -41 |
| 5 | **1.120e** | 78 | -78 |
| 6 | **1.120f** | 52 | 3 |
| 7 | **1.120g** | 90 | -29 |
| 8 | **1.120h** | 39 | 26 |

NMR and IR experiments were performed to rationalize the chelation in the reaction process. NMR results suggested that the pyridine is coordinated to the metal and phosphine part is involved in the coordination. IR showed that the amide group is free in the chelated intermediate. More results were obtained which suggested bidentate coordination and a chelation complex as shown in Figure 1.10 was proposed to account for the results.

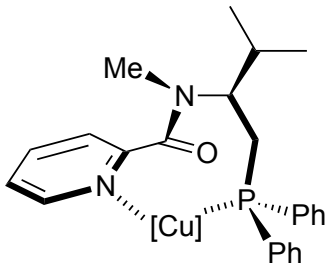


Figure 1.10. Proposed Chelation
in Cu (II)-**1.120b** Complex

The chiral relay ligand with fluxional group can also be applied in diethylzinc addition to aldehydes.[60] In this case, it was found that the size of the fluxional group on the ligand also correlates with level of enantioselectivity of the product. The results are shown in Table 1.18.

Table 1.18. Chiral Relay Ligands in Diethylzinc Addition to
Benzaldehyde

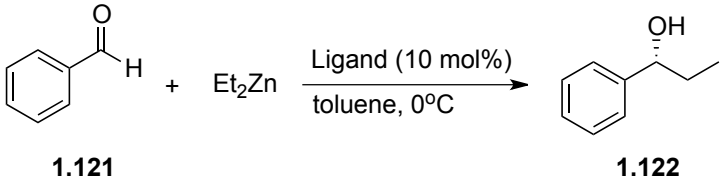


**1.121** **1.122**

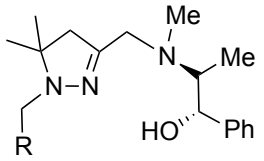


**1.123a** R = $CH_3$
**1.123b** R = Ph
**1.123c** R = Mesityl
**1.123d** R = Benzhydryl
**1.123e** R = 2-Naphthyl
**1.123f** R = 1-Naphthyl
**1.123g** R = 9-Anthracenyl

| entry | Ligand | Yield% | *ee*% |
|---|---|---|---|
| 1 | **1.123a** | 96 | 50 |
| 2 | **1.123b** | 97 | 77 |
| 3 | **1.123c** | 88 | 81 |
| 4 | **1.123d** | 98 | 76 |
| 5 | **1.123e** | 99 | 81 |
| 6 | **1.123f** | 99 | 89 |
| 7 | **1.123g** | 99 | 93 |

Reaction with ligand **1.123a** with a small R (methyl) group is less selective than **1.123b** with a benzyl group. The trend is consistent except for **1.123d** with a benzhydryl group (entry 4). A large 9-anthracenyl substituted substituted ligand **1.123g** exhibited the highest selectivity. These results demonstrated that the size of the fluxional group on the nitrogen plays an important role in determining the enantioselectivity of the product. Using the optimized reaction conditions, a range of aromatic aldehydes was studied and the addition products were obtained with good enantioselectivities and excellent yields.

Hitchcock and coworkers prepared a series of chiral oxazolidine ligands derived from *ephedra alkaloids* as ligands for the addition of diethylzinc to aldehydes.[61] Good yields and moderate selectivities were obtained for aromatic and aliphatic aldehydes. It was proposed that the stereogenic nitrogen center in the oxazolidine ring played a role of relaying the stereochemical information from the adjacent substituents on the oxazolidine ring and the coordination with the zinc reagent.

**1.6. Chiral Catalysts with Fluxional Groups**

Smith and coworkers designed a new type of *N*-heterocyclic carbenes (NHCs), derived from (1*R*, 2*R*)-cyclohexane-1, 2-diamine, for [2+2] cycloaddition of ketenes and imines.[62] In this case, the chiral relay effect in the NHC catalyst was found to dictate the stereochemical outcome of the β-lactam product.

The imidazolinium salts with different substituents as precatalysts were evaluated in the [2+2] cycloaddition to form the β-lactam product (Table 1.19). The use of precatalyst with a *N*-methyl group, **1.127a**, gave the β-lactam with good conversion but low enantioselectivity (entry 1). *N*-ethyl substituted precatalyst **1.127b** also produced the lactam with good conversion and improved enantioselectivity (entry 2). The much bulkier *N*-Bn or *N*-naphthylmethyl substituted

precatalysts exhibited optimal stereochemical control, giving the product with 51-70 %ee (entries 3-7).

Table 1.19. Asymmetric NHC Catalyzed β-Lactam Synthesis

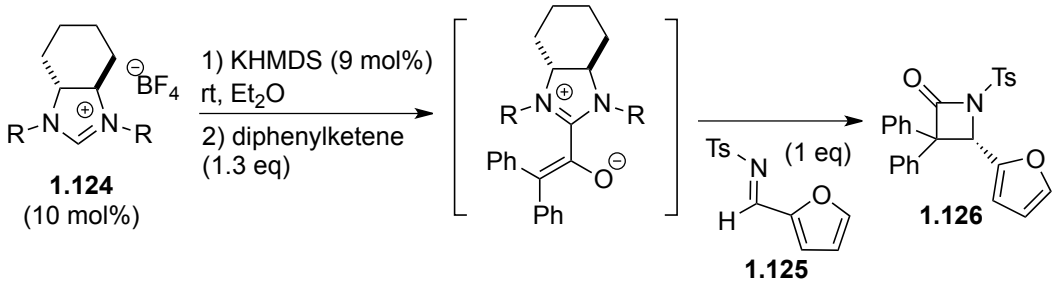


| entry | Ligand | R | Conv.% | *ee*% |
|---|---|---|---|---|
| 1 | **1.127a** | Methyl | 94 | 10 |
| 2 | **1.127b** | Ethyl | 90 | 30 |
| 3 | **1.127c** | Benzyl | quant. | 61 |
| 4 | **1.127d** | 4-Methoxybenzyl | 43 | 58 |
| 5 | **1.127e** | 4-Trifluorobenzyl | 40 | 66 |
| 6 | **1.127f** | 2-Naphthylmethyl | quant. | 51 |
| 7 | **1.127g** | 1-Naphthylmethyl | quant. | 70 |
| 8 | **1.127h** | Mesitylmethyl | 72 | 1 |
| 9 | **1.127i** | Neopentyl | 40 | 17 |
| 10 | **1.127j** | Phenyl | NA | - |
| 11 | **1.127k** | 2-Methylphenyl | NA | - |
| 12 | **1.127l** | 2-Isopropylphenyl | NA | - |

The best result was obtained by using N-1-naphthylmethyl substituted compound as precatalyst, which gave the product with quantitative conversion and 70 %ee (entry 7). The catalyst with either electron-withdrawing or electron-donating substituents led to the decreased conversion without affecting enantioselectivity (entries 4 and 5). Unfortunately, the incorporation of further steric bulky *N*-substituents gave only product with low conversions and

poor enantioselectivity (entries 8 and 9). All *N*-aryl substituted NHCs didn't give the lactam product (entries 10-12). The above results demonstrate that enantioselectivity is highly dependent on the size of the substituent on the nitrogen with larger and more fluxional groups producing the optimal enantioselectivity.

The authors proposed a mechanism and stereochemical model based on the observed enantioselectivity in this process (Scheme 1.20). This transformation proceeds through the initial addition of NHC to the ketene to give an azolium enolate, followed by the addition of the Ts-imine to generate the [2+2] product. The conformation of azolium enolate affected the steric outcome. The *trans*-fused cyclohexane framework would make the two hydrogens on the bicyclic bridge to adopt the antiperiplanar orientation, which further made the two adjacent *N*-benzyl(1-naphthylmethyl) groups to take *syn*-conformation to the neighboring hydrogens on the bridge. Ketene was activated by imidazolinium to form enolate and one enolate face was shielded by *N*-substituent, thus the addition of imine *anti* to this face and the smallest imine substituent preferred to stay in the more sterically demanding position. The above effects produced the lactam with observed stereocontrol. In the proposed model, the *N*-benzyl or *N*-1-naphthylmethyl group exhibited chiral relay effect that is important for the selectivity control.

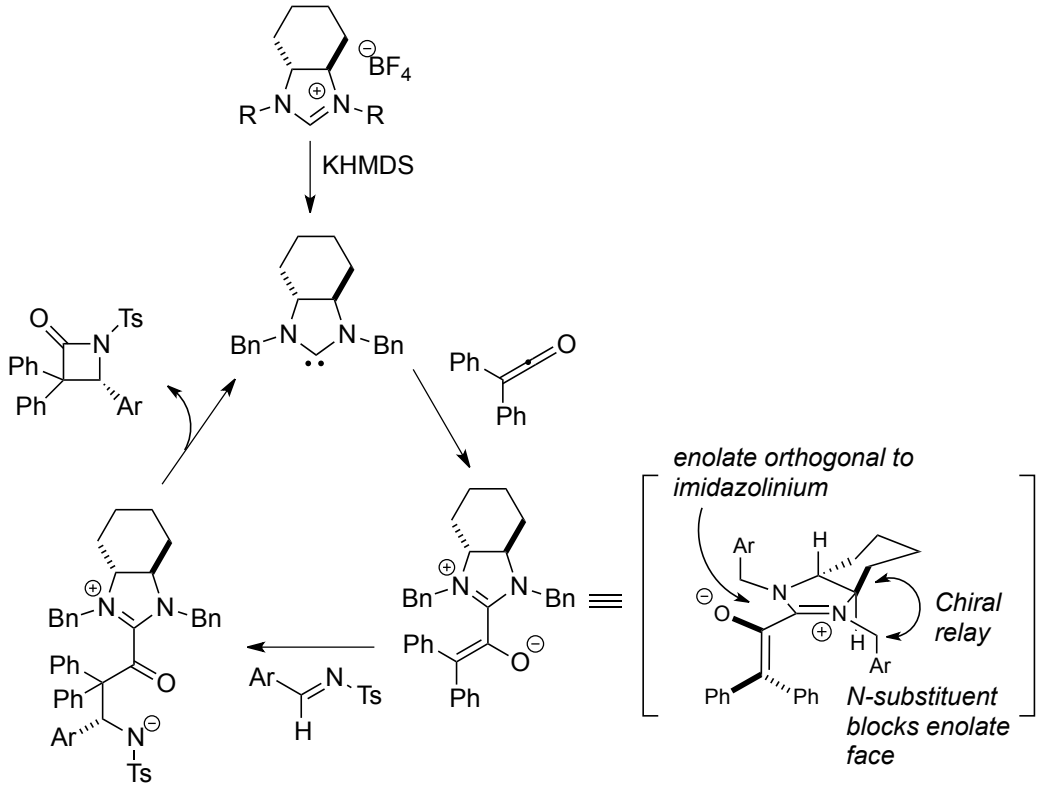


Scheme 1.20. Proposed Mechanism and Stereochemical Model

## 1.7. Conclusion

The chiral relay concept has been applied to govern the stereochemical outcome of a range of diastereo- and enantioselective reactions in a number of systems. The representative examples of this approach were introduced. If one looks back on the history of chiral relay, many breakthroughs led the chiral relay principle to promote asymmetric control better and better. From the chiral template to achiral template, from the stoichiometric amount of chiral source to catalytic amount of chiral source and from templates, additives, ligands to catalysts, chiral relay has exhibited many possibilities to fulfill the role of 'indispensible tool' for asymmetric catalysis and provide a great oppotunity for enantiocontrol.

## 1.8. Objective of Research

Enzymes, typically proteins with molecular weight ~20000 unit or higher, catalyze reactions that are important biological processes to sustain our life. Catalysts can lower the activation energy for reactions and enzymes are biological catalysts, which can speed up reactions in our body by lowering the activation energy. Almost all metabolic processes in the cell need enzymes in order to occur or accelerate to produce enantiopure compounds. Much like our right and left hands, enantiopure molecules exist as one of two possible structures that are chemically identical but arranged such that they are mirror images of each other. The existence of these molecules is determined by a concept known as chirality. Enantiopure compounds play a significant role in our life.

Nearly all biological macromolecules are homochiral. All amino acids in proteins are left-handed. While all sugars that make up the helical backbone of DNA, RNA, and in the metabolic pathways are right-handed. More dramatic and crucially important is chirality in many pharmacologically active natural products and therapeutic molecules. Enantiomers of drugs (therapeutics) that have different biological effects have been demonstrated in many instances. One enantiomer may be helpful, while the other may be inactive or even toxic. One example is thalidomide, a sedative or hypnotic drug for pregnant women. Some women who took the drug in the racemic form had babies with severe birth defects. A later study revealed that one enantiomer of thalidomide has the desired sedative activity, while the other form may cause birth defects. The enantiomers of thalidomide interacted differently with the chiral biomolecules in the body such as enzymes.

Organic chemists have for a long time been interested in the development of simple enzyme mimics with molecular weight of <500 that can function as effective catalysts.

Compared with enzymes, small organocatalysts have several important advantages. Organocatalysts offer simple handling and storage of the catalysts. More significantly, the use of organocatalysts in place of enzymes in the synthesis of pharmaceutical products can solve the disadvantages with enzymes, such as limited substrate scope, access to purified form, sensitivity to moisture and air, and limited solvent choices. Many significant accomplishments have been reported using organocatalysts.

During the past several years our group has initiated and examined in detail a novel concept called 'Chiral Relay' which utilizes fluxional chirality in achiral templates, ligands, and additives to provide a general method for the enhancement of enantioselectivity in a variety of transformations, and allows us to address some fundamental issues related to reactivity and selectivity in functionalized acyclic substrates. The chiral relay concept has been effectively used in the development of several highly enantioselective methods for the construction of heterocycles. As an extension of this strategy we became interested in developing efficient and broadly applicable and adjustable fluxional organocatalysts based on the chiral relay strategy. The organocatalyst design will contribute to superior atom efficiency, avoiding the incorporation of template in the substrate and the subsequent template cleavage in the product, and allowing the direct synthesis of structurally complex molecules. Can organocatalysts that incorporate fluxional groups provide enhanced selectivity in asymmetric transformations? To address this we designed a chiral Lewis base, 4-dialkylaminopyridine catalyst containing fluxional chirality. We surmised that a fluxional group would be effective in relaying stereochemical information from the fixed chiral center to the catalytic center in this type of catalyst thus control the stereochemistry in the product.

The super nucleophilic base, 4-dimethylaminopyridine (DMAP), was found to have general applicability for the catalysis of a wide variety of reactions. In view of the versatility of DMAP catalysis, the next step was to devise a chiral variant that would achieve asymmetric catalysis. In the search of reactive catalytic center to design an expected small chiral organocatalyst, we became interested in investigating DMAP catalysts that incorporate fluxional groups to provide steric control of reactivity and provide a platform to conduct enantioselective transformations.

In this thesis, the novelty and utility of the chiral DMAPs in kinetic resolution of secondary alcohols, biaryls with high selectivity was demonstrated. Dynamic kinetic resolution of biaryl substrates with good selectivity was investigated. Additionally, the enantioselective allylic amination of Moria-Baylis-Hillman adduct was first carried out by the use of chiral DMAP type catalyst. These methodologies provided different types of chiral products, which contain important class of skeletons for the broad applications, such as pharmaceutical industries and catalysis ligand development. Summary of several research projects accomplished on the application of novel chiral 4-dimethylaminopyridine catalyst with fluxional groups during my graduate work is presented in this thesis.

**1.9. References**


1. Papadopoulos, M. G.; Sadlej, A. J.; Leszczynski, J. Non-Linear Optical Properties of Matter: From Molecules to Condensed Phases. Springer, **2007**.
2. a) Siegel, J. S. Biochemistry: Single-Handed Cooperation. *Nature* **2001**, *409*, 777-778; b) Blackmond, D. G. The Origin of Biological Homochirality. *Cold Spring Harb. Perspect. Biol.* **2010**; 2:a002147; c) Ball, P. Giving Life a Hand. *Chem. World* **2007**, *4*, 30-31.

3. a) Mori, K. Bioactive Natural Products and Chirality. *Chirality* **2011**, *23*, 449-462; b) Thomson, R. H. The Chemistry of Natural Products. Springer, **2012**.
4. a) Ariens, E. J. Stereochemistry, A Basis for Sophisticated Nonsense in Pharmacokinetics and Clinical Pharmacology. *Eur. J. Clin. Pharmacol.* **1984**, *26*, 663-668; b) Nguyen, L. A.; He, H.; Pham-Huy, C. Chiral Drugs: An Overview. *Int. J. Biomed Sci.* **2006**, *2*, 85-100; c) Caner, H.; Groner, E.; Levy, L.; Agranat, I. Trends in the Development of Chiral Drugs. *Drug Discov. Today* **2004**, *9*, 105-110.
5. a) Botting, J. The History of Thalidomide. *Drug News Perspect.* **2002**, *15*, 604-611; b) Ridings, J. E. The Thalidomide Disaster, Lessons from the Past. *Methods Mol. Biol.* **2013**, *947*, 575-586.
6. a) Faigl, F.; Kozma, D. Enantiomer Separation: Fundamentals and Practical methods. ed. Toda, F. Kluwer Academic Press, **2004**; b) Palovics, E.; Szeleczky, Z.; Fodi, B.; Faigl, F.; Fogassy, E. Prediction of the Efficiency of Diastereoisomer Separation on the Basis of the Behavior of Enantiomeric Mixtures. *RSC Adv.* **2014**, *4*, 21254-21261.
7. a) Ward, T. J.; Ward, K. D. Chiral Separations: A Review of Current Topics and Trends." *Anal. Chem.* **2012**, *84*, 626-635; b) Lämmerhofer, M. Chiral Recognition by Enantioselective Liquid Chromatography. *J. Chromatogr. A* **2010**, *1217*, 814-856.
8. a) Jacobsen, E. N.; Pfaltz, A.; Yamamoto, H. Comprehensive Asymmetric Catalysis. Springer, **2012**; b) Trost, B. M. Asymmetric Catalysis: An Enabling Science. *Proc. Natl. Acad. Sci. U.S.A.* **2004**, *101*, 5348-5355; c) Taylor, M. S.; Jacobsen, E. N. Asymmetric Catalysis in Complex Target Synthesis. *Proc. Natl. Acad. Sci. U.S.A.* **2004**, *101*, 5368-5373; d) Weiner, B.; Szymanski, W.; Janssen, D. B.; Minnaard, A. J.; Feringa, B. L.

Recent Advances in the Catalytic Asymmetric Synthesis of β-Amino Acids. *Chem. Soc. Rev.* **2010**, *39*, 1656-1691.

9. a) Gruttadauria, M.; Giacalone, F. Catalytic Methods in Asymmetric Synthesis: Advanced Materials, Techniques, and Applications. Wiley, **2011**; b) Dalko, P. I.; Moisan, L. Enantioselective Organocatalysis. *Angew. Chem. Int. Ed.* **2001**, *40*, 3726-3748; c) Bauer, E. B. Chiral-at Metal Complexes and Their Catalytic Applications in Organic Synthesis. *Chem. Soc. Rev.* **2012**, *41*, 3153-3167; d) Special Issue: List, B. Organocatalysis. *Chem. Rev.* **2007**, *107*, 5413-5883.
10. a) Meyers, A. I.; Knaus, G.; Kamata, K.; Ford, M. E. Asymmetric Synthesis of *R* and *S*-(α)-Alkylalkanoic Acids from Metalation and Alkylation of Chiral 2-Oxazolines. *J. Am. Chem. Soc.* **1976**, *98*, 567-576; b) Gnas, Y.; Glorius, F. Chiral Auxiliaries-Principles and Recent Applications. *Synthesis* **2006**, *12*, 1899-1930.
11. a) Evans, D. A.; Helmchen, G.; Rüping, M. Chiral Auxiliaries in Asymmetric Synthesis. In M. Christmann, Asymmetric Synthesis-The Essentials. Wiley, **2007**; b) Seyden-Penne, J. Chiral Auxiliaries and Ligands in Asymmetric Synthesis. Wiley, **1995**.
12. a) Seebach, D.; Sting, A. R.; Hoffmann, M. Self-Regeneration of Stereocenters (SRS)-Applications, Limitations, and Abandonment of a Synthetic Principle. *Angew. Chem. Int. Ed.* **1996**, *35*, 2708-2748; b) Schöllkopf, U.; Groth, U.; Deng, C. Enantioselective Syntheses of (*R*)-Amino Acids Using L-Valine as Chiral Agent. *Angew. Chem. Int. Ed.* **1981**, *20*, 798-799.
13. Schöllkopf, U.; Groth, U.; Deng, C. Enantioselective Syntheses of (*R*)-Amino Acids Using L-Valine as Chiral Agent. *Angew. Chem. Int. Ed.* **1981**, *20*, 798-799.

14. Bull, S. D.; Davies, S. G.; Fox, D. J.; Garner, A. C.; Sellers, T. G. R. Chiral Relay Auxiliaries. *Pure Appl. Chem.* **1998**, *70*, 1501-1506.

15. a) Corminboeuf, O.; Quaranta, L.; Renaud, P.; Liu, M.; Jasperse, C. P.; Sibi, M. P. Chiral Relay: A Novel Strategy for the Control and Amplification of Enantioselectivity in Chiral Lewis Acid Promoted Reactions. *Chem. Eur. J.* **2003**, *9*, 28-35; b) Bull, S. D.; Davies, S. G.; Epstein, S. W.; Ouzman, J. V. A. Chiral Relay Auxiliary for the Synthesis of Enantiomerically Pure α-Amino Acids. *Chem. Commun.* **1998**, 659-660; c) Bull, S. D.; Davies, S. G.; Epstein, S. W.; Leech, M. A.; Ouzman, J. V. A. A Chiral Relay Auxiliary for the Synthesis of Homochiral a-Amino Acids. *J. Chem. Soc., Perkin Trans. 1* **1998**, 2321-2330; d) Bull, S. D.; Davies, S. G.; Fox, D. J.; Sellers, T. G. R. Chiral relay Effects influence the Facial Selectivity of *N*-Alkylated 5-Phenylmorpholin-2-One Enolates. *Tetrahedron: Asymm.* **1998**, *9*, 1483-1487; e) Clayden, J.; Vassiliou, N. Stereochemical Relays: Communication *via* Conformation. *Org. Biomol. Chem.* **2006**, *4*, 2667-2678; f) Davies, S. G.; Fletcher, A. M.; Thomson, J. E. Direct Asymmetric Syntheses of Chiral Aldehydes and Ketones via N-Acyl Chiral Auxiliary Derivatives including Chiral Weinreb Amide Equivalents. *Chem. Commun.* **2013**, *49*, 8586-8598.

16. Bull, S. D.; Davies, S. G.; Epstein, S. W.; Leech, M. A.; Ouzman, J. V. A. A Chiral Relay Auxiliary for the Synthesis of Homochiral α-Amino Acids. *J. Chem. Soc., Perkin Trans. 1* **1998**, 2321-2330.

17. Dellaria Jr., J. F.; Santarsiero, B. D. Enantioselective Synthesis of α-amino Acid Derivatives via the Stereoselective Alkylation of A Homochiral Glycine Enolate Synthon. *J. Org. Chem.* **1989**, *54*, 3916-3926.

18. Bull, S. D.; Davies, S. G.; Fox, D. J.; Sellers, T. G. R. Chiral relay Effects influence the Facial Selectivity of *N*-Alkylated 5-Phenylmorpholin-2-One Enolates. *Tetrahedron: Asymm.* **1998**, *9*, 1483-1487.

19. Craig, D.; McCague, R.; Potter, G. A.; Williams, M. R. V. 1,4-Bis(arylsulfonyl)-1,2,3,4-Tetrahydropyridines in Synthesis. Highly Regio- and Stereoselective $S_N1'$ and Alkylation Reactions. *Synlett* **1998**, 55-57.

20. Bowles, P.; Clayden, J.; Tomkinson, M. Diastereoisomeric Atropisomers from the addition of Lithiated N,N-Dialkyl-1-Naphthamides to Aldehydes. *Tetrahedron Lett.* **1995**, *36*, 9219-9222.

21. Clayden, J.; Pink, J. H.; Yasin, S. A. Conformationally Interlocked Amides: Remote Asymmetric Induction by Mechanical Transfer of Stereochemical Information. *Tetrahedron Lett.* **1998**, *39*, 105-108.

22. Casper, D. M.; Burgeson, J. R.; Esken, J. M.; Ferrence, G. M.; Hitchcock, S. R. Toward the Development of a Structurally Novel Class of Chiral Auxiliaries: Diastereoselective Aldol Reactions of a (1*R*, 2*S*)-Ephedrine-Based 3,4,5,6-Tetrahydro-2H-1,3,4-oxadiazin-2-one. *Org. Lett.* **2002**, *4*, 3739-3742.

23. Hitchcock, S. R.; Casper, D. M.; Vaughn, J. F.; Finefield, J. M.; Ferrence, G. M.; Esken, J. M. Intramolecular Chiral Relay at Stereogenic Nitrogen. Synthesis and Application of a New Chiral Auxiliary Derived from (1*R*, 2*S*)-Norephedrine and Acetone. *J. Org. Chem.* **2004**, *69*, 714-718.

24. Vasse, J. -L.; Dupas, G.; Duflos, J.; Quéguiner, G.; Bourguignon, J.; Levacher, V. Design of New Axially Chiral NADH Mimics. Mechanistic Investigation of the Enantioselective Hydride Transfer. *Tetrahedron Lett.* **2001**, *42*, 4613-4616.

25. Chernega, A. N.; Davies, S. G.; Goodwin, C. J.; Hepworth, D.; Kurosawa, W.; Roberts, P. M.; Thomson, J. E. The Chiral Auxiliary *N*-1-(1'-Naphthyl)ethyl-*O*-tert-butylhydroxylamine: A Chiral Weinreb Amide Equivalent. *Org. Lett.* **2009**, *11*, 3254-3257.

26. Davies, S. G.; Goodwin, C. J.; Hepworth, D.; Roberts, P. M.; Thomson, J. E. On the Origins of Diastereoselectivity in the Alkylation of Enolates Derived from N-1-(1'-Naphthyl)ethyl-O-tert-butylhydroxamates: Chiral Weinreb Amide Equivalents. *J. Org. Chem.* **2010**, *75*, 1214-1227.

27. For reviews and accounts covering aspects of chiral Lewis acid catalysis, see: a) Narasaka, K. Chiral Lewis Acids in Catalytic Asymmetric Reactions. *Synthesis* **1991**, 1-11; b) Jørgensen, K. A.; Johannsen, M.; Yao, S.; Audrain, H.; Thorhauge, J.; Catalytic Asymmetric Addition Reactions of Carbonyls. A Common Catalytic Approach. *Acc. Chem. Res.* **1999**, *32*, 605-613; c) Kobayashi, S.; Ogawa, C. New Entries to Water-Compatible Lewis Acids. *Chem. Eur. J.* **2006**, *12*, 5954-5960; d) Christoffers, J.; Koripelly, G.; Rosiak A.; Rössle, M. Recent Advances in Metal-Catalyzed Asymmetric Conjugate Additions. *Synthesis* **2007**, 1279-1300; e) North, M.; Usanov, D. L.; Young, C. Lewis Acid Catalyzed Asymmetric Cyanohydrin Synthesis. *Chem. Rev.* **2008**, *108*, 5146-5226; f) Rasappan, R.; Laventine, D.; Reiser, O. Metal-bis(oxazoline) Complexes: From Coordination Chemistry to Asymmetric Catalysis. *Coord. Chem. Rev.* **2008**, *252*, 702-714.

28. a) Johnson, J. S.; Evans, D. A. Chiral Bis(oxazoline) Copper(II) Complexes: Versatile Catalysts for Enantioselective Cycloaddition, Aldol, Michael, and Carbonyl Ene Reactions. *Acc. Chem. Res.* **2000**, *33*, 325-335; b) Desimoni, G.; Faita, G.; Jørgensen, K.

A. Update 1 of: $C_2$-Symmetric Chiral Bis(oxazoline) Ligands in Asymmetric Catalysis. *Chem. Rev.* **2011**, *111*, 284-437; c) Liao, S.; Sun, X. -L.; Tang, Y. Side Arm Strategy for Catalyst Design: Modifying Bisoxazolines for Remote Control of Enantioselection and Related. *Acc. Chem. Res.*, **2014**, *47*, 2260-2272.

29. a) Evans, D. A.; Bartroli, J.; Shih, T. L. Enantioselective Aldol Condensations. 2. Erythro-selective Chiral Aldol Condensations via Boron Enolates. *J. Am. Chem. Soc.* **1981**, *103*, 2127-2129; b) Evans, D. A.; Ennis, M. D.; Mathre, D. J. Asymmetric Alkylations Reactions of Chiral Imide Enolates. A Practical Approach to the Enantioselective Synthesis of α-Substituted Carboxylic Acid Derivatives. *J. Am. Chem. Soc.* **1982**, *104*, 1737-1739; c) Evans, D. A.; Chapman, K. T.; Bisaha, J. New Asymmetric Diels-Alder Cycloaddition Reactions. Chiral α, β-Unsaturated Carboximides as Practical Chiral Acrylate and Crotonate Dienophile Synthons. *J. Am. Chem. Soc.* **1984**, *106*, 4261-4263; d) Evans, D. A.; Chapman, K. T.; Hung, D. T.; Kawaguchi, A. T. Transition State π-Solvation by aromatic Rings: An Electronic Contribution to Diels-Alder Reaction Diastereoselectivity. *Anew. Chem. Int. Ed.* **1987**, *26*, 1184-1186; e) Hargaden, G. C.; Guiry, P. J. Recent Applications of Oxazoline-Containing Ligands in Asymmetric Catalysis. *Chem. Rev.* **2009**, *109*, 2505-2550.
30. Sibi, M. P.; Venkatraman, L.; Liu, M.; Jasperse, C. P. A New Approach to Enantiocontrol and Enantioselectivity Amplification: Chiral Relay in Diels-Alder Reactions. *J. Am. Chem. Soc.* **2001**, *123*, 8444-8445.
31. Sibi, M. P.; Stanley, L. M.; Nie, X.; Venkatraman, L.; Liu, M.; Jasperse, C. P. The Role of Achiral Pyrazolidinone Templates in Enantioselective Diels-Alder Reactions: Scope, Limitations, and Conformational Insights. *J. Am. Chem. Soc.* **2007**, *129*, 395-405.

32. Sibi, M. P.; Nie, X.; Shackleford, J. P.; Stanley, L. M.; Bouret, F. Exo- and Enantioselective Diels-Alder Reactions: Pyrazolidinone Auxiliaries as a Means to Enanhanced *exo* Selectivity. *Synlett* **2008**, *17*, 2655-2658.

33. Evans, D. A.; Miller, S. J.; Lectka, T.; von Matt, P. Chiral Bis(oxazoline)copper (II) Complexes as Lewis Acid Catalysts for the Enantioselective Diels-Alder Reaction. *J. Am. Chem. Soc.* **1999**, *121*, 7559-7573.

34. a) Ishihara, K.; Fushimi, M. Catalytic Enantioselective [2+4] and [2+2] Cycloaddition Reactions with Propiolamides. *J. Am. Chem. Soc.* **2008**, *130*, 7532; b) Ishihara, K.; Kondo, S.; Kurihara, H.; Yamamoto, H.; Ohashi, S.; Inagaki, S. *J. Org. Chem.* **1997**, *62*, 3026-3027; c) Payette, J. N.; Yamamoto, H. Cationic-Oxazaborolidine-Catalyzed Enantioselective Diels-Alder Reaction of α, β-Unsaturated Acetylenic Ketones. *Angew. Chem. Int. Ed.* **2009**, *48*, 8060-8062; d) Corey, E. J.; Lee, T. W. Enantioselective Diels-Alder Reactions Between Cyclopentadiene and α,β-acetylenic Aldehydes Catalyzed by A Chiral Super Lewis Acid. *Tetrahedron Lett.* **1997**, *38*, 5755; e) Maruoka, K.; Concepcion, A. B.; Yamamoto, H. Asymmetric Diels-Alder Reaction of Cyclopentadiene and Methyl Acrylate Catalyzed by Chiral Organoaluminum Reagents. *Bull. Chem. Soc. Jpn.* **1992**, *65*, 3501.

35. Sibi, M. P.; Cruz Jr. W.; Stanley, L. M. Enantioselective Diels-Alder Cycloadditions with β-Substituted Pyrazolidinone Propiolimides. *Synlett* **2010**, *6*, 889-892.

36. Quaranta, L.; Corminboeuf, O.; Renaud, P. Chiral Relay Effect: 4-Substituted 1,3-Benzoxazol-2-(3H)-ones as Achiral Templates for Enantioselective Diels-Alder Reactions. *Org. Lett.* **2002**, *4*, 39-42.

37. a) Gothelf, K. V.; Jørgensen, K. A. Asymmetric 1,3-Dipolar Cycloaddition Reactions. *Chem. Rev.* **1998**, *98*, 863-909; b) Hashimoto, T.; Maruoka, K. Recent Advances of Catalytic Asymmetric 1,3-Dipolar Cycloaddition. *Chem. Rev.* **2015**, *115*, 5366-5412; c) Stanley, L. M.; Sibi, M. P. Enantioselective Copper-Catalyzed 1,3-Dipolar Cycloadditions. *Chem. Rev.* **2008**, *108*, 2887-2902; d) Bădoiu, A.; Brinkmann, Y.; Viton, F.; Kündig, E. P. Asymmetric Lewis Acid Catalyzed 1,3-Dipolar cycloadditions. *Pure Appl. Chem.* **2008**, *80*, 1013-1018; e) Kano, T.; Hashimoto, T.; Maruoka, K. Asymmetric 1,3-Dipolar Cycloaddition Reaction of Nitrones and Acrolein with A Bis-Titanium Catalyst as Chiral Lewis Acid. *J. Am. Chem. Soc.* **2005**, *70*, 11926-11927; f) Viton, F.; Bernardinelli, G.; Kündig, E. P. Iron and Ruthenium Lewis Acid Catalyzed Asymmetric 1,3-Dipolar Cycloaddition Reactions Between Nitrones and Enals. *J. Am. Chem. Soc.* **2002**, *124*, 4968-4969.

38. Sibi, M. P.; Ma, Z.; Jasperse, C. P. Exo Selective Enantioselective Nitrone Cycloadditions. *J. Am. Chem. Soc.* **2004**, *126*, 718-719.

39. Kozikowski, A. P. The Isoxazoline Route to the Molecules of Nature. *Acc. Chem. Res.* **1984**, *17*, 410.

40. Sibi, M. P.; Itoh, K.; Jasperse, C. P. Chiral Lewis Acid Catalysis in Nitrile Oxide Cycloadditions. *J. Am. Chem. Soc.* **2004**, *126*, 5366-5367.

41. Sibi, M. P.; Stanley, L. M.; Soeta, T. Enantioselective 1,3-Dipolar Cycloaddition of Nitrile Imines to α-Substituted and α, β-Disubstituted α, β-Unsaturated Carbonyl Substrates: A Method for Synthesizing Dihydropyrazoles Bearing a Chiral Quaternary Center. *Adv. Synth. Catal.* **2006**, *348*, 2371-2375.

42. Sibi, M. P.; Stanley, L. M.; Soeta, T. Enantioselective 1,3-Dipolar Cycloadditions of Diazoacetate Electron-Deficient Olefins. *Org. Lett.* **2007**, *9*, 1553-1556.

43. a) Allway, P.; Grigg, R. Chiral Cobalt (II) and Manganese (II) Catalysts for the 1,3-Dipolar Cycloaddition Reactions of Azomethine Ylides Derived from Arylidene Imines of Glycine. *Tetrahedron Lett.* **1991**, *32*, 5817-5820; b) Hashimoto, T.; Maruoka, K. Recent Advances of Catalytic Asymmetric 1,3-Dipolar Cycloaddition. *Chem. Rev.* **2015**, *115*, 5366-5412.

44. Sibi, M. P.; Rane, D.; Stanley, L. M.; Soeta, T. Copper (II)-Catalyzed Exo and Enantioselective Cycloadditions of Azomethine Imines. *Org. Lett.* **2008**, *10*, 2971-2974.

45. Suga, H.; Adachi, Y.; Fujimoto, K.; Furihata, Y.; Tsuchida, T.; Kakehi, A.; Baba, T. Asymmetric 1,3-Dipolar Cycloaddition Reactions of Nitrile Oxides Catalyzed by Chiral Binaphthyldiimine-Ni(II) Complexes. *J. Org. Chem.* **2009**, *74*, 1099-1113.

46. Sibi, M. P.; Liu, M. Enantioselective Conjugate Addition of Hydroxylamines to Pyrazolidinone Acrylamides. *Org. Lett.* **2001**, *3*, 4181-4184.

47. Adachi, S.; Takeda, N.; Sibi, M. P. Evaluation of Achiral Templates with Fluxional Bronsted Basic Substituents in Enantioselective Conjugate Additions. *Org. Lett.* **2014**, *16*, 6440-6443.

48. a) Renaud, P.; Gerster, M. Use of Lewis Acids in Free Radical Reactions. *Angew. Chem. Int. Ed.* **1998**, *37*, 2562-2579; b) Sibi, M. P.; Ji, J.; Wu, J. H.; Gürtler, S.; Porter, N. A. Chiral Lewis Acid Catalysis in Radical Reactions: Enantioselective Conjugate Radical Additions. *J. Am. Chem. Soc.* **1996**, *118*, 9200-9201; c) Sibi, M. P.; Ji, J. Practical and Efficient Enantioselective Conjugate Radical Additions. *J. Org. Chem.* **1997**, *62*, 3800-

3801; d) Miyabe, H.; Takemoto, Y. Enantioselective Radical Cyclizations: A New Approach to Stereocontrol of Cascade Reactions. *Chem. Eur. J.* **2007**, *13*, 7280-7286.

49. Sibi, M. P.; Prabagaran, N. Chiral Relay in Enantioselective Conjugate Radical Additions Using Pyrazolidinone Templates. How Does Metal Geometry Impact Selectivity? *Synlett* **2004**, *13*, 2421-2424.
50. Sibi, M. P.; Yang, Y. -H.; Lee, S. Tin-Free Enantioselective Radical Reactions Using Silanes. *Org. Lett.* **2008**, *10*, 5349-5352.
51. Oppolzer, W. Camphor as A Natural Source of Chirality in Asymmetric Synthesis. *Pure Appl. Chem.* **1990**, *62*, 1241-1250.
52. a) Pellissier, H. Chiral Sulfur-Containing Ligands for Asymmetric Catalysis. *Tetrahedron* **2007**, *63*, 1297-1330; b) Hiroi, K.; Sone, T. Chiral Sulfur Ligands for Catalytic Asymmetric Synthesis. *Curr. Org. Syn.* **2008**, *5*, 305-320.
53. Watanabe, Y.; Mase, N.; Furue, R.; Toru, T. Enantioselective Allylation of the a-Sulfonyl Radical Controlled by Coordination of A Chiral Lewis Acid to An Enantiotopic Sulfonyl Oxygen. *Tetrahedron Lett.* **2001**, *42*, 2981-2984.
54. Sibi, M. P.; Sausker, J. B. The Role of the Achiral Template in Enantioselective Transformations. Radical Conjugate Additions to α-Methacrylates Followed by Hydrogen Atom Transfer. *J. Am. Chem. Soc.* **2002**, *124*, 984-991.
55. a) Vogl, E. M.; Groger, H.; Shibasaki, M. Towards Perfect Asymmetric Catalysis: additives and Cocatalysts. *Angew. Chem. Int. Ed.* **1999**, *38*, 1570-1577; b) Walsh, P. J.; Lurain, A. E.; Balsells, J. Use of Achiral and meso Ligands to convey Asymmetry in Enantioselective Catalysis. *Chem. Rev.* **2003**, *103*, 3297-3344; c) Itoh, K.; Kanemasa, S. Enantioselective Michael Addition of Nitrogen by A Catalytic Double Activation using

Chiral Lewis Acid and Achiral Amine Catalysts. *J. Am. Chem. Soc.* **2002**, *124*, 13394-13395.

56. Sibi, M. P.; Manyem, S.; Palencia, H. Fluxional Additives: A Second Generation Control in Enantioselective Catalysis. *J. Am. Chem. Soc.* **2006**, *128*, 13660-13661.
57. Sibi, M. P.; Zhang, R.; Manyem, S. A New Class of Modular Chiral Ligands with Fluxional Groups. *J. Am. Chem. Soc.* **2003**, *125*, 9306-9307.
58. Malkov, A. V.; Hand, J. B.; Kočovsky, P. A Long-Range Chiral Relay via Tertiary Amide Group in Asymmetric Catalysis: New Amino Acid-derived N, P-Ligands for Copper-Catalysed Conjugates Addition. *Chem. Commun.* **2003**, 1948-1949.
59. Morimoto, T.; Yamaguchi, Y.; Suzuki, M.; Saitoh, A. Enantioselective Copper-Catalyzed Conjugate Addition of Diethylzinc to Enones Using New Chiral P, N ligands Composed of (*S*)-2-alkyl-2-Aminoethylphosphines and α-Substututed Pyridine. *Tetrahedron Lett.* **2000**, *41*, 10025-10029.
60. Sibi, M. P.; Stanley, L. M. Enantioselective Diethylzinc Additions to Aldehydes Catalyzed by Chiral Relay Ligands. *Tetrahedron: Asymm.* **2004**, *15*, 3353-3356.
61. Parrott II, R. W.; Hitchcock, S. R. Intramolecular chiral Relay at Stereogenic Nitrogen: Oxazolidine Catalysts Derived From Ephedra Alkaloids. *Tetrahedron: Asymm.* **2007**, *18*, 377-382.
62. Duguet, N.; Donaldson, A.; Leckie, S. M.; Douglas, J.; Shapland, P.; Brown, T. B.; Churchill, G.; Slawin, A. M. Z.; Smith, A. D. Chiral Relay in NHC-Mediated Asymmetric β-Lactam Synthesis I; Substituent Effects in NHCs Derived from (1*R*, 2*R*)-Cyclohexane-1,2-Diamine. *Tetrahedron: Asymm.* **2010**, *21*, 582-600.

# CHAPTER 2. FLUXIONALLY CHIRAL 4-DIMETHYL AMINO PYRIDINE CATALYST DESIGN AND SYNTHESIS

## 2.1. Introduction

The broad utility of synthetic chiral compounds as single-enantiomer drug molecules, as components in macromolecules with novel properties and as probes of biological function, has made asymmetric catalysis an attractive area of investigation.[1] Modern asymmetric catalysis is built on three areas: biocatalysis, metal catalysis, and organocatalysis.

Asymmetric organocatalysis uses small chiral organic molecules predominantly composed of C, H, O, N, S and P, to accelerate organic transformations. An inorganic element is not part of the active principle.[2] The level of efficiency and selectivity of many organocatalytic reactions meet the standards of established organic reactions.[3] Compared to conventional organometallic and biocatalysis, organocatalysis has several important advantages.[4] Organocatalysis offers simple handling and storage of the catalysts. Of particular importance is that most reactions are insensitive to moisture and air, and are often easy to perform. The absence of metal in organocatalysis makes this type of reaction an attractive tool for the synthesis of agrochemical and pharmaceutical compounds, in which the presence of hazardous metallic traces do not contaminate the final product. They have more wide substrate scope than biocatalysis and can produce both enantiomers since both enantioseries of catalyst are available. Typical transition metal mediated coupling reactions, such as Suzuki,[5] Sonogashira,[6] Ullmann,[7] and Heck-type coupling reactions,[8] as well as the Tsuji-Trost reaction,[9] can now be performed under metal-free conditions. Organocatalysis has several advantages not only because of its synthetic advantages but also for economic reasons. The ready availability, low cost, and easy incorporation onto a solid support, makes organocatalyst attractive from synthetic standpoint.

Recent years have seen impressive developments in organocatalysis. The growth has been reflected in the development of very large number of new organocatalytic systems.[10] The application included exploration of new reaction types, organocatalysts supported on solid surfaces and in unusual reaction media, applications in polymerizations and total synthesis of natural products and drug-discovery, and many more (Figure 2.1). Many researchers from academia and the chemical industry are involved in this field, with most of the efforts focused on the development of new reaction and asymmetric methodology to produce environmentally friendly access to enantiomerically enriched compounds.

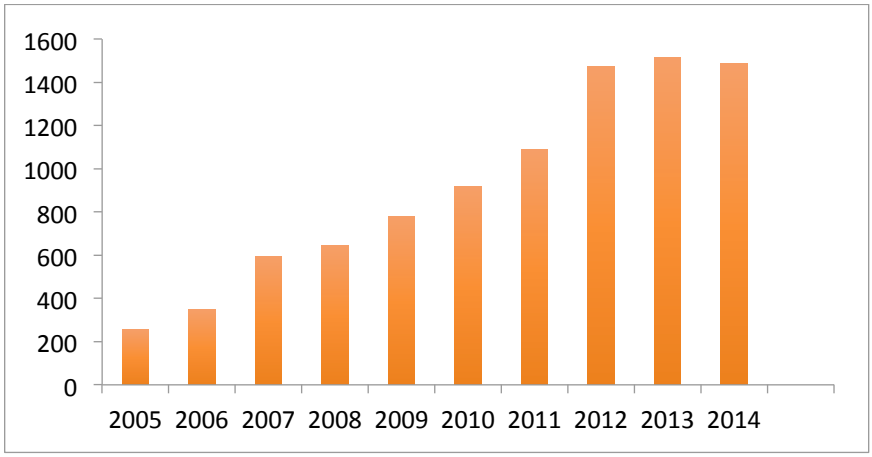


Figure 2.1. Number of References using the Concept "organocatalysis" Since the Year 2005 from SciFinder

Organocatalysts have two main functions. They can activate the electrophile or the nucleophile or both, or/and they create an asymmetric environment that is responsible for setting the chirality of the product. There are commonly four types of organocatalysts, Lewis bases, Lewis acids, Brønsted bases and Brønsted acids (Figure 2.2).

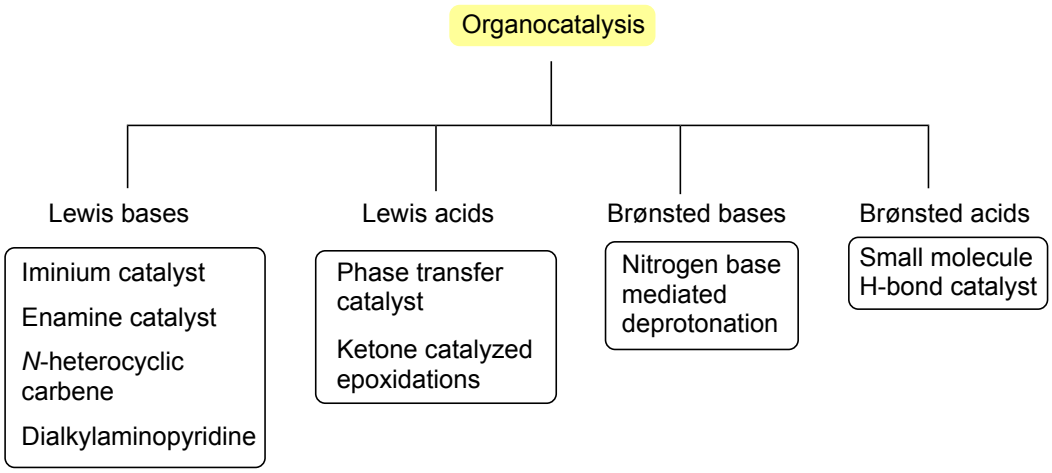


Figure 2.2. Classification of Organocatalysis

Lewis bases initiate the catalytic cycle via nucleophilic addition to the substrate and the mode of activation[11] can be through an enamine, iminium ion, acyl ammonium ions, carbene catalysis, *etc*. Whereas Lewis acids catalysis activates nucleophilic substrates, the famous cases are phase transfer catalysts and epoxidation catalysts.[12] In contrast, Brønsted base and acid catalytic cycles are initiated via a (partial) deprotonation or protonation, respectively.[13] Urea and thiourea catalysts are most common Brønsted acid catalysts and they can activate imines through hydrogen bonding.[14] Typical Brønsted bases include guanidine, amidine and cinchona alkaloid, *etc.*, which contain nitrogen as the basic site for deprotonation. It should be noted that the catalytic role of those catalysts may not always act through a single activation mode.[15] There are also some miscellaneous organocatalyst, such as small peptide catalyst.[16]

The need from chemical industry, especially the pharmaceutical sector, for reliable asymmetric transformations of molecular skeletons is high. Thus the diversity and power of asymmetric organocatalysis has attracted many research groups' attention and has become an important field of research.

Our group has designed useful templates, ligands, and additives that use fluxional groups to control and/or enhance stereoselectivity in a variety of asymmetric transformations.[17] A key feature of this strategy is that the size of the fluxional substituent can be varied readily. As an extension of this strategy we became interested in developing efficient and broadly applicable and adjustable fluxional organocatalysts based on the chiral relay strategy. The organocatalyst design will contribute to superior atom efficiency, avoiding the incorporation of template in the substrate and the subsequent template cleavage in the product, and allowing the direct synthesis of structurally complex molecules. Can organocatalysts that incorporate fluxional groups provide enhanced selectivity in asymmetric transformations? To address this we designed a chiral Lewis base, 4-dialkylaminopyridine catalysts containing fluxional chirality. We surmised that a fluxional group would be effective in relaying stereochemical information from the fixed chiral center to the catalytic center of DMAP.

4-Dialkylaminopyridine is a derivative of pyridine. It is of great interest because in one case, 4-dimethylaminopyridine (DMAP) was found to be able to provide a $10^4$-fold rate enhancement than pyridine in the benzoylation of 3-chloroaniline,[18] owing to the resonance stabilization of the dimethyl amino group. Because of its high basicity, 4-dialkylaminopyridine is a useful nucleophilic catalyst for catalysis of a wide variety of reactions,[19] such as esterifications with anhydrides, the Morita-Baylis-Hillman reaction, hydrosilylations, tritylation, the Steglich rearrangement, Staudinger synthesis of β-lactams and many more. There are thousands of examples on the use of DMAP in far ranging fields of chemistry in both patents and research literature. Several pharmaceutical and agricultural products that rely on DMAP's superior catalytic properties in their synthetic sequences have been produced for years. There are a large

number of functional groups and class of compounds that are involved in reactions with DMAP.[20]

In view of the versatility of DMAP as a Lewis base in different types of reactions, researchers started to think about designing the chiral variant of DMAP that would catalyze enantioselective transformations. Vedejs reported the first example in 1996 and they are using stoichiometric amount of chiral 2-substituted DMAP for the kinetic resolution of racemic secondary alcohols.[21] After this initial work, a lot of new chiral DMAP catalysts were developed and have been applied to a range of reactions with substoichiometric amount to control stereochemical outcome,[22] such as kinetic resolutions, asymmetric cycloadditions, asymmetric protonation of ketenes, C-acylations, *etc*, (Figure 2.3).

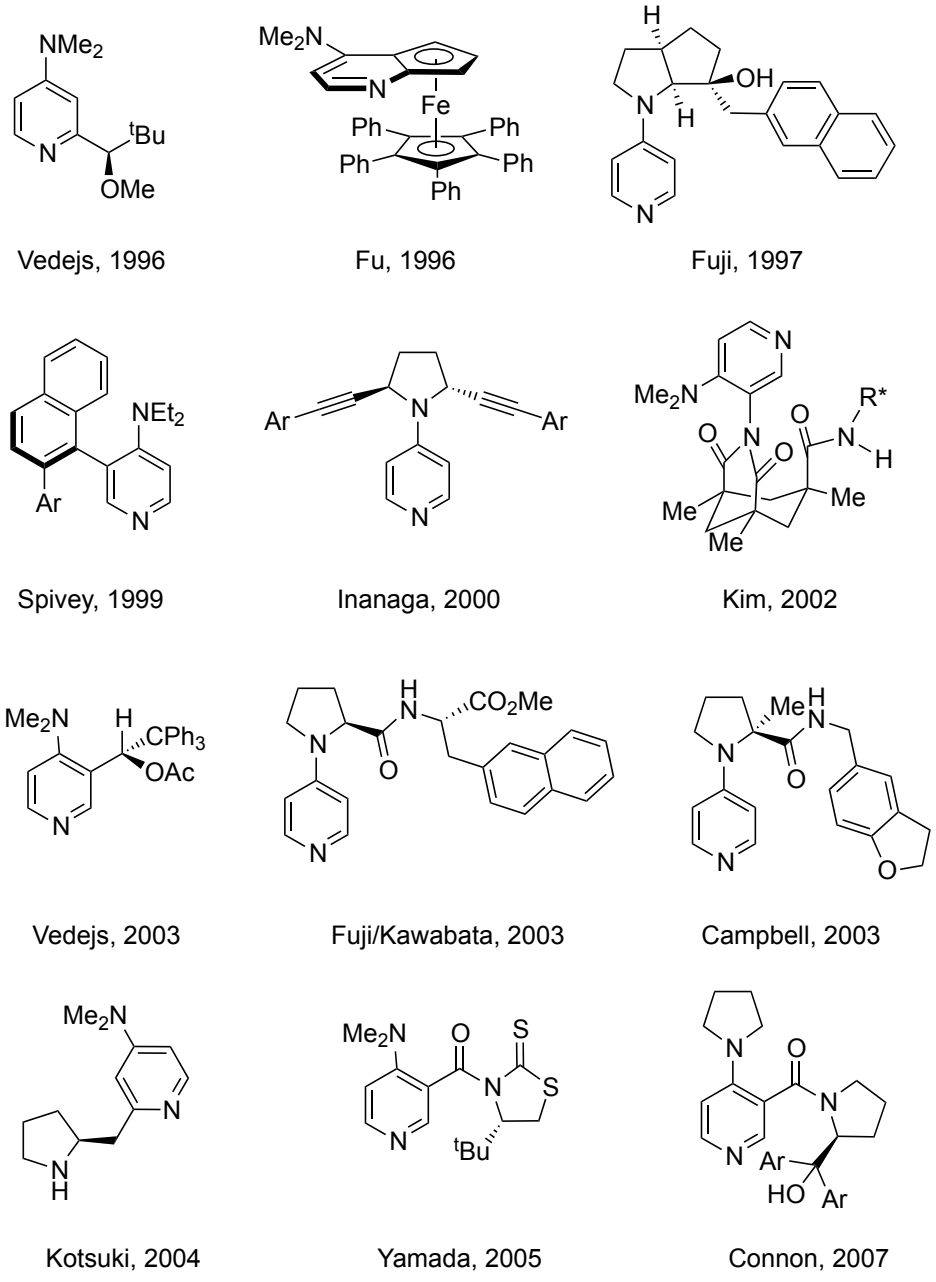


Figure 2.3. Chiral DMAP Catalysts

The general idea for designing chiral DMAP is incorporating an appropriate substituent in the 2-position. But the original study showed the presence of even a small group adjacent to the nitrogen would have a negative effect on the nucleophilicity of DMAP, probably because of the steric hindrance.[22] The reactivity of 2-substituted pyridine is one twentieth of pyridine in

benzoylation of simple alcohols (Scheme 2.1). This principle should be under consideration in the design of a new chiral DMAP catalyst.

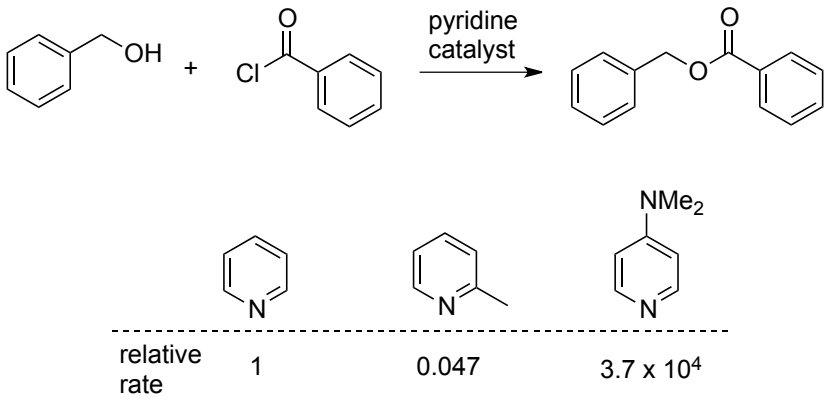


Scheme 2.1. Reactivity Comparisons of Pyridine Derivatives

**2.2. Catalyst Design Scenario**

Inspired by the previous success of achiral pyrazolidinone skeleton in templates, additives and ligands design, we envisioned that an organocatalyst that incorporates chiral pyrazolidinone with fluxional groups might be able to provide enhanced selectivity in asymmetric transformations. A paper published in 2009 provided us an idea of how to incorporate a fluxional group into a chiral unit.[23] In this case, the chiral pyrazolidinones were resolved with high selectivity through a process that utilizes a relay of stereochemical information from a permanent chiral center to a fluxional chiral center to enhance the inherent selectivity of the chiral Lewis acid and allowed the synthesis of C5-substituted pyrazolidinones with good to excellent enantioselectivity (Scheme 2.2). After separation of the enantiomerically enriched starting material and the Diels-Alder cycloadduct, the **2.5** and **2.6** are liberated by reaction of **2.3** and **2.4** with the lithium alkoxide of *p*-methoxybenzyl alcohol, respectively. The

final chiral pyrazolidinones were isolated in moderate to good yields with minimal erosion of the enantiomeric excess.

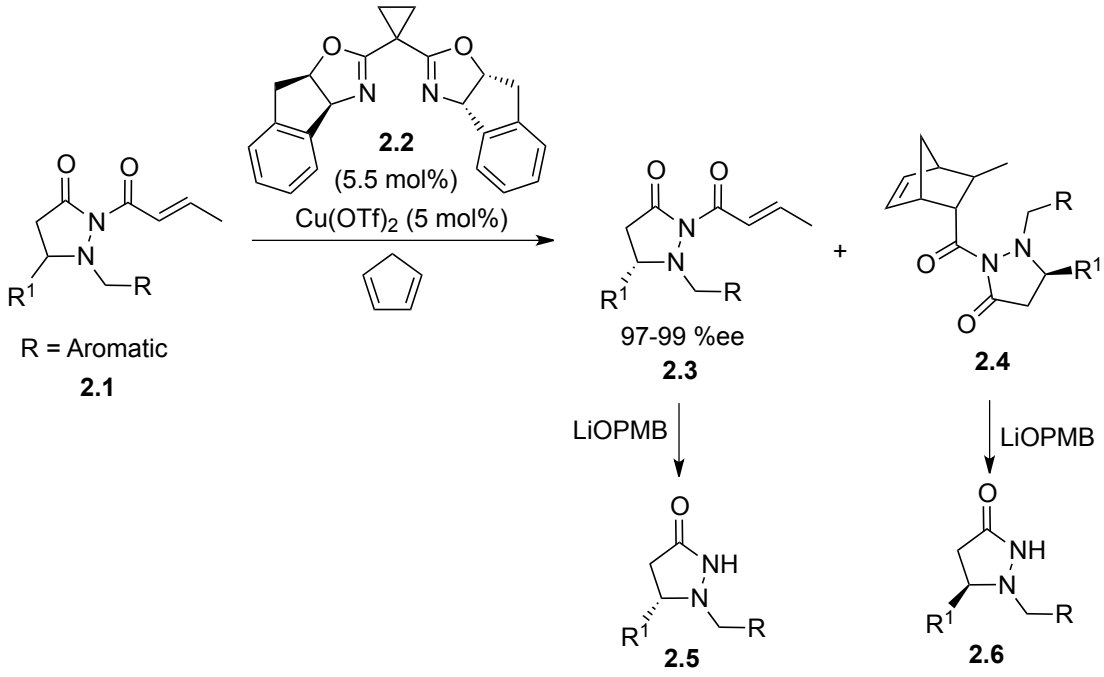


Scheme 2.2. Diels-Alder Cycloaddition Strategy for Kinetic Resolution of Chiral Pyrazolidinones

The design criteria for the new chiral DMAP catalysts were based on well-established principles in the literature. The initial evaluation involved the proper placement of the fluxional group on the pyridine ring. Early investigations showed that even a small group (methyl) adjacent to the pyridine nitrogen markedly erodes their activity as nucleophilic catalysts. Thus, 2-substituents in DMAP catalyst design are generally not desirable (Structure A, Scheme 2.3). Furthermore, 4-substituted pyridines are likely to provide minimal steric shielding due to the remote architecture between the catalytic center and the stereocontrol element (Structure B, Scheme 2.3). Based on these considerations, we connected the 3-position of the pyridine with the chiral pyrazolidinone template containing the fluxional group (Structure C, Scheme 2.3). We

expected that reactivity should be reasonable, and the proximity between the fluxional group and the pyridine might afford conformational definition.

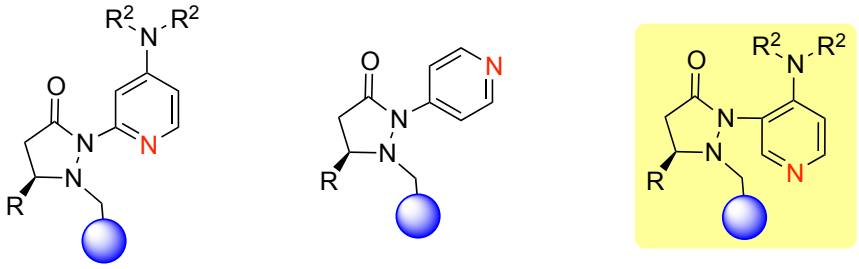


2-substituted pyridine
*Reactivity challenge
*N-C2 bond rotation issue

4-substituted pyridine
Modest basicity
Blocking?

3-Substituted pyridine
*Good blocking possibilities
*N-C3 bond rotation controllable
*Good reactivity

Scheme 2.3. Design of Novel Chiral DMAP Catalysts with Fluxional Chirality

Our chiral DMAP catalysts is highly modular and consists of three components: 4-(*N*,*N*-dialkylamino)pyridine (DMAP analogues) as the catalytic site, chiral pyrazolidinone as a chirality element and a fluxional substituent whose size can readily be varied as a blocking group (Figure 2.4). Conceptually the $R^1$ group dictates the orientation of the $CH_2R^2$ group, which in turn both influences the orientation of the DMAP group and provides steric discrimination during enantioselective reaction. The 4-(*N*, *N*-dialkylamino)pyridine is connected to the chiral pyrazolidinone at the *meta*-position. Additionally, the nucleophilicity of the pyridine can be tuned by varying the dialkylamino substituent $R^3$. Synthesis of these catalysts were straightforward. Several novel chiral DMAP catalysts were prepared.

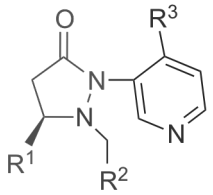


*fluxionality*

**2.7** $R^1$ = *i*-Pr, $R^2$ = phenyl, $R^3$ = dimethylamino
**2.8** $R^1$ = *t*-Bu, $R^2$ = phenyl, $R^3$ = dimethylamino
**2.9** $R^1$ = *t*-Bu, $R^2$ = 1-naphthyl, $R^3$ = dimethylamino
**2.10** $R^1$ = *t*-Bu, $R^2$ = 9-anthracenyl, $R^3$ = dimethylamino
**2.11** $R^1$ = *t*-Bu, $R^2$ = 2-naphthyl, $R^3$ = dimethylamino
**2.12** $R^1$ = *t*-Bu, $R^2$ = 1-naphthyl, $R^3$ = pyrrolidine
**2.13** $R^1$ = *t*-Bu, $R^2$ = 1-naphthyl, $R^3$ = di-*n*-butylamino

Figure 2.4. Novel Fluxionally Chiral DMAP Catalysts

## 2.3. Synthesis of Fluxionally Chiral DMAP Catalysts

### 2.3.1. Synthesis of Achiral 5-Substituted-Pyrazolidin-3-One

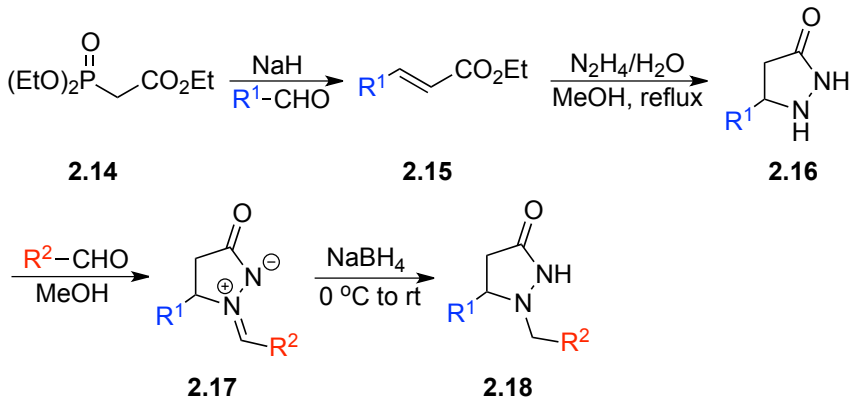


Scheme 2.4. Synthesis of Achiral Pyrazolidinone

Several chiral DMAP catalysts containing fluxional groups have been prepared from readily available pyrazolidinones **2.18** (Scheme 2.5). The Horner-Wadsworth-Emmons reaction between triethyl phosphonoacetate **2.14** and a variety of aldehydes $R^1$-CHO gave (*E*)-α,β-unsaturated esters **2.15**, which refluxed with hydrazine monohydrate to produce 5-alkylpyrazolidine-3-ones **2.16**. The reaction mixture was concentrated and the resulting residue

was used without any further purification. At 0 °C, the appropriate aldehyde $R^2$-CHO was added a solution of appropriate **2.16** and the more reactive N1 on **2.16** will react with aldehyde, followed by reductive amination with sodium borohydride to produce achiral pyrazolidinone **2.18**.

### 2.3.2. Synthesis of Chiral 5-Substituted-Pyrazolidin-3-One

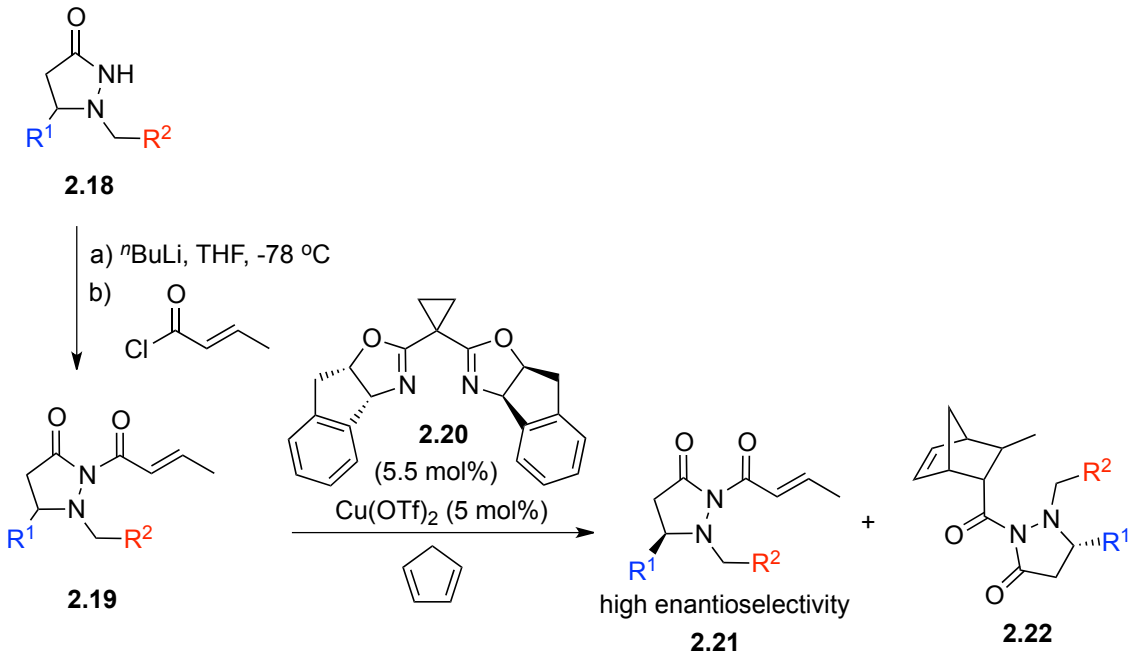


Scheme 2.5. Synthesis of Chiral Pyrazolidinone Crotonimide **2.22** by Kinetic Resolution Strategy

The chiral pyrazolidinone was obtained through the kinetic resolution strategy. Starting from the preparation of pyrazolidinone crotonimide **2.19**, then using the Diels-Alder cycloaddition strategy for the kinetic resolution of chiral pyrazolidinone crotonimide **2.21** with high enantiomeric excess. Under the influence of chiral Lewis acid and fluxional N1-substituent, the two enantiomers of pyrazolidinone react with different rates with cyclopentadiene. The (*S*)-isomer reacted faster to form the Diels-Alder product **2.22**, resulting in an enantioenriched

sample of the less reactive (*R*)-enantiomer **2.21** (97-99% ee). Then the (*R*)-N-H pyrazolidinone **2.23** was liberated by reaction of **2.21** with the lithium alkoxide of *p*-methoxybenzyl alcohol (Scheme 2.6).

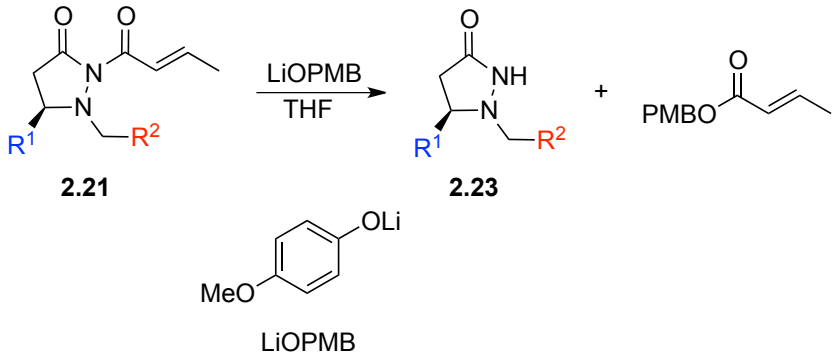


Scheme 2.6. Conversion of N2-Acylated Pyrazolidinone **2.21** to N2-H Pyrazolidinone **2.23**

This kinetic strategy to obtain the chiral pyrazolidinone allows for the synthesis of C5-substituted pyrazolidinone efficiently, however, it still required several steps from the achiral pyrazolidinone, such as acylation, Diels-Alder reaction, deacylation. In addition, Lewis acid participated reactions are less tolerant of moisture. Once again, to catch the optimum time to stop kinetic resolution for the best enantiomeric excess of compounds is also not easy to handle. In the end, the substrate scope for this strategy is also an issue. To solve these problems, we started to think about an alternative way to obtain the chiral pyrazolidinones.

After the study, we tried the diastereomer separation strategy to get the optically pure pyrazolidinone (Scheme 2.7). L-Proline is readily available naturally occurring amino acid and is easy to obtain in high enantiomeric purity. It contains a free chiral carboxylic acid group and a secondary amine group. The *tert*-butoxycarbonyl (Boc) protected *L*-proline can connect with the achiral pyrazolidinone unit through amide bond formation to produce two diastereomers. Using

flash column chromatography, the two diastereomers can be separated as two single isomers **2.24** and **2.25**.

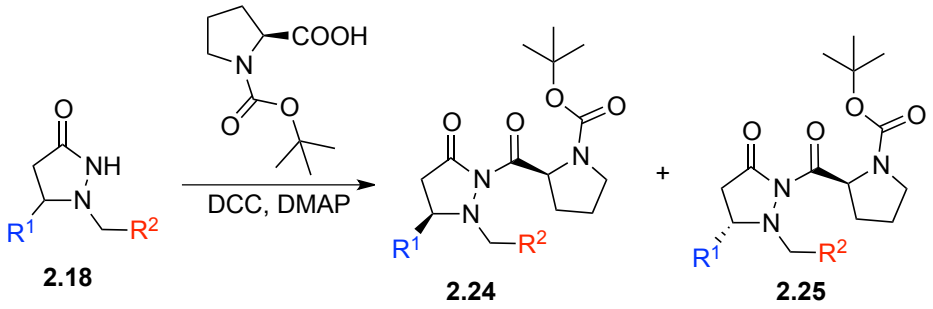


Scheme 2.7. Diastereomer Separation Strategy

Treatment of proline attached single isomer **2.24** with a catalytic amount of $Er(OTf)_3$ in methanol provided the optically pure pyrazolidinone **2.23** in high yield (Scheme 2.8). Compared to the kinetic resolution strategy, this diastereomer separation method took less steps and was easier to handle.

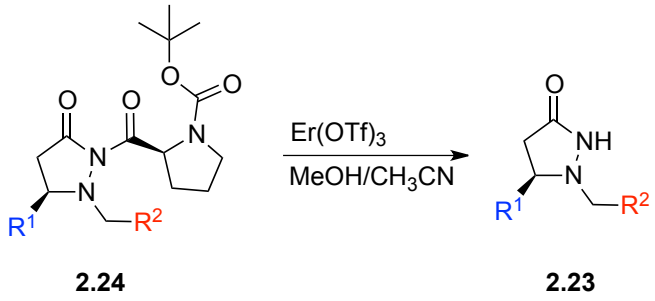


Scheme 2.8. Transformation of Diastereomer to Chiral Pyrazolidinone

### 2.3.3. Synthesis of Chiral DMAP Catalysts

The preparation of new DMAP catalysts started from enantiometically pure pyrazolidinones **2.23** and required three steps, which proceeded in good overall yields. The coupling reaction between **2.23** and 3-bromo-4-nitro pyridine oxide **2.26** was catalyzed by

$Pd_2(dba)_3$/Xantphos, and the coupling product was obtained with high yield. We also screened other organophosphorus ligands and Xantphos ligand gave the optimal yield for product **2.27** (Scheme 2.9).

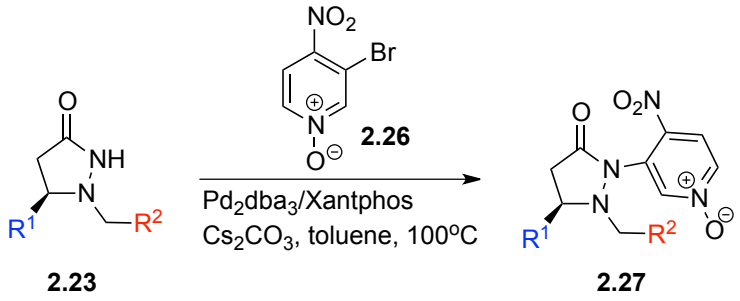


Scheme 2.9. Coupling Reaction with 3-Bromo-4-Nitro Pyridine Oxide

To produce final catalyst **2.29**, the nitro group in **2.27** was replaced with dimethyl amino substituent, and then underwent iron-mediated reduction (Scheme 2.10).

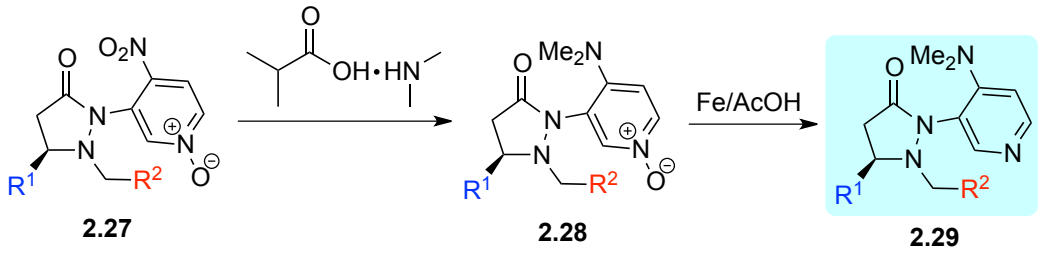


Scheme 2.10. Synthesis of Chiral 4-Dimethylamino Pyridine Catalysts

For other amino substituents, the corresponding pyrazolidinone-4-aminopyridine *N*-oxides were prepared in a different way. The nitro group was replaced by chloro and then underwent further substitution with amino group and iron-mediated reduction (Scheme 2.11).

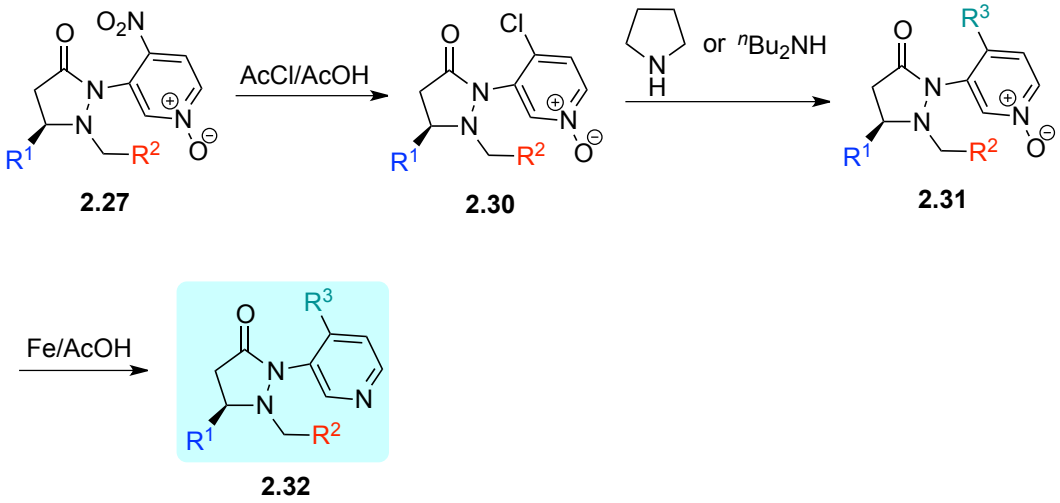


Scheme 2.11. Synthesis of Other Chiral 4-Aminoalkyl Pyridine Catalysts

## 2.4. Conclusion

We designed a new type of fluxionally chiral 4-dialkylamino pyridine catalyst based on 'chiral relay' concept and developed the synthetic methodology of these catalysts, which is amenable for scale up and diversity can be introduced in the fluxional group, C5 substituent on the pyrolidinone as well as the pyridine 4-substituent without much difficulty. Different catalysts were synthesized with different $R^1$, $R^2$ and $R^3$ substituents for evaluation. The reactivity and selectivity of these catalysts could be controlled by tuning different substituents. We expected the stereochemical information could be relayed from static C5 substituent to catalytic ceneter through the N-fluxional group.

## 2.5. Experimental

### 2.5.1. General

All solvents were dried and degassed by standard methods and stored under nitrogen. Flash chromatography was performed using EM Science silica gel 60 (230-400 mesh). $^1$H NMR spectra were recorded on Varian Unity/Inova-400 NB (400 MHz) spectrometer or Bruker

Ascend™ 400 (400 MHz for $^{1}H$) spectrometer. $^{13}C$ NMR spectra were recorded on Varian Unity/Inova-400 NB (100 MHz) spectrometer or Bruker Ascend™ 400 (100 MHz for $^{13}C$) spectrometer. HPLC analyses were carried out with Waters 515 HPLC pumps and a 2487 dual wavelength absorbance detector connected to a PC with Empower workstation. Rotations were recorded on a JASCO-DIP-370 polarimeter. FT-IR spectra were recorded on a Bruker Optics Vertex 70 FTIR. High resolution mass spectra were obtained at a Bruker Daltonics BioTOF HRMS spectrometer.

**2.5.2. Reaction Procedure and Compounds Characterization**

The racemic pyrazolidinones were prepared according to the literature reported.[23] The chiral pyrazolidinones for catalyst **2.7**, **2.8** and **2.11** were prepared according to the procedure reported in the literature.[23]

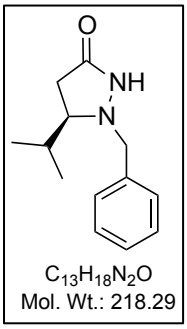


Chiral pyrazolidinone for catalyst **2.7**. $[\alpha]_D^{25}$ +140.2 (*c* 0.52, $CHCl_3$). $^{1}H$ NMR ($CDCl_3$, 400 MHz) δ 0.87 (d, *J* = 6.8 Hz, 3H), 0.91 (d, *J* = 6.8 Hz, 3H), 1.68-1.77 (m, 1H), 2.15 (dd, *J* = 16.8, 4.0 Hz, 1H), 2.73 (dd, *J* = 17.2, 8.8 Hz, 1H), 2.98-3.03 (m, 1H), 3.74 (d, *J* = 12.4 Hz, 1H), 3.91 (d, *J* = 12.4 Hz, 1H), 7.02 (br s, 1H), 7.26-7.33 (m, 5H); $^{13}C$ NMR ($CDCl_3$, 100 MHz) δ 18.4, 18.9, 31.9, 32.2, 64.6, 68.3, 128.1, 128.8, 129.6, 136.6, 174.4. HPLC analysis: HPLC (UV 220 nm, Chiralpak AD-H, *i*-PrOH/Hexane = 4/96, 1 mL/min), $t_1$ (major) = 15.9 min, $t_2$ (minor) = 23.6 min.

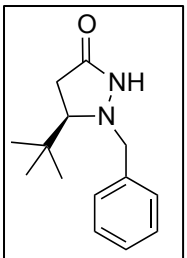


$C_{14}H_{20}N_2O$
Mol. Wt.: 232.32

Chiral pyrazolidinone for catalyst **2.8**. $[\alpha]_D^{25}$ +137.8 (*c* 0.56, $CHCl_3$). $^1H$ NMR ($CDCl_3$, 400 MHz) δ 0.84 (s, 9H), 2.16 (dd, *J* = 17.6, 2.4 Hz, 1H), 2.68 (dd, *J* = 17.6, 10.0 Hz, 1H), 2.94 (dd, *J* = 9.6, 2.4 Hz, 1H), 3.77 (d, *J* = 12.4 Hz, 1H), 3.87 (d, *J* = 12.4 Hz, 1H), 7.24-7.33 (m, 5H), 7.60 (br s, 1H); $^{13}C$ NMR ($CDCl_3$, 100 MHz) δ 25.6, 30.6, 35.1, 65.7, 70.7, 128.1, 128.7, 129.9, 136.6, 174.8. HPLC analysis: HPLC (UV 220 nm, Chiralpak OD-H, *i*-PrOH/Hexane = 3/97, 1 mL/min), $t_1$ (major) = 16 min, $t_2$ (minor) = 20.7 min.

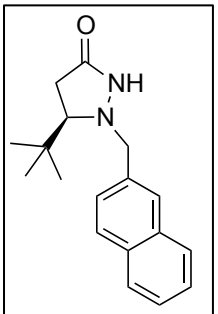


$C_{18}H_{22}N_2O$
Mol. Wt.: 282.38

Chiral pyrazolidinone for catalyst **2.11**. $[\alpha]_D^{25}$ +135.4 (*c* 0.50, $CHCl_3$). $^1H$ NMR ($CDCl_3$, 400 MHz) δ 0.88 (s, 9H), 2.18 (dd, *J* = 17.2, 2.4 Hz, 3H), 2.73 (m, 1H), 3.00 (dd, *J* = 10.0, 2.4 Hz, 1H), 3.92 (m, 2H), 7.24 (br s, 1H), 7.45 (m, 3H), 7.72 (m, 1H), 7.80 (m, 3H); $^{13}C$ NMR ($CDCl_3$, 100 MHz) δ 25.7, 30.5, 35.2, 66.1, 71.1, 126.3, 126.5, 127.6, 127.9, 128.0, 128.7, 133.2, 133.4, 134.3, 174.7. HPLC analysis: HPLC (UV 220 nm, Chiralpak AD-H, *i*-PrOH/Hexane = 4/96, 1 mL/min), $t_1$ (major) = 21.1 min, $t_2$ (minor) = 36.3 min.

The chiral pyrazolidinones for catalyst **2.9**, **2.10, 2.12** and **2.13** were prepared by a diastereomeric resolution strategy (Scheme 2.12).

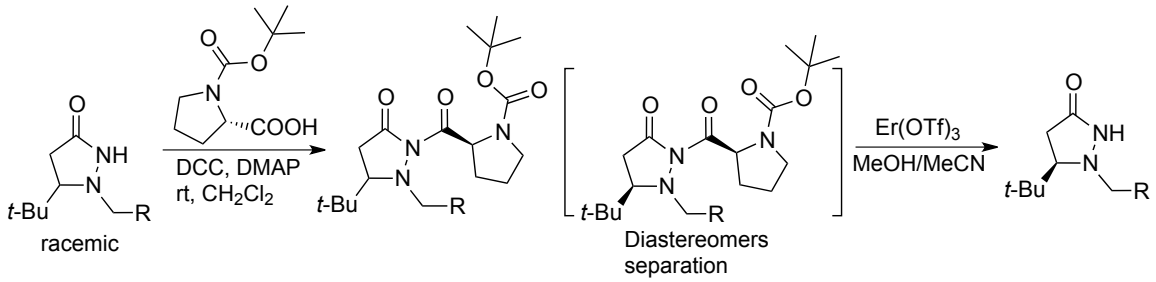


Scheme 2.12. General Procedure for the Preparation of Chiral Pyrazolidinones

A mixture of Boc-proline (1 equiv), racemic pyrazolidinone (1.2 equiv), DCC (1 equiv) and a catalytic amount of DMAP (0.2 equiv) in $CH_2Cl_2$ (10 mL) was stirred at room temperature for 48 h. The reaction mixture was filtered and subjected to silica-gel column chromatography (acetone/hexane = 1/5) to separate both diastereomers. To a solution of one diastereomer (1 equiv) in MeOH/MeCN (ratio = 3/2) was added $Er(OTf)_3$ (5 mol%) at room temperature.[24] After TLC evaluation showed all starting material has been consumed, the reaction mixture was evaporated and purified by silica-gel column chromatography (hexane/ethyl acetate = 1/1) to get the enantiopure chiral pyrazolidinone (85-95% yield).

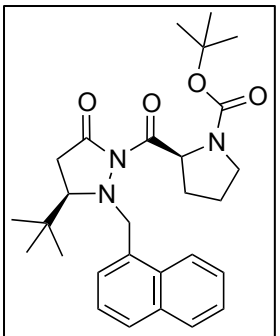

$C_{28}H_{37}N_3O_4$
Mol. Wt.: 479.61

Single pyrazolidinone-proline diastereomer for catalyst **2.9**, **2.12** and **2.13**. $[\alpha]_D^{25}$ -36.9 (*c* 0.58, $CHCl_3$). $^1H$ NMR ($CDCl_3$, 400 MHz) δ 0.48 (s, 9H), 1.43 (s, 6H), 1.51 (s, 3H), 1.88-1.98 (m, 3H), 2.4-2.47 (m, 1H), 2.56 (d, *J* = 18 Hz, 1H), 3.03 (dd, *J* = 16, 9.6 Hz, 1H), 3.18 (dd, *J* = 18, 9.6 Hz, 1H), 3.46-3.58 (m, 1H), 3.67-3.73 (m, 1H), 3.9 (d, *J* = 11.2 Hz, 1H), 4.84 (d, *J* = 11.2 Hz, 1H), 5.36 (dd, *J* = 8.8, 2 Hz, 1H), 7.36-7.44 (m, 2H), 7.5-7.56 (m, 1H), 7.64-7.7 (m, 1H), 7.85 (t, *J* = 7.2 Hz, 2H), 9.07 (d, *J* = 8 Hz, 1H); $^{13}C$ NMR ($CDCl_3$, 100 MHz) δ 22.5, 25.5, 28.4, 31.4, 31.7, 34.3, 46.7, 59.7, 60.4, 63.6, 77.2, 79.8, 124.5, 126.2, 126.6, 126.7, 127.9, 129.1, 129.4, 131.9, 133.1, 133.7, 154.1, 168.8, 174.3; IR (NaCl) 1748, 1706, 1687, 1402, 1384, 1215, 1166, 785 $cm^{-1}$; ESI-HRMS: *m/z* calcd. for $(C_{28}H_{37}N_3O_4Na)^+$ 502.2676; found 502.2673.

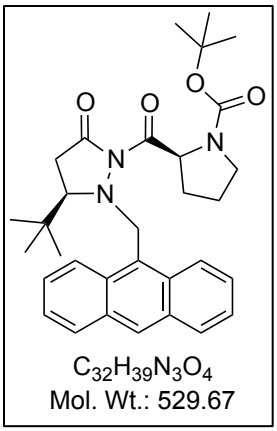

$C_{32}H_{39}N_3O_4$
Mol. Wt.: 529.67

Single pyrazolidinone-proline diastereomer for catalyst **2.10**. $[\alpha]_D^{25}$ -25.7 (*c* 0.95, $CHCl_3$). $^1H$ NMR ($CDCl_3$, 400 MHz, 60 °C) δ 0.38 (s, 9H), 1.47 (s, 9H), 1.93 (m, 3H), 2.46 (s, 1H), 2.61 (dd, *J* = 18, 1.2 Hz, 1H), 2.86 (d, *J* = 9.6 Hz, 1H), 3.31 (br, 1H), 3.56 (br, 1H), 3.7 (br, 1H), 4.85 (d, *J* = 12 Hz, 1H), 5.17 (d, *J* = 12 Hz, 1H), 5.43 (dd, *J* = 8.8, 2.4 Hz, 1H), 7.48-7.52 (m, 2H), 7.62-7.66 (m, 2H), 8.03 (d, *J* = 8.4 Hz, 2H), 8.48 (s, 1H), 8.83 (br, 2H); $^{13}C$ NMR ($CDCl_3$, 100 MHz) δ 22.5, 25.4, 28.5, 29.6, 31.5, 32.5, 34.3, 46.8, 52.3, 60.5, 63.8, 77.1, 79.7, 125.0, 126.5, 128.6, 128.9, 131.3, 132.1, 154.1, 174.4, 188.2; IR (NaCl) 1748, 1698, 1479, 1460, 1385, 1166, 1123, 762 $cm^{-1}$; ESI-HRMS: *m/z* calcd. for $(C_{32}H_{39}N_4O_4Na)^+$ 552.2833; found 552.2826.

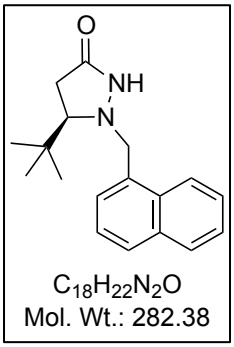

$C_{18}H_{22}N_2O$
Mol. Wt.: 282.38

Chiral pyrazolidinone for catalyst **2.9**, **2.12** and **2.13**. $[\alpha]_D^{25}$ 158.4 (*c* 0.54, $CHCl_3$). $^1H$ NMR ($CDCl_3$, 400 MHz) δ 0.86 (s, 9H), 2.27 (dd, *J* = 17.6, 2.4 Hz, 3H), 2.96 (dd, *J* = 17.6, 9.6 Hz, 1H), 3.12 (dd, *J* = 9.6, 2.4 Hz, 1H), 4.21 (d, *J* = 12.0 Hz, 1H), 4.37 (d, *J* = 12.0 Hz, 1H), 6.71 (br s, 1H), 7.40-7.42 (m, 2H), 7.47-7.56 (m, 2H), 7.80-7.87 (m, 2H), 8.24 (d, *J* = 8.0 Hz, 1H);

$^{13}$C NMR ($CDCl_3$, 100 MHz) δ 25.8, 30.2, 35.1, 64.1, 72.0, 124.6, 125.4, 126.1, 126.4, 128.8, 129.1, 129.2, 132.3, 132.4, 134.1, 174.5. HPLC analysis: HPLC (UV 220 nm, Chiralpak AD-H, *i*-PrOH/Hexane = 4/96, 1 mL/min), $t_1$ (major) = 24.3 min, $t_2$ (minor) = 28.6 min.

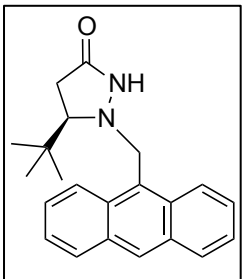


$C_{22}H_{24}N_2O$
Mol. Wt.: 332.44

Chiral pyrazolidinone for catalyst **2.10**. $[\alpha]_D^{25}$ 51.3 (c 0.89, $CHCl_3$). $^1$H NMR ($CDCl_3$, 400 MHz) δ 0.84 (s, 9H), 2.38 (d, *J* = 14.8 Hz, 1H), 3.21(dd, *J* = 23.6, 9.2 Hz, 1H), 3.23 (s, 1H), 4.82 (d, *J* = 12.4 Hz, 1H), 5.01 (d, *J* = 12.4 Hz, 1H), 6.66 (s, 1H), 7.49-7.61 (m, 4H), 8.05 (d, *J* = 8.4 Hz, 2H), 8.43 (d, *J* = 8.8 Hz, 2H), 8.5 (s, 1H); $^{13}$C NMR ($CDCl_3$, 100 MHz) δ 25.7, 30.2, 34.9, 56.6, 71.7, 124.4, 125.0, 126.4, 126.9, 127.2, 128.6, 129.2, 131.3, 131.4, 134.1, 174.5. HPLC analysis: HPLC (UV 254 nm, Chiralpak OD-3, *i*-PrOH/Hexane = 5/95, 1 mL/min), $t_1$ (major) = 22.7 min, $t_2$ (minor) = 26.7 min.

The chiral DMAP catalysts **2.7**, **2.8**, **2.9**, **2.10** and **2.11** were prepared from commercially available 3-bromo-4-nitropyridine *N*-oxide according to the following Scheme 2.13.

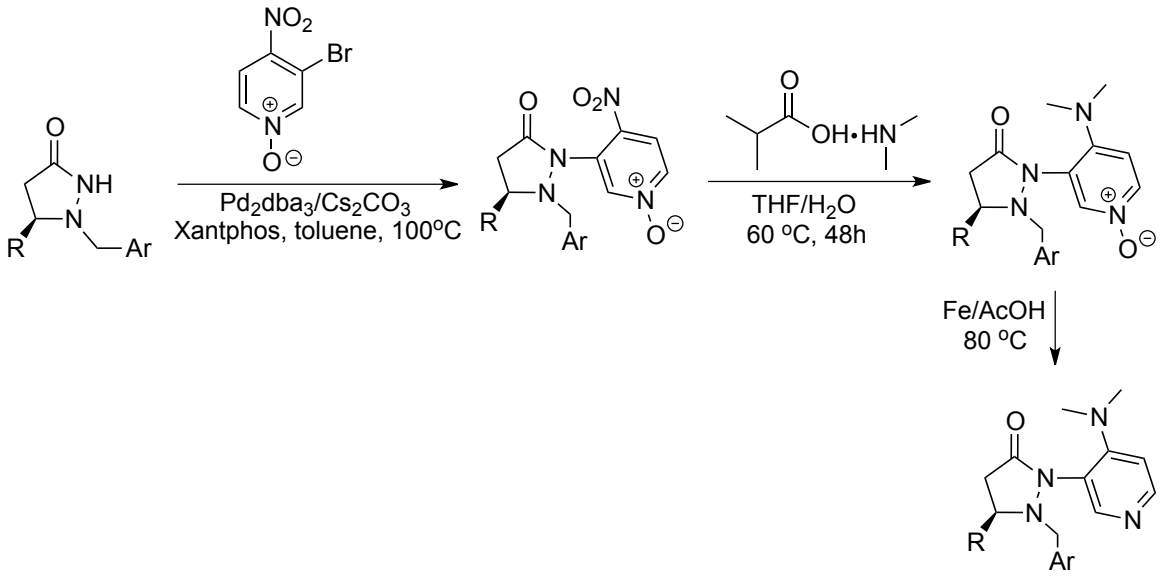


Scheme 2.13. General Procedure for the Prapararion of Chiral DMAP Catalyst

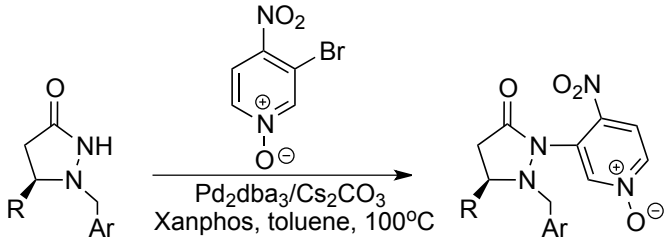


Scheme 2.14. General Procedure for the Preparation
of Chiral Pyrazolidinone-4-Nitropyridine *N*-Oxide

General procedure for synthesis of chiral pyrazolidinone-4-nitropyridine *N*-oxide (Scheme 2.14). A flask equipped with a stirrer and a reflux condenser was charged with chiral pyrazolidinone (1.0 equiv), 3-bromo-4-nitro-pyridine *N*-oxide (1.0 equiv), $Pd_2dba_3$ (5 mol%), Xantphos (5 mol%), cesium carbonate (1.2 equiv). The mixture was degassed and backfilled with argon, after adding the toluene, then stirring for 12 h at 100 °C, the reaction mixture was cooled to room temperature, filtered through Celite, and concentrated. The crude material was purified using column chromatography (hexane/ethyl acetate = 1/1-1/2) to give the product as a yellow solid; average yields are 80-90%.

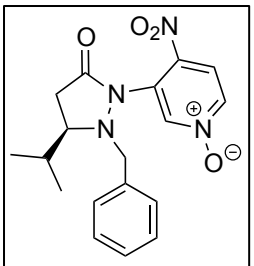

$C_{18}H_{20}N_4O_4$
Mol. Wt.: 356.38

Chiral pyrazolidinone-4-nitropyridine *N*-oxide for catalyst **2.7**. $[\alpha]_D^{25}$ -735.9 (*c* 0.53, $CHCl_3$). $^1H$ NMR ($CDCl_3$, 400 MHz) δ 0.82 (d, *J* = 6.8 Hz, 3H), 0.91 (d, *J* = 6.8 Hz, 3H), 1.59-1.68 (m, 1H), 2.37 (d, *J* = 16.0 Hz, 1H), 3.09-3.18 (m, 2H), 4.04 (d, *J* = 12.4 Hz, 1H), 4.14 (d, *J* = 12.4 Hz, 1H), 7.18-7.27 (m, 3H), 7.32-7.35 (m, 2H), 7.65 (d, *J* = 7.2 Hz, 1H), 7.83 (dd, *J* = 7.2, 1.6 Hz, 1H), 8.49 (d, *J* = 2.0 Hz, 1H); $^{13}C$ NMR ($CDCl_3$, 100 MHz) δ 18.6, 18.9, 32.3, 32.7, 63.4, 66.1, 121.8, 128.7, 130.2, 130.3, 134.8, 135.1, 136.1, 171.2; IR (NaCl) 1724, 1601, 1567, 1521, 1466, 1267, 750 $cm^{-1}$; ESI-HRMS: *m/z* calcd. for $(C_{18}H_{20}N_4O_4Na)^+$ 379.1377; found 379.1394.

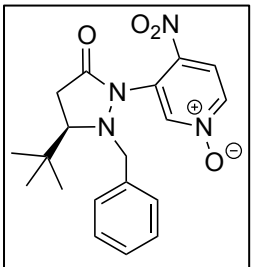

$C_{19}H_{22}N_4O_4$
Mol. Wt.: 370.40

Chiral pyrazolidinone-4-nitropyridine *N*-oxide for catalyst **2.8**. $[\alpha]_D^{25}$ -761.1 (*c* 0.58, $CHCl_3$). $^1H$ NMR ($CDCl_3$, 400 MHz) δ 0.81 (s, 9H), 2.42 (d, *J* = 17.2 Hz, 1H), 3.01-3.15 (m, 2H), 4.08 (dd, *J* = 28, 12.4 Hz, 2H), 7.19-7.26 (m, 3H), 7.33-7.35 (m, 2H), 7.65 (d, *J* = 6.8 Hz, 1H), 7.81-7.83 (m, 1H), 8.52 (d, *J* =2.0 Hz, 1H); $^{13}C$ NMR ($CDCl_3$, 100 MHz) δ 25.7, 31.2, 35.1,

64.4, 68.9, 121.8, 128.7, 128.8, 129.7, 130.6, 134.5, 134.7, 135.8, 137.2, 171.2; IR (NaCl) 1727, 1600, 1567, 1521, 1467, 1272, 750 $cm^{-1}$; ESI-HRMS: *m/z* calcd. for $(C_{19}H_{22}N_4O_4Na)^+$ 393.1533; found 393.1531.

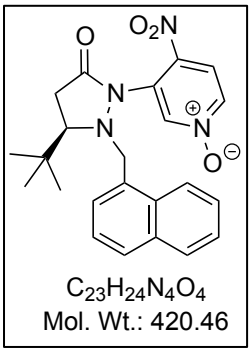


Chiral pyrazolidinone-4-nitropyridine *N*-oxide for catalyst **2.9**, **2.12** and **2.13**. $[\alpha]_D^{25}$ -455.7 (*c* 0.52, $CHCl_3$). $^1H$ NMR ($CDCl_3$, 400 MHz) δ 0.85 (s, 9H), 2.50 (dd, *J* = 14.0, 2.4 Hz, 1H), 3.27-3.35 (m, 2H), 4.51 (d, *J* = 12.0 Hz, 1H), 4.63 (d, *J* = 12.0 Hz, 1H), 7.15-7.19 (m, 1H), 7.47-7.58 (m, 4H), 7.63-7.70 (m, 2H), 7.8 (d, *J* = 8.0 Hz, 1H), 8.07 (d, *J* = 2.0 Hz, 1H), 8.18 (d, *J* = 8.8 Hz, 1H); $^{13}C$ NMR ($CDCl_3$, 100 MHz) δ 25.9, 31.0, 35.2, 63.1, 70.2, 121.4, 123.4, 124.9, 126.6, 127.6, 129.1, 129.6, 130.0, 130.3, 130.4, 132.1, 133.5, 134.4, 135.6, 136.2, 171.1; IR (NaCl) 1726, 1600, 1567, 1519, 1467, 1272, 750 $cm^{-1}$; ESI-HRMS: *m/z* calcd. for $(C_{23}H_{24}N_4O_4Na)^+$ 443.1690; found 443.1692.

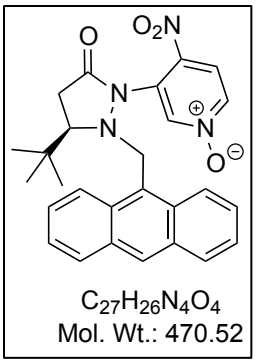


Chiral pyrazolidinone-4-nitropyridine *N*-oxide for catalyst **2.10**. $[\alpha]_D^{25}$ -363.2 (*c* 0.53, $CHCl_3$). $^1H$ NMR ($CDCl_3$, 400 MHz) δ 0.47 (s, 9H), 2.56 (d, *J* = 17.6 Hz, 1H), 3.14 (d, *J* = 9.2 Hz, 1H), 3.47 (dd, *J* = 17.2, 9.2 Hz, 1H), 5.16 (d, *J* = 12.8 Hz, 1H), 5.26 (d, *J* = 12.8 Hz, 1H), 7.51-7.55 (m, 2H), 7.66-7.7 (m, 2H), 7.77 (d, *J* = 7.2 Hz, 1H), 7.97 (dd, *J* = 7.2, 2 Hz, 1H), 8.04 (d, *J* = 8.4 Hz, 2H), 8.34-8.36 (m, 2H), 8.47 (s, 1H), 8.73 (d, *J* = 1.6 Hz, 1H); $^{13}C$ NMR ($CDCl_3$, 100 MHz) δ 25.5, 30.9, 34.5, 54.4, 67.4, 121.9, 124.9, 125.3, 127.2, 129.2, 129.2, 129.4, 131.1, 131.4, 134.8, 136.3, 137.3, 171.0; IR (NaCl) 1726, 1625, 1600, 1569, 1522, 1469, 1273, 734 $cm^{-1}$; ESI-HRMS: *m/z* calcd. for $(C_{27}H_{26}N_4O_4Na)^+$ 493.1846; found 493.1839.

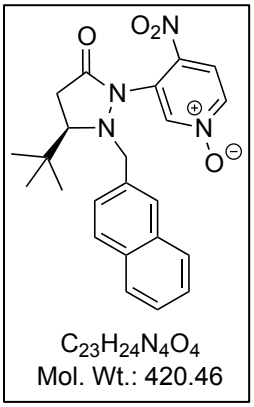


Chiral pyrazolidinone-4-nitropyridine *N*-oxide for catalyst **2.11**. $[\alpha]_D^{25}$ -725.0 (*c* 0.50, $CHCl_3$). $^1H$ NMR ($CDCl_3$, 400 MHz) δ 0.83 (s, 9H), 2.42 (m, 1H), 3.05 (m, 1H), 3.19 (m, 1H), 4.19 (dd, *J* = 26, 12.4 Hz, 1H), 7.41-7.52 (m, 4H), 7.60 (dd, *J* = 7.2, 2.0 Hz, 1H), 7.67-7.69 (m,

1H), 7.74-7.76 (m, 2H), 7.80 (d, $J$ = 8.0 Hz, 1H), 8.50 (d, $J$ = 2.0 Hz, 1H); $^{13}$C NMR ($CDCl_3$, 100 MHz) δ 25.7, 31.3, 35.2, 64.7, 68.9, 121.5, 126.8, 127.9, 128.6, 129.6, 130.0, 132.1, 133.0, 133.1, 134.4, 135.5, 137.0, 171.1; IR (NaCl) 1727, 1600, 1567, 1521, 1467, 1272, 751 cm$^{-1}$; ESI-HRMS: *m/z* calcd. for $(C_{23}H_{24}N_4O_4Na)^+$ 443.1690; found 443.1686.

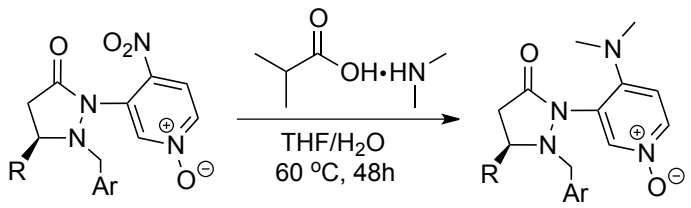


Scheme 2.15. General Procedure for the Preparation of Chiral Pyrazolidinone-4-Dimethylamino Pyridine *N*-Oxides

General procedure for synthesis of chiral pyrazolidinone-4-dimethylaminopyridine *N*-oxides. To a solution of the 2-(4-nitro-1-oxy-pyridin-3-yl)-pyrazolidin-3-one (1 equiv.) in THF/$H_2O$ (ratio = 10/1) was added the *N, N*-dimethylammonium *N*', *N*'-dimethylcarbamate (5 equiv.) dropwise. After stirring at 60 °C for 48 h, the reaction mixture was cooled to room temperature, filtered through Celite, and concentrated. The residue was purified by column chromatography (methanol/ethyl acetate = 1/10) to give the product as a yellow solid; average yields are 80-90%.

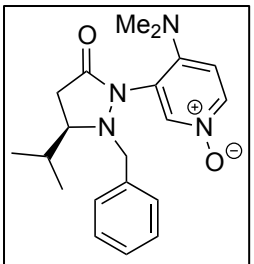


$C_{20}H_{26}N_4O_2$
Mol. Wt.: 354.45

Chiral pyrazolidinone-4-dimethylaminopyridine *N*-oxide for catalyst **2.7**. $[\alpha]_D^{25}$ -16.4 (*c* 0.52, $CHCl_3$). $^1H$ NMR ($CDCl_3$, 400 MHz) δ 0.72-0.75 (m, 6H), 1.58-1.63 (m, 1H), 2.36 (dd, *J* = 16.8, 3.2 Hz, 1H), 2.88 (s, 6H), 2.94-2.99 (m, 1H), 3.06-3.12 (m, 1H), 3.84 (d, *J* = 12.4 Hz, 1H), 4.1 (d, *J* = 12.4 Hz, 1H), 6.48 (d, *J* = 7.6 Hz, 1H), 7.17-7.23 (m, 5H), 7.8 (dd, *J* = 3.6, 2.0 Hz, 1H), 8.26 (d, *J* = 2.0 Hz, 1H); $^{13}C$ NMR ($CDCl_3$, 100 MHz) δ 18.2, 19.4, 31.4, 32.5, 41.5, 61.4, 65.4, 113.1, 123.2, 128.1, 128.5, 129.6, 135.8, 137.9, 138.6, 146.4, 170.6; IR (NaCl) 1703, 1506, 1425, 750 $cm^{-1}$; ESI-HRMS: *m/z* calcd. for $(C_{20}H_{26}N_4O_2Na)^+$ 377.1948; found 377.1938.

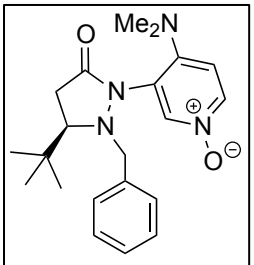


$C_{21}H_{28}N_4O_2$
Mol. Wt.: 368.47

Chiral pyrazolidinone-4-dimethylaminopyridine *N*-oxide for catalyst **2.8**. $[\alpha]_D^{25}$ -13.2 (*c* 0.57, $CHCl_3$). $^1H$ NMR ($CDCl_3$, 400 MHz) δ 0.66 (s, 9H), 2.45 (dd, *J* = 17.2, 5.6 Hz, 1H), 2.92 (s, 6H), 3.01 (dd, *J* = 9.6, 1.6 Hz, 1H), 3.25 (dd, *J* = 17.2, 9.6 Hz, 1H), 3.86 (d, *J* = 11.6 Hz, 1H), 4.2 (d, *J* = 11.6 Hz, 1H), 6.61 (d, *J* = 7.2 Hz, 1H), 7.25-7.29 (m, 5H), 7.87 (dd, *J* = 7.2, 2.0 Hz, 1H), 8.6 (d, *J* = 2.4 Hz, 1H); $^{13}C$ NMR ($CDCl_3$, 100 MHz) δ 25.9, 31.3, 34.7, 41.0, 62.2, 66.8,

113.8, 123.3, 128.5, 128.6, 130.3, 135.4, 136.4, 137.3, 145.4, 169.1; IR (NaCl) 1704, 1508, 1425, 747 $cm^{-1}$; ESI-HRMS: *m/z* calcd. for $(C_{21}H_{28}N_4O_2Na)^+$ 391.2104; found 391.2112.

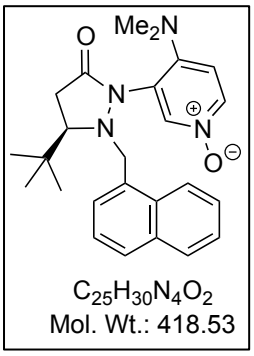


Chiral pyrazolidinone-4-dimethylaminopyridine *N*-oxide for catalyst **2.9**. $[\alpha]_D^{25}$ -127.3 (*c* 0.52, $CHCl_3$). $^1H$ NMR ($CDCl_3$, 400 MHz) δ 0.45 (s, 9H), 2.46 (dd, *J* = 17.2, 1.2 Hz, 1H), 2.96 (s, 6H), 3.12-3.14 (m, 1H), 3.31 (dd, *J* = 17.2, 10.0 Hz, 1H), 4.2 (d, *J* = 11.6 Hz, 1H), 4.81 (d, *J* = 11.6 Hz, 1H), 6.66 (d, *J* = 7.2 Hz, 1H), 7.35-7.4 (m, 2H), 7.45-7.49 (m, 1H), 7.60-7.64 (m, 1H), 7.78-7.82 (m, 2H), 7.92-7.95 (m, 2H), 8.62 (d, *J* = 2.4 Hz, 1H); $^{13}C$ NMR ($CDCl_3$, 100 MHz) δ 25.7, 31.1, 34.6, 41.3, 59.9, 66.4, 113.9, 123.3, 123.7, 124.9, 126.4, 127.4, 128.9, 129.5, 129.7, 131.2, 132.6, 133.8, 137.3, 137.7, 146.0, 169.7; IR (NaCl) 1703, 1509, 1425, 751 $cm^{-1}$; ESI-HRMS: *m/z* calcd. for $(C_{25}H_{30}N_4O_2Na)^+$ 441.2261; found 441.2280.

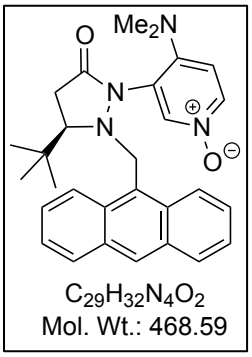


Chiral pyrazolidinone-4-dimethylaminopyridine *N*-oxide for catalyst **2.10**. $[\alpha]_D^{25}$ -118.1 (*c* 0.5, $CHCl_3$). $^1H$ NMR ($CDCl_3$, 400 MHz) δ 0.26 (s, 9H), 2.52 (d, *J* = 16.8 Hz, 1H), 3.06 (d, *J*

= 9.6 Hz, 1H), 3.15 (s, 6H), 3.5 (dd, *J* = 17.2, 9.6 Hz, 1H), 5.08 (d, *J* = 12 Hz, 1H), 5.23 (d, *J* = 12 Hz, 1H), 6.84 (d, *J* = 7.2 Hz, 1H), 7.51-7.54 (m, 2H), 7.67-7.71 (m, 2H), 8.05 (d, *J* = 8.4 Hz, 2H), 8.13 (dd, *J* = 7.2, 2 Hz, 1H), 8.24 (d, *J* = 8.8 Hz, 2H), 8.52 (s, 1H), 8.8 (d, *J* = 2 Hz, 1H); $^{13}$C NMR ($CDCl_3$, 100 MHz) δ 25.3, 25.8, 29.7, 31.1, 34.3, 41.2, 52.3, 65.7, 113.6, 122.8, 123.4, 125.2, 125.2, 127.2, 129.1, 129.5, 131.2, 131.5, 136.9, 137.7, 146.4, 169.6; IR (NaCl) 1704, 1525, 1384, 735 cm$^{-1}$; ESI-HRMS: *m/z* calcd. for $(C_{29}H_{32}N_4O_2Na)^+$ 491.2417; found 491.2421.

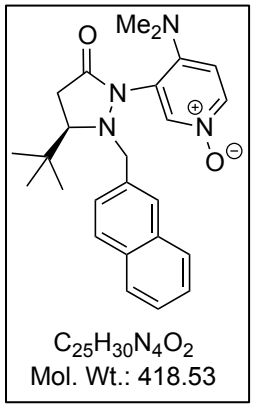


Chiral pyrazolidinone-4-dimethylaminopyridine *N*-oxide for catalyst **2.11**. $[\alpha]_D^{25}$ -0.20 (*c* 0.53, $CHCl_3$). $^1$H NMR ($CDCl_3$, 400 MHz) δ 0.66 (s, 9H), 2.45 (dd, *J* = 17.2, 1.6 Hz, 1H), 2.92 (s, 6H), 3.07 (dd, *J* = 9.6, 1.6 Hz, 1H), 3.27 (dd, *J* = 17.2, 9.6 Hz, 1H), 4.03 (d, *J* = 7.6 Hz, 1H), 4.34 (d, *J* = 12.0 Hz, 1H), 6.54 (d, *J* = 7.2 Hz, 1H), 7.43-7.47 (m, 3H), 7.66 (s, 1H), 7.76-7.80 (m, 3H), 7.84 (dd, *J* = 7.2, 2.0 Hz, 1H), 8.65 (d, *J* = 2.0 Hz, 1H); $^{13}$C NMR ($CDCl_3$, 100 MHz) δ 26.0, 31.4, 34.7, 41.1, 62.5, 66.8, 113.7, 123.3, 126.5, 127.9, 128.0, 128.4, 130.0, 133.0, 133.0, 133.1, 133.2, 136.5, 137.3, 145.5, 169.2; IR (NaCl) 1703, 1508, 1425, 748 cm$^{-1}$; ESI-HRMS: *m/z* calcd. for $(C_{25}H_{30}N_4O_2Na)^+$ 441.2261; found 441.2267.

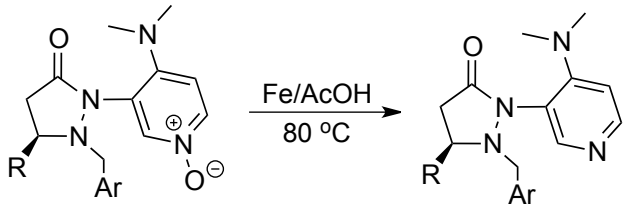


Scheme 2.16. General Procedure for the Preparation of Chiral Pyrazolidinone-4-Dimethylamino Pyridine Catalyst **2.7**, **2.8**, **2.9**, **2.10** and **2.11**

Iron powder (10 mmol) and the chiral 4-dimethylamine pyridyl-*N*-oxide (2 mmol) was suspended in glacial acetic acid (10 mL) and heated at 85 °C for 8 hours. The reaction mixture was poured onto the crushed ice, and was neutralized with 6 N sodium hydroxide to basic, the solution was filtered through Celite, and extracted with dichloromethane three times (50 mL × 3), the combined organic extracts were dried over $Na_2SO_4$ and concentrated *in vacuo*. The residue was chromatographed on silica gel (methanol / EtOAc = 1 / 10) to give the catalyst in 80-85% yield.

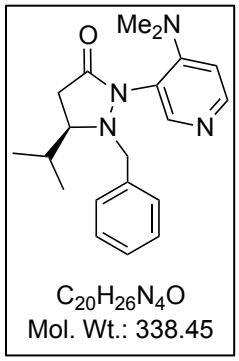


Catalyst **2.7**. $[\alpha]_D^{25}$ -54.3 (*c* 0.65, $CHCl_3$). $^1H$ NMR ($CDCl_3$, 400 MHz) δ 0.72-0.80 (m, 6H), 1.65-1.72 (m, 1H), 2.36-2.41 (m, 1H), 2.89 (s, 6H), 2.91-3.05 (m, 2H), 3.78 (d, *J* = 12.8 Hz, 1H), 4.07 (d, *J* = 12.8 Hz, 1H), 6.41-6.43 (m, 1H), 7.10-7.14 (m, 5H), 8.02 (dd, *J* = 5.6, 2.8 Hz, 1H), 8.29 (s, 1H); $^{13}C$ NMR ($CDCl_3$, 100 MHz) δ 18.2, 19.6, 31.0, 32.9, 41.4, 60.9, 66.1, 111.0,

127.6, 128.2, 129.4, 136.6, 149.1, 151.7, 153.5, 170.8; IR (NaCl) 1698, 1591 $cm^{-1}$; ESI-HRMS: *m/z* calcd. for $(C_{20}H_{26}N_4ONa)^+$ 361.1999; found 361.2009.

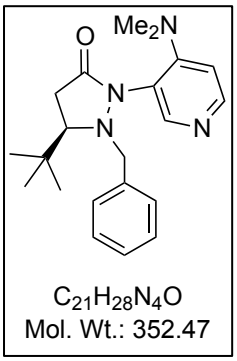


Catalyst **2.8**. $[\alpha]_D^{25}$ -4.6 (*c* 0.41, $CHCl_3$). $^1H$ NMR ($CDCl_3$, 400 MHz) δ 0.71 (s, 9H), 2.47 (dd, *J* = 16.8, 2.0 Hz, 1H), 2.93 (s, 6H), 2.99 (dd, *J* = 9.6, 2.0 Hz, 1H), 3.23 (dd, *J* = 17.2, 9.6 Hz, 1H), 3.85 (d, *J* = 12.0 Hz, 1H), 4.24 (d, *J* = 12.0 Hz, 1H), 6.55 (d, *J* = 6.0 Hz, 1H), 7.19-7.23 (m, 5H), 8.08 (d, *J* = 6.0 Hz, 1H), 8.76 (s, 1H); $^{13}C$ NMR ($CDCl_3$, 100 MHz) δ 26.0, 31.8, 34.8, 40.9, 61.9, 67.0, 111.5, 121.5, 128.0, 128.3, 130.0, 136.3, 148.3, 148.8, 152.2, 169.1; IR (NaCl) 1691, 1191 $cm^{-1}$; ESI-HRMS: *m/z* calcd. for $(C_{21}H_{28}N_4ONa)^+$ 375.2155; found 375.2185.

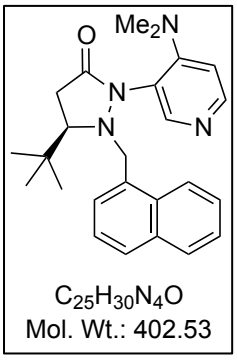


Catalyst **2.9**. $[\alpha]_D^{25}$ -133.3 (*c* 0.53, $CHCl_3$). $^1H$ NMR ($CDCl_3$, 400 MHz) δ 0.46 (s, 9H), 2.46 (dd, *J* = 17.2, 1.6 Hz, 1H), 3.0 (s, 6H), 3.12 (dd, *J* = 10.0, 1.6 Hz, 1H), 3.27-3.34 (m, 1H), 4.12 (d, *J* = 11.6 Hz, 1H), 4.89 (d, *J* = 12.0 Hz, 1H), 6.67 (d, *J* = 5.6 Hz, 1H), 7.35-7.44 (m, 4H), 7.76-7.84 (m, 3H), 8.20 (d, *J* = 5.6 Hz, 1H), 8.80 (s, 1H); $^{13}C$ NMR ($CDCl_3$, 100 MHz) δ 25.7,

31.5, 34.6, 41.3, 59.7, 66.4, 111.7, 121.5, 121.6, 124.3, 124.9, 126.1, 126.6, 128.6, 129.1, 129.4, 132.1, 132.8, 133.8, 148.8, 149.9, 153.0, 169.9; IR (NaCl) 1697, 1591 $cm^{-1}$; ESI-HRMS: *m/z* calcd. for $(C_{25}H_{30}N_4ONa)^+$ 425.2312; found 425.2305.

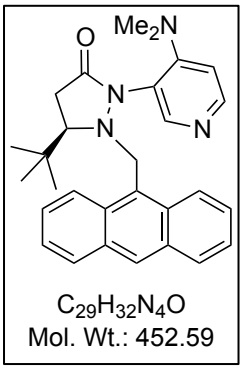


Catalyst **2.10**. $[\alpha]_D^{25}$ -136.8 (*c* 0.5, $CHCl_3$). $^1H$ NMR ($CDCl_3$, 400 MHz) δ 0.29 (s, 9H), 2.55 (dd, *J* = 16.8, 1.2 Hz, 1H), 3.09 (d, *J* = 9.6 Hz, 1H), 3.18 (s, 6H), 3.5 (dd, *J* = 17.2, 9.6 Hz, 1H), 5.09 (d, *J* = 12.4 Hz, 1H), 5.23 (d, *J* = 12 Hz, 1H), 6.85 (d, *J* = 6 Hz, 1H), 7.48-7.52 (m, 2H), 7.55-7.59 (m, 2H), 8.03 (d, *J* = 8.4 Hz, 2H), 8.23 (d, *J* = 8.8 Hz, 2H), 8.33 (d, *J* = 5.6 Hz, 2H), 8.49 (s, 1H), 8.97 (s, 1H); $^{13}C$ NMR ($CDCl_3$, 100 MHz) δ 25.4, 31.6, 34.3, 41.3, 51.9, 65.8, 111.7, 121.3, 123.8, 125.0, 126.1, 126.6, 128.7, 129.3, 131.2, 131.5, 169.8; IR (NaCl) 1702, 1590 $cm^{-1}$; ESI-HRMS: *m/z* calcd. for $(C_{29}H_{32}N_4ONa)^+$ 475.2468; found 475.2455.

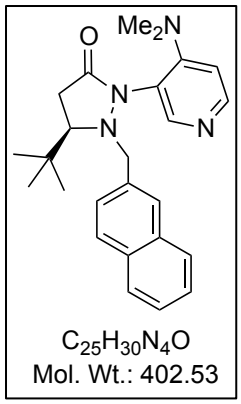


Catalyst **2.11**. $[\alpha]_D^{25}$ -25.2 (*c* 0.52, $CHCl_3$). $^1H$ NMR ($CDCl_3$, 400 MHz) δ 0.72 (s, 9H), 2.49 (dd, *J* = 17.2, 2.4 Hz, 1H), 2.95 (s, 6H), 3.08 (dd, *J* = 10, 2.4 Hz, 1H), 3.27 (dd, *J* = 16.8, 9.6 Hz, 1H), 4.04 (d, *J* = 12.0 Hz, 1H), 4.40 (d, *J* = 12.0 Hz, 1H), 6.50 (d, *J* = 5.6 Hz, 1H), 7.38 (dd, *J* = 8.4, 1.6 Hz, 1H), 7.44-7.47 (m, 2H), 7.64 (s, 1H), 7.71-7.80 (m, 3H), 8.06 (dd, *J* = 6.0, 2.0 Hz, 1H), 8.85 (s, 1H); $^{13}C$ NMR ($CDCl_3$, 100 MHz) δ 26.1, 31.9, 34.8, 41.0, 62.2, 67.1, 111.5, 121.5, 126.3, 126.4, 127.9, 128.0, 128.1, 128.5, 133.1, 133.2, 134.0, 148.2, 148.7, 152.2, 169.2; IR (NaCl) 1698, 1591 $cm^{-1}$; ESI-HRMS: *m/z* calcd. for $(C_{25}H_{31}N_4O)^+$ 403.2492; found 403.2499.

Chiral pyrazolidinone-4-aminopyridine *N*-oxides for catalyst **2.12** and **2.13** were prepared according to the following Scheme 2.17.

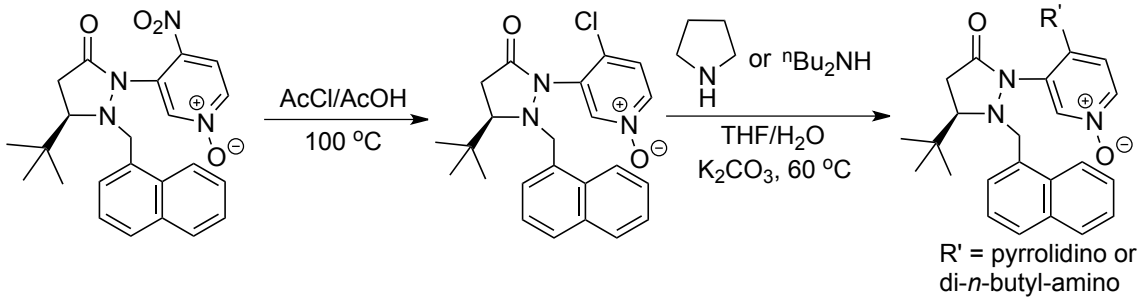


Scheme 2.17. General Procedure for the Preparation of Other Chiral Pyrazolidinone-4-Aminoalkyl Pyridine *N*-Oxides

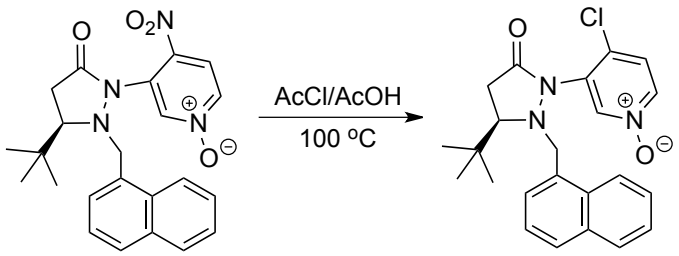


Scheme 2.18. General Procedure for the Preparation of Chiral Pyrazolidinone-4-Chloro Pyridine *N*-Oxide

Acetic acid (10 mL) and acetic chloride (50 mmol) were added to 2-(4-nitro-1-oxy-pyridin-3-yl)-pyrazolidin-3-one (5 mmol) at room temperature. The reaction was heated with stirring at 100 °C for 2 hours. The reaction mixture was poured onto the crushed ice, and was basified using 6 M NaOH and extracted with dichloromethane three times (50 mL × 3). The combined organic extracts were dried over $Na_2SO_4$ and concentrated *in vacuo*. The residue was purified by flash column chromatography (methanol/ethyl acetate = 1/10) to afford 2-(4-chloro-1-oxy-pyridin-3-yl)-pyrazolidin-3-one; average yields are 90-97%. $[\alpha]_D^{25}$ -28.2 (*c* 0.57, $CHCl_3$). $^1$H NMR ($CDCl_3$, 400 MHz) δ 0.85 (s, 9H), 2.49 (d, *J* = 16.8 Hz, 1H), 3.18 (d, *J* = 9.6 Hz, 1H), 3.3 (dd, *J* = 16.8, 9.6 Hz, 1H), 4.35 (d, *J* = 12 Hz, 1H), 4.45 (d, *J* = 12 Hz, 1H), 6.87 (d, *J* = 7.2 Hz, 1H), 7.23-7.28 (m, 1H), 7.4 (d, *J* = 7.2 Hz, 1H), 7.46-7.5 (m, 1H), 7.54-7.57 (m, 1H), 7.61-7.66 (m, 2H), 7.72 (d, *J* = 8.4 Hz, 1H), 8.06 (d, *J* = 8.4 Hz, 1H), 8.12 (d, *J* = 2.0 Hz, 1H); $^{13}$C NMR ($CDCl_3$, 100 MHz) δ 26.0, 31.1, 35.2, 63.2, 69.7, 123.8, 125.0, 126.5, 126.6, 127.3, 127.8, 128.7, 129.7, 129.8, 130.6, 131.9, 133.4, 134.8, 136.9, 137.2, 169.8; IR (NaCl) 1720, 1470, 1265, 753 cm$^{-1}$; ESI-HRMS: *m/z* calcd. for $(C_{23}H_{24}ClN_3O_2Na)^+$ 432.1449; found 432.1450.

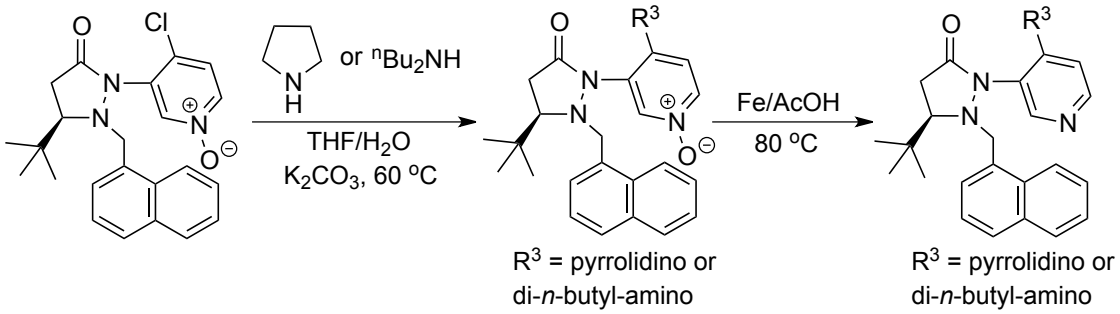


Scheme 2.19. General Procedure for the Preparation of Catalyst **2.12** and **2.13**

To a solution of the 2-(4-chloro-1-oxy-pyridin-3-yl)-pyrazolidin-3-one (2 mmol) in 10 mL THF and 1 mL $H_2O$ was added the corresponding amine. After stirring the mixture at 60 °C for 48 hours, the reaction mixture was cooled to room temperature, and extracted with dichloromethane three times (50 mL × 3), the combined organic extracts were dried over $Na_2SO_4$ and concentrated *in vacuo*. To the residue was added Iron powder (10 mmol), glacial acetic acid (10 mL) and heated at 80 °C for 8 hours. The reaction mixture was poured onto crushed ice, and was basified with 6 N NaOH. The solution was filtered through Celite and extracted with dichloromethane three times (50 mL × 3). The combined organic extracts were dried over $Na_2SO_4$ and concentrated *in vacuo*. The residue was chromatographed on silica gel (methanol/ethyl acetate = 1/10) to give the desired product; the average total yields of two steps are 70-80%.

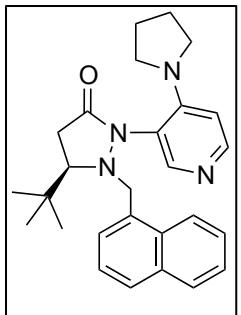

$C_{27}H_{32}N_4O$
Mol. Wt.: 428.57

Catalyst **2.12**. $[\alpha]_D^{25}$ -193.6 (*c* 0.50, $CHCl_3$). $^1H$ NMR (DMSO-d6, 400 MHz) δ 0.45 (s, 9H), 1.86-1.89 (m, 4H), 2.31-2.36 (m, 1H), 3.14 (d, *J* = 10 Hz, 1H), 3.38-3.5 (m, 5H), 4.33 (d, *J* = 12.4 Hz, 1H), 4.72 (d, *J* = 12.4 Hz, 1H), 6.58 (d, *J* = 6.0 Hz, 1H), 7.28-7.32 (m, 1H), 7.37-7.44 (m, 2H), 7.53 (d, *J* = 6.8 Hz, 1H), 7.75 (d, *J* = 8.8 Hz, 1H), 7.79-7.84 (m, 2H), 8.03 (d, *J* = 5.6 Hz, 1H), 8.46 (s, 1H); $^{13}C$ NMR ($CDCl_3$, 100 MHz) δ 25.7, 25.8, 31.8, 34.7, 49.2, 59.8, 66.3, 110.2, 119.0, 124.5, 124.9, 126.1, 126.6, 128.6, 129.1, 129.4, 132.1, 132.8, 133.8, 148.7, 150.0, 170.5; IR (NaCl) 1693, 1592 $cm^{-1}$; ESI-HRMS: *m/z* calcd. for $(C_{23}H_{24}ClN_3O_2Na)^+$ 432.1449; found 432.1450.

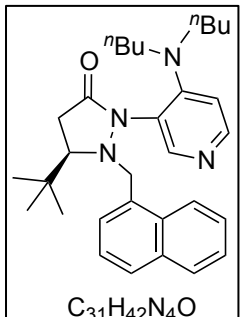

$C_{31}H_{42}N_4O$
Mol. Wt.: 486.69

Catalyst **2.13**. $[\alpha]_D^{25}$ -110.7 (*c* 0.50, $CHCl_3$). $^1H$ NMR ($CDCl_3$, 400 MHz) δ 0.46 (s, 9H), 0.88 (t, *J* = 7.2 Hz, 1H), 1.26-1.35 (m, 4H), 1.49-1.63 (m, 4H), 2.48 (dd, *J* = 16.8, 1.2 Hz, 1H), 3.14-3.25 (m, 3H), 3.32 (dd, *J* = 16.8, 9.6 Hz, 1H), 3.42-3.49 (m, 2H), 4.13 (d, *J* = 11.6 Hz, 1H), 4.88 (d, *J* = 11.6 Hz, 1H), 6.82 (d, *J* = 6 Hz, 1H), 7.39 (d, *J* = 5.2 Hz, 2H), 7.45-7.47 (m, 2H),

7.80-7.86 (m, 3H), 8.25 (d, $J$ = 5.6 Hz, 1H), 8.89 (s, 1H); $^{13}$C NMR ($CDCl_3$, 100 MHz) δ 14.2, 20.6, 25.7, 30.0, 31.4, 34.6, 50.6, 60.0, 66.2, 114.0, 123.6, 124.4, 124.9, 126.2, 126.7, 128.6, 129.2, 129.5, 132.1, 132.8, 133.8, 148.7, 150.0, 152.4, 169.4; IR (NaCl) 2957, 2932, 1700, 1586, 1498, 1362, 793 cm$^{-1}$; ESI-HRMS: *m/z* calcd. for $(C_{31}H_{43}N_4ONa)^+$ 487.3431; found 487.3427.

**2.6. References**


1. a) Sharpless, K. B. Searching for New Reactivity. *Angew. Chem. Int. Ed.* **2002**, *41*, 2024-2032; b) Noyori, R. Asymmetric Catalysis: Science and Opportunities. *Angew. Chem. Int. Ed.* **2002**, *41*, 2008-2022; c) Knowles, W. S. Asymmetric Hydrogenations. *Angew. Chem. Int. Ed.* **2002**, *41*, 1998-2007.
2. List, B. Introduction: Organocatalysis. *Chem. Rev.* **2007**, *107*, 5413-5415.
3. Dalko, P. I.; Moisan, L. In the Golden Age of Organocatalysis. *Angew. Chem. Int. Ed.* **2004**, *43*, 5138-5175.
4. a) Pellissier, H. Asymmetric Organocatalysis. *Tetrahedron* **2007**, *63*, 9267-9331; b) Gaunt, M. J.; Johansson, C. C. C.; McNally, A.; Vo, N. T. Enantioselective Organocatalysis. *Drug Discov. Today* **2007**, *12*, 8-27; c) Shaikh, I. R. Organocatalysis: Key Trends in Green Synthetic Chemistry, Challenges, Scope towards Heterogenization, and Importance from Research and Industrial Point of View. *Journal of Catalysts* **2014**, *2014*, Article ID 402860.
5. a) Leadbeater, N. E.; Marco, M. Transition-Metal-Free Suzuki-Type Coupling Reactions. *Angew. Chem. Int. Ed.* **2003**, *42*, 1407-1409; b) Leadbeater, N. E.; Macro, M. Transition-Metal-Free Suzuki-Type Coupling Reactions. Scope and Limitations of the Methodology. *J. Org. Chem.* **2003**, *68*, 5660-5667.

6. a) Leadbeater, N. E.; Marco, M.; Tominack, B. J. First Example of Transition-Metal Free Sonogashira-Type Couplings. *Org. Lett.* **2003**, *5*, 3919-3922; b) Appukkuttan, P.; Dehaen, W.; Van der-Eycken, E. Transition-Metal-Free Sonogashira-Type Coupling Reactions in Water. *Eur. J. Org. Chem.* **2003**, 4713-4716.
7. Ma, D.; Cai, Q. *L*-Proline Promoted Ullmann-Type Coupling Reactions of Aryl Iodides with Indoles, Pyrroles, Imidazoles or Pyrazoles. *Synlett* **2004**, 128-130.
8. Zhang, R.; Zhao, F.; Sato, M.; Ikushima, Y. Noncatalytic Heck Coupling Reaction Using Supercritical Water. *Chem. Commun.* **2003**, 1548-1549.
9. Chevrin, C.; Le Bras, J.; Hénin, F.; Muzart, J. Water-mediated Transition-Metal-Free Tsuji-Trost-type Reaction. *Tetrahedron Lett.* **2003**, *44*, 8099-8102.
10. a) Bertelsen, S.; Jørgensen, K. A. Organocatalysis-After the Gold Rush. *Chem. Soc. Rev.* **2009**, *38*, 2178-2189; b) Alemán, J.; Cabrera, S. Applications of Asymmetric Organocatalysis in Medicinal Chemistry. *Chem. Soc. Rev.* **2013**, *42*, 774-793; c) Jacobsen, E. N.; MacMillan, D. W. C. *Proc. Natl. Acad. Sci. USA* **2010**, *107*, 20618-20619.
11. MacMillan, D. W. C. The Advent and Development of Organocatalysis. *Nature* **2008**, *455*, 304-308.
12. Sereda, O.; Tabassum, S.; Wilhelm, R. Lewis Acid Organocatalysts. *Top. Curr. Chem.* **2010**, *291*, 349-393.
13. Seayad, J.; List, B. Asymmetric Organocatalysis. *Org. Biomol. Chem.* **2005**, *3*, 719-724.
14. Doyle, A. G.; Jacobsen, E. N. Small-Molecule H-Bonds Donors in Asymmetric Catalysis. *Chem. Rev.* **2007**, *107*, 5713-5743.

15. Palomo, C.; Oiarbide, M.; Lopez, R. Asymmetric Organocatalysis by Chiral Brønsted Bases: Implications and Applications. *Chem. Soc. Rev.* **2009**, *38*, 632-653.

16. Davie, E. A. C.; Mennen, S. M.; Xu, Y.; Miller, S. J. Asymmetric Catalysis Mediated by Synthetic Peptides. *Chem. Rev.* **2007**, *107*, 5759-5812.

17. a) Sibi, M. P.; Venkatraman, L.; Liu, M.; Jasperse, C. P. A New Approach to Enantiocontrol and Enantioselectivity Amplification: Chiral Relay in Diels-Alder Reactions. *J. Am. Chem. Soc.* **2001**, *123*, 8444-8445; b) Sibi, M. P.; Zhang, R.; Manyem, S. A New Class of Modular Chiral Ligands with Fluxional Groups. *J. Am. Chem. Soc.* **2003**, *125*, 9306-9307; c) Sibi, M. P.; Manyem, S.; Palencia, H. Fluxional Additives: A Second Generation Control in Enantioselective Catalysis. *J. Am. Chem. Soc.* **2006**, *128*, 13660-13661; d) Sibi, M. P.; Stanley, L. M.; Nie, X.; Venkatraman, L.; Liu, M.; Jasperse, C. P. The Role of Achiral Pyrazolidinone Templates in Enantioselective Diels-Alder Reactions: Scope, Limitations, and Conformational Insights. *J. Am. Chem. Soc.* **2007**, *129*, 395-405; e) Sibi, M. P.; Kawashima, K.; Stanley, L. Diels-Alder Cycloaddition Strategy for Kinetic Resolution of Pyrazolidinones. *Org. Lett.* **2009**, *11*, 3894-3897.

18. Steglich, W.; Höfle, G.; *N*,*N*-Dimethyl-4-Pyridinamine, A Very Effective Acylation Catalyst. *Angew. Chem. Int. Ed.* **1969**, *8*, 981.

19. a) Höfle, G.; Steglich, W.; Vorbrüggen, H.; 4-Dialkylaminopyridines as Highly Active Acylation Catalysts. *Angew. Chem. Int. Ed.* **1978**, *17*, 569-583; b) Scriven, E. F. V. 4-Dialkylaminopyridines: Super Acylation and Alkylation Catalysts. *Chem. Soc. Rev.* **1983**, *12*, 129-161; c) Ranarsson, U.; Grehn, L. Novel Amine Chemistry Based on DMAP-Catalyzed Acylation. *Acc. Chem. Res.* **1998**, *31*, 494-501; d) Garnier, J.; Kennedy, A. R.; Berlouis, L. E. A.; Turner, A. T.; Murphy, J. A. Structure and Reactivity in Neutral

Organic Electron Donors Derived from 4-Dimethylaminopyridine. *Beilstein J. Org. Chem.* **2010**, *6*, 1-8; e) Spivey, A. C.; Arseniyadis, S. Nucleophilic Catalysis by 4-(Dialkylamino)pyridines Revisited-The Search for Optimal Reactivity and selectivity. *Angew. Chem. Int. Ed.* **2004**, *43*, 5436-5441.

20. Berry, D. J.; DiGiovanna, C. V.; Metrick, S. S.; Murugan, R. Catalysis by 4-Dialkylaminopyridines. *ARKIVOC* **2001**, 201-226.
21. Vedejs, E.; Chen, X. Kinetic Resolution of Secondary Alcohols. Enantioselective Acylation Mediated by A Chiral (Dimethylamino)pyridine Derivative. *J. Am. Chem. Soc.* **1996**, *118*, 1809-1810.
22. Wurz, R. P. Chiral Dialkylaminopyridine Catalysts in Asymmetric Synthesis. *Chem. Rev.* **2007**, *107*, 5570-5595.
23. Sibi, M. P.; Kawashima, K.; Stanley, L. M. Diels-Alder Cycloaddition Strategy for Kinetic Resolution of Chiral Pyrazolidinones. *Org. Lett.* **2009**, *11*, 3894-3897.
24. Hoashi, Y.; Okino, T.; Takemoto, Y. Enantioselective Michael Addition to α,β-Unsaturated Imides Catalyzed by A Bifunctional Organocatalyst. *Angew. Chem. Int. Ed.* **2005**, *44*, 4032-4035.

# CHAPTER 3. KINETIC RESOLUTION OF SECONDARY ALCOHOLS AND AXIALLY CHIRAL BIARYL COMPOUNDS USING FLUXIONALLY CHIRAL 4-DIMETHYLAMINO PYRIDINE (DMAP) CATALYSTS

## 3.1. Introduction

The resolution of racemic substrates to get enantioenriched product or enantioenriched substrate is a significant process in organic synthesis. Kinetic resolution is a process leading to the partial or complete separation of enantiomers by the unequal rates of reaction of the enantiomers with a chiral agent (reagent, catalyst, solvent, etc.), according to the 1996 IUPAC definition.[1] It allows the preparation of samples that are enantiomerically pure and this feature is very attractive to both academic and industrial applications. In a typical catalytic kinetic resolution, two enantiomers react with different reaction rates with a chiral catalyst in a chemical reaction, resulting in one of the enantiomers being transformed to the product, and the other enantiomer is recovered unchanged[2] (Scheme 3.1). In contrast to chiral resolution, kinetic resolution does not rely on the different physical properties but rely on the different chemical properties of racemic substrate. The efficiency of a kinetic resolution is typically evaluated by selectivity factor ($s$) or $k_{rel} = k_{fast} / k_{slow}$, the relative rates of reaction, which reflects the free energy difference of two diastereomeric transition states in the selectivity-determining step of the catalytic reaction (In some cases, this is also referred to as the $E$ factor). Usually in simple kinetic resolution experiments, the following equation is used**:** $s = \ln[1-c(1+ee_{pro})]/\ln[1-c(1-ee_{pro})]$ (based on *ee* of the product) or equation: $s = \ln[(1-c)(1-ee_{sm})]/\ln[(1-c)(1+ee_{sm})]$ (based on *ee* of the recovered substrate) to calculate the selectivity factor ($s$), where c is the conversion. The enantiomeric excess of the substrate and the product in a simple kinetic resolution change as a function of conversion, so the selectivity factor ($s$) is generally considered as the evaluation of

the efficiency of kinetic resolution.[3] A sufficient rate difference allows the consumption of one enantiomer and recovery of the other. The maximum theoretical yield in simple kinetic resolution is 50%. High selectivity factors are necessary to obtain high enantioselectivity for the product in kinetic resolution.

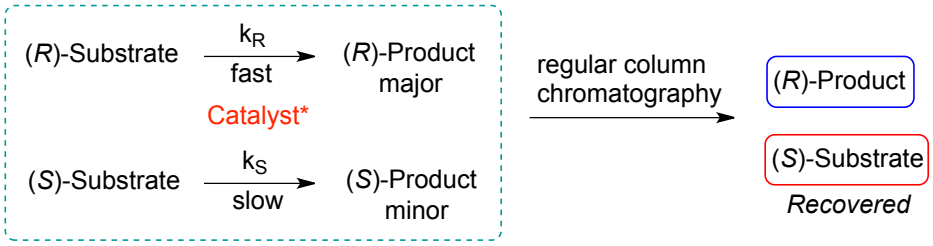


Scheme 3.1. General Scheme for Catalytic Kinetic Resolution

Kinetic resolution exhibits advantages among other preparation methods if the racemate are not expensive and the catalyst can be recycled; and if the starting material and the product are easily separated.

The kinetic resolution of racemic substances can be achieved by biocatalysis, metal catalysis and organocatalysis. Microorganisms, such as lipase, or isolated enzymes catalyze resolution in an effective way to produce optically pure enantiomers. Thus chiral recognition of alcohols by enzyme has been widely used in synthesis in the past few years. A large number of hydrolytic lipases have been successfully used for the kinetic resolution of racemic secondary alcohols.[4] However, only very limited number of enzymes are able to resolve racemates and enzymeric reactions are usually require high standards for their use in organic reactions, for example, the use of enzymes in organic solvents would decrease their catalytic activities.

Recent advances based on a non-enzymatic kinetic resolution strategy have been achieved with high efficiency comparable to biocatalysts,[5] such as the acylation of alcohols or amines, oxidative kinetic resolution of alcohols, Mitsunobu reactions of alcohols, alcoholysis of

racemic carbonyl derivatives, ring opening reactions of epoxides, epoxidation of alkenes, oxidative transfer hydrogenation, ring closing metathesis, hydrogenation of alkenes and imines, hydrosilylation or hydroboration strategies, Pd-catalyzed allylic alkylation, 1,4-conjugate addition. Moreover, important advances in the application of non-enzymatic chiral catalysts for dynamic kinetic resolution have also been made.[6]

### 3.2. Kinetic Resolution of Secondary Alcohols

#### 3.2.1. Background

Enantiomerically pure secondary alcohols are very important synthetic building blocks and key targets in the manufacture of a wide range of chemical products, such as agrochemicals, pharmaceuticals and fine chemicals.

Consequently, a wide variety of methodologies have been developed for preparing these synthons in high enantiomeric excess, including asymmetric hydrogenation of prochiral ketones catalyzed by metal complexes,[7] enantioselective addition of carbon nucleophiles to aldehydes,[8] hydration of alkenes,[9] ring opening of epoxides,[10] the enzymatic kinetic resolution of racemic secondary alcohols through acylation,[11] and non-enzymatic kinetic resolution.[12] In the non-enzymeric kinetic resolution of secondary alcohols, many research groups have developed several methods to obtain optically pure alcohols, such as asymmetric nucleophilic acyl transfer reactions, Sharpless asymmetric epoxidation of allylic alcohols, selective oxidation of alcohols to ketones, asymmetric hydrogenation of allylic alcohols and $S_N2$ displacement/Mitsunobu reactions, *etc* (Scheme 3.2). Among these methodologies, the kinetic resolution of racemic alcohols via asymmetric acylation has been widely used to construct various chiral alcohol skeletons, since the acylation reagents like anhydrides, acyl halides, and carboxylic acids are commercially available and can react under mild conditions. The challenge of developing easily

accessible and effective non-enzymatic asymmetric acylation catalysts has attracted many research groups over the last decade.

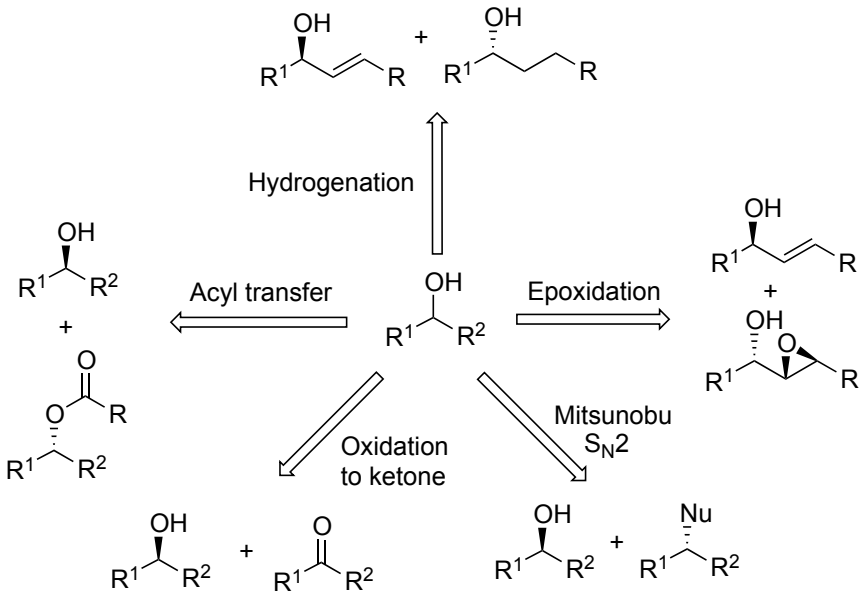


Scheme 3.2. Alcohol Non-Enzymeric Kinetic Resolution Strategies

The mechanism of asymmetric nucleophilic catalyst catalyzed acyl transfer in the kinetic resolution of secondary alcohols can be considered as a three-step process[13] (Scheme 3.3). Step A involves attack of the chiral nucleophilic catalyst on an achiral acylating agent. The resulting chiral acylium cation intermediate will be further attacked by a racemic mixture of nucleophilic secondary alcohols (Step B). Two enantiomeric secondary alcohols react with different reaction rates in a chemical reaction with this chiral acylating intermediate and result in a resolution process. Both the enantioenriched starting material and enantioenriched acylation product are formed. The chiral nucleophilic catalyst is regenerated by a stoichiometric amount of achiral base (Step C). The role of the base is still under investigation and it is generally accepted that the base neutralizes the acid produced during the reaction to avoid catalyst deactivation by protonation.[14]

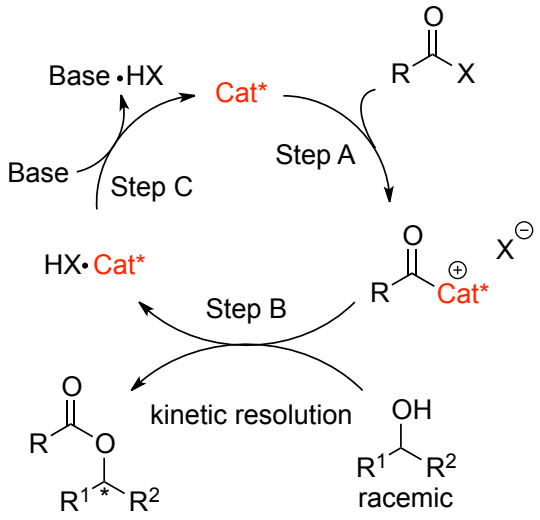


Scheme 3.3. Catalytic Cycle of an Asymmetric Nucleophilic Catalyst in the Kinetic Resolution of A Secondary Alcohol

A significant number of efficient acyl transfer catalysts has been developed for the kinetic resolution of racemic secondary alcohols and they can be divided into different groups, including 4-dialkylamino pyridine derivatives, *N*-alkylimidazoles, amidines, vicinal diamines, phosphines and phosphoric acids, *N*-heterocylic carbenes, etc.

**3.2.1.1. 4-Dialkylamino Pyridine Derived Chiral Catalyst**

Vedejs and Chen designed the first chiral 4-dimethylamino pyridine (DMAP) catalyst **3.1** with a chiral center incorporated on the 2-position of the pyridine ring. The kinetic resolution of secondary alcohols required stoichiometric amount of catalyst, excess Lewis acids and bases. The established principle showed that the closer the chirality center to the active reaction center, the lesser the activity the catalyst would exhibit.[15] This study provided a starting point for the design of chiral DMAP analogues in the application of secondary alcohol resolutions. Shortly after, Fu and coworkers independently designed and synthesized planar-chiral ferrocenyl DMAP analogues **3.2** with a chiral plane.[16] This type of catalyst realized the effective kinetic resolution

of variety of alcohols, amines, and diols with low catalyst loading. The incorporation of a ferrocene skeleton brought two advantages: it can differentiate two mirror planes of DMAP; on the other hand, the iron would increase the nucleophilicity of pyridine and stabilize the acylium cation intermediate.[17] Additionally, there were no substituents at the cyclopentadiene ring besides DMAP. The less hindered space at 2-position of DMAP won't affect the catalytic activity.

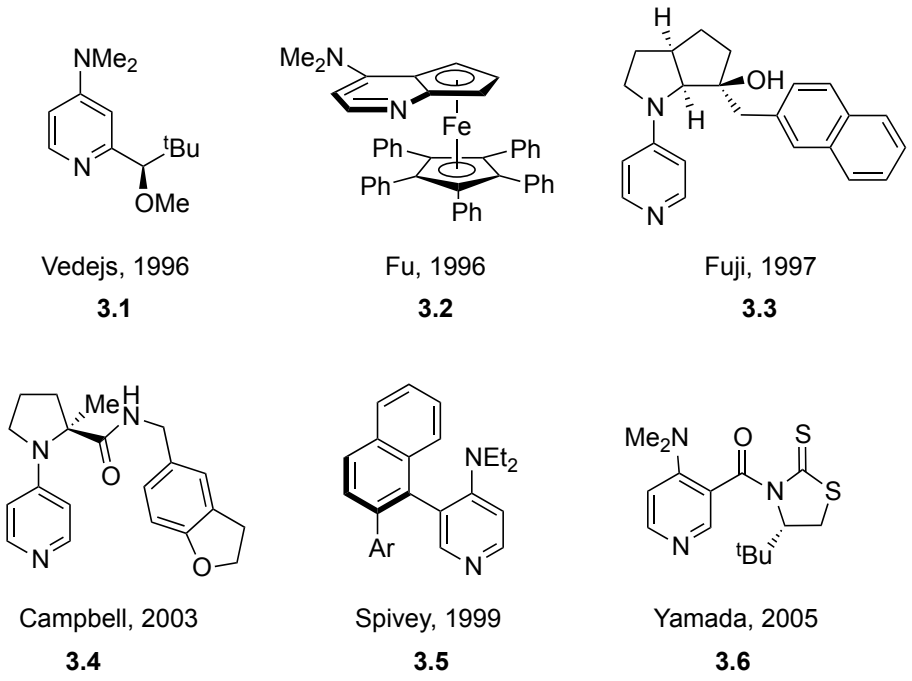


Figure 3.1. Selective Examples of 4-Dialkylamino Pyridine Chiral Catalysts for Kinetic Resolution of Alcohols

Fuji and coworkers designed chiral 4-pyrrolidinopyridine derivatives **3.3**, which promotes the kinetic resolution of racemic alcohols with $s$ = 4.7-12.3, through an "induced fit" mechanism like natural enzymes.[18] Campbell's chiral 4-pyrrolidinopyridine catalyst **3.4** is based on the proline chirality and is more efficient for the kinetic resolution of monoprotected *cis*-cyclohexane-1,2-diol than secondary monoalcohols.[19] Spivey and cowokers developed the first axially chiral 4-dialkylamino pyridine type catalyst **3.5**, which relied on the high rotation barrier

of aryl-aryl bond at 3-position of DMAP to form single atropisomer for kinetic resolution by acylation.[20] These catalysts provided moderate to good selectivities for the kinetic resolution of secondary alcohols. Yamada and coworkers developed a chiral DMAP catalyst possessing chiral thiazolidine-2-thione.[21] This type of catalyst was able to resolve allyl-alkyl, propargyl-alkyl, alkyl-alkyl alcohols, diols and *meso* diols with moderate to excellent selectivities. Besides the catalyst mentioned here, there are still some other chiral 4-dialkylamino pyridine derived catalysts, which showed high efficiency in the kinetic resolution of secondary alcohols (Figure 3.1).[22]

**3.2.1.2. Amidines**

Amidine derivatives became increasingly popular acyl transfer catalysts due to their high nucleophilicity. Birman and coworkers have developed a number of excellent catalysts for the kinetic resolution of secondary alcohols. Their first contribution in this area is the design of **3.7**, which was shown to be effective in the kinetic resolution of benzylic secondary alcohols.[23] The transition states are proposed to form π-π or cation-π interactions between the pyridinium ring of the catalyst and the aryl part of the alcohol. The alcohol enantiomer with less steric repulsive alkyl group orientation was favored. After several structure optimizations, the homobenzotetramisole (HBTM) core **3.8** seems to be efficient catalysts for the kinetic resolution of benzylic, cinnamoyl, propargyl and cyclic secondary alcohols.[24] Fossey and Deng group combined Birman's amidine design and Fu's planar chiral DMAP design principles to synthesize catalyst **3.9**, which exhibited remarkable selectivity control for the resolution of benzylic alcohols (Figure 3.2).[25]

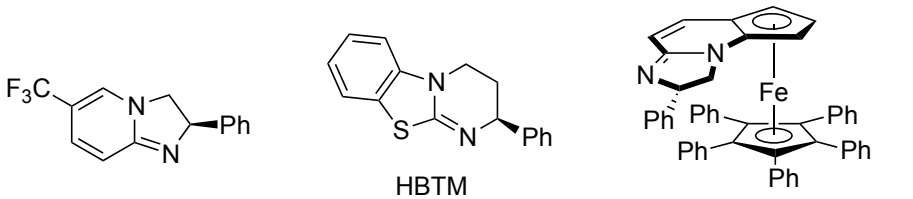


Birman, 2004 **3.7** | HBTM Birman, 2008 **3.8** | Deng and Fossey, 2010 **3.9**

Figure 3.2. Selective Examples of Amidine and Isothiourea Derivatives for the Kinetic Resolution of Secondary Alcohols

### 3.2.1.3. *N*-Alkylimidazoles

Miller and coworkers developed the first small peptide catalysts with nucleophilic *N*-alkylimidazole moiety for the kinetic resolution of secondary alcohols.[26] Later they developed a screening assay employing fluorescence and applied this assay to discover a highly selective octapeptide catalyst **3.10** for the kinetic resolution of aryl-alkyl and also alkyl-alkyl secondary alcohols.[27] Further studies showed that the peptide backbone might serve to recognize and stabilize the transition state leading to acylated product. The *p*-methyl histidine and *t*-trityl histidine moieties play an important role in the recognition.

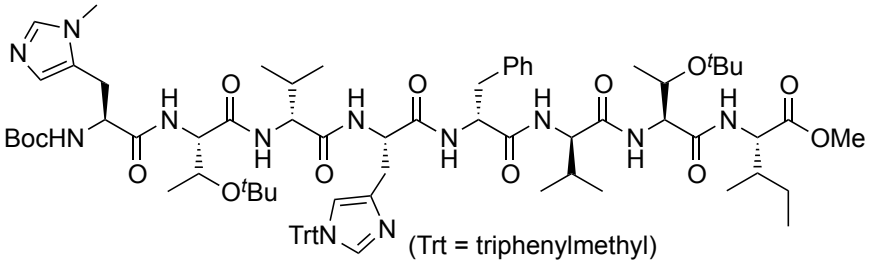


Miller, 2001 **3.10**

Figure 3.3. Selective Peptide Catalyst for the Kinetic Resolution of Secondary Alcohols

### 3.2.1.4. Vicinal Diamines and Phosphines

Oriyama and coworkers developed di(*tert*-amine) catalyst **3.11** based on chiral proline. **3.11** was proved to be highly selective in the kinetic resolution of racemic secondary alcohols.[28] Vedejs and coworkers first applied chiral phosphines in the kinetic resolutions. After catalyst structure exploration, the bicyclic phosphine catalysts **3.12** showed the best performance in the resolution of aryl-alkyl, aryl-aryl secondary alcohols.[29] Furthermore, phosphine catalyst **3.12** was also found efficient for the kinetic resolution of allylic alcohols and desymmetrizations. The π-π interactions between catalysts and substrates may play a role in the resolution process.

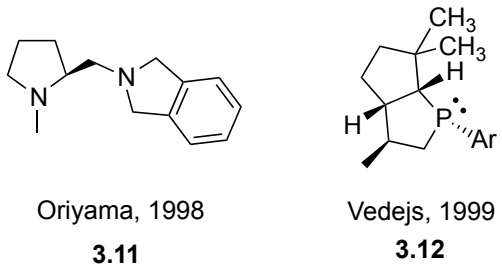


Oriyama, 1998 **3.11**

Vedejs, 1999 **3.12**

Figure 3.4. Selective Examples of Chiral Vicinal Diamine and Phosphine

### 3.2.1.5. *N*-Heterocyclic Carbenes

Suzuki group published the first example of *N*-heterocyclic carbene catalyzed acylative kinetic resolution of racemic secondary aryl-alkyl alcohols with moderate selectivities.[30] Later, Maruoka and coworkers found that in the presence of **3.13a** or **3.13b** (Scheme 3.4), vinyl diphenylacetate can be used as the acyl transfer agent to resolve aryl-alkyl and allyl-alkyl alcohols and increased the selectivities significantly.[31] The carbene is formed *in situ* after deprotonation of their precursor salts using strong base like $^{t}$BuOK. Compared to the acylation of secondary alcohols catalyzed by nucleophilic catalyst with acid chloride or acid anhydrides, these two examples proceeded via transesterification process.

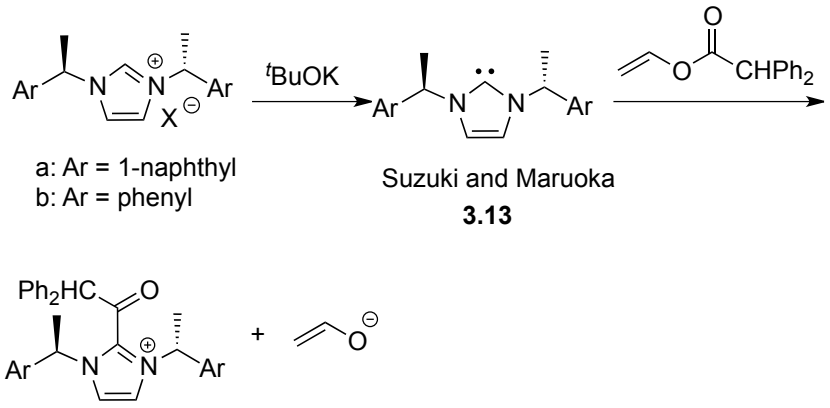


Scheme 3.4. Proposed Chiral Carbene Activation Process

Another way of asymmetric esterification of alcohols is employing chiral acyl azolium species generated from aldehydes catalyzed by oxidative *N*-heterocyclic carbene catalysis.[32] This strategy was initiated by the nucleophilic addition of chiral carbene to aldehyde to generate tetrahedral intermediate, followed by the oxidation to provide a chiral acylazolium ion and subsequent stereoselective acylation of the racemic alcohol (Scheme 3.5). Studer and coworkers reported the first case of NHC-catalyzed oxidative kinetic resolution of secondary alcohols and moderate to good selectivities were obtained using catalyst **3.14**.[33]

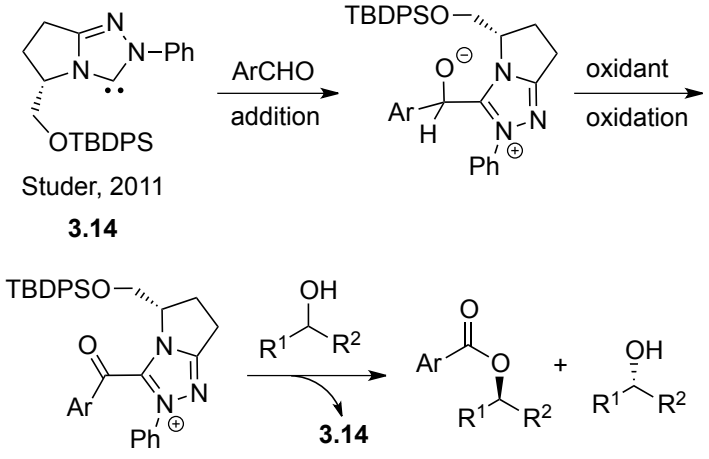


Scheme 3.5. Generation of Acylazolium Ions by NHC Catalyzed Oxidative Esterification

### 3.2.1.6. Chiral Phosphoric Acids and Thiourea Derivatives

Takasu and coworkers demonstrated the conventional method for kinetic resolution of secondary alcohols using chiral phosphoric acids.[34] Compared to the nucleophilic catalysts that generates chiral acylating reagents *in situ*, Brønsted acid can activate the acylating agent by hydrogen bonding. The binaphthyl-based phosphoric acid **3.15** with two nitro groups at the 6,6'-positions was found to promote the resolution of *cis*-2-arylcycloalkanol with high selectivities. Reaction procedure was simple and no additives were required. The geometry of proposed transition state was calculated and suggested the phosphonic acid played a bifunctional role involving selective coordination of one alcohol enantiomer and protonation of acyl agent[35] (Figure 3.5).

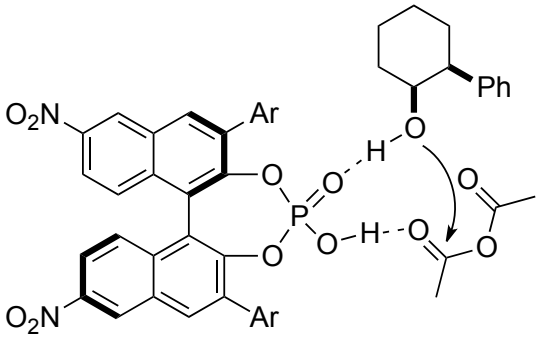


Ar = 2,4,6-(*i*Pr)$_3$C$_6$H$_2$

Takasu, 2013

**3.15**

Figure 3.5. Proposed Transition State for the Kinetic Resolution of Secondary Alcohols by Phosphonic Acid

The selective functionalization of a variety of hydroxyl groups in different molecules is an essential problem for molecular constructions. Besides the catalysts discussed above, others have also served as a tool for the kinetic resolution of a variety types of alcohols and provide a

catalyst library. The development of new selective catalysts for different hydroxyl groups' transformation is still an important task for the synthetic organic community.

### 3.2.2. Results and Discussion

The kinetic resolution of racemic secondary alcohols has always served as the primary testing reactions at the beginning of novel chiral dialkylamino pyridine development. Herein the synthesis of novel fluxionally chiral DMAP catalysts and their application in the acylative kinetic resolution of *sec*-alcohols is presented. In our design, we surmised that a fluxional group in the newly designed DMAP catalyst would be effective in relaying stereochemical information from the fixed chiral center to the catalytic center of pyridine ring, therefore the stereochemistry outcome could be controlled.

#### 3.2.2.1. Solvent Effects on the Kinetic Resolution of Secondary Alcohols

We initiated the evaluation of the kinetic resolution of *sec*-alcohols using 1-(2-naphthyl) ethanol *rac*-**3.16a** as a test substrate and isobutyric anhydride as acylation reagent (Table 3.1). Five different solvents were tested. Using THF as the solvent, we were pleased to see a selectivity factor of 9 (entry 1). Diethyl ether gave the best result among all the solvents tested (entry 2). Toluene as the solvent gave similar result as diethyl ether (entry 3). Interestingly, using more polar solvents, such as acetonitrile and dichloromethane, decreased selectivity factors were observed (entries 4 and 5). Diethyl ether was selected for further screening.

Table 3.1. Solvent Effects for the Kinetic Resolution of Secondary Alcohols

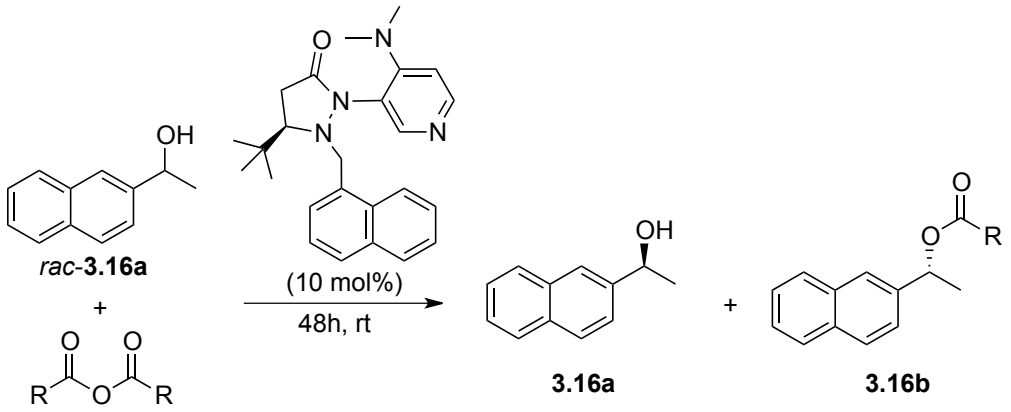


| entry | R | Solvents | Conv.(%) | *s* factor[a-c] |
|---|---|---|---|---|
| 1 | *i*-Pr | THF | 57 | 9 |
| 2 | *i*-Pr | $Et_2O$ | 59 | 12 |
| 3 | *i*-Pr | PhMe | 59 | 11 |
| 4 | *i*-Pr | $CH_3CN$ | 57 | 4 |
| 5 | *i*-Pr | $CH_2Cl_2$ | 55 | 6 |

[a] Conditions: racemic alcohol (1 equiv.) and anhydride (0.6 equiv.) in the presence of a chiral DMAP catalyst, solvent (2 ml), rt, 48h; [b] Conversions and selective factors were calculated by the method of Kagan and Fiaud: Conv. = $ee_{alcohol}$ / ($ee_{product}$ + $ee_{alcohol}$). *s* factor = ln[1-conv(1+$ee_{ester}$)] / ln[1-conv(1-$ee_{ester}$)]. [c] Determined by HPLC analysis.

### 3.2.2.2. Novel 4-Dialkylamino Pyridine Catalysts and Temperature Evaluation

Six different chiral DMAP catalysts were synthesized and evaluated in the kinetic resolution of secondary alcohols (Figure 3.6). Using 10 mol% catalyst loading and $Et_2O$ as solvent, the catalyst evaluation results are shown in table 3.2. Catalyst **3.17** bearing an *i*-propyl chiral group at the C-5 position and a benzyl fluxional group gave low selectivity for the resolution (*s* = 4, Table 3.2, entry 1). The selectivity factor (*s*) was largely influenced by the chiral substituent; replacement of the *i*-propyl group in **3.17** by the more sterically demanding *t*-butyl group (**3.18**) raised the *s* factor from 4 to 15 (entry 2). Increasing the size of the relay group from benzyl to 1-naphthylmethyl (**3.19**) gave the best result: *s* = 23 (entry 3). However, installing

an even larger 9-methylanthracenyl fluxional group (**3.20**) reduced selectivity compared to **3.19** (*s* = 14, entry 4). The dialkylamino group on the pyridine unit of the catalyst was also investigated and found to impact selectivity: **3.19** bearing a dimethylamino group gave higher selectivity (*s* = 23) than **3.20** (*s* = 11) or **3.21** (*s* = 9) with pyrrolidine or di-*n*-butylamino substituents respectively (Table 3.2, compare entry 3 with entries 5-6). Results of catalyst screening thus demonstrate that **3.19** is the best catalyst for the kinetic resolution of rac-**3.16a**. These results suggested that the size of the fluxional substituent, C-5 substituent as well as amino substituents on the pyridine ring could work together to affect the stereochemical outcome due to steric effects or electronic effects. $R^1$, $R^2$ and $R^3$ can be tuned to obtain the optimal enantiomeric control. Catalyst **3.19** was selected for the following evaluations.

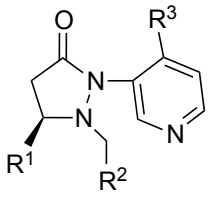


**3.17** $R^1$ = *i*-Pr, $R^2$ = phenyl, $R^3$ = dimethylamino

**3.18** $R^1$ = *t*-Bu, $R^2$ = phenyl, $R^3$ = dimethylamino

**3.19** $R^1$ = *t*-Bu, $R^2$ = 1-naphthyl, $R^3$ = dimethylamino

**3.20** $R^1$ = *t*-Bu, $R^2$ = 9-anthracenyl, $R^3$ = dimethylamino

**3.21** $R^1$ = *t*-Bu, $R^2$ = 1-naphthyl, $R^3$ = pyrrolidine

**3.22** $R^1$ = *t*-Bu, $R^2$ = 1-naphthyl, $R^3$ = di-*n*-butylamino

Figure 3.6. Fluxionally Chiral DMAP Catalysts

The effect of temperature was also investigated (Table 3.2). Using the optimal catalyst **3.19**, the inverse relationship was observed between the temperature and selectivity factor. When the temperature decreased, the selectivity factor increased correspondingly. At room temperature, kinetic resolution gave *s* factor = 12 (entry 7). Lowering the temperature to 0 °C, there was a remarkable increase of *s* factor compared to room temperature (entry 3). Lowering the

temperature from 0 °C (*s* = 23) to -10 °C (*s* = 24) showed limited improvement (entry 3 and entry 8). But when the reaction was carried out at -50 °C, the *s* factor increased dramatically to 37 (entry 9). Notably, in this case, addition of a base, such as 2,6-di-*tert*-butylpyridine, was detrimental to the selectivity (*s* = 22, entry 10).

Table 3.2. Catalyst and Temperature Screening

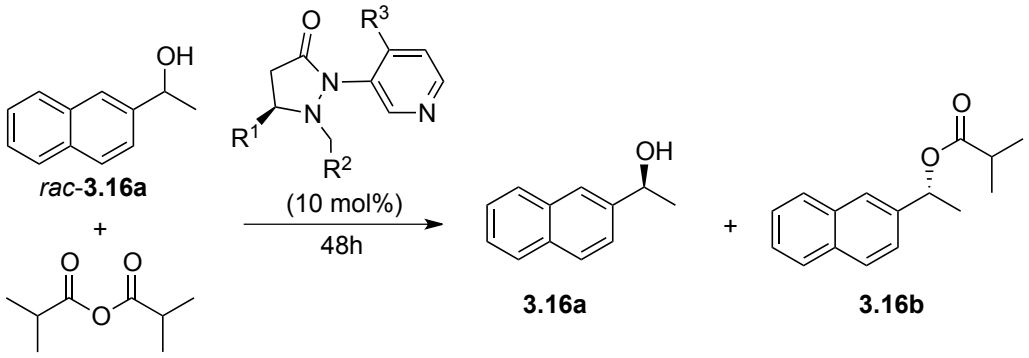


| entry | Cat. | Temp.(°C) | Conv.(%) | *s* factor[a-c] |
|---|---|---|---|---|
| 1 | **3.17** | 0 | 53 | 4 |
| 2 | **3.18** | 0 | 54 | 15 |
| 3 | **3.19** | 0 | 56 | 23 |
| 4 | **3.20** | 0 | 49 | 14 |
| 5 | **3.21** | 0 | 52 | 11 |
| 6 | **3.22** | 0 | 51 | 9 |
| 7 | **3.19** | rt | 59 | 12 |
| 8 | **3.19** | -10 | 57 | 24 |
| 9 | **3.19** | -50 | 47 | 37 |
| 10[d] | **3.19** | -50 | 47 | 22 |

[a]Conditions: racemic alcohol (1 equiv.) and anhydride (0.6 equiv.) in the presence of chiral catalysts, $Et_2O$ (2 ml), 48h; [b,c]see table 3.1 notes; [d]2,6-di-*tert*-butyl pyridine (0.6 equiv.) was added.

### 3.2.2.3. Evaluation of Different Anhydrides

Our screening of anhydrides revealed that isobutyric anhydride was optimal, affording higher selectivity factor than other anhydrides (Table 3.3, entry 2). Small anhydride acetic

anhydride showed similar selectivity as larger anhydride, like diphenylacetic anhydride (entry 1 and entry 3). Surprisingly, the use of 2-naphthyl substituted anhydride showed dramatically lower selectivity (entry 4).

Table 3.3. Evaluation of Different Anhydrides

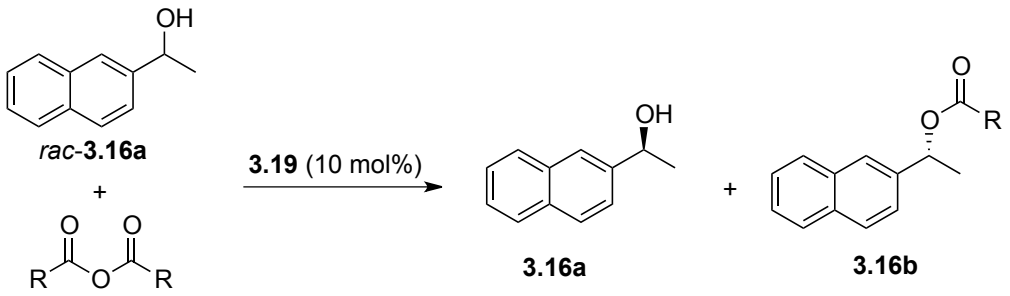


| entry | R | Conv.(%) | *s* factor[a-c] |
|---|---|---|---|
| 1 | $CH_3$ | 51 | 14 |
| 2 | *i*-Pr | 56 | 23 |
| 3 | $Ph_2CH$ | 33 | 15 |
| 4 | 2-Naphthyl | 4 | 2 |

[a] Conditions: racemic alcohol (1 equiv.) and anhydride (0.6 equiv.) in the presence of catalyst **3.19**, $Et_2O$ (2 ml), 0 °C, 48h; [b,c] see table 3.1 notes.

### 3.2.2.4. Substrate Scope for the Kinetic Resolution of Secondary Alcohols

On the basis of these investigations, we conducted the kinetic resolution of various racemic secondary alcohols with isobutyric anhydride (0.6 equiv.) and **3.19** (10 mol %) at -50 °C, and the results are summarized in Scheme 3.6.

The 2-naphthyl (*rac*-**3.16a**) and propargylic (*rac*-**3.27a**) alcohols could be efficiently resolved within 48 h with *s* factor = 17-37. In contrast, resolution of 1-naphthyl based alcohol, rac-**3.23a,** gave lower selectivity (*s* = 6). The steric bulk of the alkyl group on secondary alcohols **3.24a-3.26a** had a significant impact on selectivity factors. More bulky *t*-butyl (*rac*-**3.25a**, *s* = 10) and ethyl groups (*rac*-**3.26a**, *s* = 12) displayed higher selectivity factors than methyl substituted benzyl alcohol (*rac*-**3.24a**, *s* = 6).

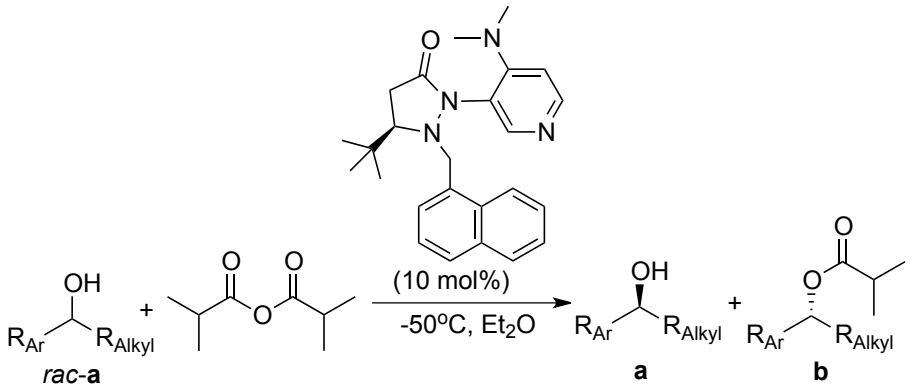


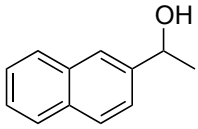

*rac*-**3.16a**

ester: 88%ee, alcohol: 77%ee
48h, 47% conv., *s* factor: 37

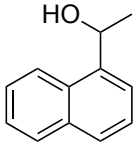

*rac*-**3.23a**

ester: 61%ee, alcohol: 44%ee
48h, 42% conv., *s* factor: 6

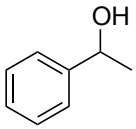

*rac*-**3.24a**

ester: 55%ee, alcohol: 61%ee
5d, 53% conv., *s* factor: 6

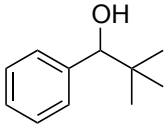

*rac*-**3.25a**

ester: 70%ee, alcohol: 57%ee
7d, 45% conv., *s* factor: 10

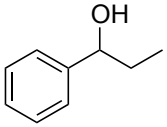

*rac*-**3.26a**

ester: 71%ee, alcohol: 67%ee
7d, 49% conv., *s* factor: 12

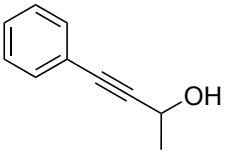

*rac*-**3.27a**

ester: 78%ee, alcohol: 73%ee
48h, 48% conv., *s* factor: 17

[a] Conditions: racemic alcohol (1 equiv.) and anhydride (0.6 equiv.) in the presence of chiral catalyst **3.19**, $Et_2O$ (2 ml), -50 °C; [b,c] see table 3.1 notes.

Scheme 3.6. Substrate Scope for the Kinetic Resolution of Secondary Alcohols[a,b,c]

### 3.2.3. Conclusion

In conclusion, we have developed an efficient non-enzymatic acylative kinetic resolution of racemic secondary alcohols with novel fluxionally chiral 4-dialkylamino pyridine catalysts. A number of secondary alcohols were resolved with moderate to good selectivities (*s* factor up to 37), which are comparable to other chiral pyridine catalysts in the kinetic resolution of secondary alcohols. The α-methyl-2-naphthalenemethanol was resolved with the best result. The suitable

substrates in this study are limited currently. Additionally, this study defined a new benchmark for the application of fluxional chirality in chiral catalyst design.

### 3.2.4. Experimental

#### 3.2.4.1. General

All solvents were dried and degassed by standard methods and stored under nitrogen. Flash chromatography was performed using EM Science silica gel 60 (230-400 mesh) or on an ISCO Combiflash. $^{1}$H NMR spectra were recorded on Varian Unity/Inova-400 NB (400 MHz) spectrometer or Bruker Ascend$^{TM}$ 400 (400 MHz for $^{1}$H) spectrometer. $^{13}$C NMR spectra were recorded on Varian Unity/Inova-400 NB (100 MHz) spectrometer or Bruker Ascend$^{TM}$ 400 (100 MHz for $^{13}$C) spectrometer. HPLC analyses were carried out with Waters 515 HPLC pumps and a 2487 dual wavelength absorbance detector connected to a PC with Empower workstation. High resolution mass spectra were obtained at a Bruker Daltonics BioTOF HRMS spectrometer. Racemic secondary alcohols are purchased from Sigma-Aldrich.

#### 3.2.4.2. General Procedure for the Kinetic Resolution of Racemic *sec*-Alcohols

To a solution of racemic alcohol (0.1 mmol) and catalyst (0.01 mmol) in 2 mL $Et_2O$ was added isobutyric anhydride (0.06 mmol) at -50 °C. After stirring for indicated time in Table 2, the reaction mixture was purified by column chromatography (hexane/ethyl acetate = 9/1) to afford alcohol and the corresponding ester. The optical purity of the alcohol was determined by HPLC, the conversion was determined using chiral HPLC, where conversion (%)= $ee_{alcohol}$ / ($ee_{alcohol}$ + $ee_{ester}$), the *s* factor = ln[1-conv(1+$ee_{ester}$)] / ln[1- conv(1-$ee_{ester}$)].

#### 3.2.4.3. Characterization of Recovered Substrates and Products

Rac-**3.16a**, *rac*-**3.23a**, *rac*-**3.24a**, *rac*-**3.25a**, *rac*-**3.26a** and *rac*-**3.27a** were purchased from Sigma-Aldrich®. The absolute configuration of the recovered alcohol **3.16a**, **3.23a**, **3.24a**,

**3.25a** and **3.26a** was assigned to be *S* by comparison with the known literature retention time on the same column which establishes that the major enantiomer is the *S* isomer.[36] **3.26a** was assigned by comparison with the known literature retention time.[37]

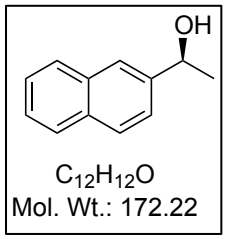


**3.16a** (77% ee) HPLC analysis: HPLC (UV 254 nm, Chiralpak OJ-H, *i*-PrOH/Hexane = 5/95, 1 mL/min), $t_1$ (major)= 28.2 min, $t_2$ (minor)= 38.3 min.

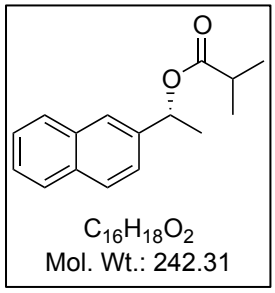


**3.16b** (88% ee) HPLC analysis: HPLC (UV 254 nm, Chiralpak OJ-H, *i*-PrOH/Hexane = 4/96, 1 mL/min), $t_1$ (major) = 8.5 min, $t_2$ (minor) = 11.7 min. $^1$H NMR ($CDCl_3$, 400 MHz) δ 1.19 (d, *J* = 7.2 Hz, 3H), 1.22 (d, *J* = 7.2 Hz, 3H), 1.62 (d, *J* = 6.8 Hz, 3H), 2.58-2.65 (m, 1H), 6.05-6.1 (m, 1H), 7.47-7.51 (m, 3H), 7.82-7.86 (m, 4H); $^{13}$C NMR ($CDCl_3$, 100 MHz) δ 19.2, 22.5, 34.4, 72.3, 124.3, 125.1, 126.2, 126.4, 127.9, 128.3, 128.6, 133.2, 133.5, 139.5, 176.5.

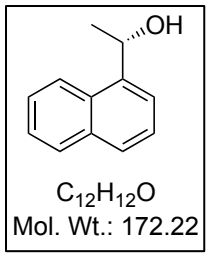


$C_{12}H_{12}O$
Mol. Wt.: 172.22

**3.23a** (44% ee) HPLC analysis: HPLC (UV 254 nm, Chiralpak OD-H, *i*-PrOH/Hexane = 4/96, 1 mL/min), $t_1$ (major)= 18.8 min, $t_2$ (minor)= 30.2 min.

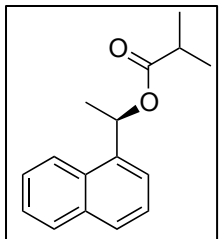


$C_{16}H_{18}O_2$
Mol. Wt.: 242.31

**3.23b** (61% ee). The ester obtained was hydrolyzed by heating to reflux in 5% NaOH/MeOH (2 mL) for 20 min and passed through a short flash silica column and eluted with ethyl acetate. The enantiomeric excess for the alcohol obtained by ester (**3.23b**) saponification was established by HPLC (UV 254 nm, Chiralpak OD-H, *i*-PrOH/Hexane = 4/96, 1.0 mL/min), $t_1$ (minor) = 18.5 min, $t_2$ (major) = 29.1 min. $^1$H NMR ($CDCl_3$, 400 MHz) δ 1.18 (d, $J$ = 7.2 Hz, 3H), 1.22 (d, $J$ = 7.2 Hz, 3H), 1.7 (d, $J$ = 6.8 Hz, 3H), 2.59-2.66 (m, 1H), 6.63-6.68 (m, 1H), 7.45-7.55 (m, 3H), 7.61 (d, $J$ = 7.2 Hz, 1H), 7.78-7.88 (m, 2H), 8.09 (d, $J$ = 8 Hz, 1H); $^{13}$C NMR ($CDCl_3$, 100 MHz) δ 19.2, 21.9, 34.5, 69.4, 123.3, 123.5, 125.6, 125.9, 126.4, 128.6, 129.1, 130.5, 134.1, 137.9, 176.5.

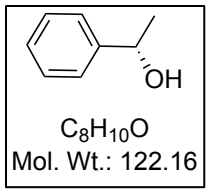


$C_8H_{10}O$
Mol. Wt.: 122.16

**3.24a** (61% ee) HPLC analysis: HPLC (UV 254 nm, Chiralpak OD-H, *i*-PrOH/Hexane = 1/99, 1 mL/min), $t_1$ (minor)= 23.0 min, $t_2$ (major)= 31.4 min.

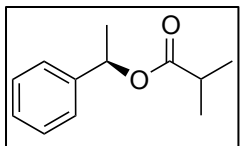


$C_{12}H_{16}O_2$
Mol. Wt.: 192.25

**3.24b** (55% ee) The ester obtained was hydrolyzed by heating to reflux in 5% NaOH/MeOH (2 mL) for 20 min and passed through a short flash silica column and eluted with EtOAc. The enantiomeric excess for the alcohol obtained by ester (**3.24b**) saponification was established by HPLC (UV 254 nm, Chiralpak OD-H, *i*-PrOH/Hexane = 1/99, 1.0 mL/min), $t_1$ (major) = 23.6 min, $t_2$ (minor) = 34.6 min. $^1$H NMR ($CDCl_3$, 400 MHz) δ 1.15 (d, $J$ = 6.8 Hz, 3H), 1.18 (d, $J$ = 6.8 Hz, 3H), 1.52 (d, $J$ = 6.8 Hz, 3H), 2.53-2.6 (m, 1H), 5.85-5.9 (m, 1H), 7.24-7.35 (m, 5H); $^{13}$C NMR ($CDCl_3$, 100 MHz) δ 19.1, 22.5, 34.4, 72.1, 126.1, 127.9, 128.7, 142.2, 176.5.

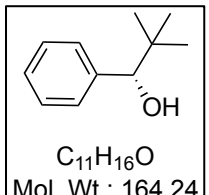


$C_{11}H_{16}O$
Mol. Wt.: 164.24

**3.25a** (57% ee) HPLC analysis: HPLC (UV 254 nm, Chiralpak OD-H, *i*-PrOH/Hexane = 3/97, 0.5 mL/min), $t_1$ (major)= 19.0 min, $t_2$ (minor)= 24.5 min.

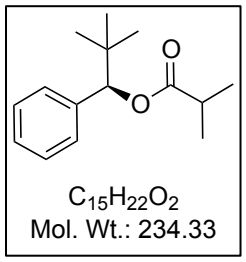


$C_{15}H_{22}O_2$
Mol. Wt.: 234.33

**3.25b** (70% ee). The ester obtained was hydrolyzed by heating to reflux in 5% NaOH/MeOH (2 mL) for 20 min and passed through a short flash silica column and eluted with EtOAc. The enantiomeric excess for the alcohol obtained by ester (**3.25b**) saponification was established by HPLC (UV 254 nm, Chiralpak OD-H, *i*-PrOH/Hexane = 3/97, 0.5 mL/min), $t_1$ (minor) = 19.1 min, $t_2$ (major) = 24.1 min. $^1$H NMR ($CDCl_3$, 400 MHz) δ 0.92 (s, 9H), 1.17 (d, *J* = 6.8 Hz, 3H), 1.19 (d, *J* = 7.2 Hz, 3H), 2.56-2.63 (m, 1H), 5.46 (s, 1H), 7.23-7.28 (m, 5H); $^{13}$C NMR ($CDCl_3$, 100 MHz) δ 19.1, 19.2, 26.3, 34.0, 34.6, 35.4, 82.6, 127.6, 127.8, 127.9, 138.8, 176.0.

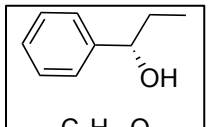


$C_9H_{12}O$
Mol. Wt.: 136.19

**3.26a** (67% ee) HPLC analysis: HPLC (UV 254 nm, Chiralpak OD-H, *i*-PrOH/Hexane = 2/98, 0.5 mL/min), $t_1$ (minor)= 28.8 min, $t_2$ (major)= 36.5 min.

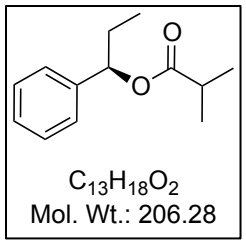


$C_{13}H_{18}O_2$
Mol. Wt.: 206.28

**3.26b** (71% ee). The ester obtained was hydrolyzed by heating to reflux in 5% NaOH/MeOH (2 mL) for 20 min and passed through a short flash silica column eluted with EtOAc. The enantiomeric excess for the alcohol obtained by ester (**3.26b**) saponification was established by HPLC (UV 254 nm, Chiralpak OD-H, *i*-PrOH/Hexane = 2/98, 0.5 mL/min), $t_1$ (major) = 28.5 min, $t_2$ (minor) = 36.1 min. $^1$H NMR ($CDCl_3$, 400 MHz) δ 0.88 (d, *J* = 7.2 Hz, 3H), 1.14 (d, *J* = 6.8 Hz, 3H), 1.18 (d, *J* = 6.8 Hz, 3H), 1.76-1.94 (m, 2H), 2.54-2.60 (m, 1H), 5.64-5.67 (m, 1H), 7.24-7.34 (m, 5H); $^{13}$C NMR ($CDCl_3$, 100 MHz) δ 10.1, 19.1, 19.2, 29.7, 34.4, 77.1, 126.6, 127.9, 128.5, 141.1, 176.5.

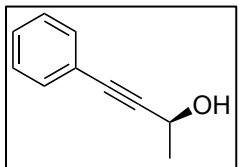


$C_{10}H_{10}O$
Mol.Wt.: 146.19

**3.27a** (73% ee) HPLC analysis: HPLC (UV 254 nm, Chiralpak OD-H, *i*-PrOH/Hexane = 3/97, 1 mL/min), $t_1$ (minor)= 15.9 min, $t_2$ (major)= 53.9 min.

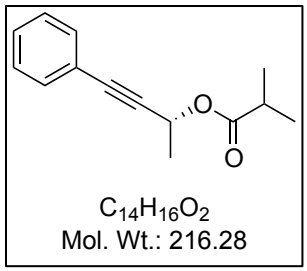


$C_{14}H_{16}O_2$
Mol. Wt.: 216.28

**3.27b** (78% ee). The ester obtained was hydrolyzed by heating to reflux in 5% NaOH/MeOH (2 ml) for 20 min and passed through a short flash silica column and eluted with EtOAc. The enantiomeric excess for the unreacted alcohol (*S*)-**6a** and the alcohol obtained by ester (**6b**) saponification was established by HPLC (UV 254 nm, Chiralpak OD-H, *i*-PrOH/Hexane = 3/97, 1.0 mL/min), $t_1$ (major) = 15.4 min, $t_2$ (minor) = 53.2 min. $^1$H NMR ($CDCl_3$, 400 MHz) δ 1.17-1.19 (m, 6H), 1.55 (d, *J* = 6.8 Hz, 3H), 2.53-2.60 (m, 1H), 5.66-5.71 (m, 1H), 7.24-7.30 (m, 3H), 7.41-7.43 (m, 2H); $^{13}$C NMR ($CDCl_3$, 100 MHz) δ 19.0, 19.1, 21.7, 34.2, 60.7, 84.6, 87.8, 122.6, 128.4, 128.7, 132.0, 176.2.

### 3.3. Kinetic Resolution of Axially Chiral Biaryls

#### 3.3.1. Background

In principle, the two conformers of biaryl scaffolds can interconvert thermally through a single bond. Atropisomerism refers to stereoisomerism resulting from hindered rotation around a single bond where the energy barrier to rotation is high enough to allow for the isolation of the conformers[38] thus for those with a half-life of interconversion of ~1000s or longer, analytical separation is possible (Figure 3.7).[39]

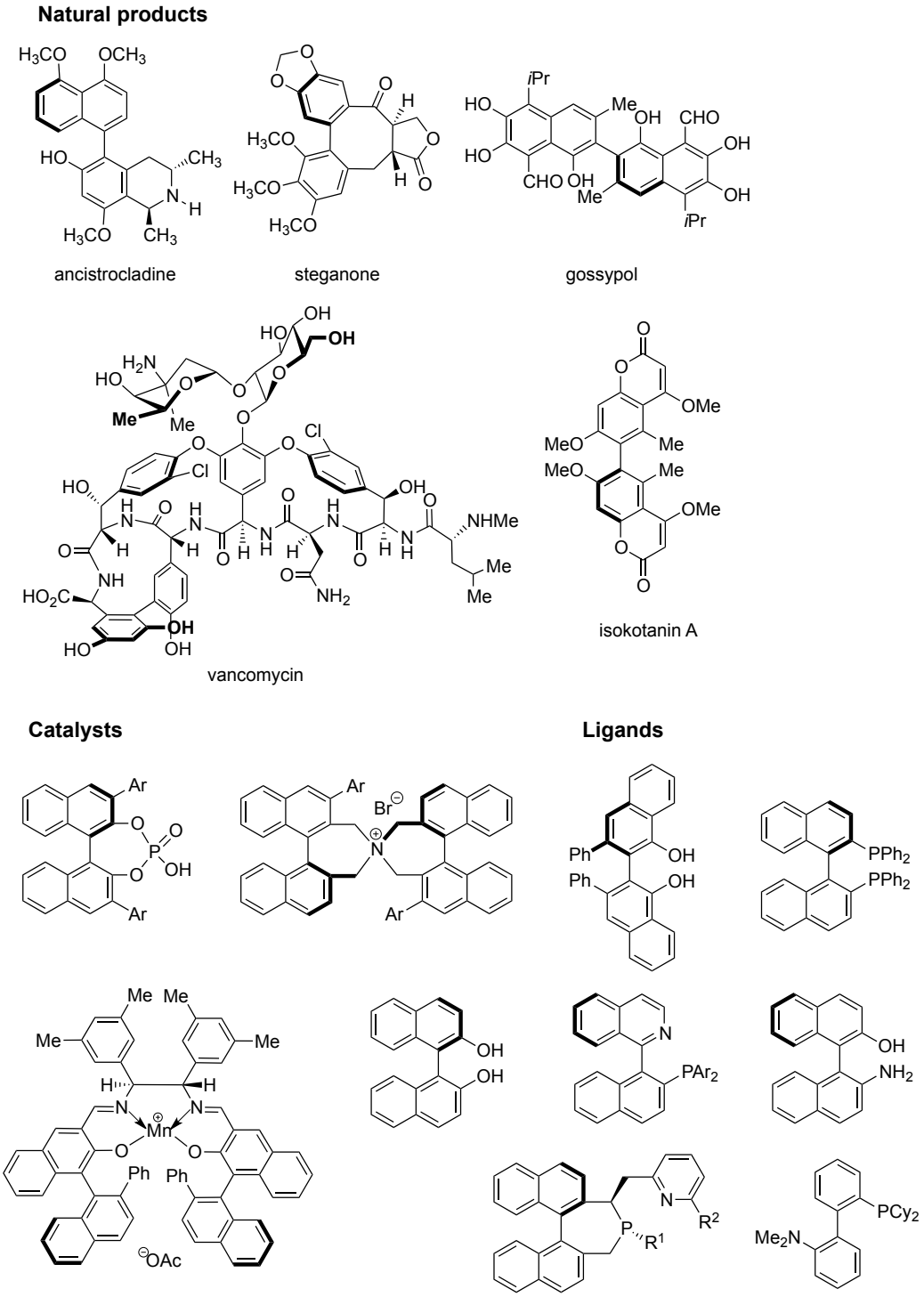


Figure 3.7. Selected Examples of Axially Chiral Molecules in Natural Products, Catalysts and Ligands

The importance of atropisomers arises to a significant degree from their stability as they can display axial chirality. This form of chirality most frequently occurs in biaryls and nonbiaryls. Ryoji Noyori was co-awarded the Nobel Prize in Chemistry, in part for his work with highly selective catalysts derived from the axially chiral 2,2'-bis(diphenylphosphino)-1,1'-binaphthyl (BINAP) ligand.[40] Chiral biaryl skeletons are prolific among useful organic molecules. The unique structures and special biological activities make the investigation of axially chiral natural biaryls highly attractive.[41] Axially chiral molecules also process excellent chiral control elements and serve as a privileged scaffold for chiral auxiliaries, ligands, and catalysts in asymmetric synthesis.[42] $C_2$-symmetric dihydroxy biaryl derivatives have been extensively applied in a variety of enantioselective processes.[43]

Owing to the importance of axially chiral biaryl compounds, a variety of synthetic approaches to this structural motif have been developed. These can be divided into three major categories.[44] They are: (1) stereoselective biaryl coupling of two aryl counterparts, (2) kinetic resolution/desymmetrization of prostereogenic biaryls and (3) aryl axis formation from non-aryl substituents attached to an aromatic ring.

The first example of kinetic resolution of 2,2'-dihydroxy-1,1'-binaphthyl via a microbial asymmetric hydrolysis of diester of dihydroxy binaphthyl was reported by Ikekawa group in 1985.[45] Two years later, Miyano and coworkers reported that a commercial porcine pancreatic lipase (PPL) could be utilized as an atropselective hydrolysis reagent for 2,2'-dihydroxy-1,1'-binaphthyl based valeric acid diester **3.28**.[46] The reaction was carried out by vigorously stirring an emulsion of *rac*-**3.28** in EtOH/hexane/0.1M phosphate buffer with PPL. When the reaction was terminated at 46% conversion, (*S*)-**3.29** was obtained with 95 %ee (Scheme 3.7).

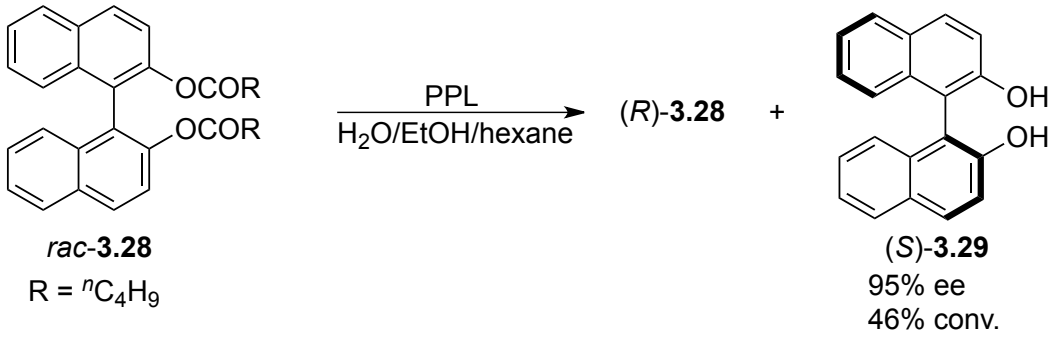


Scheme 3.7. Enzymatic Hydrolysis of Racemic 1,1'-Binaphthyl-2,2'-Diester

Later, Aoyagi group and Seki group developed an enzymatic kinetic resolution of biaryl compounds by introducing variety of microorganisms and high enantiomeric excess was obtained in most cases.[47] Although the enzymatic kinetic resolution strategy is a widely used method, this strategy can suffer from drawbacks such as high cost, stability of the catalyst, less solvent choices, and narrow substrate scope. The non-enzymetic kinetic resolution was much more attractive for the kinetic resolution of biaryls.

Palladium catalyzed kinetic resolution of 2,2'-dihydroxy-1,1'-biaryls by atropselective alcoholysis of their vinyl ethers was reported by Tsuji, Tokunaga and coworkers (Table 3.4).[48] The ligand derived from (*R*,*R*)-1,2-cyclohexanediamine **3.31** showed higher selectivity than other diamine ligands. In addition, the effect of the relative bulkiness of the acyl group on BINOL was examined. The nonacylated compound **3.30a** showed almost no selectivity. The selectivity factor increased from **3.30b** < **3.30c** < **3.30d** < **3.30e** with larger substituents on BINOL. The scope of this reaction system was applicable to different types of substrates, including 1,1'-bi-phenols as well as 1,1'-bi-2-naphthols, giving moderate to high selectivity (*s* factor = 12.1-35.8).

Table 3.4. Atropselective Alcoholysis Kinetic Resolution of 2,2'-Dihydroxy-1,1'-Biaryls Catalyzed by Palladium Catalyst

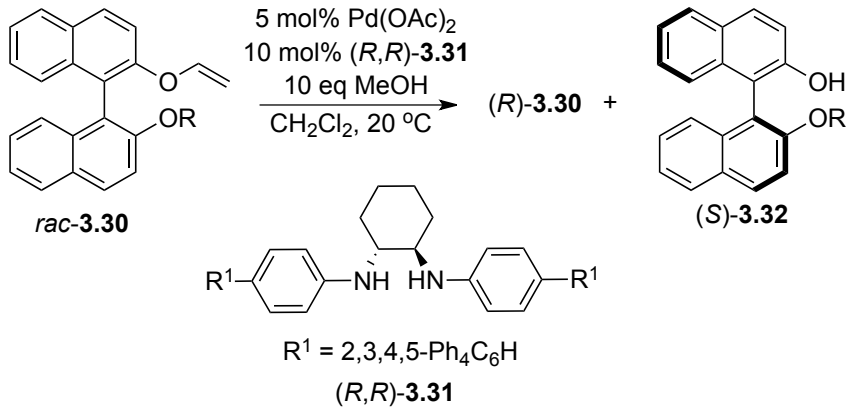


| Entry | BINOL (*rac*) | R | % conv. | % ee (*R*)-**3.30** | % ee (*S*)-**3.32** | *s* factor |
|---|---|---|---|---|---|---|
| 1 | **3.30a** | H | 43 | 4 | 6 | 1.1 |
| 2 | **3.30b** | $COCH_3$ | 49 | 54 | 57 | 6.1 |
| 3 | **3.30c** | $CO(^nC_6H_{13})$ | 44 | 61 | 77 | 14.3 |
| 4 | **3.30d** | $CO(^tBu)$ | 58 | 96 | 69 | 20.3 |
| 5 | **3.30e** | CO(1-adamantyl) | 56 | 96 | 77 | 28.7 |

Axially chiral amino compounds have found many applications in the synthesis of chiral ligands, catalysts, and biologically active compounds. An efficient approach towards the kinetic resolution of axially chiral 2-amino-1,1'-biaryls by a phase-transfer-catalyzed *N*-allylation method was developed by Maruoka and coworkers in 2013 (Scheme 3.8).[49]

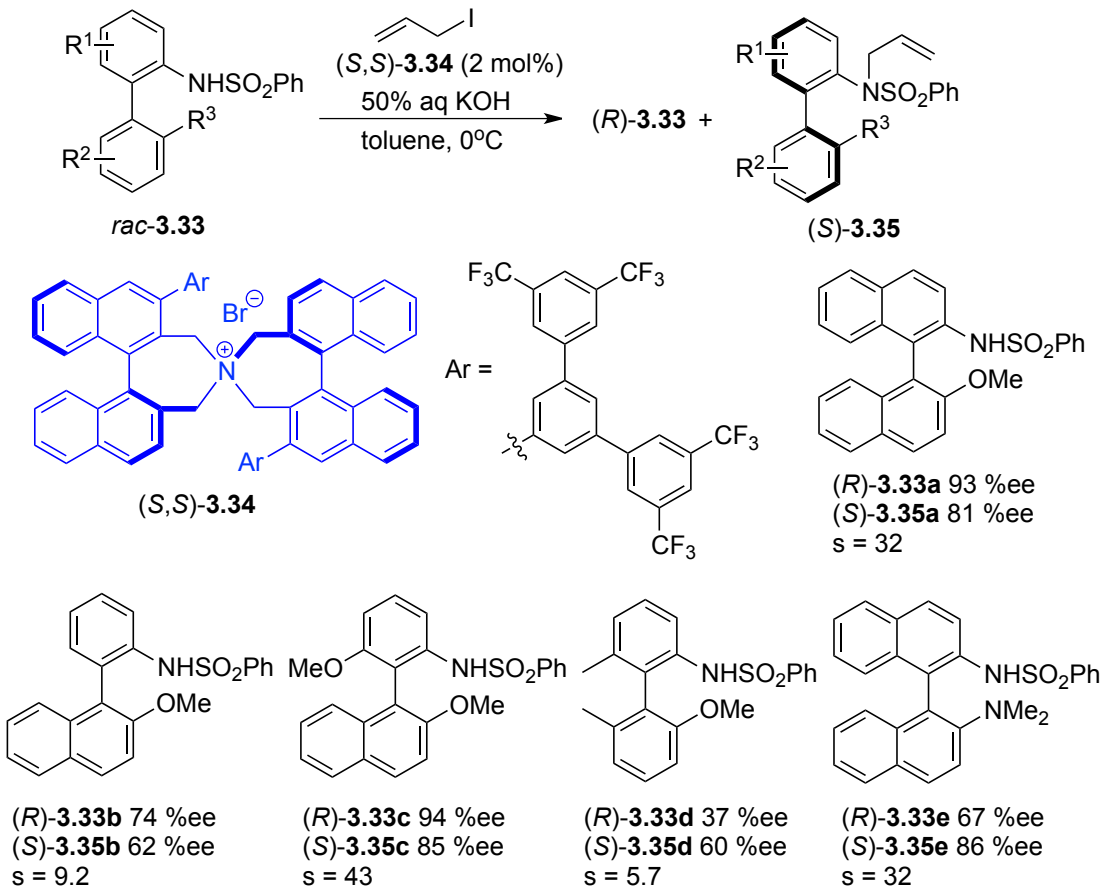


Scheme 3.8. Kinetic Resolution of Axially Chiral 2-Amino-1,1'-Biaryls by a Phase-Transfer-Catalyzed *N*-Allylation

They proposed that a phase-transfer catalyst might directly interact with axially chiral amino compounds by the formation of an ion pair, which may facilitate the efficient chiral recognition of the amino compound. The asymmetric alkylation was catalyzed by a binaphthyl-modified chiral quaternary ammonium salt (*S*,*S*)-**3.34**. The reaction conditions could tolerate substrates containing binaphthyl or biphenyl structures. 2-Amino-1,1'-biaryls possessing other functional groups were also tolerated in this kinetic resolution. Good to high selectivities were achieved in this process.

Tan, Liu, Tian and coworkers developed the kinetic resolution of axially chiral 1,1'-binaphthyl-2,2'-diamine (BINAM) with high selectivity factors.[50] This work used a chiral

Brønsted acid-catalyzed imine formation and transfer hydrogenation cascade process (Scheme 3.9). They found that the installation of a bulky group in one of the amines of racemic BINAM could increase the rotation energy barrier and provide steric interaction to improve enantioselectivity. The reaction was performed between racemic BINAM **3.36** and aryl aldehyde, using chiral phosphoric acid **3.37** as the Brønsted acid catalyst and Hantzsch ester **3.38** as a hydride source in ethyl acetate at room temperature. Screening of functional groups on the aldehydes showed that 2-naphthaldehyde gave the best result in terms of stereoselectivity for both the product and recovered starting material, suggesting that an aromatic stacking interaction during the transfer hydrogenation step. This reaction also showed excellent compatibility with different types of protecting groups. Furthermore, the reaction also tolerated functional groups at the 6-position or 6,6'-positions of BINAM skeleton of the substrates, such as *rac*-**3.36d**, *rac*-**3.36e**, etc. The substrates with silicon-based functional groups also showed excellent *s* factor (*rac*-**3.36f**). Further study demonstrated that the first imine formation step might not be the stereo determining step in the resolution, but the cooperation of Hantzsch ester and phosphoric acid for the transfer hydrogenation might play a role in the kinetic resolution process.

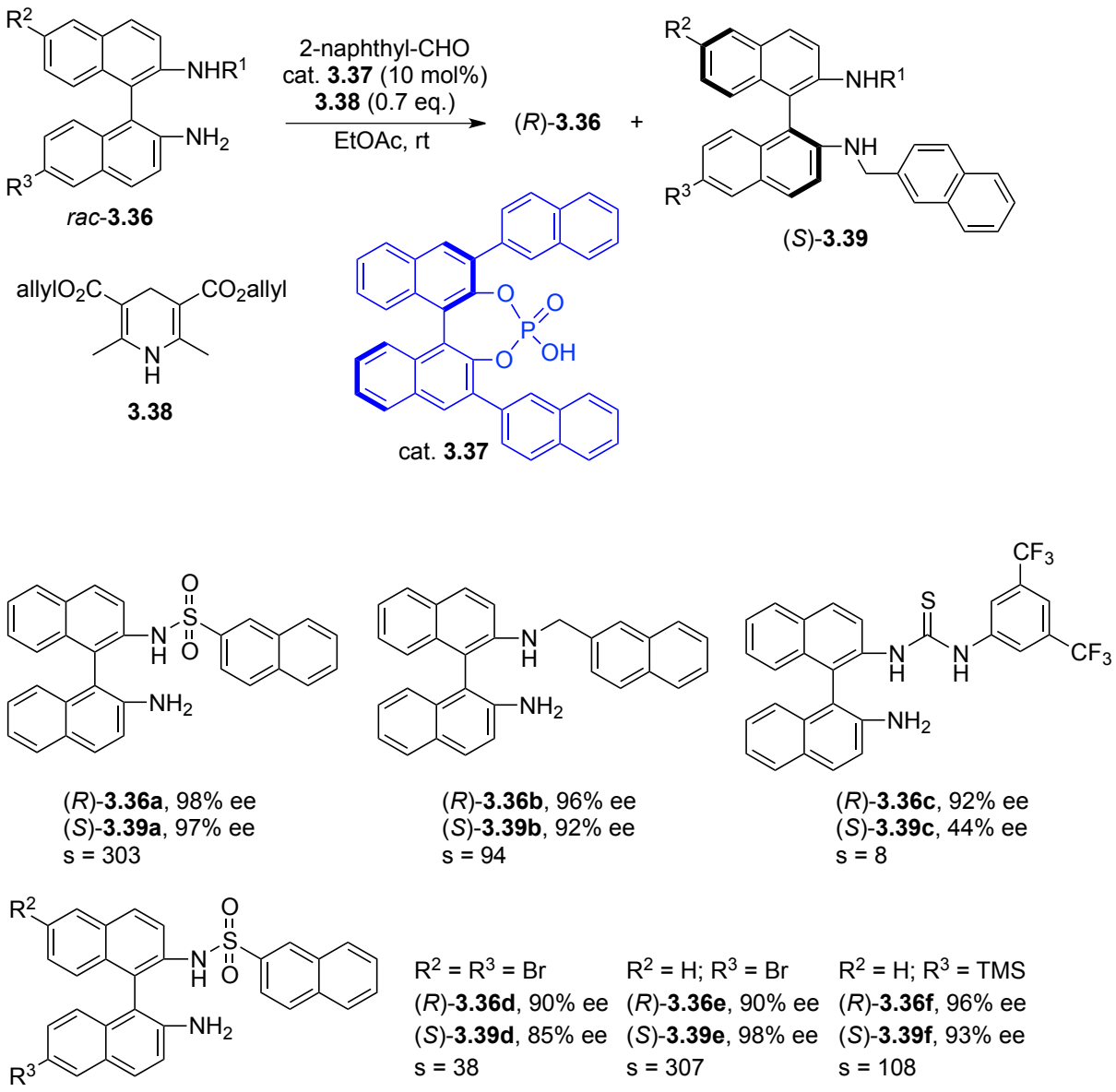


Scheme 3.9. Kinetic Resolution of BINAM by Chiral Brønsted Acids

A *N*-heterocylic carbene (NHC)-catalyzed atroposelective kinetic resolution of 1,1'-biaryl-2,2'-diols (BINOL) and protected 2-amino-2'-hydroxy-1,1'-binaphthyls (NOBIN) was reported by Zhao and coworkers (Scheme 3.10).[51] The selectivity in the resolution was largely influenced by the aldehyde substituent, which is incorporated into the chiral acyl azolium intermediate and has a significant effect on the enantioselectivity of the process.

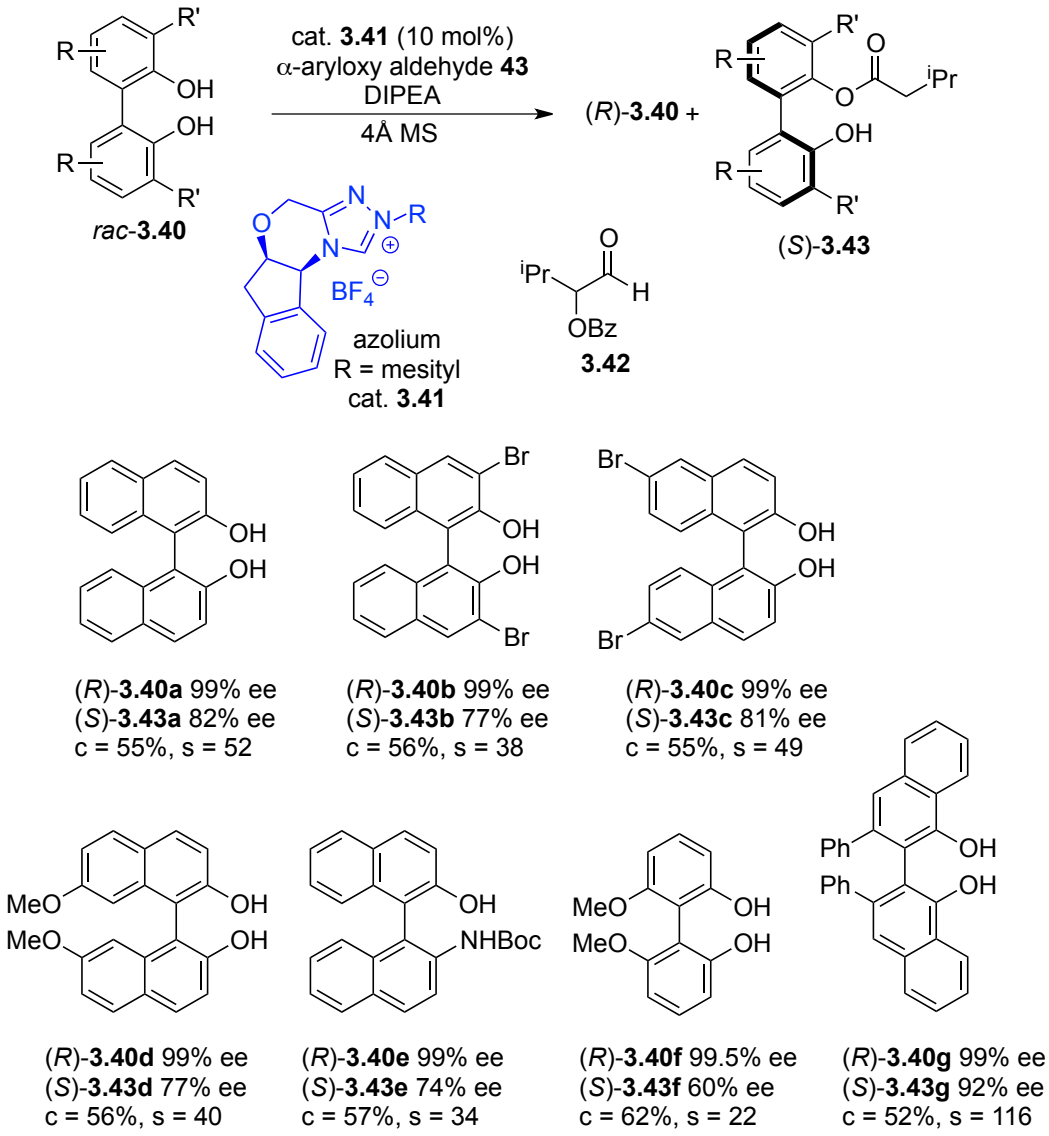


Scheme 3.10. *N*-Heterocyclic Carbene Catalyzed Kinetic Resolution of Axially Chiral Biaryls

After screening many different aldehydes, a α-aryloxy aldehyde showed the best result. The scope of this catalytic system is very broad. Various binaphthyl and biphenyl diols with different substitution patterns were tested and all substrates were recovered in ≥99 %ee. For the different binaphthyl diols such as *rac*-**3.40a**, *rac*-**3.40b**, *rac*-**3.40c**, *rac*-**3.40d**, *etc*, the substitution pattern did not have a significant impact on selectivities. Substrates *rac*-**3.40f** containing a biphenyl showed relatively lower selectivity. Remarkably, the widely used ligand

VANOL *rac*-**3.40g** with phenyl substituent was resolved with an excellent selectivity of 116. It was also discovered that the kinetic resolution of acyl- or Boc-protected NOBIN worked well with *s* factor = 34 (*rac*-**3.40e**). Further study found that an intramolecular H-bond interaction between the two phenols (or with aniline) of the substrate presumably increases the nucleophilicity of the substrate and/or help to organize the substrate conformation leading to better enantioselectivity.

Spivey and coworkers developed the first organocatalytic kinetic resolution of the atropisomeric anilines (Scheme 3.11).[52] In this work, the chiral pyridine-based nucleophilic catalyst was used to selectively *N*-acylate one isomer of NOBIN derivative *rac*-**3.44**. Attempted *N*-acylative kinetic resolution of atropisomeric aniline *rac*-**3.44** was achieved with a selectivity factor of 4.4±1 at 31.4% conversion using just 1 mol% of catalyst **3.45**. This is the only example of chiral DMAP catalyzed acylative kinetic resolution of 1,1'-binaphthyl derivatives proceeding with modest selectivities.

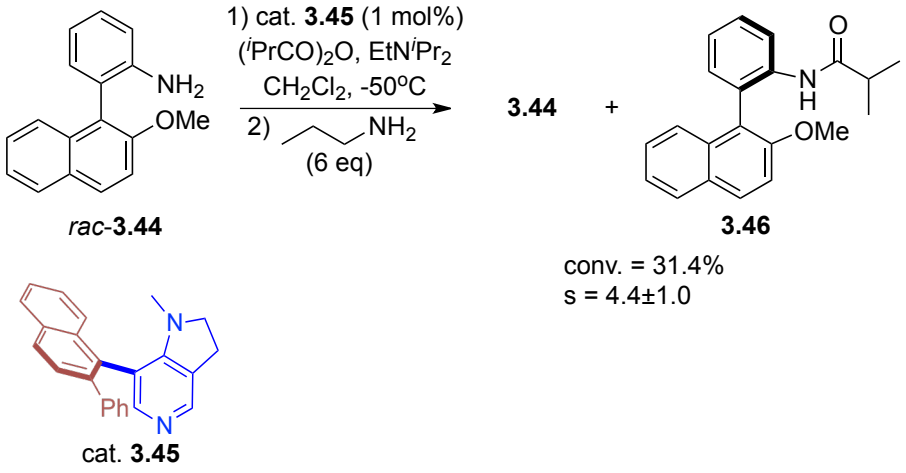


Scheme 3.11. Kinetic Resolution of Atropisomeric Aniline using Axially Chiral 4-Dialkylamino Pyridine Derivatives

### 3.3.2. Results and Discussion

Encouraged by the previous results of kinetic resolution of *sec*-alcohols catalyzed by fluxionally chiral 4-dialkylaminopyridine catalysts, we began the study on kinetic resolution of biaryl compounds. Our investigation started with the acylation of dihydroxy biaryl compounds. Optically active 2,2'-dihydroxy-1,1'-biaryls have received significant attention as they are highly effective as ligands and also serve as precursors for the synthesis of many important biaryl compounds.

#### 3.3.2.1. Kinetic Resolution Study of (±)-1,1'-Bi(2-naphthol) (BINOL) by Chiral Dialkylamino Catalysts

At the beginning, we selected (±)-1,1'-Bi(2-naphthol) (BINOL) *rac*-**3.47** as the dihydroxy substrate for reaction condition optimization. It reacted with half amount of isobutyric anhydride in the presence of 5 mol% catalyst **3.19** and produced the acylated product **3.47b**. The unreacted Bi(2-naphthol) was recovered with a low selectivity factor (Scheme 3.12, $s$ = 1.8).

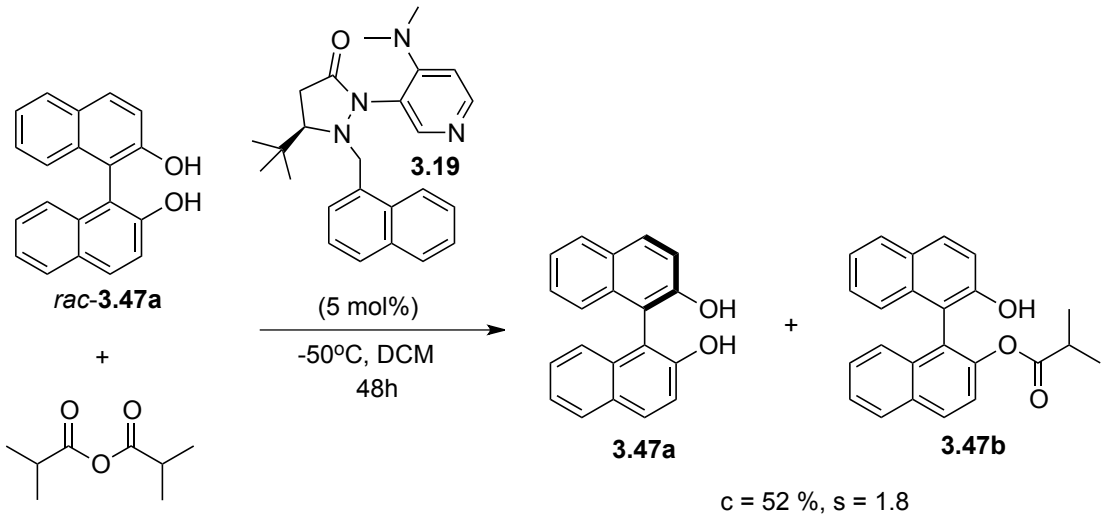


Scheme 3.12. Kinetic Resolution of (±)-1,1'-Bi(2-naphthol) by Chiral DMAP Catalyst

### 3.2.2.2. Catalyst Screening Study of (±)-Bi-2-Naphthol

Considering two reactive hydroxyl groups on Bi-2-naphthol might contribute more background reactions, we set out to synthesize mono-hydroxyl substituted biaryl compound 1,1'-binaphthalen-2-ol *rac*-**3.49a** and investigated its reactivity in the chiral DMAP catalyst (Scheme 3.13). To our delight, at -50 °C in the presence of catalyst **3.19**, the selectivity factor for *rac*-**3.49a** was improved to 10. We started to evaluate different chiral 4-dialkylamino pyridine catalysts to examine effect of the substituents. The N1 fluxional group was found to affect the selectivity. It seems that when N1 was substituted by 1-naphthylenemethyl group, the reaction gave the optimal selectivity. However, smaller size like benzyl substituted **3.18**, less sterically demanding 2-naphthylene-methyl substituted **3.50** and larger 9-anthracene-methyl substituted **3.20** lowered the selectivity. This observation suggested that the proper size of fluxional group is crucial to control the selectivity. Replacing *tert*-butyl substituent on C5 with *iso*-propyl group (**3.17**) led to poor selectivity. The dialkylamino group evaluation showed the **3.19** bearing dimethylamino group is still the best choice. Moreover, pyrrolidine substituted catalyst **3.21** provided much higher selectivity than di-*tert*-butylamino substituted **3.22**.

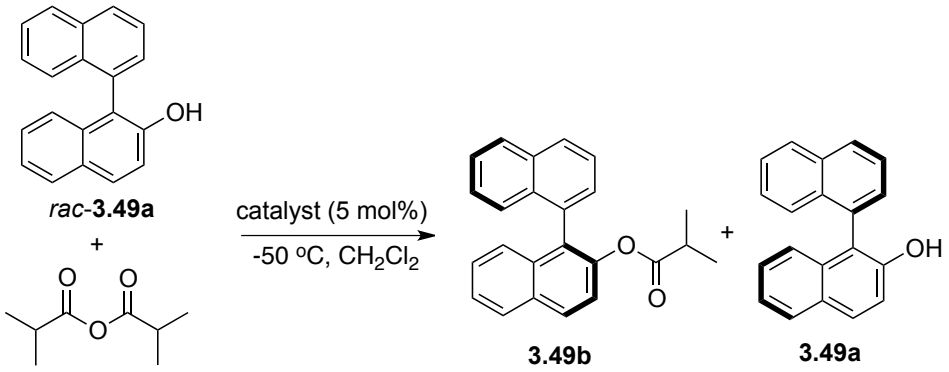


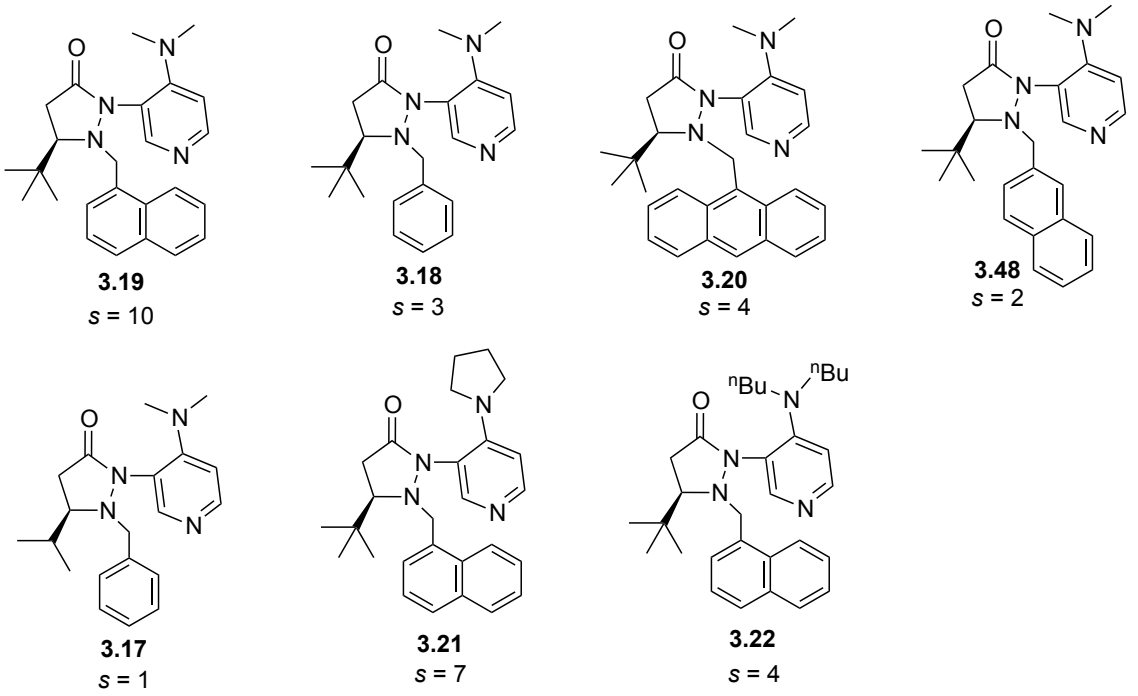


Scheme 3.13. Catalysts Screening for Kinetic Resolution of 1,1'-Binaphthalen-2-ol

### 3.3.2.3. Solvents and Anhydrides Effect Investigation of (±)-Bi-2-naphthol

The anhydride screening results showed isobutyric anhydride is still the best acylating reagent in this study (Table 3.5, entry 3). The selectivity factor increased gradually as the size of acyl group increased from acetic anhydride to propionic anhydride to isobutyric anhydride (entries 1-3). The bulky anhydride, such as trimethylacetic anhydride, exhibited low reactivity

and moderate selectivity (entry 4). The kinetic resolution with aliphatic anhydride gave higher selectivity than aromatic anhydride in this case.

Table 3.5. Anhydride Screening in the Kinetic Resolution of Biaryl Compound

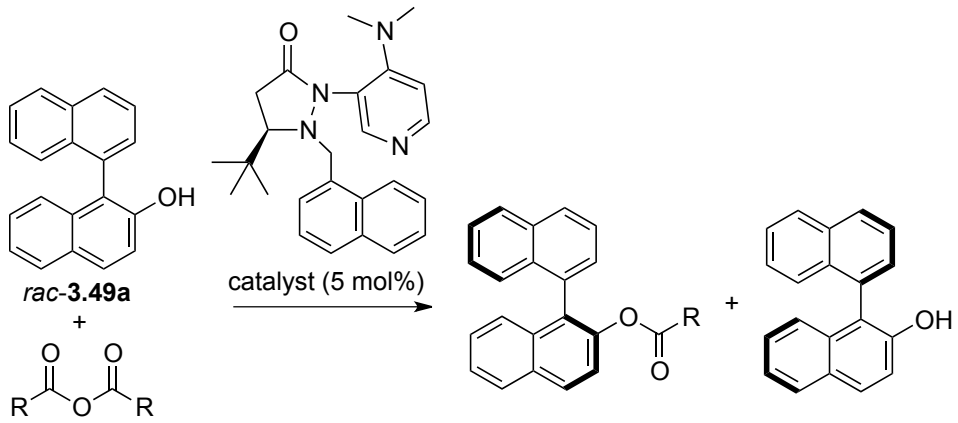


| entry | R | Solvent | Time | Temp.(°C) | Conv.(%) | *s* factor[a-c] |
|---|---|---|---|---|---|---|
| 1 | Methyl | $CH_2Cl_2$ | 2d | -50 | 35 | 3 |
| 2 | Ethyl | $CH_2Cl_2$ | 2d | -50 | 28 | 5 |
| 3 | *iso*-Propyl | $CH_2Cl_2$ | 4d | -50 | 31 | 10 |
| 4 | *tert*-Butyl | $CH_2Cl_2$ | 10d | -50 | 4 | 6 |
| 5 | Ph | $CH_2Cl_2$ | 1d | -50 | 38 | 2 |
| 6 | *iso*-propyl | $Et_2O$ | 6d | -50 | 39 | 7 |
| 7 | *iso*-propyl | $CH_3CN$ | 4d | -30 | 41 | 4 |
| 8 | *iso*-propyl | *t*-BuOH | 1d | r.t. | 46 | 4 |
| 9 | *iso*-propyl | THF | 6d | -50 | 40 | 10 |

[a] Conditions: racemic phenol (1 equiv.) and anhydride (0.6 equiv.) in the presence of a chiral DMAP catalyst, solvent (2 ml); [b] Conversions and selective factors were calculated by the method of Kagan and Fiaud: Conv. = $ee_{alcohol}$ / ($ee_{product}$ + $ee_{alcohol}$). *s* factor = ln[1-conv(1+$ee_{ester}$)] / ln[1-conv(1-$ee_{ester}$)]. [c] Determined by HPLC analysis.

The solvent effect was examined next (Table 3.5). Similar to dichloromethane, reaction conducted in tetrehydrofuran also gave good selectivity (entry 9). In contrast to the kinetic resolution of secondary alcohols, no significant improvement was observed when the reaction was conducted in diethylether (entry 6). At an elevated temperature, reaction conducted in acetonitrile or *tert*-butyl alcohol showed reduced selectivities (entries 7 and 8).

The results of kinetic resolution of 1,1'-binaphthalen-2-ol were good but still in need of improvement. The breakthrough was achieved by choosing mono-methylated Bi-2-naphthol (BINOL) *rac*-**3.50a** as the biaryl substrate.

### 3.3.2.4. Kinetic Resolution of mono-Methylated Bi-2-Naphthol

We examined the kinetic resolution of mono-methylated bi-2-naphthol (BINOL) *rac*-**3.50a** under various conditions with catalyst **3.19** and isobutyric anhydride (0.6 equiv). In the presence of 5 mol % catalyst at room temperature, after 72 hours, *rac*-**3.50a** was resolved with an *s* factor of 9. Lowering the reaction temperature led to increased selectivity (Table 3.6, entries 1-3), and at -50 °C, catalytic resolution gave $s$ = 33, although the acylation proceeded slowly with 24% conversion. Use of higher amounts of the catalyst improved conversion (Table 3.6, entries 3-5). Using 15 mol% **3.19**, (*R*)-**3.50a** was produced with increased selectivity ($s$ = 38, 49% conversion, Table 3.6, entry 5).

We speculated that adding a base might lead to a higher acylation rate, because base could remove the byproduct isobutyric acid and thus prevent deactivation of the catalyst. To our delight, as shown in Table 3.6 (entries 6-9), the bulky 2,6-di-*tert*-butylpyridine was the best among the tested bases, providing sufficient selectivity (s = 36) and 41% conversion in 84 hours with 15 mol% **3.19**. We observed diminished *s* value with 1,8-bis(dimethylamino)-naphthalene (proton sponge). The absolute configuration of the product alcohol was assigned by HPLC comparison with an authentic sample of mono-methylated enantiopure BINOL.

Table 3.6. Optimization of the Reaction Conditions for mono-Methylated Bi-2-Naphthol Resolution

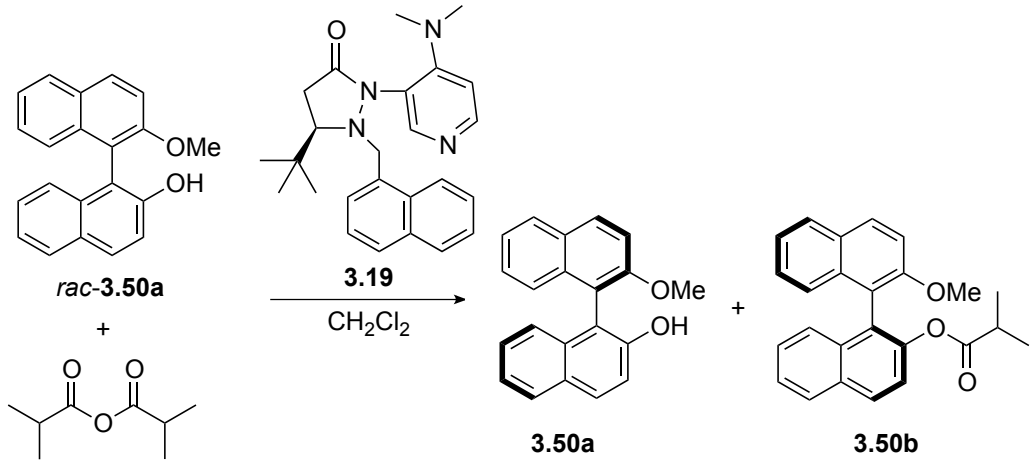


| entry | Cat. Loading (mol%) | Temp. (°C) | Additive (0.6 eq.) | Time (h) | Conv. (%) | ee% (ester) | ee% (alcohol) | *s* factor[a-c] |
|---|---|---|---|---|---|---|---|---|
| 1 | 5 | rt | - | 72 | 44 | 69 | 54 | 9 |
| 2 | 5 | -30 | - | 72 | 46 | 82 | 71 | 20 |
| 3 | 5 | -50 | - | 144 | 24 | 92 | 30 | 33 |
| 4 | 10 | -50 | - | 120 | 39 | 90 | 56 | 34 |
| 5 | 15 | -50 | - | 120 | 49 | 87 | 84 | 38 |
| 6 | 15 | -50 | 2,6-di-*tert*-butyl pyridine | 84 | 41 | 90 | 63 | 36 |
| 7 | 15 | -50 | 2,6-Lutidine | 60 | 45 | 88 | 71 | 34 |
| 8 | 15 | -50 | pyridine | **60** | 50 | 84 | 84 | 31 |
| 9 | 15 | -50 | proton sponge | 60 | 50 | 81 | 79 | 21 |

[a] Conditions: racemic phenol (1 equiv.) and anhydride (0.6 equiv.) in the presence of **3.19**, additives, $CH_2Cl_2$ (2 ml); [b] Conversions and selective factors were calculated by the method of Kagan and Fiaud: Conv. = $ee_{alcohol}$ / ($ee_{product}$ + $ee_{alcohol}$). *s* factor = ln[1-conv(1+$ee_{ester}$)] / ln[1-conv(1-$ee_{ester}$)]. [c] Determined by HPLC analysis.

### 3.3.2.5. Substrate Scope Investigation of Dihydroxy Biaryl Derivatives

The scope of the kinetic resolution was investigated using the optimal conditions (Scheme 3.14) and a variety of substrates (*rac*-**3.49a** to *rac*-**3.58a**) were competent in the resolution. A number of 2-hydroxyl-1,1'-biaryl analogues were resolved with good to excellent

selectivities ($s$ = 10-51). Biaryls without substituents at the β'-position, like *rac*-**3.49a**, gave reduced selectivity factor ($s$ = 10). Notably, compounds with electron-rich groups at the β'-position gave higher selectivity factors: resolution of substrates *rac*-**3.50a**, *rac*-**3.51a**, *rac*-**3.52a**, *rac*-**3.53a**, *rac*-**3.54a** proceeded with $s$ values more than 18. In contrast, compounds with electron-deficient groups at the β'-position gave lower selectivities (*rac*-**3.55a**, *rac*-**3.56a**). Pyridine was used for more bulky substituents, like *rac*-**3.54a** and *rac*-**3.55a**, to increase conversion.

The catalytic kinetic resolution of 2-amino-2'-hydroxy-1,1'-binaphthyl (NOBIN) derivatives remains a challenging problem and only limited examples have been reported. Among them, the reported chiral DMAP acylation showed only modest selectivity. To expand the utility of our DMAP catalysts, we synthesized NOBIN derivative *rac*-**3.57a** and resolved it. To our surprise, the kinetic resolution afforded the acylation product with 35% conversion and high selectivity factor ($s$ = 21). Remarkably, the substrate possessing a biaryl structure *rac*-**3.58a** was resolved with very high selectivity and $s$ factor of 51 with 50% conversion.

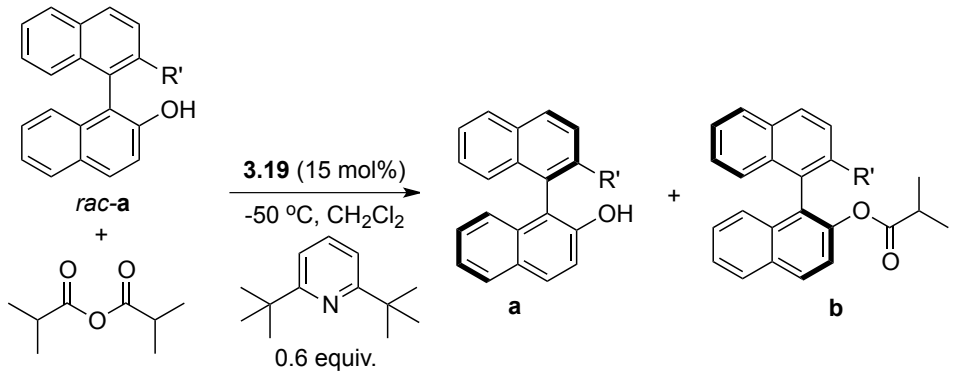


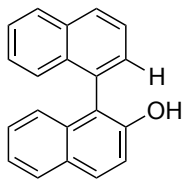


*rac*-**3.49a**
4d, 54% conv.
ester: 63%ee
alcohol: 73%ee
s factor: 10

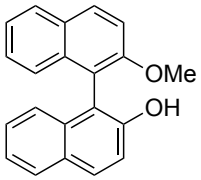


*rac*-**3.50a**
3.5d, 41% conv.
ester: 90%ee
alcohol: 63%ee
s factor: 36

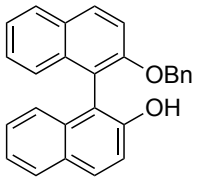


*rac*-**3.51a**
5d, 47% conv.
ester: 83%ee
alcohol: 72%ee
s factor: 23

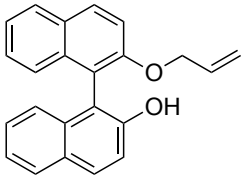


*rac*-**3.52a**
5d, 44% conv.
ester: 84%ee
alcohol: 68%ee
s factor: 25

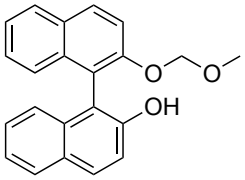


*rac*-**3.53a**
5d, 42% conv.
ester: 85%ee
alcohol: 62%ee
s factor: 23

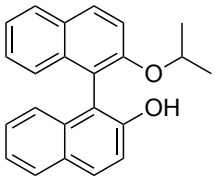


*rac*-**3.54a**
6d, 45% conv.*
ester: 80%ee
alcohol: 67%ee
s factor: 18

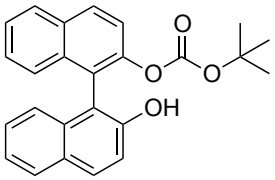


*rac*-**3.55a**
6d, 47% conv.*
ester: 71%ee
alcohol: 63%ee
s factor: 11

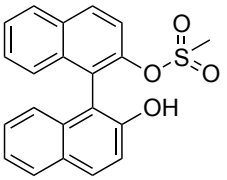


*rac*-**3.56a**
4d, 57% conv.
ester: 60%ee
alcohol: 85%ee
s factor: 11

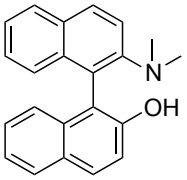


*rac*-**3.57a**
6d, 35% conv.
ester: 86%ee
alcohol: 46%ee
s factor: 21

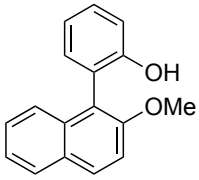


*rac*-**3.58a**
3.5d, 50% conv.
ester: 89%ee
alcohol: 90%ee
s factor: 51

*0.6 equiv. pyridine was used instead of 2,6-di-*tert*-butyl pyridine. Conditions: racemic phenol (1 equiv.) and anhydride (0.6 equiv.) in the presence of **3.19**, additives, $CH_2Cl_2$.

Scheme 3.14. Substrate Scope for Kinetic Resolution of BINOL Derivatives

### 3.3.2.6. Crystal Structure Analysis for Catalyst 3.19

In order to get insight into the origin of the catalytic activity and stereoselectivity, we obtained the single-crystal X-ray structure of catalyst **3.19** (Figure 3.8).

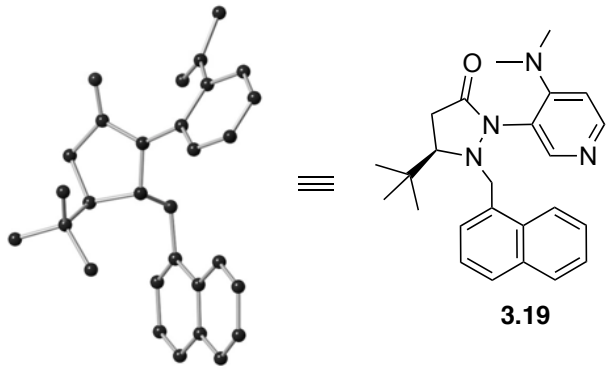


Figure 3.8. X-ray Analysis of Catalyst **3.19**

According to the X-ray structure, the pyridine ring lies at the top of the fluxional naphthalene ring. Similar to our prior observation, the *t*-butyl group and the fluxional naphthylmethyl substituent are on opposite face of the five membered ring due to steric interaction. The fluxional group blocked the backside as well as bottom side. Thus, based on the experimental results and structure analysis, we propose a stereochemical model for selectivity as shown Figure 3.9. In the proposed stereochemical model, the DMAP ring and the acyl group of the acylpyridinium ion lie approximately in a single plane. One naphthalene ring **A** with hydroxyl group attacks the *N*-acyl group from the top face and the other ring **B** approaches from the backside. To minimize steric repulsion between naphthylmethyl group of pyrazolidinone and **B** ring, the OR' side of **B** ring prefers to approach the catalyst, thus (*S*)-BINOL derivative is more favored than (*R*)-BINOL derivative to afford the acylation product. However, the bulky substituents on **B** ring having relatively strong repulsion showed decreased selectivity. The high

selectivity exhibited by β'-OR' substituted biaryls possibly results from the intervention of attractive π-π interaction between *N*-acyl and OR' group.

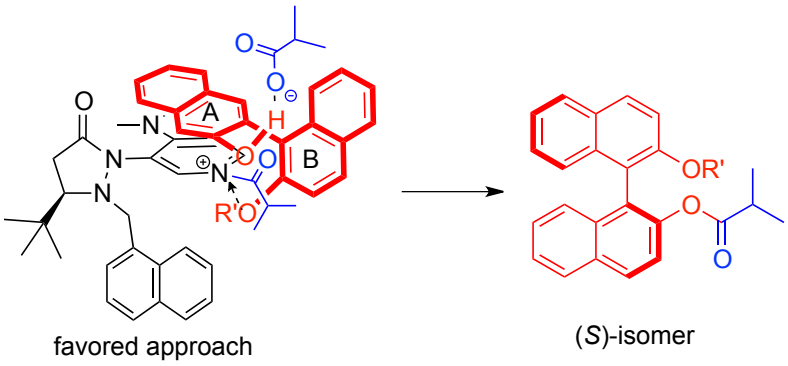


Figure 3.9. Proposed Stereochemical Model for Kinetic Resolution of Biaryl Compounds

### 3.3.3. Conclusion

In summary, we have established that novel fluxionally chiral DMAP molecules serve as an effective acylation catalyst for the kinetic resolution of racemic *sec*-alcohols, and especially biaryl compounds. This report adds a new family of DMAP based organocatalysts to the field of nucleophilic acylation catalysis. Biaryl substrates were resolved with selectivity factors of up to 51 by using this catalyst system. To the best of our knowledge, the selectivities obtained for kinetic resolution of biaryl compounds are better than previously reported asymmetric acylation catalysts. In addition, we proposed a stereochemical model to illustrate the enantioselectivities in this process. Further applications of the chiral DMAP catalysts in other asymmetric transformations are underway.

### 3.3.4. Experimental

#### 3.3.4.1. General

All solvents were dried and degassed by standard methods and stored under nitrogen. Flash chromatography was performed using EM Science silica gel 60 (230-400 mesh). $^{1}$H NMR spectra were recorded on Varian Unity/Inova-400 NB (400 MHz) spectrometer or Bruker Ascend$^{TM}$ 400 (400 MHz for $^{1}$H) spectrometer. $^{13}$C NMR spectra were recorded on Varian Unity/Inova-400 NB (100 MHz) spectrometer or Bruker Ascend$^{TM}$ 400 (100 MHz for $^{13}$C) spectrometer. HPLC analyses were carried out with Waters 515 HPLC pumps and a 2487 dual wavelength absorbance detector connected to a PC with Empower workstation. Rotations were recorded on a JASCO-DIP-370 polarimeter. High resolution mass spectra were obtained at a Bruker Daltonics BioTOF HRMS spectrometer.

#### 3.3.4.2. Preparation of Biaryl Compounds

Racemic substrates, *rac*-**3.50a**[53], *rac*-**3.51a**[54], *rac*-**3.52a**[55], *rac*-**3.53a**[56] and *rac*-**3.54a**[55] were prepared using the following method.

To a solution of a racemic mixture of 1,1'-binaphthalene-2,2'-diol (3 mmol) in acetone was added potassium carbonate (3.2 mmol). After stirring for 10 min, RX (X = I or Br, 3.2 mmol) in acetone was added dropwise at room temperature and the mixture stirred for 30h. The mixture was filtered and washed with acetone three times. Acetone was evaporated under reduced pressure and the racemic mixture was purified by column chromatography (hexane/ethyl acetate = 20/1) to afford the corresponding mono-protected 1,1'-binaphthalene-2,2'-diol, average yield 70-80%.

*Rac*-**3.49a** was prepared according to the literature.[57] 1-Bromo-2-naphthol (4.78mmol), 1-naphthylboronic acid (9.56 mmol), dry $K_3PO_4$ (9.56 mmol), *t*-$Bu_3P$ (0.239 mmol) and

$Pd(OAc)_2$ (0.12 mmol) were placed under Argon in a two-necked round bottom flask. Toluene was then added and heated to reflux for 12h. Solid was then filtered off and washed with toluene. The solvent was removed in vacuum, and the residue was separated by column chromatography on silica gel using hexane/ethyl acetate = 1/1 as eluent. The *rac*-**3.49a** was obtained in 60% yield.

*Rac*-**3.55a** was prepared according to the literature.[58] A round bottom flask was charged with 1,1'-binaphthalene-2,2'-diol (3 mmol), DMAP (0.3mmol), $CH_2Cl_2$ (10 mL) and $NEt_3$ (3.3 mmol). $Boc_2O$ (3.3 mmol) was added to the reaction vessel, and the reaction was stirred until the bubbling subsided (about 15 min). The solution was transferred to a separatory funnel, and $NaHSO_4$ (0.5 M, 9 mL) was added. The layers were separated, and the aqueous layer was extracted with $CH_2Cl_2$. The combined organic layers were washed with brine, dried over $MgSO_4$, and concentrated under reduced pressure. The crude residue was purified by flash chromatography (hexane/ethyl acetate = 9/1) to yield *rac*-**3.55a** as a white solid (80%).

*Rac*-**3.56a** was prepared according to the literature.[59] To a solution of a racemic mixture of 1,1'-binaphthalene-2,2'-diol (3 mmol) and pyridine (1.4 mL) in dichloromethane (20.0 mL) was added methanesulfonyl chloride (3.9 mmol) at 0 °C. The reaction mixture was stirring at room temperature for 12 hours. The reaction mixture was quenched with saturated aqueous ammonium chloride, and the resulting mixture was extracted with ethyl acetate. The combined organic extracts were washed with brine, dried over magnesium sulfate, filtered, and concentrated under reduced pressure. The mixture was purified by silica gel column chromatography (hexane/ethyl acetate = 5/1 to 2/1) to afford *rac*-**3.56a** (89%).

*Rac*-**3.57a** was prepared according to the literature.[60] A solution of racemic α-methylbenzylamine (10 mmol) in degassed 2-propanol (10 mL) was added to a solution of $CuCl_2$

$4H_2O$ (2.5 mmol) in degassed propanol (10 mL), the mixture was stirred for 10 min under argon, and then a solution of a mixture of 2-naphthylamine (1 mmol) and 2-naphthol (1 mmol) in degassed propanol (10 ml) was added. The mixture was stirred under argon at rt for 20h. After evaporating the solvent, the reaction mixture was washed by water, extracted using dichloromethane and purified by column chromatography (hexane/ethyl acetate = 4/1) to afford the 2-amino-2'-hydroxy-1,1'-binaphthyl (70 %). To a solution of 2-amino-2'-hydroxy-1,1'-binaphthyl (0.35 mmol) in glacial acetic acid (10 mL) was added $(HCHO)_n$ (1.05 mmol), followed by $NaBH_3CN$ (1.05 mmol). The reaction mixture were was stirred for 1 h at 40 °C, then another $(HCHO)_n$ (1.05 mmol) and $NaBH_3CN$ (1.05 mmol) were added. The mixture was stirred for 16 h at 40 °C. The solvent was removed under reduced pressure. The residues were partitioned between ethyl acetate and water. The organic layer was collected and dried over $Na_2SO_4$, filtered and concentrated under reduced pressure. The crude product was purified by column chromatography on silica gel, eluting with hexane/ethyl acetate = 9/1 to afford *rac*-**3.57a** (85%).

*Rac*-**3.58a** was prepared according to the literature.[52] A mixture of 2-methoxynaphthalene-1-boronic acid (1.5 mmol), 2-hydroxy-1-bromobenzene (1 mmol), $Pd_2dba_3$ (0.01 mmol, 1 mole %), 2-dicyclohexylphosphino-2′-(*N,N*′-dimethylamino)biphenyl (0.03 mmol, 2.4 mole %) and $K_3PO_4$ (1.8 mmol) in dry toluene (10 mL) was stirred under nitrogen at 70 °C for 5h. The mixture was diluted with ethyl acetate, washed with saturated $NaHCO_3$ solution, water, brine, dried over $Na_2SO_4$ and the solvent was removed *in vacuo*. Flash chromatography eluting with hexane/EtOAc = 9/1 gave compound *rac*-**3.58a** (60%).

### 3.3.4.3. General Procedure for the Kinetic Resolution of Racemic Biaryl Compounds

To a solution of racemic biaryl compounds (0.1 mmol), and catalyst (0.015 mmol) in 2 mL $CH_2Cl_2$ was added 2,6-di-*tert*-butyl pyridine (0.06 mmol). Under -50 °C, isobutyric anhydride (0.06 mmol) was added. After stirring for indicated time in Table 3.7, the reaction mixture was purified by column chromatography (hexane/ethyl acetate = 9/1) to afford alcohol and the corresponding ester, separately. The optical purity of the recovered alcohol and obtained ester were determined by chiral HPLC, the conversion was determined using chiral HPLC, where conversion (%) = $ee_{alcohol}$ / ($ee_{alcohol}$ + $ee_{ester}$), the *s* factor = ln[1-conv(1+$ee_{ester}$)] / ln[1-conv(1-$ee_{ester}$)].

### 3.3.4.4. Characterization of Recovered Substrates and Products

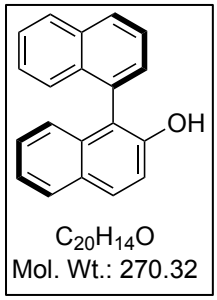


$C_{20}H_{14}O$
Mol. Wt.: 270.32

**3.49a** (73 %ee) HPLC (UV 220 nm, Chiralpak OD-H, *i*-PrOH/Hexane = 4/96, 0.5 mL/min), $t_1$ (major) = 19.6 min, $t_2$ (minor) = 35.9 min. $[\alpha]_D^{25}$ -70.8 (*c* 0.5, $CHCl_3$). $^1H$ NMR ($CDCl_3$, 400 MHz) δ 4.95 (s, 1H), 7.14 (d, *J* = 8.4 Hz, 1H), 7.25-7.29 (m, 1H), 7.34-7.44 (m, 4H), 7.54-7.59 (m, 2H), 7.7 (dd, *J* = 8.4, 7.2 Hz, 1H), 7.9 (d, *J* = 8 Hz, 1H), 7.94 (d, *J* = 8.8 Hz, 1H), 8.01 (d, *J* = 8 Hz, 1H), 8.06 (d, *J* = 8.4 Hz, 1H); $^{13}C$ NMR ($CDCl_3$, 100 MHz) δ 117. 5, 118.8, 123.4, 125.0, 125.8, 126.0, 126.6, 126.6, 126.9, 128.0, 128.5, 129.0, 129.3, 129.7, 129.9, 131.4, 132.8, 133.9, 134.2, 151.0; ESI-HRMS: *m/z* calcd. for $(C_{20}H_{14}ONa)^+$ 293.0937; found 293.0932.

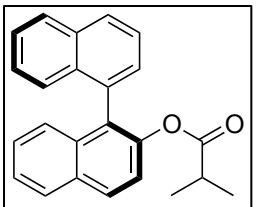

$C_{24}H_{20}O_2$
Mol. Wt.: 340.41

**3.49b** (63 %ee) HPLC (UV 220 nm, Chiralpak OD-H, *i*-PrOH/Hexane = 1/99, 0.5 mL/min), $t_1$ (minor) = 12.0 min, $t_2$ (major) = 15.8 min. $[\alpha]_D^{25}$ -28.2 (*c* 0.53, $CHCl_3$). $^1H$ NMR ($CDCl_3$, 400 MHz) δ 0.65 (d, *J* = 7.2 Hz, 1H), 0.7 (d, *J* = 6.8 Hz, 1H), 2.33 (m, 1H), 7.31-7.38 (m, 4H), 7.4 (d, *J* = 8.8 Hz, 1H), 7.44 (dd, *J* = 6.8, 1.2 Hz, 1H), 7.48-7.52 (m, 2H), 7.6 (dd, *J* = 8.4, 7.2 Hz, 1H), 7.94-7.99 (m, 3H), 8.03 (d, *J* = 8.8 Hz, 1H), 8.01 (d, *J* = 8 Hz, 1H), 8.06 (d, *J* = 8.4 Hz, 1H); $^{13}C$ NMR ($CDCl_3$, 100 MHz) δ 18.1, 18.3, 33.8, 121.8, 125.3, 125.6, 125.9, 126.1, 126.3, 126.6, 128.0, 128.0, 128.2, 128.3, 129.0, 129.2, 131.8, 132.7, 132.9, 133.5, 133.9; ESI-HRMS: *m/z* calcd. for $(C_{24}H_{20}O_2Na)^+$ 363.1356; found 363.1360.

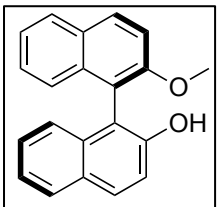

$C_{21}H_{16}O_2$
Mol. Wt.: 300.35

**3.50a** (63 %ee) HPLC (UV 220 nm, Chiralpak OD-H, *i*-PrOH/Hexane = 4/96, 0.5 mL/min), $t_1$ (major) = 30.6 min, $t_2$ (minor) = 47.7 min. $[\alpha]_D^{25}$ -28.9 (*c* 0.51, $CHCl_3$). $^1H$ NMR ($CDCl_3$, 400 MHz) δ 3.83 (s, 3H), 4.94 (s, 1H), 7.08 (d, *J* = 8.4 Hz, 1H), 7.21 (d, *J* = 8.8 Hz, 1H), 7.23-7.34 (m, 3H), 7.36-7.42 (m, 2H), 7.51 (d, *J* = 9.2 Hz, 1H), 7.88-7.95 (m, 3H), 8.08 (d, *J* = 9.2 Hz, 1H); $^{13}C$ NMR ($CDCl_3$, 100 MHz) δ 56.7, 113.8, 115.0, 115.3, 117.5, 123.2, 124.2,

124.8, 124.9, 126.4, 127.3, 128.1, 128.2, 129.1, 129.4, 129.8, 131.1, 133.8, 134.0, 151.2, 156.0; ESI-HRMS: *m/z* calcd. for $(C_{21}H_{16}O_2Na)^+$ 323.1043; found 323.1102.

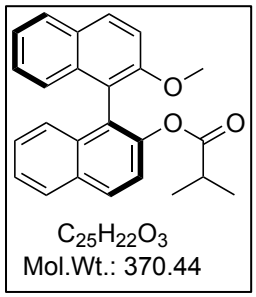


**3.50b** (90 %ee) HPLC (UV 220 nm, Chiralpak AD-H, *i*-PrOH/Hexane = 2/98, 0.5 mL/min), $t_1$ (major) = 25.9 min, $t_2$ (minor) = 38.1 min. $[\alpha]_D^{25}$ -26.8(*c* 0.53, $CHCl_3$). $^1H$ NMR ($CDCl_3$, 400 MHz) δ 0.64 (d, *J* = 7.2 Hz, 3H), 0.71 (d, *J* = 7.2 Hz, 3H), 2.34 (m, 1H), 3.9 (s, 3H), 4.94 (s, 1H), 7.16 (d, *J* = 8.4 Hz, 1H), 7.24-7.28 (m, 1H), 7.31-7.36 (m, 3H), 7.44 (d, *J* = 2.8 Hz, 1H), 7.46-7.5 (m, 2H), 7.87 (d, *J* = 8.4 Hz, 1H), 7.97 (d, *J* = 8.4 Hz, 1H), 8.0 (d, *J* = 8.8 Hz, 1H), 8.02 (d, *J* = 8.8 Hz, 1H); $^{13}C$ NMR ($CDCl_3$, 100 MHz) δ 18.2, 33.8, 56.8, 113.6, 117.9, 122.0, 123.7, 125.2, 125.3, 125.4, 126.1, 126.4, 126.6, 127.7, 128.1, 129.0, 129.0, 129.9, 131.8, 133.7, 133.8, 146.7, 155.0, 174.9; ESI-HRMS: *m/z* calcd. for $(C_{25}H_{22}O_3Na)^+$ 393.1461; found 393.1479.

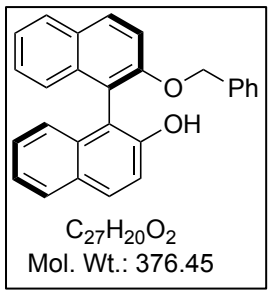


**3.51a** (72 %ee) HPLC (UV 220 nm, Chiralpak OD-H, *i*-PrOH/Hexane = 4/96, 0.5 mL/min), $t_1$ (major) = 33.7 min, $t_2$ (minor) = 47.1 min. $[\alpha]_D^{25}$ 5.29 (*c* 0.5, $CHCl_3$). $^1H$ NMR ($CDCl_3$, 400 MHz) δ 4.97 (s, 1H), 5.13 (m, 2H), 7.06-7.14 (m, 3H), 7.2-7.43 (m, 9H), 7.49 (d, *J*

= 8 Hz, 1H), 7.91-8.02 (m, 4H); $^{13}$C NMR ($CDCl_3$, 100 MHz) δ 71.1, 115.1, 116.0, 116.8, 117.5, 123.3, 124.4, 125.0, 125.1, 126.4, 126.9, 127.3, 127.7, 128.1, 128.2, 128.3, 129.2, 129.7, 129.9, 130.9, 133.8, 134.1, 136.9, 151.3, 155.0; ESI-HRMS: *m/z* calcd. for $(C_{27}H_{20}O_2Na)^+$ 399.1356; found 399.1367.

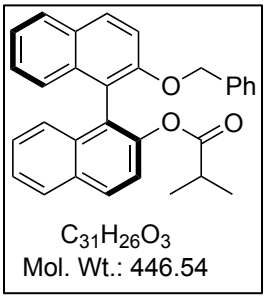


**3.51b** (83 %ee) HPLC (UV 220 nm, Chiralpak OD-3, *i*-PrOH/Hexane = 2/98, 0.5 mL/min), $t_1$ (minor) = 15.0 min, $t_2$ (major) = 17.3 min. $[\alpha]_D^{25}$ -40.9 (*c* 0.51, $CHCl_3$). $^1$H NMR ($CDCl_3$, 400 MHz) δ 0.59 (d, *J* = 7.2 Hz, 3H), 0.73 (d, *J* = 7.2 Hz, 3H), 2.35 (m, 1H), 5.11 (d, *J* = 2.4 Hz, 2H), 7.07-7.09 (m, 2H), 7.19-7.41 (m, 8H), 7.42 (d, *J* = 9.2 Hz, 1H), 7.48-7.52 (m, 2H), 7.86 (d, *J* = 8 Hz, 1H), 7.94 (d, *J* = 9.2 Hz, 1H), 8.0 (d, *J* = 8 Hz, 1H), 8.05 (d, *J* = 8.8 Hz, 1H); $^{13}$C NMR ($CDCl_3$, 100 MHz) δ 18.18, 18.2, 71.1, 115.5, 119.0, 122.1, 123.9, 125.3, 125.4, 125.5, 126.2, 126.4, 126.6, 126.8, 127.4, 127.6, 128.1, 128.2, 129.0, 129.2, 129.7, 131.8, 133.8, 133.9, 137.4, 146.8, 153.9, 175.0; ESI-HRMS: *m/z* calcd. for $(C_{31}H_{26}O_3Na)^+$ 469.1774; found 469.1768.

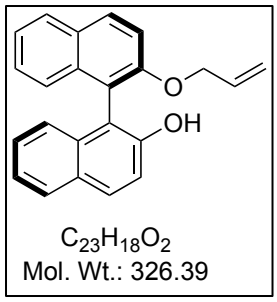


$C_{23}H_{18}O_2$
Mol. Wt.: 326.39

**3.52a** (68 %ee) HPLC (UV 220 nm, Chiralpak OD-H, *i*-PrOH/Hexane = 4/96, 0.5 mL/min), $t_1$ (major) = 23.2 min, $t_2$ (minor) = 30.9 min. $[\alpha]_D^{25}$ -15.8 (*c* 0.5, $CHCl_3$). $^1H$ NMR ($CDCl_3$, 400 MHz) δ 4.57-4.6 (m, 2H), 4.98 (s, 1H), 5.07 (t, *J* = 1.6 Hz, 1H), 5.11 (dd, *J* = 4, 1.6 Hz, 1H), 5.79 (m, 1H), 7.11 (d, *J* = 8.4 Hz, 1H), 7.23-7.43 (m, 6H), 7.47 (d, *J* = 8.4 Hz, 1H), 7.89-7.95 (m, 3H), 8.04 (d, *J* = 9.2 Hz, 1H); $^{13}C$ NMR ($CDCl_3$, 100 MHz) δ 70.0, 115.1, 115.8, 116.5, 117.2, 117.5, 123.2, 124.4, 124.9, 125.1, 126.4, 127.3, 128.1, 128.2, 129.1, 129.7, 129.8, 130.8, 133.1, 133.8, 134.1, 151.2, 155.0; ESI-HRMS: *m/z* calcd. for $(C_{23}H_{18}O_2Na)^+$ 349.1199; found 349.1198.

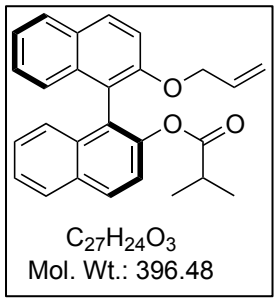


$C_{27}H_{24}O_3$
Mol. Wt.: 396.48

**3.52b** (84 %ee) HPLC (UV 220 nm, Chiralpak AD-H, *i*-PrOH/Hexane = 2/98, 0.5 mL/min), $t_1$ (major) = 18.7 min, $t_2$ (minor) = 24.9 min. $[\alpha]_D^{25}$ -36.4 (*c* 0.53, $CHCl_3$). $^1H$ NMR ($CDCl_3$, 400 MHz) δ 0.61 (d, *J* = 6.8 Hz, 3H), 0.71 (d, *J* = 6.8 Hz, 3H), 2.33 (m, 1H), 4.54-4.56 (m, 1H), 5.02-5.09 (m, 2H), 5.74-5.83 (m, 1H), 7.19 (d, *J* = 8.4 Hz, 1H), 7.24-7.29 (m, 1H), 7.31-7.37 (m, 3H), 7.46 (d, *J* = 8.8 Hz, 1H), 7.46-7.5 (m, 1H), 7.86 (d, *J* = 8 Hz, 1H), 7.95 (d, *J* =

4.8 Hz, 1H), 7.97 (d, *J* = 3.6 Hz, 1H), 8.01 (d, *J* = 8.8 Hz, 1H); $^{13}$C NMR ($CDCl_3$, 100 MHz) δ 18.2, 33.8, 70.0, 115.3, 116.6, 118.7, 122.0, 123.8, 125.2, 125.4, 125.5, 126.2, 126.3, 126.5, 127.6, 128.1, 128.9, 129.1, 129.6, 131.7, 133.6, 133.7, 133.8, 146.7, 154.0, 174.9; ESI-HRMS: *m/z* calcd. for $(C_{27}H_{24}O_3Na)^+$ 419.1618; found 419.1623.

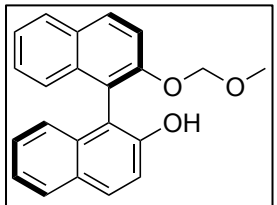


$C_{22}H_{18}O_3$
Mol. Wt.: 330.38

**3.53a** (62 %ee) HPLC (UV 220 nm, Chiralpak OD-H, *i*-PrOH/Hexane = 4/96, 0.5 mL/min), $t_1$ (major) = 21.9 min, $t_2$ (minor) = 28.4 min. $[\alpha]_D^{25}$ -18.1 (*c* 0.56, $CHCl_3$). $^1$H NMR ($CDCl_3$, 400 MHz) δ 3.21 (s, 1H), 5.02 (s, 1H), 5.11 (dd, *J* = 19, 7.2 Hz, 2H), 7.1 (d, *J* = 8.4 Hz, 1H), 7.23-7.28 (m, 2H), 7.3-7.37 (m, 2H), 7.39 (d, *J* = 8.4 Hz, 1H), 7.42-7.46 (m, 1H), 7.63 (d, *J* = 9.2 Hz, 1H), 7.9 (d, *J* = 8 Hz, 1H), 7.94 (m, 2H), 8.05 (d, *J* = 8.8 Hz, 1H); $^{13}$C NMR ($CDCl_3$, 100 MHz) δ 56.2, 95.0, 115.1, 117.1, 117.5, 117.6, 123.3, 124.8, 124.8, 125.1, 126.5, 127.3, 128.1, 128.2, 129.1, 129.8, 130.2, 131.0, 133.8, 134.0, 151.3, 153.7; ESI-HRMS: *m/z* calcd. for $(C_{22}H_{18}O_3Na)^+$ 353.1148; found 353.1150.

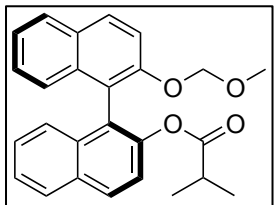


$C_{26}H_{24}O_4$
Mol. Wt.: 400.47

**3.53b** (85 %ee) HPLC (UV 220 nm, Chiralpak OD-H, *i*-PrOH/Hexane = 1/99, 0.5 mL/min), $t_1$ (minor) = 14.4 min, $t_2$ (major) = 17.6 min. $[\alpha]_D^{25}$ -39.7 (*c* 0.54, $CHCl_3$). $^1H$ NMR ($CDCl_3$, 400 MHz) δ 0.62 (d, *J* = 7.2 Hz, 3H), 0.69 (d, *J* = 6.8 Hz, 3H), 2.33 (m, 1H), 3.22 (s, 3H), 5.06 (dd, *J* = 18.4, 6.8 Hz, 1H), 7.17 (d, *J* = 8.8 Hz, 1H), 7.24-7.28 (m, 1H), 7.31-7.39 (m, 3H), 7.45 (d, *J* = 8.8 Hz, 1H), 7.46-7.58 (m, 1H), 7.58 (d, *J* = 9.2 Hz, 1H), 7.87 (d, *J* = 7.6 Hz, 1H), 7.95-7.97 (m, 2H), 8.02 (d, *J* = 8.8 Hz, 1H); $^{13}C$ NMR ($CDCl_3$, 100 MHz) δ 18.2, 33.8, 55.9, 95.0, 116.6, 119.3, 122.0, 124.1, 125.2, 125.5, 125.5, 126.1, 126.4, 126.5, 127.6, 128.1, 129.0, 129.6, 129.8, 131.7, 133.7, 146.8, 152.7, 175.0; ESI-HRMS: *m/z* calcd. for $(C_{26}H_{24}O_4Na)^+$ 423.1567; found 423.1574.

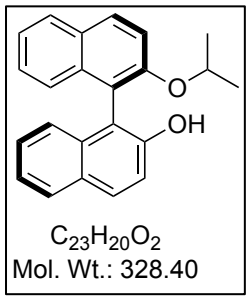


**3.54a** (67 %ee) HPLC (UV 220 nm, Chiralpak OD-H, *i*-PrOH/Hexane = 4/96, 0.5 mL/min), $t_1$ (major) = 16.0 min, $t_2$ (minor) = 19.0 min. $[\alpha]_D^{25}$ -51.3 (*c* 0.5, $CHCl_3$). $^1H$ NMR ($CDCl_3$, 400 MHz) δ 1.02 (d, *J* = 6 Hz, 3H), 1.15 (d, *J* = 6 Hz, 3H), 4.47 (m, 1H), 5.09 (s, 1H), 7.09 (d, *J* = 8.4 Hz, 1H), 7.19-7.35 (m, 4H), 7.37-7.42 (m, 2H), 7.47 (d, *J* = 9.2 Hz, 1H), 7.9 (dd, *J* = 12, 8 Hz, 2H), 7.92 (d, *J* = 8.8 Hz, 1H), 8.02(d, *J* = 8.8 Hz, 1H); $^{13}C$ NMR ($CDCl_3$, 100 MHz) δ 22.2, 22.3, 72.6, 115.6, 117.6, 118.1, 123.1, 124.3, 125.2, 125.3, 126.2, 127.1, 128.0, 128.1, 129.1, 129.6, 129.8, 130.7, 133.8, 134.2, 151.3, 154.6; ESI-HRMS: *m/z* calcd. for $(C_{23}H_{20}O_2Na)^+$ 351.1356; found 351.1361.

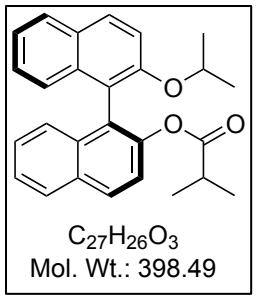

$C_{27}H_{26}O_3$
Mol. Wt.: 398.49

**3.54b** (80 %ee) HPLC (UV 220 nm, Chiralpak OD-3_OD connection, *i*-PrOH/Hexane = 1/99, 0.5 mL/min), $t_1$ (minor) = 20.2 min, $t_2$ (major) = 22.7 min. $[\alpha]_D^{25}$ -29.1 (*c* 0.5, $CHCl_3$). $^1H$ NMR ($CDCl_3$, 400 MHz) δ 0.63 (d, *J* = 7.2 Hz, 3H), 0.74 (d, *J* = 6.8 Hz, 3H), 1.0 (d, *J* = 2 Hz, 3H), 1.1 (d, *J* = 2 Hz, 3H), 2.35 (m, 1H), 4.45 (m, 1H), 7.17 (d, *J* = 8.4 Hz, 1H), 7.23-7.27 (m, 1H), 7.3-7.36 (m, 3H), 7.41 (d, *J* = 8.8 Hz, 1H), 7.45-7.49 (m, 2H), 7.86 (d, *J* = 8 Hz, 1H), 7.95 (d, *J* = 9.2 Hz, 1H), 7.96 (d, *J* = 8 Hz, 1H), 8.0 (d, *J* = 8.8 Hz, 1H); $^{13}C$ NMR ($CDCl_3$, 100 MHz) δ 18.2, 18.2, 22.2, 22.3, 71.9, 117.2, 119.9, 122.0, 123.7, 125.3, 125.4, 125.5, 126.1, 126.4, 126.4, 127.6, 128.0, 128.6, 129.2, 129.5, 131.6, 133.7, 134.0, 146.7, 153.6, 174.9; ESI-HRMS: *m/z* calcd. for $(C_{27}H_{26}O_3Na)^+$ 421.1774; found 421.1790.

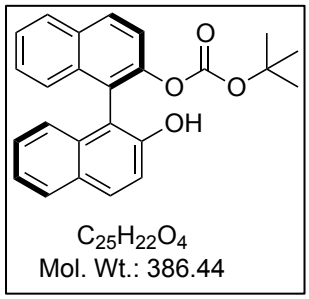

$C_{25}H_{22}O_4$
Mol. Wt.: 386.44

**3.55a** (63 %ee) HPLC (UV 220 nm, Chiralpak OD-H, *i*-PrOH/Hexane = 4/96, 0.5 mL/min), $t_1$ (major) = 15.1 min, $t_2$ (minor) = 18.7 min. $[\alpha]_D^{25}$ 55.2 (*c* 0.52, $CHCl_3$). $^1H$ NMR ($CDCl_3$, 400 MHz) δ 1.29 (s, 9H), 5.41 (s, 1H), 7.05 (d, *J* = 8 Hz, 1H), 7.24-7.3 (m, 2H), 7.33-7.39 (m, 3H), 7.49-7.55 (m, 2H), 7.88 (d, *J* = 8 Hz, 1H), 7.93 (d, *J* = 8 Hz, 1H), 8.0 (d, *J* = 8 Hz,

1H), 8.1 (d, $J$ = 8 Hz, 1H); $^{13}$C NMR ($CDCl_3$, 100 MHz) δ 27.3, 84.0, 114.1, 118.5, 121.5, 123.5, 123.6, 124.7, 125.8, 126.3, 126.7, 127.4, 127.9, 128.2, 129.1, 130.4, 130.8, 132.3, 133.6, 133.6, 148.1, 151.9, 152.6; ESI-HRMS: *m/z* calcd. for $(C_{25}H_{22}O_4Na)^+$ 409.1410; found 409.1536.

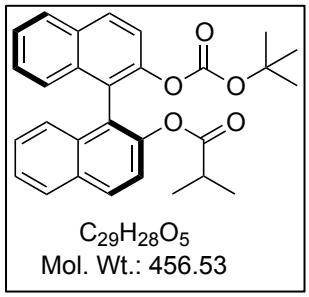


$C_{29}H_{28}O_5$
Mol. Wt.: 456.53

**3.55b** (71 %ee) HPLC (UV 220 nm, Chiralpak OD-3, *i*-PrOH/Hexane = 1/99, 0.5 mL/min), $t_1$ (minor) = 11.7 min, $t_2$ (major) = 17.6 min. $[\alpha]_D^{25}$ -4.9 (*c* 0.55, $CHCl_3$). $^1$H NMR ($CDCl_3$, 400 MHz) δ 0.6 (d, $J$ = 7.2 Hz, 3H), 0.74 (d, $J$ = 8 Hz, 3H), 1.23 (s, 9H), 2.36 (m, 1H), 7.29-7.33 (m, 4H), 7.45-7.52 (m, 4H), 7.92-7.96 (m, 2H), 8 (d, $J$ = 7.2 Hz, 1H), 8.03 (d, $J$ = 7.2 Hz, 1H); $^{13}$C NMR ($CDCl_3$, 100 MHz) δ 18.1, 18.1, 27.3, 33.8, 83.1, 121.6, 121.9, 123.4, 123.8, 125.5, 125.7, 126.3, 126.6, 126.7, 127.8, 127.9, 129.5, 129.5, 131.5, 131.6, 133.3, 133.4, 146.9, 146.9, 151.5, 175.0; ESI-HRMS: *m/z* calcd. for $(C_{29}H_{28}O_5Na)^+$ 479.1829; found 479.1805.

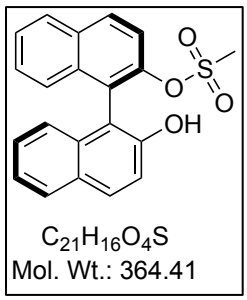


$C_{21}H_{16}O_4S$
Mol. Wt.: 364.41

**3.56a** (85 %ee) HPLC (UV 220 nm, Chiralpak AD-H, *i*-PrOH/Hexane = 10/90, 0.5 mL/min), $t_1$ (minor) = 43.0 min, $t_2$ (major) = 48.5 min. $[\alpha]_D^{25}$ 27.6 (*c* 0.52, $CHCl_3$). $^1$H NMR ($CDCl_3$, 400 MHz) δ 2.47 (s, 3H), 5.17 (s, 1H), 7.08 (d, $J$ = 8.4 Hz, 1H), 7.29-7.33 (m, 1H),

7.36-7.44 (m, 4H), 7.56-7.6 (m, 1H), 7.73 (d, $J$ = 8.8 Hz, 1H), 7.9 (d, $J$ = 8 Hz, 1H), 7.97 (d, $J$ = 8.8 Hz, 1H), 8.02 (d, $J$ = 8 Hz, 1H), 8.12 (d, $J$ = 9.2 Hz, 1H); $^{13}$C NMR ($CDCl_3$, 100 MHz) δ 38.5, 113.8, 118.0, 122.0, 123.6, 123.9, 124.5, 126.0, 126.9, 127.2, 127.9, 128.2, 128.5, 129.0, 130.9, 131.2, 132.6, 133.3, 133.4, 146.3, 151.9, 145.5, 146.9, 175.0; ESI-HRMS: *m/z* calcd. for $(C_{21}H_{16}O_4SNa)^+$ 387.0662; found 387.0668.

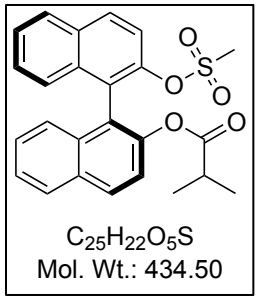


**3.56b** (60 %ee) HPLC (UV 220 nm, Chiralpak IA, *i*-PrOH/Hexane = 2/98, 1 mL/min), $t_1$ (major) = 23.8 min, $t_2$ (minor) = 26.6 min. $[\alpha]_D^{25}$ 7.4 (*c* 0.57, $CHCl_3$). $^1$H NMR ($CDCl_3$, 400 MHz) δ 0.72 (d, $J$ = 8 Hz, 3H), 0.8 (d, $J$ = 8 Hz, 3H), 2.4 (m, 1H), 2.41 (s, 3H), 7.29-7.32 (m, 2H), 7.35-7.40 (m, 2H), 7.48-7.55 (m, 3H), 7.71 (d, $J$ = 8 Hz, 1H), 7.98 (dd, $J$ = 4, 4 Hz, 2H), 8.06 (t, $J$ = 4 Hz, 2H); $^{13}$C NMR ($CDCl_3$, 100 MHz) δ 18.2, 33.9, 38.4, 121.5, 122.1, 122.8, 124.1, 126.0, 126.1, 126.4, 126.5, 127.1, 127.2, 128.0, 128.2, 129.9, 130.2, 131.4, 131.9, 133.2, 133.2, 145.5, 146.9, 175.0; ESI-HRMS: *m/z* calcd. for $(C_{25}H_{22}O_5SNa)^+$ 457.1080; found 457.1075.

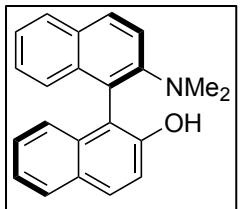


$C_{22}H_{19}NO$
Mol. Wt.: 313.39

**3.57a** (46 %ee) HPLC (UV 220 nm, Chiralpak AD-3, *i*-PrOH/Hexane = 2/98, 1.0 mL/min), $t_1$ (minor) = 8.6 min, $t_2$ (major) = 14.0 min. $[\alpha]_D^{25}$ -52.7 (*c* 0.55, $CHCl_3$). $^1H$ NMR ($CDCl_3$, 400 MHz) δ 2.65 (s, 6H), 7.06-7.08 (m, 1H), 7.11-7.24 (m, 4H), 7.3-7.34 (m, 2H), 7.4 (d, *J* = 8.8 Hz, 1H), 7.5 (d, *J* = 9.2 Hz, 1H), 7.84 (d, *J* = 8 Hz, 1H), 7.87 (d, *J* = 8 Hz, 1H), 7.9 (d, *J* = 9.2 Hz, 1H), 7.95 (d, *J* = 9.2 Hz, 1H); $^{13}C$ NMR ($CDCl_3$, 100 MHz) δ 43.9, 118.6, 118.7, 119.7, 122.4, 123.5, 124.4, 126.0, 126.1, 126.6, 126.8, 128.2, 128.4, 129.5, 129.9, 130.2, 130.3, 134.2, 134.4, 149.7, 151.9; ESI-HRMS: *m/z* calcd. for $(C_{22}H_{20}NO)^+$ 314.1539; found 314.1540.

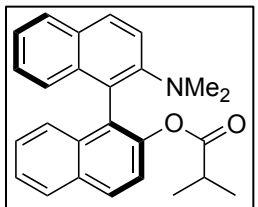


$C_{26}H_{25}NO_2$
Mol. Wt.: 383.48

**3.57b** (86 %ee) HPLC (UV 220 nm, Chiralpak AD-3, *i*-PrOH/Hexane = 1/99, 0.5 mL/min), $t_1$ (major) = 15.9 min, $t_2$ (minor) = 25.5 min. $[\alpha]_D^{25}$ -13.0 (*c* 0.5, $CHCl_3$). $^1H$ NMR ($CDCl_3$, 400 MHz) δ 0.68 (d, *J* = 6.8 Hz, 3H), 0.76 (d, *J* = 6.8 Hz, 3H), 2.35 (m, 1H), 2.54 (s, 3H), 7.08 (d, *J* = 8.4 Hz, 1H), 7.18 (t, *J* = 8 Hz, 1H), 7.3-7.35 (m, 3H), 7.46-7.5 (m, 3H), 7.81 (d, *J* = 8 Hz, 1H), 7.9-8.0 (m, 3H); $^{13}C$ NMR ($CDCl_3$, 100 MHz) δ 18.2, 18.3, 33.9, 43.7, 113.3, 119.5, 122.3, 123.6, 123.8, 125.4, 125.5, 126.1, 126.4, 126.5, 127.5, 128.1, 128.6, 129.2, 129.6,

131.7, 133.8, 133.8, 146.6, 150.1, 174.8; ESI-HRMS: *m/z* calcd. for $(C_{26}H_{26}NO_2)^+$ 384.1958; found 384.1955.

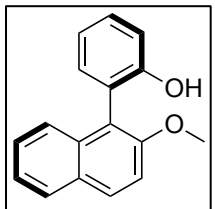


$C_{17}H_{14}O_2$
Mol. Wt.: 250.29

**3.58a** (90 %ee) HPLC (UV 220 nm, Chiralpak OD-H, *i*-PrOH/Hexane = 4/96, 0.5 mL/min), $t_1$ (major) = 28.7 min, $t_2$ (minor) = 36.4 min. $[\alpha]_D^{25}$ -30.2 (*c* 0.58, $CHCl_3$). $^1H$ NMR ($CDCl_3$, 400 MHz) δ 3.92 (s, 3H), 4.97 (s, 1H), 7.1 (td, *J* = 7.6, 1.2 Hz, 1H), 7.14 (dd, *J* = 8, 1.2 Hz, 1H), 7.25 (dd, *J* = 7.6, 2 Hz, 1H), 7.38-7.44 (m, 4H), 7.51-7.54 (m, 1H), 7.87-7.89 (m, 1H), 7.99 (d, *J* = 9.2 Hz, 1H); $^{13}C$ NMR ($CDCl_3$, 100 MHz) δ 56.8, 113.5, 116.0, 118.5, 120.5, 122.4, 124.1, 125.0, 127.1, 126.6, 126.8, 128.1, 129.4, 129.4, 130.5, 132.1, 133.7, 153.8, 154.5; ESI-HRMS: *m/z* calcd. for $(C_{17}H_{14}O_2Na)^+$ 273.0886; found 273.0894.

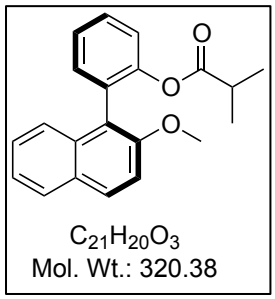


$C_{21}H_{20}O_3$
Mol. Wt.: 320.38

**3.58b** (89 %ee) HPLC (UV 220 nm, Chiralpak AD-3, *i*-PrOH/Hexane = 2/98, 0.5 mL/min), $t_1$ (minor) = 14.5 min, $t_2$ (major) = 17.7 min. $[\alpha]_D^{25}$ 62.7(*c* 0.55, $CHCl_3$). $^1H$ NMR ($CDCl_3$, 400 MHz) δ 0.66 (d, *J* = 6.8 Hz, 3H), 0.7 (d, *J* = 6.8 Hz, 3H), 2.3 (m, 1H), 3.86 (s, 3H), 7.28-7.31 (m, 1H), 7.34-7.43 (m, 6H), 7.48-7.52 (m, 1H), 7.81-7.83 (m, 1H), 7.9 (d, *J* = 9.2 Hz,

1H); $^{13}C$ NMR ($CDCl_3$, 100 MHz) δ 18.2, 18.3, 33.8, 56.7, 113.4, 120.4, 122.8, 123.6, 125.2, 125.7, 126.4, 127.6, 128.6, 128.8, 129.4, 129.5, 132.5, 133.4, 149.3, 154.2, 174.7; ESI-HRMS: *m/z* calcd. for $(C_{21}H_{20}O_3Na)^+$ 343.1305; found 343.1302.

**3.3.4.5. Determination of Absolute Configuration for Chiral Biaryl Compounds**

The absolute configuration of **3.50a** was confirmed by acylating the mono-methylated (*R*)-(+)-1,1'-bi(2-naphthol) or mono-methylated (*S*)-(+)-1,1'-bi(2-naphthol) by catalyst **3.19**. Mono-methylated (*S*)-(+)-1,1'-bi(2-naphthol) took 16 hours to complete the acylation but mono-methylated (*R*)-(+)-1,1'-bi(2-naphthol) took 8 days to complete the acylation. Compared with methylated (*R*)-(+)-1,1'-bi(2-naphthol), mono-methylated (*S*)-(+)-1,1'-bi(2-naphthol) acylated faster by isobutyric anhydride under catalyst **3.19**, which indicates that the product obtained in kinetic resolution is (*S*)-isomer, the recovered starting material is (*R*)-isomer.

The absolute configurations of **3.49a** to **3.57a** were confirmed by comparison of the retention time of HPLC with authentic samples, which were prepared from commercially available (*R*)-(+)-1,1'-bi(2-naphthol)[53,58,59,61] or (*R*)-(+)-2'-amino-1,1'-binaphthalen-2-ol.[60] The absolute configuration of **3.58a** was assigned by analogy to **3.50a**.

### 3.3.4.6. Crystal Structure of Catalyst 3.19

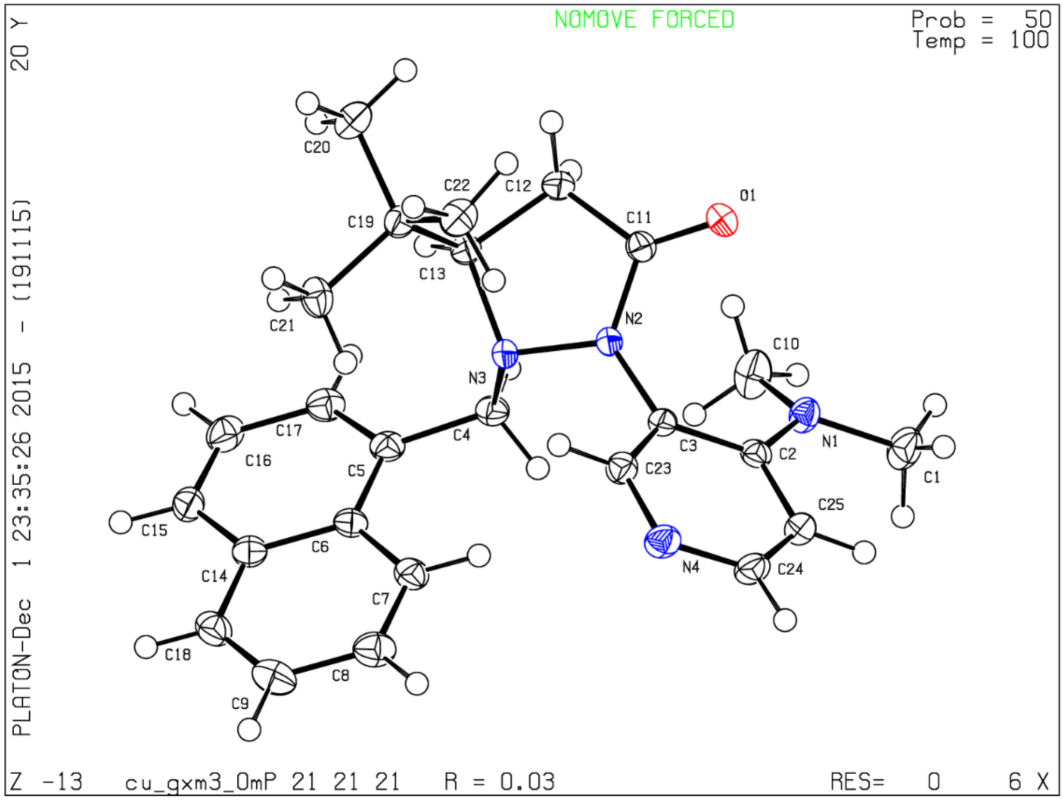


Figure 3.10. X-ray Structure Determination

Single crystal X-ray diffraction data of **3.19** was collected on a Bruker APEX-II CCD diffractometer. The crystal was kept at 100K during data collection. Cu radiation was used for the sample. Using Olex2,[62] the structure was solved with the ShelXS[63] structure solution program using Direct Methods and refined with the XL refinement package using Least Squares minimization. Basic information pertaining to crystal parameters and structure refinement is summarized in Table 3.7.

Table 3.7. Crystal Data and Structure Refinement

| | |
|---|---|
| Identification code | cu_gxm3_0m |
| Empirical formula | $C_{25}H_{30}N_4O$ |
| Formula weight | 402.53 |
| Temperature | 100K |
| Crystal system | orthorhombic |
| space group | $P2_12_12_1$ |
| *a*/Å | 11.2926(3) |
| *b*/Å | 12.7919(3) |
| *c*/Å | 15.5672(4) |
| $\alpha$, deg | 90 |
| $\beta$, deg | 90 |
| $\gamma$, deg | 90 |
| *V*, Å$^3$ | 2248.74(10) |
| *Z* | 4 |
| $d_{calcd}$, g.cm$^{-3}$ | 1.189 |
| $\mu$, mm$^{-1}$ | 0.580 |
| F(000) | 864.0 |
| Crystal size/mm$^3$ | 0.25 × 0.23 × 0.2 |
| Radiation | CuKa (l = 1.54178) |
| 2Θ range for data collection | 8.948 to 133.288 |
| Index ranges | -12 ≤ h ≤ 13, -15 ≤ k ≤ 11, -18 ≤ l ≤ 18 |
| Reflections collected | 15267 |
| Independent reflections | 3960 [$R_{int}$ = 0.0252, $R_{sigma}$ = 0.0209] |
| Data/restraints/parameters | 3960/0/276 |
| GOOF on $F^2$ | 1.057 |
| Final R indexes [I>=2σ (I)] | $R_1$ = 0.0279, $wR_2$ = 0.0693 |
| Final R indexes [all data] | $R_1$ = 0.0292, $wR_2$ = 0.0702 |
| Largest diff. peak/hole/e Å$^{-3}$ | 0.15/-0.16 |
| Flack parameter | 0.00(8) |

## 3.4. Conclusion

In summary, we have established that novel fluxionally chiral DMAP molecules serve as an effective acylation catalyst for the kinetic resolution of racemic *sec*-alcohols, and especially biaryl compounds. This report adds a new family of DMAP based organocatalysts to the field of nucleophilic acylation catalysis. Biaryl substrates were resolved with good to high selectivities with up to 51 by using this catalyst system. To the best of our knowledge, the selectivities obtained for kinetic resolution of biaryl compounds are better than previously reported asymmetric acylation catalysts. Our approaches still required improvement. The catalyst preparation could be further simplified and this approach is limited in the substrate scope, especially for the more complicated biaryl structures. The emergence of new chiral routes to access various enantiopure compounds is of importance for the discovery and the development of new bioactive compounds and catalyst for both pharmaceutical as well as chemical sciences. In addition, we proposed a stereochemical model to illustrate the enantioselective outcome in this process. The computational studies will be performed to better understand the basis for asymmetric induction in this catalytic system in the future.

## 3.5. References


1. Moss, G. P. Basic Terminology of Stereochemistry. *Pure Appl. Chem.* **1996**, *68*, 2193-2222.
2. Fiaud, J. C.; Kagan, H. B. Kinetic Resolution. In Eliel, E. L.; Wilen, S. H. *Topics in Stereochemistry* 18. Wiley, **1988**, 249-340.
3. a) Keith, J. M.; Larrow, J. F.; Jacobsen, E. N. *Adv. Synth. Catal.* **2001**, *343*, 5-26; b) Vedejs, E.; Jure, M. Efficiency in Nonenzymatic Kinetic Resolution. *Angew. Chem. Int. Ed.* **2005**, *44*, 3974-4001.

4. a) Abdel-Rahman, H. M. Lipases-Catalyzed Enantioselective Kinetic Resolution of Alcohols. *J. Chem. Pharm. Res.* **2015**, *7*, 311-322; b) Ghanem, A.; Aboul-Enein, H. Y. Application of Lipases in Kinetic Resolution of Racemates. *Chirality* **2005**, *17*, 1-15.
5. a) Robinson, D. E. J. E.; Bull, S. D. Kinetic Resolution Strategies using Non-Enzymatic Catalysts. *Tetrahedron: Asymm.* **2003**, *14*, 1407-1446; b) Pellissier, H. Catalytic Non-Enzymatic Kinetic Resolution. *Adv. Synth. Catal.* **2011**, *353*, 1613-1666.
6. a) Lee, S. Y.; Murphy, J. M.; Ukai, A.; Fu, G. C. Nonenzymatic Dynamic Kinetic Resolution of Secondary Alcohols via Enantioselective Acylation: Synthetic and Mechanistic Studies. *J. Am. Chem. Soc.* **2012**, *134*, 15149-15153; b) Pellissier, H. Recent Developments in Dynamic Kinetic Resolution. *Tetrahedron* **2008**, *64*, 1563-1601.
7. a) Tang, W.; Zhang, X. New Chiral Phosphorus Ligands for Enantioselective Hydrogenation. *Chem. Rev.* **2003**, *103*, 3029-3070; b) Ikariya, T.; Blacker, A. J. Asymmetric Transfer Hydrogenation of Ketones with Bifunctional Transition Metal-Based Molecular Catalysts. *Acc. Chem. Res.* **2007**, *40*, 1300-1308; c) Morris, R. H. Asymmetric Hydrogenation, Transfer Hydrogenation and Hydrosilylation of Ketones Catalyzed by Iron Complexes. *Chem. Soc. Rev.* **2009**, *38*, 2282-2291.
8. Pu, L.; Yu, H. -B. Catalytic Asymmetric Organozinc Additions to Carbonyl Compounds. *Chem. Rev.* **2001**, *101*, 757-824.
9. a) Smith, M. B.; March, J. March's Advanced Organic Chemistry. 5$^{th}$ ed. Wiley, **2001**; b) Guo, J.; Teo, P. Anti-Markovnikov Oxidation and Hydration of Terminal Olefins. *Dalton Trans.* **2014**, *43*, 6952-6964.

10. a) Jacobsen, E. N. Asymmetric Catalysis of Epoxide Ring-Opening Reactions. *Acc. Chem. Res.* **2000**, *33*, 421-431; b) Pineschi, M. Asymmetric Ring-Opening of Epoxides and Aziridines with Carbon Nucleophiles. *Eur. J. Org. Chem.* **2006**, *2006*, 4979-4988.
11. a) Liu, H. -L.; Anthonsen, T. Enantiopure building blocks for chiral Drugs from Racemic Mixtures of Secondary Alcohols by Combination of Lipase Catalysis and Mitsunobu Esterification. *Chirality* **2002**, *14*, 25-27; b) Larios, A.; Garcia, H. S.; Oliart, R. M.; Valerio-Alfaro, G. Synthesis of Flavor and Fragrance Esters Using Candida Antarctica Lipase. *Appl. Microbiol. Biotechnol.* **2004**, *65*, 373-376.
12. a) Somfai, P. Nonenzymatic Kinetic Resolution of Secondary Alcohols. *Angew. Chem. Int. Ed.* **1997**, *36*, 2731-2733; b) Taylor, J. E.; Bull, S. D.; Williams, J. M. Amidines, Isothioureas, and Guanidines as Nucleophilic Catalysts. *Chem. Soc. Rev.* **2012**, *41*, 2109-2121; c) Müller, C. E.; Schreiner, P. R. Organocatalytic Enantioselective Acyl Transfer onto Racemic as well as *meso* Alcohols, Amines, and Thiols. *Angew. Chem. Int. Ed.* **2011**, *50*, 6012.
13. Spivey, A. C.; Maddaford, A.; Redgrave, A. J. Asymmetric Catalysis of Acyl Transfer by Lewis Acids and Nucleophiles. A Review. *Org. Prep. Proced. Int.* **2000**, *32*, 331-365.
14. Xu, S.; Held, I.; Kempf, B.; Mayr, H.; Steglich, W.; Zipse, H. The DMAP-Catalyzed Acetylation of Alcohols-A Mechanistic Study (DMAP = 4-(Dimethylamino)pyridine). *Chem. Eur. J.* **2005**, *11*, 4751-4757.
15. Vedejs, E.; Chen, X. Kinetic Resolution of Secondary Alcohols. Enantioselective Acylation Mediated by A Chiral (Dimethylamino)pyridine Derivative. *J. Am. Chem. Soc.* **1996**, *118*, 1809-1810.

16. Fu, G. C. Enantioselective Nucleophilic Catalysis with "Planar-Chiral" Heterocycles. *Acc. Chem. Res.* **2000**, *33*, 412-420.

17. Held, I.; Villinger, A.; Zipse, H. The Stability of Acylpyridinium Cations and Their Relation to the Catalytic Activity of Pyridine Bases. *Synthesis* **2005**, 1425-1430.

18. Kawabata, T.; Nagato, M.; Takasu, K.; Fuji, K. Nonenzymatic Kinetic Resolution Resolution of Racemic Alcohols through an "Induced Fit" Process. *J. Am. Chem. Soc.* **1997**, *119*, 3169-3170.

19. Priem, G.; Pelotier, B.; Macdonald, S. J. F.; Anson, M. S.; Campbell, I. B. The Design of Novel N-4'-Pyridinyl-α-methyl Proline Derivatives as Potent Catalysts for the Kinetic Resolution of Alcohols. *J. Org. Chem.* **2003**, *68*, 3844-3848.

20. Spivey, A. C.; Fekner, T.; Spey, S. E. Axially Chiral Analogues of 4-(Dimethylamino)pyridine: Novel Catalysts for Nonenzymatic Enantioselective Acylation. *J. Org. Chem.* **2000**, *65*, 3154-3159.

21. Yamada, S.; Misono, T.; Iwai, Y.; Masumizu, A.; Akiyama, Y. New Class of Pyridine Catalyst Having a Conformation Switch System: Asymmetric Acylation of Various *sec*-Alcohols. *J. Org. Chem.* **2006**, *71*, 6872-6880.

22. a) Dálaigh, C. Ó.; Connon, S. J. Nonenzymatic Acylative Kinetic Resolution of Baylis-Hillman Adducts. *J. Org. Chem.* **2007**, *72*, 7066-7069; b) Naraku, G.; Shimomoto, N.; Hanamoto, T.; Inanaga, J. Synthesis of Enantiomerically Pure C2-Symmetric 4-Pyrrolidinopyridine Derivative as a Chiral Acyl Transfer Catalyst for the Kinetic Resolution of Secondary Alcohols. *Enantiomer* **2000**, *5*, 135-138; c) Jeong, K. -S.; Kim, S. -H.; Park, H. -J.; Chang, K. -J.; Kim, K. S. A New Nucleophilic Catalyst for Kinetic Resolution of Racemic *sec*-Alcohols. *Chem. Lett.* **2002**, *11*, 1114-1115.

23. Birman, V. B.; Uffman, E. W.; Hui, J.; Li, X. M.; Kilbane, C. J. 2,3-Dihydroimidazo[1,2-a]pyridines: A New Class of Enantioselective Acyl Transfer Catalysts and Their Use in Kinetic Resolution of Alcohols. *J. Am. Chem. Soc.* **2004**, *126*, 12226-12227.

24. Birman, V. B.; Li, X. M.; Homobenzotetramisole: An Effective Catalyst for Kinetic Resolution of Aryl-Cycloalkanols. *Org. Lett.* **2008**, *10*, 1115-1118.

25. Hu, B.; Meng, M.; Wang, Z.; Du, W. T.; Fossey, J. S.; Hu, X. Q.; Deng, W. P.; A Highly Selective Ferrocene-Based Planar Chiral PIP (Fc-PIP) Acyl Transfer Catalyst for the Kinetic Resolution of Alcohols. *J. Am. Chem. Soc.* **2010**, *132*, 17041-17044.

26. Copeland, G. T.; Jarvo, E. R.; Miller, S. J. Minimal Acylase-Like Peptides. Conformational Control of Absolute Stereospecificity. *J. Org. Chem.* **1998**, *63*, 6784-6785.

27. Copeland, G. T.; Miller, S. J. Selection of Enantioselective Acyl Transfer Catalysts from a Pooled Peptide Library Through a Fluorescence-based Activity Assay: An Approach to Kinetic Resolution of Secondary Alcohols of Broad Structural Scope. *J. Am. Chem. Soc.* **2001**, *123*, 6496-6502.

28. Oriyama, T.; Hori, Y.; Imai, K.; Sasaki, R. Nonenzymatic Enantioselective Acylation of Racemic Secondary Alcohols Catalyzed by A $SnX_2$-Chiral Diamine Complex. *Tetrahedron Lett.* **1996**, *37*, 8543-8546.

29. Vedejs, E.; Daugulis, O. 2-Aryl-4,4,8-trimethyl-2-phosphabicyclo[3.3.0]octanes: Reactive Chiral Phosphine Catalysts for Enantioselective Acylation. *J. Am. Chem. Soc.* **1999**, *121*, 5813-5814.

30. Suzuki, Y.; Yamauchi, K.; Muramatsu, K.; Sato, M. First Example of Chiral *N*-heterocyclic Carbenes as Catalysts for Kinetic Resolution. *Chem. Commun.* **2004**, 2770-2771.

31. Kano, T.; Sasaki, K.; Maruoka, K. Enantioselective Acylation of Secondary Alcohols Catalyzed by Chiral *N*-Heterocyclic Carbenes. *Org. Lett.* **2005**, *7*, 1347-1349.

32. Maki, B. E.; Chan, A.; Phillips, E. M.; Scheidt, K. A. *N*-Heterocyclic Carbene-Catalyzed Oxidations. *Tetrahedron* **2009**, *65*, 3102-3109.

33. De Sarkar, S.; Biswas, A.; Song, C. H.; Studer, A.; Kinetic Resolution of Secondary Alcohols by NHC-Catalyzed Oxidative Esterification. *Synthesis* **2011**, *12*, 1974-1983.

34. Harada, S.; Kuwano, S.; Yamaoka, Y.; Yamada, K.; Takasu, K.; Kinetic Resolution of Secondary Alcohols Catalyzed by Chiral Phosphoric Acids. *Angew. Chem. Int. Ed.* **2013**, *52*, 10227-10230.

35. Parmar, D.; Sugiono, E.; Raja, S.; Rueping, M. Complete Field Guide to Asymmetric BINOL-Phosphate Derived Brønsted Acid and Metal Catalysis: History and Classification by Mode of Activation; Brønsted Acidity, Hydrogen Bonding, Ion Pairing, and Metal Phosphates. *Chem. Rev.* **2014**, *114*, 9047-9153.

36. Crittall, M. R.; Rzepa, H. S.; Carbery, D. R. Design, Synthesis, and Evaluation of A Helicenoidal DMAP Lewis Base Catalyst. *Org. Lett.* **2011**, *13*, 1250-1253.

37. Birman, V. B.; Guo, L. Kinetic Resolution of Propargylic Alcohols Catalyzed by Benzotetramisole. *Org. Lett.* **2006**, *8*, 4859-4861.

38. Bringmann, G.; Mortimer, A. J. P.; Keller, P. A.; Gresser, M. J.; Garner, J.; Breuning, M. Atroposelective Synthesis of Axially Chiral Biaryl Compounds. *Angew. Chem. Int. Ed.* **2005**, *44*, 5384-5427.

39. Oki, M. Advances in Atropisomerism. *Topics in Stereochem*. **1983**, *14*, 1-81.

40. Noyori, R.; Takaya, H. BINAP: An Efficient Chiral Element for Asymmetric Catalysis. *Acc. Chem. Res.* **1990**, *23*, 345-350.

41. a) Chang, J.; Reiner, J.; Xie, J. Progress on the Chemistry of Dibenzocyclooctadiene Lignans. *Chem. Rev.* **2005**, *105*, 4581-4609; b) Kozlowski, M. C.; Morgan, B. J.; Linton, E. C. Total Synthesis of Chiral Biaryl Natural Products by Asymmetric Biaryl Couping. *Chem. Soc. Rev.* **2009**, *38*, 3193-3207; c) LaPlante, S. R.; Fader, L. D.; Fandrick, K. R.; Fandrick, D. R.; Hucke, O.; Kemper, R.; Miller, S. P. F.; Edwards, P. J. Assessing Atropisomer Axial Chirality in Drug Discovery and Development. *J. Med. Chem.* **2011**, *54*, 7005-7022; d) Clayden, J.; Moran, W. J.; Edwards, P. J.; LaPlante, S. R. The Challenge of Atropisomerism in Drug Discovery. *Angew. Chem. Int. Ed.* **2009**, *48*, 6398-6401.

42. a) Noyori, R.; Takaya, H. BINAP: An Efficient Chiral Element for Asymmetric Catalysis. *Acc. Chem. Res.* **1990**, *23*, 345-350; b) Tang, W.; Zhang, X. New Chiral Phosphorus Ligands for Enantioselective Hydrogenation. *Chem. Rev.* **2003**, *103*, 3029-3070; c) Xie, J.-H.; Zhou, Q.-L. Chiral Diphosphine and Monodentate Phosphorus Ligands on A Spiro Scaffold for Transition-Metal-Catalyzed Asymmetric Reactions. *Acc. Chem. Res.* **2008**, *41*, 581-593.

43. a) Akiyama, T.; Itoh, J.; Fuchibe, K. Recent Process in Chiral Brønsted Acid Catalysis. *Adv. Synth. Catal.* **2006**, *348*, 999-1010; b) Brunel, J. M. BINOL: A Versatile Chiral Reagent. *Chem. Rev.* **2005**, *105*, 857-898; c) Chen, Y.; Yekta, S.; Yudin, A. K. Modified BINOL Ligands in Asymmetric Catalysis. *Chem. Rev.* **2003**, *103*, 3155-3212; d) Rueping, M.; Kuenkel, A.; Atodiresei, I. Chiral Brønsted Acids in Enantioselective

Carbonyl Activations-Activation Modes and Applications. *Chem. Soc. Rev.* **2011**, *40*, 4539-4549.

44. Bringmann, G.; Mortimer, A. J. P.; Keller, P. A.; Gresser, M. J.; Garner, J.; Breuning,M. Atroposelective Synthesis of Axially Chiral Biaryl Compounds. *Angew. Chem. Int. Ed.* **2005**, *44*, 5384-5427.
45. Fujimoto, Y.; Iwadate, H.; Ikekawa, N. Preparation of Optically Active 2,2'-Dihydroxy-1,1'-binaphthyl via Microbial Resolution of the Corresponding Racemic Diester. *J. Chem. Soc., Chem. Commun.* **1985**, 1333-1334.
46. Miyano, S.; Kawahara, K.; Inoue, Y.; Hashimoto, H.; A Convenient Preparation of Optically Active 1,1'-Binaphthyl-2,2'-diol via Enzymatic Hydrolysis of the Racemic Diester. *Chem. Lett.* **1987**, 355-356.
47. a) Aoyagi, N.; Izumi, T. Kinetic Resolution of 1,1'-Binaphthylamines via Lipase-Catalyzed Amidation. *Tetrahedron Lett.* **2002**, *43*, 5529-5531; b) Aoyagi, N.; Kawauchi, S.; Izumi, T. Effect of the Alkyl Chain Length of 1,1'-Binaphthyl Esters in Lipase-Catalyzed Amidation. *Tetrahedron Lett.* **2003**, *44*, 5609-5612; c) Aoyagi, N.; Ohwada, T.; Izumi, T. Facile Synthesis of Chiral 2-Formyl-1,1'-binaphthyl via Lipase-Catalyzed Acylation and Hydrolysis of 1,1'-Binaphthyl Oximes. *Tetrahedron Lett.* **2003**, *44*, 8269-8272; d) Furutani, T.; Hatsuda, M.; Imashiro, R.; Seki, M. Facile Synthesis of Enantiopure 1,1'-Binaphthyl-2,2'-Dicarboxylic Acid via Lipase-Catalyzed Kinetic Resolution. *Tetrahedron: Asymm.* **1999**, *10*, 4763-4768; e) Seki, M.; Furutani, T.; Hatsuda, M.; Imashiro, R. Facile Synthesis of $C_2$-Symmetric Chiral Binaphthyl Ketone Catalysts. *Tetrahedron Lett.* **2000**, *41*, 2149-2152.

48. Aoyama, H.; Tokunaga, M.; Kiyosu, J.; Iwasawa, T.; Obora, Y.; Tsuji, Y. Kinetic Resolution of Axially Chiral 2,2'-Dihydroxy-1,1'-Biaryls by Palladium-Catalyzed Alcoholysis. *J. Am. Chem. Soc.* **2005**, *127*, 10474-10475.

49. Shirakawa, S.; Wu, X.; Maruoka, K. Kinetic Resolution of Axially Chiral 2-Amino-1,1'-Biaryls by Phase-Transfer-Catalyzed *N*-Allylation. *Angew. Chem. Int. Ed.* **2013**, *52*, 14200-14203.

50. Cheng, D.-J.; Yan, L.; Tian, S.-K.; Wu, M.-Y.; Wang, L.-X.; Fan, Z.-L.; Zheng, S.-C.; Liu, X.-Y.; Tan, B. Highly Enantioselective Kinetic Resolution of Axially Chiral BINAM Derivatives Catalyzed by A Brønsted Acid. *Angew. Chem. Int. Ed.* **2014**, *53*, 3684-3687.

51. Lu, S.; Poh, S. B.; Zhao, Y. Kinetic Resolution of 1,1'-Biaryl-2,2'-Diols and Amino Alcohols through NHC-Catalyzed Atroposelective Acylation. *Angew. Chem. Int. Ed.* **2014**, *53*, 11041-11045.

52. Arseniyadis, S.; Mahesh, M.; McDaid, P.; Hampel, T.; Davey, S. G.; Spivey, A. C. Studies Towards the *N*-Acylative Kinetic Resolution of NOBIN. *Collect. Czech. Chem. Commun.* **2011**, *76*, 1239-1253.

53. Dabbagh, H. A.; Chermahini, A. N.; Banibairami, S. A New Family of bis-Tetrazole (BIZOL) BINOL-type Ligands. *Tetrahedron Lett.* **2006**, *47*, 3929-3932.

54. Fernández-Mateos, E.; Macia, B.; Ramon, D. J.; Yus, M. Catalytic Enantioselective Addition of MeMgBr and Other Grignard Reagents to Aldehydes. *Eur. J. Org. Chem.* **2011**, *34*, 6851-6855.

55. Salvadori, P.; Rosini, C.; Pini, D.; Bertucci, C.; Altemura, P.; Uccello-Barretta, G.; Raffaelli, A. A Novel Application of Cinchona Alkaloids as Chiral Auxiliaries:

Preparation and Use of a New Family of Chiral Stationary Phases for the Chromatographic Resolution of Racemates. *Tetrahedron* **1987**, *43*, 4969-4978.

56. Jin, L.; Huang, Y.; Jing, H.; Chang, T.; Yan, P. Chiral Catalysts for the Asymmetric Cycloaddition of Carbon Dioxide with Epoxides. *Tetrahedron: Asymmetry.* **2008**, *19*, 1947-1953.
57. Wawrzyniak, P.; Heinicke, J. Microwave-promoted Suzuki-Miyaura Coupling of Aryl Boronic Acids with 1-Bromo-2-naphthol, *o*-Bromophenol and *o*-Chlorophenol. *Tetrahedron Lett.* **2006**, *47*, 8921-8924.
58. Quasdorf, K. W.; Riener, M.; Petrova, K. V.; Garg, N. K. Suzuki-Miyaura Couling of Aryl Caramates, Carbonates, and Sulfamates. *J. Am. Chem. Soc.* **2009**, *131*, 17748-17749.
59. N. Murai, M. Miyano, M. Yonaga, K. Tanaka, One-Pot Primary Aminomethylation of Aryl and Heteroaryl Halides with Sodium Phthalimidomethyltrifluoroborate. *Org. Lett.* **2012**, *14*, 2818-2821.
60. Smrcina, M.; Lorenc, M.; Hanus, V.; Sedmera, P.; Kocovsky, P. Synthesis of Enantiomerically Pure 2,2'-Dihydroxy-1,1'-binaphthyl, 2,2'-Diamino-1,1'-binaphthyl, and 2-Amino-2'-hydroxy-1,1'-binaphthyl. Comparison of Processes Operating as Diastereoselective Crystallization and as Second Order Asymmetric Transformation. *J. Org. Chem.* **1992**, *57*, 1917-1920.
61. Jiang, Y. -Q.; Shi, Y. -L.; Shi, M. Chiral Phosphine-Catalyzed Enantioselective Construction of g-Butenolides Through Substitution of Morita-Baylis-Hillman Acetates with 2-Trimethylsilyloxy Furan. *J. Am. Chem. Soc.* **2008**, *130*, 7202-7203.

62. Dolomanov, O. V.; Bourhis, L. J.; Gildea, R. J.; Howard, J. A. K.; Puschmann, H. OLEX2: A Complete Structure Solution, Refinement and Analysis Program. *J. Appl. Cryst.* **2009**, *42*, 339-341.

63. Sheldrick, G. M. A Short History of SHELX. *Acta Cryst.* **2008**, *A64*, 112-122.

# CHAPTER 4. DYNAMIC KINETIC RESOLUTION OF ATROPISOMERS BY CHIRAL DIALKYLAMINO CATALYSTS

## 4.1. Introduction

In kinetic resolution, one of the enantiomers of the racemic mixture is transformed into the desired product while the other is recovered unchanged. However, this procedure suffers from being limited to a maximum theoretical yield of 50%. The effort devoted to overcome this limitation has led to the evolution of dynamic kinetic resolution.[1] Dynamic kinetic resolution is possible when racemization of the starting material occurs during the reaction process, resulting in the conversion of both enantiomers of a racemic substrate into a single enantiomer of the product. According to the Curtin-Hammett principle, the isolation of highly enriched non-racemic product with a theoretical maximum 100% yield can be reached.[2] For this reason, dynamic kinetic resolution has practical applications in organic synthesis. A dynamic kinetic resolution reaction involving two enantiomeric substrates can be illustrated as shown in Scheme 4.1. $k_R$ and $k_S$ are the rate constants for the conversion of $Substrate_R$ and $Substrate_S$ to the corresponding $Product_R$ and $Product_S$, respectively. $k_{rac}$ is the rate for the racemization. Assume $Substrate_R$ is the fast reacting enantiomer, the design of a successful dynamic kinetic resolution system requires the following features: $k_R$, $k_S$ and $k_{rac}$ are rate constants of first-order kinetics; $Substrate_R$ and $Substrate_S$ interconvert at the same rate; $Substrate_R$ and $Substrate_S$ convert to $Product_R$ and $Product_S$ irreversibly; $Product_R$ and $Product_S$ don't racemize under reaction conditions. Dynamic kinetic resolution will become more efficient when $k_R$ / $k_S$ or $k_{rac}$ / $k_S$ increases.[3] Racemization of the substrate can be performed either chemically, biocatalytically or physically and the reaction conditions must avoid the racemization of the product.

In the past few years, significant developments in the efficiency and scope of the applications of dynamic kinetic resolution have taken place and have attracted an increasing amount of interest from both the industrial and academic perspectives. A number of excellent reviews have been published, detailing the theory and practical applications of dynamic kinetic resolution.[4]

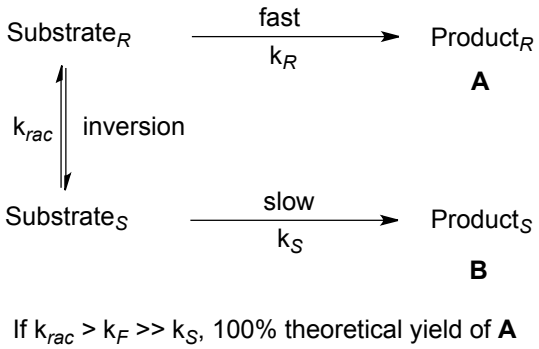


Scheme 4.1. Kinetic Scheme of Dynamic Kinetic Resolution

An atropselective alkylation of 2-(1-naphthyl)-pyridine/1-(1-naphthyl)-isoquinoline via transition metal-catalyzed C-H/olefin coupling using chiral ferrocenyl phosphine as the ligand was developed by Murai and coworkers (Scheme 4.2).[5] The low inversion barriers of these kinds of biaryl substrates make the interconversion spontaneous during the dynamic kinetic process. In contrast, the alkylation products are produced with enough inversion barriers to restrict the racemization of products.

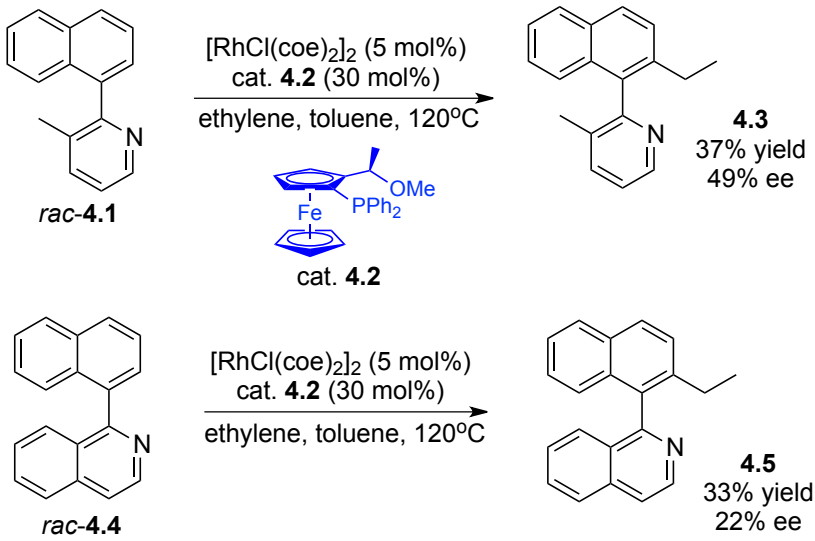


Scheme 4.2. Atropselective Alkylation of 2-(1-Naphthyl)-Pyridine/ 1-(1-Naphthyl)-Isoquinoline

Ethylene reacted with the biaryl compound *rac*-**4.1** using $[RhCl(coe)_2]_2$/**4.2** catalyst system giving the corresponding addition product **4.3** in 37 % yield with 49 %ee. Naphthyl isoquinoline **4.4** also reacted with ethylene using the same catalytic system to give product **4.5**, but the chemical yields and enantiomeric excesses were slightly lower (33 %yield and 22 %ee).

The dynamic kinetic asymmetric cross-coupling strategy in the deracemization of configurationally stable 2-aryl pyridines and analogs was investigated by Lassaletta, Fernández and coworkers (Scheme 4.3).[6] In their study, the Pd(0)-catalyzed coupling of racemic 2-triflate *rac*-**4.6** with aryl boroxines **4.7** using a TADDOL-derived phosphoramidite ligand **4.8** provided the corresponding coupling products with good to excellent enantioselectivities. This kinetic dynamic coupling process was proposed to occur via the interconversion of two diastereomers of cationic five-membered palladacylic intermediate **4.10**.

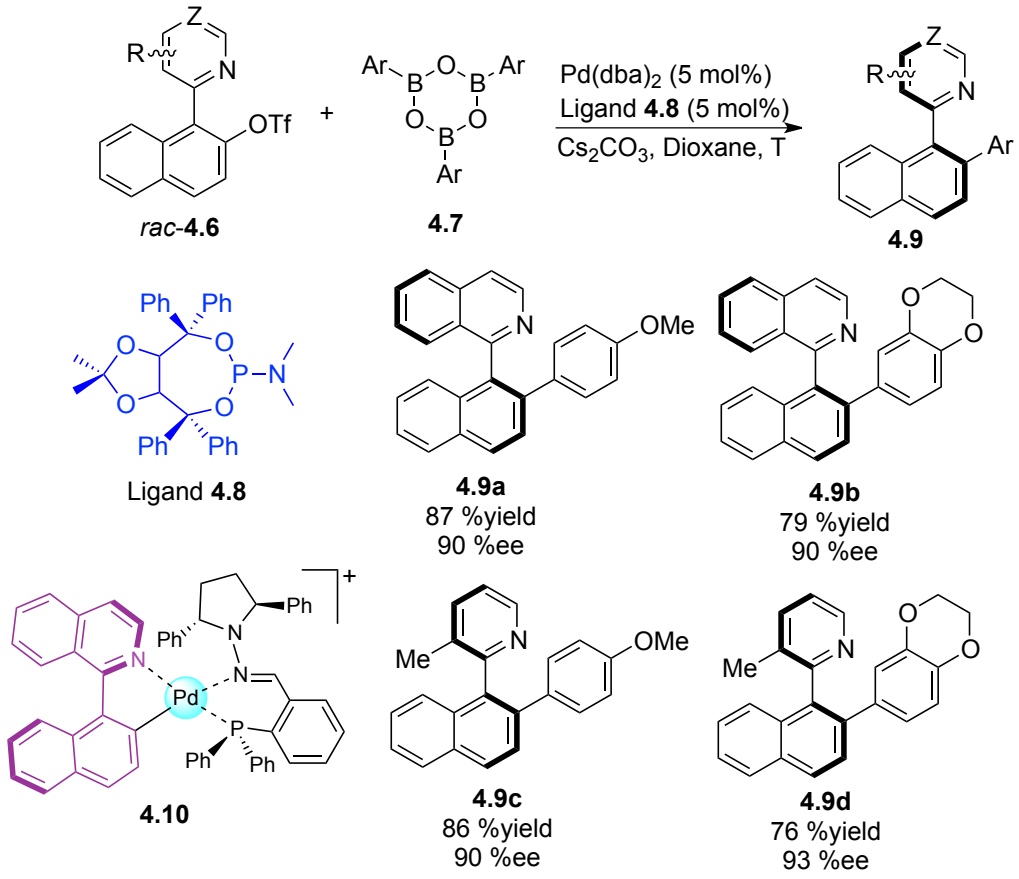


Scheme 4.3. Dynamic Kinetic Suzuki-Miyaura Coupling of Biaryls

Colobert, Wencel-Delord and coworkers investigated the stereoselective sulfoxide-directed acetoxylation and iodination of biaryls occurring through a mild C-H activation/dynamic kinetic resolution sequence.[7] An enantiopure sulfoxide substituent was used as both a chiral auxiliary and a traceless directing group in this process. The configurationally stable racemic biaryl substrate bearing the coordinating sulfoxide group underwent a direct C-H cleavage to generate a small-ring-size, metal-bridged intermediate, which could lower the rotational barrier thus facilitating an isomerization process (Scheme 4.4).

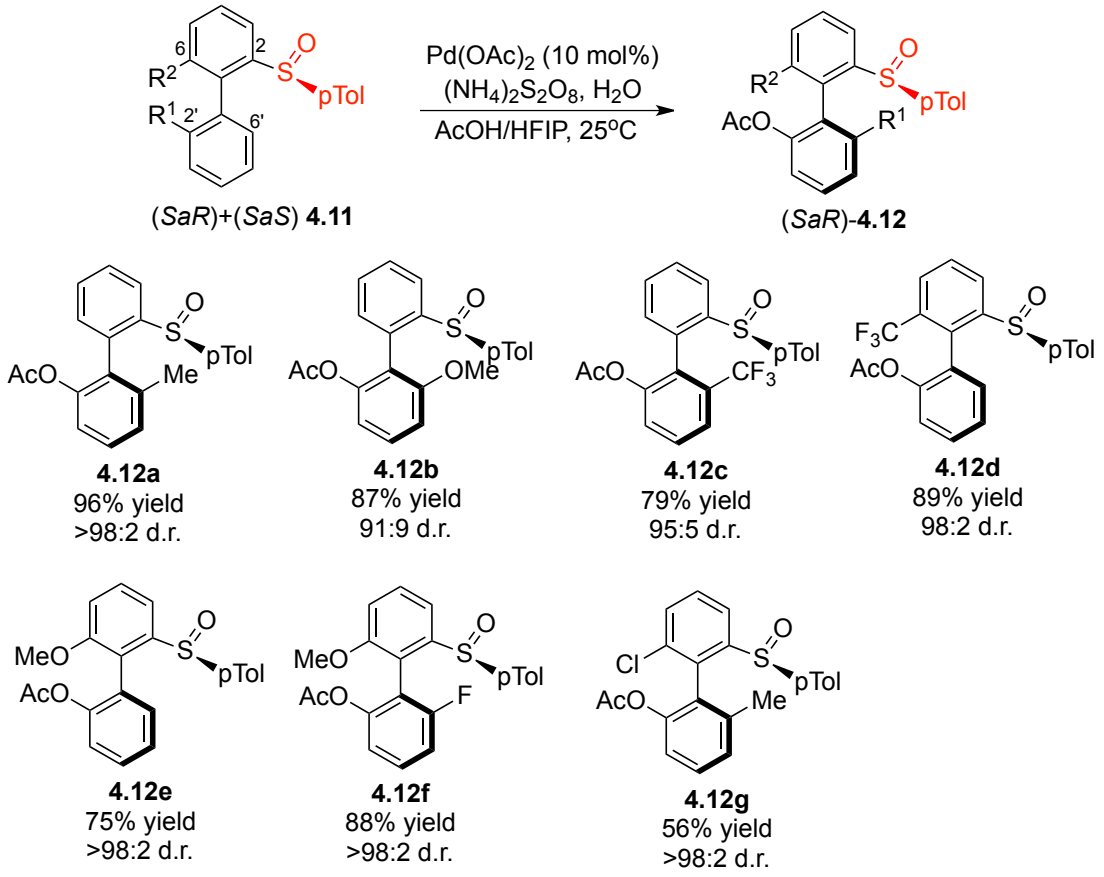


Scheme 4.4. Asymmetric Direct Acetoxylation through Dynamic Kinetic Resolution

In the acetoxylation process, substrate **4.11**, a mixture of two diastereomers, was reacted with $Pd(OAc)_2$ an acetoxylating agent and an oxidant. The reaction proceeded smoothly for an array of 2'-substituted biaryls. The catalytic system is compatible with both electron-rich and electron-poor substrates, 2,6'- and 2,6-disubstituted biaryls. The products were formed in good to excellent yields and selectivities. In contrast, for 2,6,6'-trisubstituted biaryls, bearing more sterically demanding substituents (**4.12g**), the corresponding acetoxylated products were obtained in enantiometrically pure form but in lower yields, which likely underwent a simple kinetic resolution process. They also conducted an asymmetric C-H iodination of biaryl compounds. The efficiency of iodination for *ortho*-trisubstituted substrates depended on steric

hindrance. The iodinated products were obtained in high yields with diasteroselectivities ranging from 91:9 to >98:2.

An asymmetric rhodium(III)-catalyzed C-H activation with direct alkenylation of biaryl derivatives with olefins was developed by You group.[8] The dynamic kinetic resolution of axially chiral biaryls by C-H activation requires the two sterically hindered biaryl systems to be coplanar in order to form the five-membered cyclometalated intermediate, which can interconvert during the reaction process. They first utilized a series of chiral Cp-rhodium complexes to promote the oxidative couplings in the DKR process of biaryls (Scheme 4.5). In the presence of 5 mol% of catalyst **4.15** and 5 mol% $(BzO)_2$, a variety of biaryl substrates were tested in this transformation. The desired alkenylated products were obtained with moderate to excellent yields and enantioselectivities. Both electron-donating and electron-withdrawing substituent in the substrates were tolerated in this reaction.

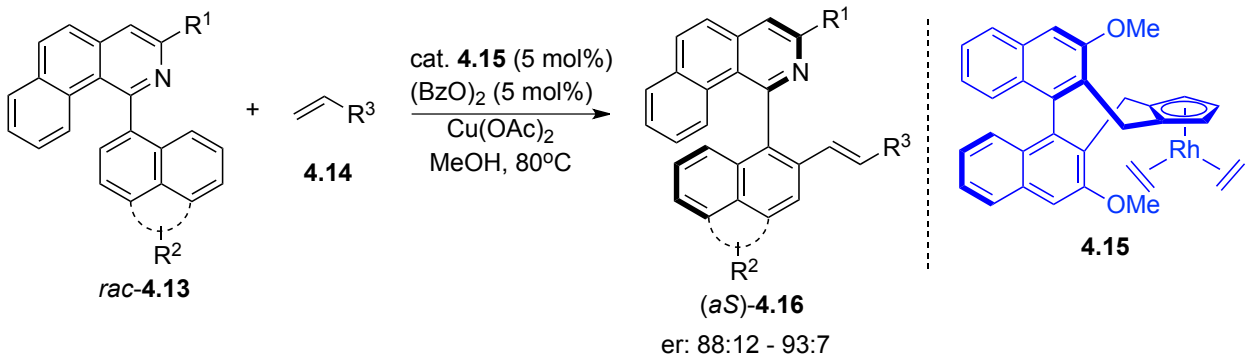


Scheme 4.5. Rhodium-catalyzed Enantioselective Alkenylation of Biaryls

A variety of chiral small organic molecules have proved to be efficient for the dynamic kinetic resolution besides transition metal complexes.

A dynamic kinetic resolution of racemic biaryl substrates via an atropisomer-selective electrophilic bromination reaction was developed by Miller group (Scheme 4.6).[9] The tripeptide-

derived small-molecule catalyst **4.18** was found to catalyze the electrophilic aromatic substitution at the *ortho*-position of biaryls resulting in chiral biaryl products with atropselectivity. When *ortho*-substituted bromo products are formed, the rotation barrier is high enough to maintain the configuration of products.[10] Substrates with electron-withdrawing or electron-donating substituents proved compatible with this transformation. The substituent pattern can also be varied. This methodology also worked well for heteroarene substrates: products such as **4.19f** and **4.19g,** both of which were produced with good selectivities.

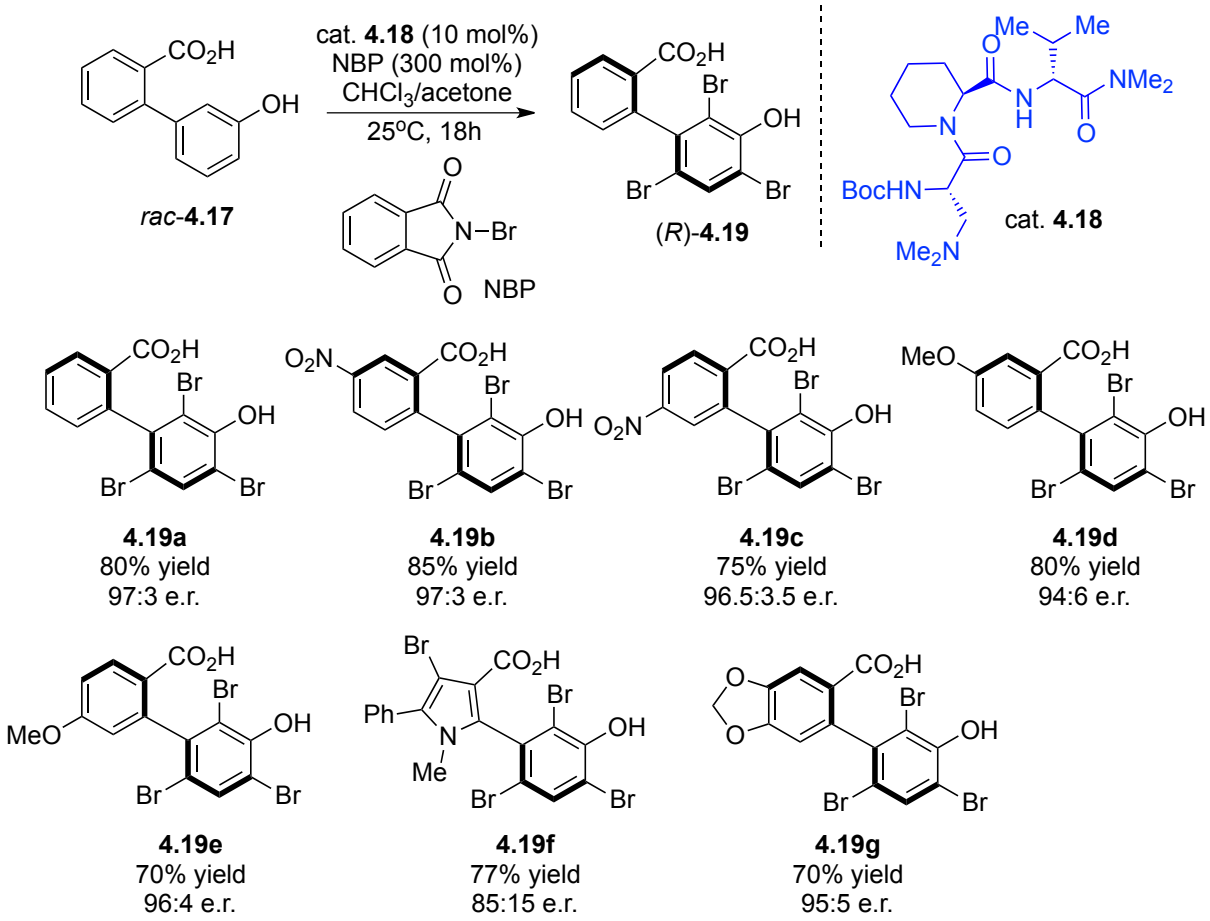


Scheme 4.6. Dynamic Kinetic Resolution of Biaryls via Small Peptide Catalyzed Electrophilic Bromination

Control experiments confirmed the possibility of amide catalysis through the activation of bromo-cation species in this process. Based on these findings and the crystal structure of the

major enantiomeric product, a docking model **4.20** was deduced[9] (Figure 4.1). The stereochemical outcome and the configuration of atropisomeric products were deduced from folding properties of the peptide, the conformation of *N*-acyl piperidines, and the hydrogen bonds between the phenolic proton and the amide diacetate.

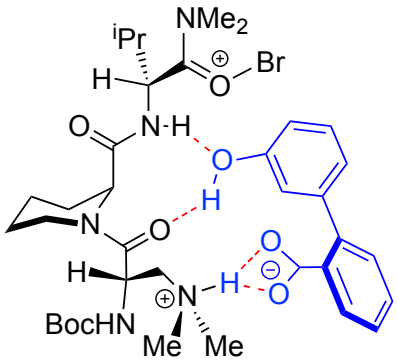


**4.20**

Figure 4.1. Proposed Docking Model

Bringmann and coworkers have developed several efficient methods for synthesizing axially chiral biaryl compounds from racemic biaryl lactones (Scheme 4.7).[11] Aromatics in **4.21** are pre-installed by an ester functionality and undergo intramolecular aryl-coupling. The helically-twisted structure of lactone-bridged biaryls shows a lower isomerization barrier than their corresponding non-bridged axially chiral derivatives. Mechanistically, this strategy constitutes a dynamic kinetic resolution of the rapidly interconverting lactone enantiomers, like **4.22** and **4.23**, then atroposelective ring opening of one lactone-bridged biaryl precursor to afford a corresponding axially chiral biaryl coumpound, which is configurationally stable. The non-reactive conformer will provide more reactive species through the rapid interconversion and thus permit a high-yield conversion of virtually all of the racemic starting material into one particular atropisomeric biaryl. Various methods for stereoselective lactone cleavage have been developed.

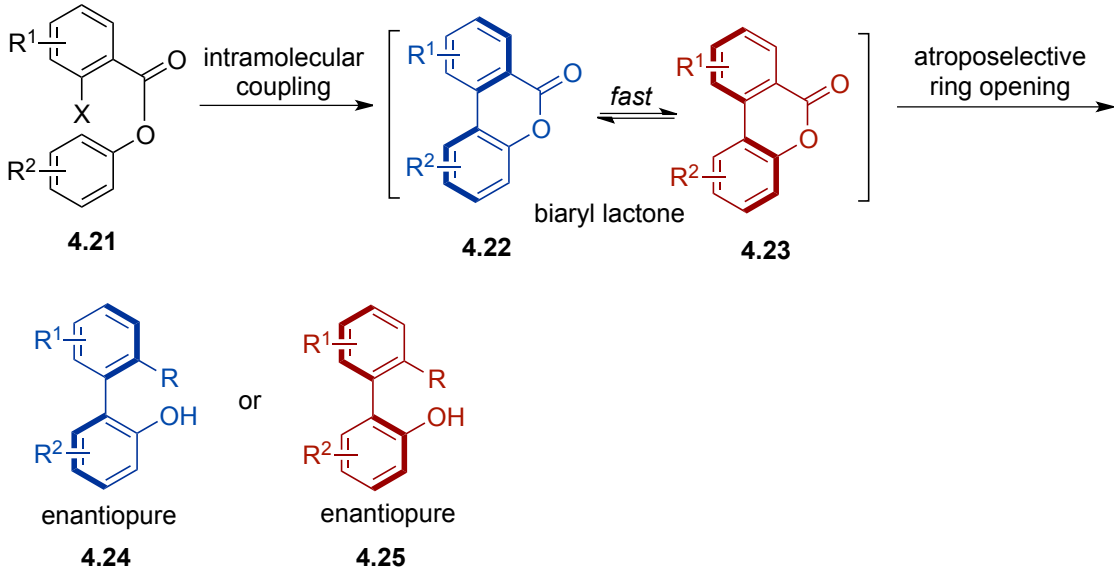


Scheme 4.7. Atropselective Cleavage of the Prochiral Biaryl Compounds

The development of highly efficient methodologies for axially chiral biaryls is of importance in synthetic organic chemistry, medicinal chemistry and material science. One way to obtain the enantiopure biaryl is by applying kinetic resolution process to differentiate two atropisomers and realize the kinetic separation of them. The methods applied in differentiating two conformers in the kinetic resolution opened the door for the development of asymmetric approaches and provided biaryl compounds with efficient stereocontrol.

## 4.2. Results and Discussion

### 4.2.1. Substrate in the Dynamic Kinetic Resolution Study

Inspired by our previous studies on regular kinetic resolution of dihydroxy biaryl derivatives, we decided to explore the dynamic kinetic resolution of atropisomeric biaryls using our novel fluxionally chiral DMAP catalysts. Our dynamic kinetic resolution approach is shown in Scheme 4.8 and the biaryl substrate possessing a phenol structure 2-(2-methoxynaphthalen-1-yl)phenol *rac*-**4.26** was selected as a model substrate. In the acylations of racemic 2-(2-methoxynaphthalen-1-yl)phenol, the interconversions between two corresponding atropisomers

take place during the reaction process due to the low rotation barriers and after acyl transfer process, product racemization must be difficult because of restricted rotation. In the presence of chiral 4-dialkylaminopyridine catalyst, two isomers will react with the acyl donor with different rates, if two enantiomers are equilibrated at a rate that is faster than that of the slow-reacting enantiomer, one enantioenriched acylated isomer will be produced exclusively.

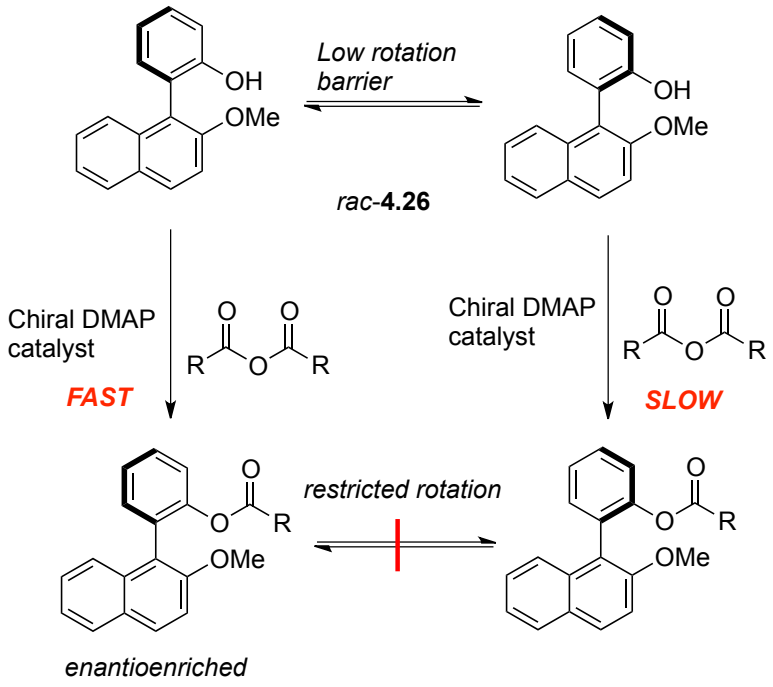


Scheme 4.8. Illustration of Dynamic Kinetic Resolution of 2-(2-Methoxynaphthalen-1-yl)phenol

### 4.2.2. Anhydride Evaluation

The reaction of *rac*-**4.26a** with different anhydrides in the presence of catalyst **4.27** was performed to see the anhydride effect (Table 4.1). Among all the anhydrides tested, isobutyric anhydride was identified as the best anhydride since it can produce more configurationally stable product in 70 %yield and 58 %ee (entry 3). Trimethylacetic anhydride can also provide the product with good enantioselectivity but the reactivity is low (entry 5). Notably, the isobutyrate

substituted product is much more configurationally stable at room temperature than propionate and acetate substituted product.[12]

Table 4.1. Anhydrides Evaluation for Dynamic Kinetic Resolution of Atropisomers

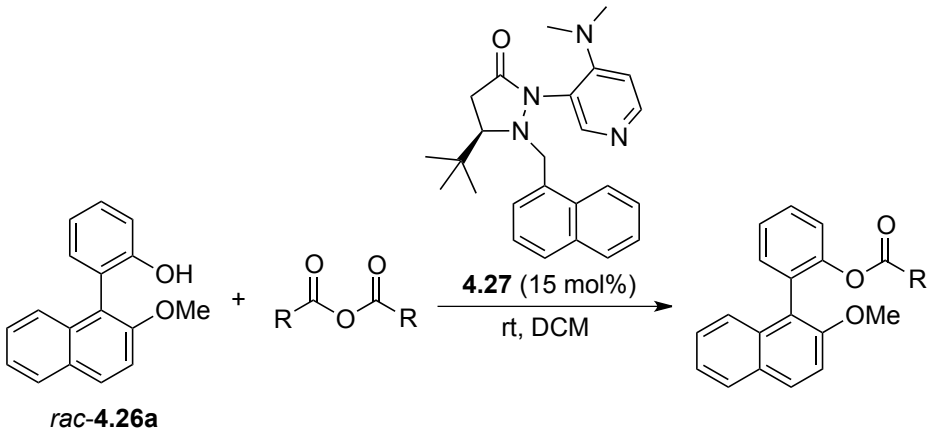


*rac*-**4.26a**

| entry[a] | R | Time | Yield% | ee%[b] |
|---|---|---|---|---|
| 1 | methyl | 12h | 85 | 49 |
| 2 | ethyl | 24h | 93 | 57 |
| 3 | isopropyl | 24h | 70 | 58 |
| 4 | phenyl | 5d | 82 | 44 |
| 5[c] | tert-butyl | 10d | 66 | 67 |

[a]conditions: racemic biaryl substrate (1 equiv.) and anhydride (1.2 equiv.) in the presence of catalyst **4.27** (15 mol%), DCM (2 ml), at room temperature; [b] Determined by HPLC; [c]Reaction was conducted at 40 $^{o}$C.

### 4.2.3. Evaluation of Different Fluxional Chiral 4-Dialkylamino Pyridine Catalysts

The next focus of our study was to evaluate our novel 4-dialkylamino pyridine catalysts, especially the effect of size of the N-1 fluxional group on enantioselectivity (Scheme 4.9). Six different chiral DMAP catalysts were evaluated. Catalyst **4.29** bearing a *t*-butyl chiral group at the C-5 position and a benzyl fluxional group gave low selectivity (25 %ee). Similar results were observed with 2-naphthylmethyl substituted catalyst **4.30** (23 %ee) and mesityl substituted catalyst **4.31** (31 %ee). It was pleased to see increasing the size of the relay group to 1-naphthylmethyl (**4.27**) provided the best result (57 %ee). Installing a larger 9-anthracenylmethyl

fluxional group (**4.32**) gave similar selectivity compared to **4.27**. These results suggested that the effective size of fluxional substituent has a dramatic effect on the enantioselectivity. The larger fluxional group can provide effective steric shielding only if its effective size matches the high selectivity chiral environment.

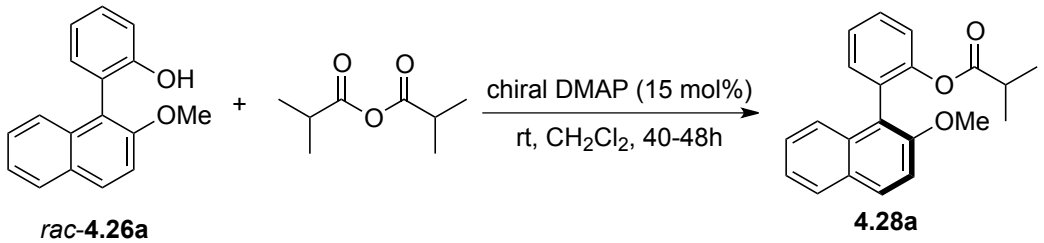


*rac*-**4.26a** **4.28a**

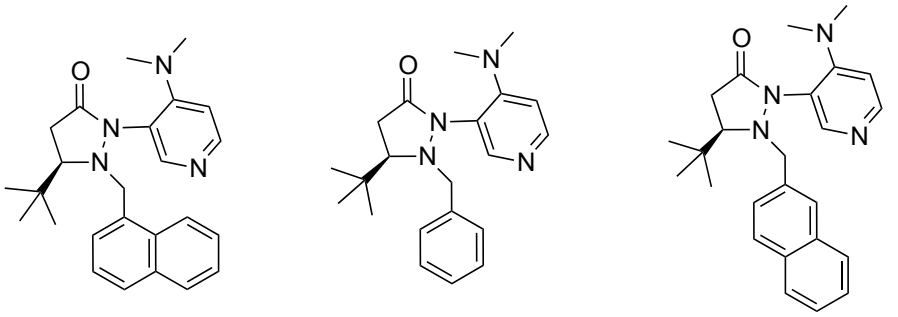

**4.27**
91 %yield, 57 %ee

**4.29**
86 %yield, 25 %ee

**4.30**
89 %yield, 23 %ee

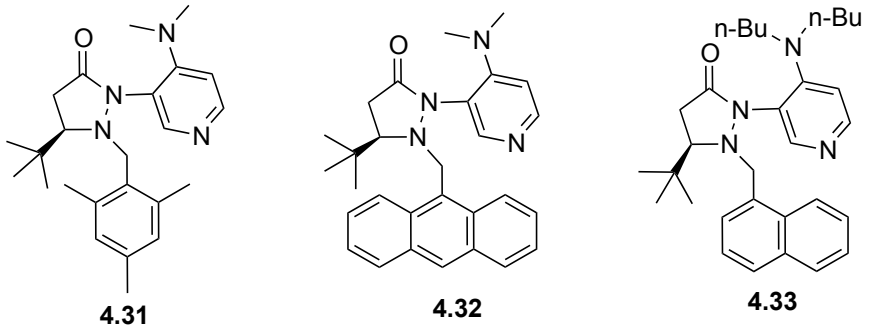

**4.31**
93 %yield, 31 %ee

**4.32**
80 %yield, 57 %ee

**4.33**
86 %yield, 41 %ee

Scheme 4.9. Survey of Chiral 4-Dialkylamino Pyridine Catalysts

The dialkylamino group on the pyridine unit of the catalyst was also investigated and found to impact selectivity: catalyst **4.27** bearing dimethylamino group gave much higher selectivity (57 %ee) than catalyst **4.33** with di-*n*-butylamino substituent (41 %ee). This result

demonstrated that large amino substituent is less selective. Results of catalyst screening thus demonstrate that **4.27** is the best catalyst for the dynamic kinetic resolution of *rac*-**4.26a**.

### 4.2.4. Temperature Screening

Previous investigation has shown that during the dynamic kinetic resolution process, a lower temperature enhanced the proper recognition of each enantiomer, whereas a higher temperature caused a fast equilibrium between them but also lead to more background reaction, which can decrease the enantioselectivity.[13] HPLC analysis of 2-(2-methoxynaphthalen-1-yl)phenol *rac*-**4.26a** suggested that at higher temperature, the lesser resolution occurred (Scheme 4.10). At room temperature, two clear peaks were assigned to two enantiomers of *rac*-**4.26a**. When raising the temperature, two peaks were getting close and started overlapping at 55 °C. Finally a single peak was observed at 80 °C.

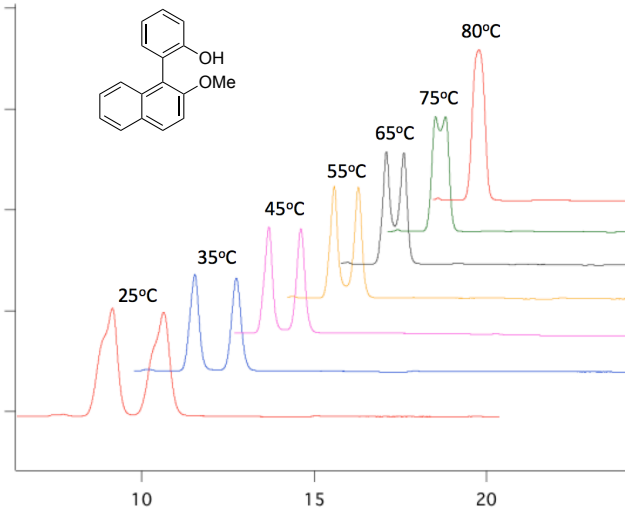


Scheme 4.10. HPLC Racemization Test (Chiralpak OD-H)

The temperature might play an important role in tuning the enantioselectivity, thus the reaction temperature was examined in this case. The temperature effect is shown in Table 4.2.

When the reaction was carried out at a low temperature like 0 °C, it took a long reaction

time and the corresponding acylated biaryl **4.28a** was obtained with low enantioselectivity (Table 4.2, entry 1). Increasing to the room temperature, the enantioselectivity for the product increased remarkably to 57 % and the reactivity was also largely improved (Table 4.2, entry 2).

Table 4.2. Examination of Reaction at Different Temperatures

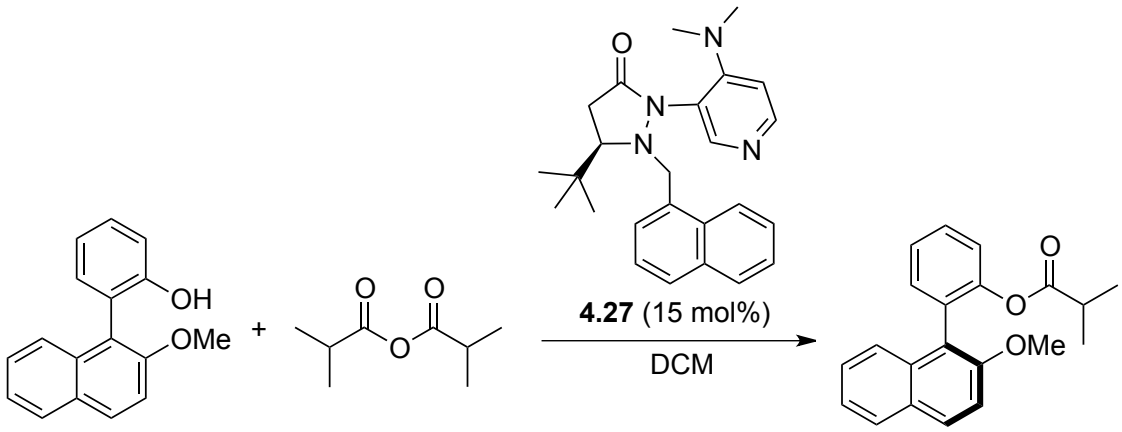


*rac*-**4.26a** **4.28a**

| entry[a] | T (°C) | Time | Yield% | ee%[b] |
|---|---|---|---|---|
| 1 | 0 | 5d | 77 | 19 |
| 2 | rt | 48h | 91 | 57 |
| 3 | 35 | 48h | 94 | 74 |
| 4 | 45 | 48h | 93 | 73 |
| 5 | 55 | 48h | 93 | 65 |
| 6 | 75 | 24h | 96 | 50 |
| 7 | 40 | 48h | 95 | 74 |

[a]Conditions: racemic biaryl substrate *rac*-**4.26** (1 equiv.) and anhydride (1.2 equiv.) in the presence of catalyst **4.27** (15 mol%), DCM (2 ml), at different temperatures; [b]Determined by HPLC.

These two trials encouraged us to explore more temperature variations. To our delight, the reaction at 35 °C gave the biaryls in 74 %ee (Table 4.2, entry 3). At a higher reaction temperature (45 °C), the enantioselectivity was similar to the result at 35 °C, with a slight decrease in the selectivity (entry 4). Interestingly, when the temperature was raised to 55 °C, the

selectivity was reduced (entry 5). This might be because the high temperature also promoted more racemization of the product. The reaction conducted at 75 °C showed remarkable reduction (entry 6). We then put attention to temperature between 35 °C and 45 °C. Finally, it was found that 40 °C was the best reaction temperature for the catalytic atropselective acylation of 2-(2-methoxynaphthalen-1-yl)phenol *rac*-**4.26a** and the product was obtained with 74 %ee (entry 7).

**4.2.5. Evaluation of Solvents**

In terms of solvent effects, better results were observed with alkyl halide solvents (Table 4.3, entry 1, 3 and 5) and chloroform exhibited relatively higher selectivity. Using ethereal solvent (THF) provided moderate selectivity (entry 2). An aromatic solvent like toluene was more effective in controlling the selectivity than ethereal solvents (entry 4). Amide and ester solvents were also tested and unfortunately they didn't improve the enantioselectivity (entry 6 and 7).

Table 4.3. Evaluation of Solvents

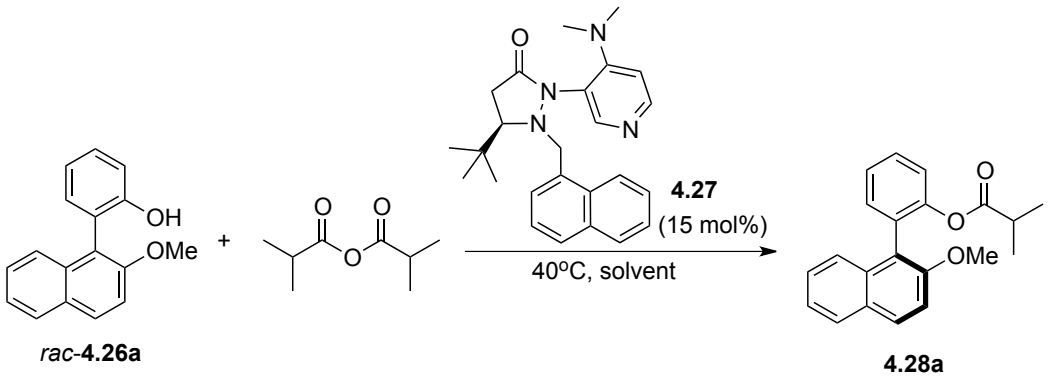


*rac*-**4.26a** **4.28a**

| entry[a] | Solvents | Time | Yield% | ee%[b] |
|---|---|---|---|---|
| 1 | $CH_2Cl_2$ | 48h | 95 | 74 |
| 2 | THF | 3d | 64 | 43 |
| 3 | $ClCH_2CH_2Cl$ | 40h | 92 | 73 |
| 4 | Toluene | 40h | 95 | 69 |
| 5 | $CHCl_3$ | 48h | 95 | 75 |
| 6 | DMF | 3d | 60 | 44 |
| 7 | EtOAc | 24h | 87 | 62 |

[a]Conditions: racemic biaryl substrate *rac*-**4.26a** (1 equiv.) and anhydride (1.2 equiv.) in the presence of catalyst **4.27** (15 mol%), Solvent (2 ml), at 40 °C; [b]Determined by HPLC.

### 4.2.6. Survey of Different Types of Bases

In order to further improve the selectivity, we were interested in determining whether additional base would be able to make an impact, since base could remove the byproduct isobutyric acid and thus prevent deactivation of the catalyst. Additionally, base can also promote the proton transfer in the acylation. In the beginning, we evaluated *N*-heterocyclic bases as additives. Reaction with 2,6-di-*tert*-butyl pyridine, 2,6-dimethyl pyridine and simple pyridine as the base provided the acylated product with similar reactivity and selectivity (Table 4.4, entries 1-3). More bulky base gave slightly higher enantiocontrol. In contrast, addition of *N*-methyl imidazole had a detrimental effect on the selectivity as it may promote the background reaction (entry 4).

Table 4.4. Evaluation of Additional Aromatic Amine Bases

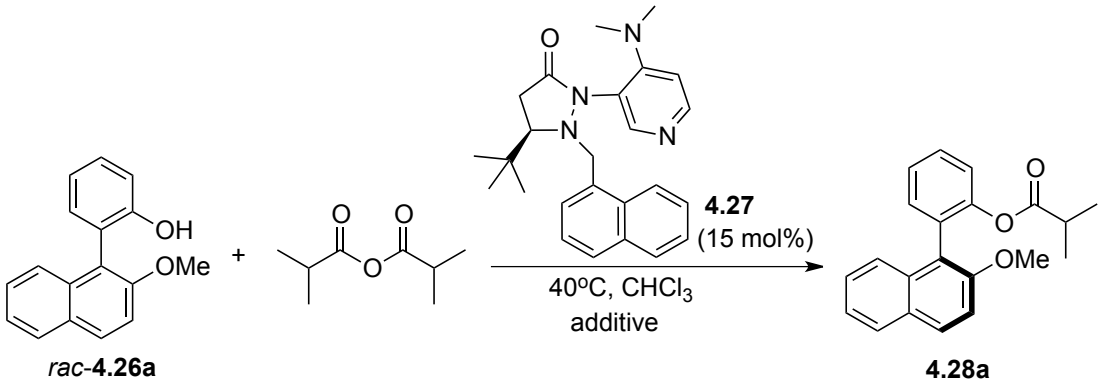


*rac*-**4.26a** **4.28a**

| entry[a] | additives | Time | Yield% | ee%[b] |
|---|---|---|---|---|
| 1 | 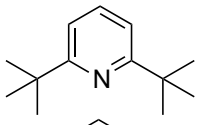 | 72h | 91 | 76 |
| 2 | 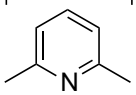 | 48h | 87 | 75 |
| 3 |  | 48h | 89 | 72 |
| 4 | 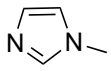 | 48h | 97 | 15 |

[a]Conditions: racemic biaryl substrate *rac*-**4.26a** (1 equiv.) and isobutyric anhydride (1.2 equiv.) in the presence of catalyst **4.27** (15 mol%), Additive (1.2 equiv.), $CHCl_3$ (2 ml), at 40 °C; [b]Determined by HPLC.

Alkyl amines as additives were also evaluated (Table 4.5). Acyclic simple tertiary amines didn't improve the selectivity and showed similar efficiency (entries 1-4). Cyclic amine gave a small decrease in enantioselectivity (entry 5). The small loss of enantioselectivity was observed in the cyclic diamine-DABCO (entry 6). In contrast, tetramethylethylenediamine as a diamine gave similar result as single tertiary amines (Table 4.5, entry 7). To our delight, addition of proton sponge (1,8-Bis(dimethylamino)naphthalene) improved the enantioselectivity slightly to 76% (entry 8). It was found that molecular sieves could further impact the selectivity (entry 9).

Table 4.5. Evaluation of Additional Alkyl Amine Bases

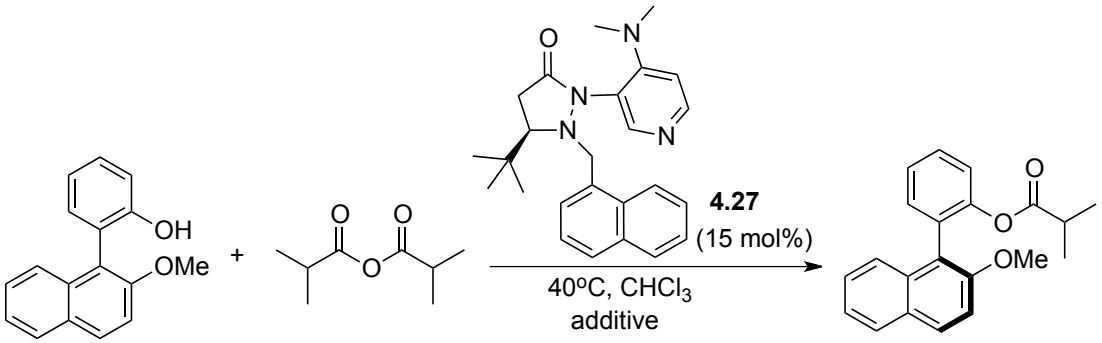


*rac*-**4.26a** **4.28a**

| entry[a] | Additives | Time | Yield% | ee%[b] | entry | Additives | Time | Yield% | ee% |
|---|---|---|---|---|---|---|---|---|---|
| 1 | $Et_3N$ | 48h | 89 | 74 | 6 | 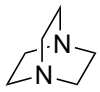 | 48h | 95 | 69 |
| 2 | $^nBu_3N$ | 60h | 90 | 75 | | | | | |
| 3 | 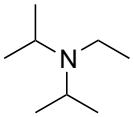 | 60h | 85 | 74 | 7 | 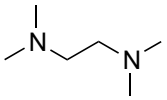 | 72h | 95 | 72 |
| 4 | 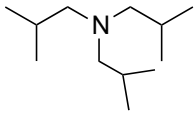 | 60h | 92 | 75 | 8 | 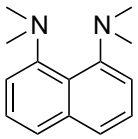 | 48h | 87 | 76 |
| 5 | 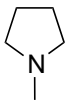 | 60h | 96 | 70 | 9[c] | 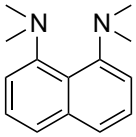 | 48h | 81 | 80 |

[a]Conditions: racemic biaryl substrate *rac*-**4.26a** (1 equiv.) and isobutyric anhydride (1.2 equiv.) in the presence of catalyst **4.27** (15 mol%), Additive (1.2 equiv.), $CHCl_3$ (2 ml), at 40 °C; [b]Determined by HPLC; [c] with Molecule sieve 13X.

We were also interested in the efficiency of inorganic bases to affect dynamic kinetic resolution. The counter anion of inorganic salt as Lewis base could help to promote the proton transfer. In order to avoid the Lewis acidity of metal salts, the alkali metal carbonates were selected (Table 4.6). Not surprisingly, when using cesium carbonate as additive, no selectivity was observed since cesium cation was able to act as strong Lewis acid, which can activate the anhydride by coordination and facilitate the acyl transfer (entry 1). Potassium carbonate, a weaker Lewis acid, gave the product with moderate selectivity (entry 2). In contrast, sodium and

lithium carbonates imporoved the selectivity to levels comparable to organic bases and sodium carbonate showed better reactivity than lithium carbonate (entries 3 and 4). Two other sodium salts were also tested. Sodium acetate exhibited similar selectivity as sodium carbonate (entry 5). Loss of enantioselectivity was observed by adding sodium methoxide since methoxide may promote uncatalyzed background reactions to some extent (entry 6).

Table 4.6. Evaluation of Additional Inorganic Salts

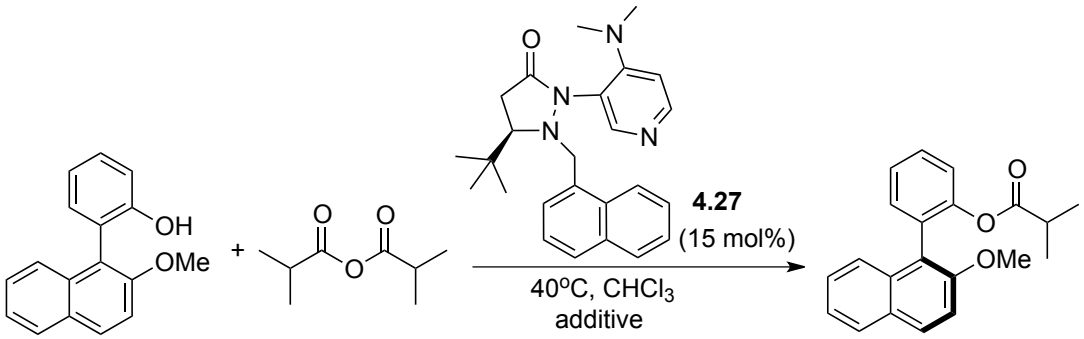


*rac*-**4.26a** **4.28a**

| entry[a] | Additives | Time | Yield% | ee%[b] |
|---|---|---|---|---|
| 1 | $Cs_2CO_3$ | 24h | 96 | racemic |
| 2 | $K_2CO_3$ | 48h | 94 | 37 |
| 3 | $Na_2CO_3$ | 48h | 91 | 73 |
| 4 | $Li_2CO_3$ | 60h | 74 | 70 |
| 5 | NaOAc | 60h | 87 | 70 |
| 6 | NaOMe | 60h | 96 | 62 |

[a]Conditions: racemic biaryl substrate *rac*-**4.26a** (1 equiv.) and isobutyric anhydride (1.2 equiv.) in the presence of catalyst **4.27** (15 mol%), Additive (1.2 equiv.), $CHCl_3$ (2 ml), at 40 °C; [b]Determined by HPLC.

### 4.2.7. Substrate Scope of Dynamic Kinetic Resolution of Biaryls

With an optimized set of reaction conditions in hand, we set out to investigate biaryl substrates in the newly developed dynamic kinetic resolution strategy (Scheme 4.11). The size of R group was found to affect the enantioselectivity. Larger size decreased the reaction efficiency.

The reaction with methoxy substituted biaryl *rac*-**4.26a** (R = OMe) gave the best result. Replacing methoxy group with ethoxy group (R = OEt) slightly lowered the enantioselectivity and reactivity. Lower enantioselectivity was observed when the R was replaced by larger benzyloxy group (67 %ee). It seems alkoxy substituent at R position is essential in the dynamic kinetic resolution outcome. For example, methoxy methyl substituted biaryl substrate (*rac*-**4.26d**) experienced a remarkable decrease of enantioslectivity. Switching 2-substituent with 2'-substituent of *rac*-**4.26a** formed substrate *rac*-**4.26e**, which was synthesized and tested. However, significant decrease of enantioselectivity was observed in *rac*-**4.26e** case compared to *rac*-**4.26a**. To further extend the scope for this methodology, a survey of substitution pattern in the substrate was conducted. It was found that substitution at bottom naphthyl ring in **4.26** had detrimental effect on the enantioselectivity of product. 4'-methyl substituted *rac*-**4.26f** only provided the corresponding product with 25 %ee and moderate reactivity. In contrast, substitution at the top phenyl ring displayed much more promising results. The corresponding products were obtained with high enantioselectivities. Furthermore, substrates with electron-donating or mild electron-withdrawing substituted phenol ring were well tolerated in the dynamic kinetic resolution process.

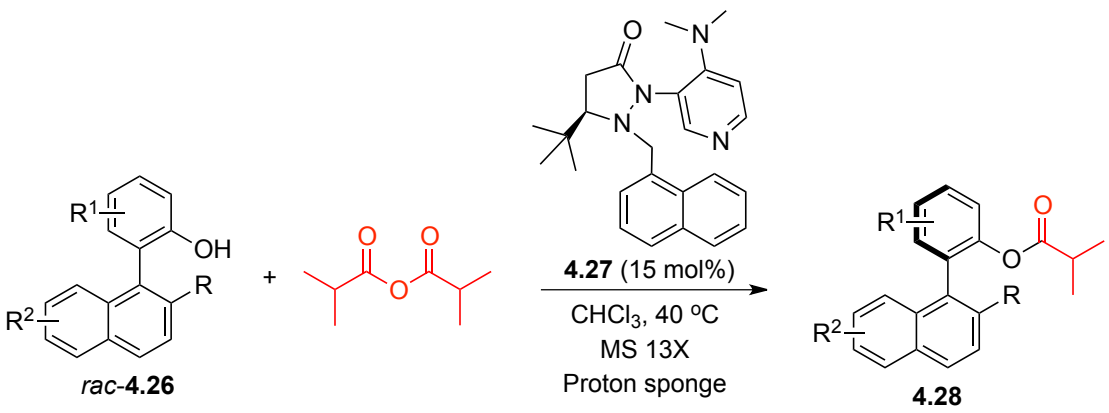


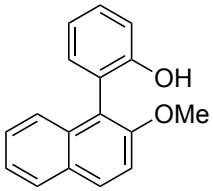


*rac*-**4.26a**

**4.28a**, 48h
81 %yield, 80 %ee

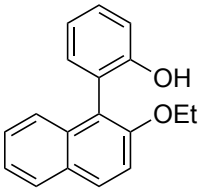


*rac*-**4.26b**

**4.28b**, 48h
74 %yield, 77 %ee

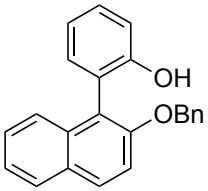


*rac*-**4.26c**

**4.28c**, 72h,
68 %yield, 67 %ee

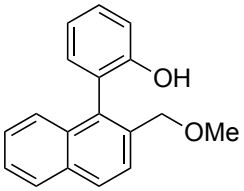


*rac*-**4.26d**

**4.28d**, 48h
78 %yield, 11 %ee

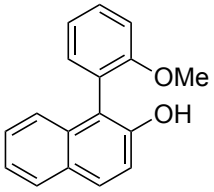


*rac*-**4.26e**

**4.28e**, 48h
71 %yield, 23 %ee

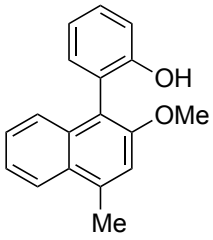


*rac*-**4.26f**

**4.28f**, 6d
70 %yield, 25 %ee

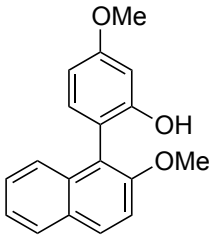


*rac*-**4.26g**

**4.28g**, 48h
92 %yield, 72 %ee

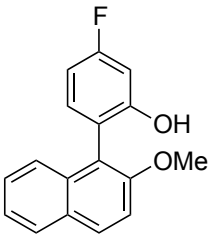


*rac*-**4.26h**

**4.28h**, 48h,
88 %yield, 67 %ee

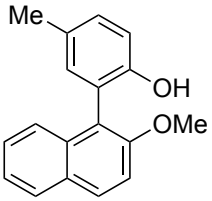


*rac*-**4.26i**

**4.28i**, 48h
89 %yield, 78 %ee

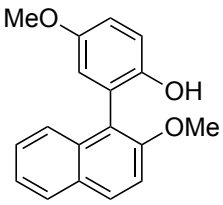


*rac*-**4.26j**

**4.28j**, 48h
91 %yield, 75 %ee

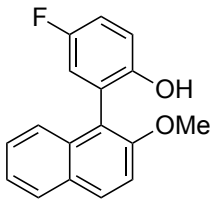


*rac*-**4.26k**

**4.28k**, 48h,
80 %yield, 75 %ee

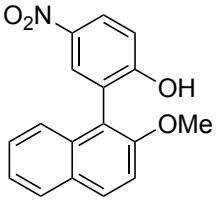


*rac*-**4.26l**

**4.28l**, 24h
94 %yield, 2 %ee

Scheme 4.11. Substrate Scope for Dynamic Kinetic Resolution of Biaryls Catalyzed by Chiral DMAP Catalysts

The enantioselectivity for the substrate with substitution at 4-position of phenyl ring showed good enantioselectivity and reactivity (*rac*-**4.26g** and *rac*-**4.26h**). The improvement was observed when phenyl ring had 5-substitution. 5-methyl and 5-methoxy substituted substrate *rac*-**4.26i** and *rac*-**4.26j** gave the product with 78 %ee and 75 %ee, respectively. The differentiation was observed when electron-withdrawing groups were substituted at the 5-position. The mild electron-withdrawing group, like fluoro substituted biaryl (*rac*-**4.26k**) still can provide efficient stereocontrol. However, *rac*-**4.26l** with strong electron-withdrawing nitro group showed poor selectivity in the corresponding product, presumably because the hydroxyl group became very active and took part in the uncatalyzed background reactions.

### 4.2.8. Stereochemical Model

Based on the experimental results, we propose the stereochemical model as shown in Scheme 4.12. The DMAP ring and the acyl group of the acylpyridinium ion lie approximately in a single plane. The naphthalene ring with methoxy group approaches the *N*-acyl group from the top face due to the intervention of attractive π-π interaction between *N*-acyl and OMe group. The hydroxyl group on the phenol ring will stay at the bottom and attack the acyl group to generate the *S*-isomer.

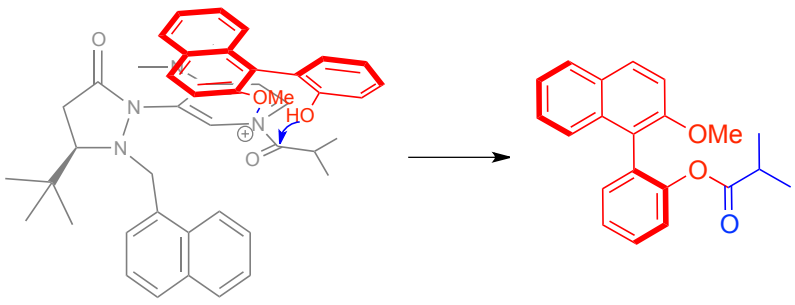


Scheme 4.12. Proposed Stereochemical Model

## 4.3. Conclusion

The development of highly efficient methodologies for axially chiral biaryls is of significance in synthetic organic chemistry, medicinal chemistry and material science. In this chapter, we have demonstrated that the novel fluxionally chiral 4-dialkylamino pyridine molecules can serve as an effective acylation catalyst for the dynamic kinetic resolution of biaryl compounds. The equilibrium between the atropoisomers of the biaryl substrates was demonstrated from chiral HPLC analysis and the temperature was found to be a key point in controlling the stereochemical outcome of acylative dynamic kinetic resolution. Good yield and enantioselectivities were obtained for configurationally stable biaryl product. The best enantioselectivity was achieved with 80 %ee. Fluxional organocatalysts can be used in enantioselective processes and transfer stereochemical information, and enantioselectivity can be affected by changing fluxional groups. Compared to simple kinetic resolution of biaryls, the dynamic kinetic resolution of configurationally unstable biaryls shows less effciency under higher temperature. In the substrate scope study, the enantioselectivity is largely affected by the biaryl substrate's structure. Additionally, the parameters that influenced the reactivity were also investigated. Our present protocol provides a new approach for the preparation of optically active biaryl compounds. Mechanistic and computational studies are currently underway to better understand the basis for asymmetric induction in this system.

## 4.4. Experimental

### 4.4.1. General

All solvents were dried and degassed by standard methods and stored under nitrogen. Flash chromatography was performed using EM Science silica gel 60 (230-400 mesh). $^{1}$H NMR spectra were recorded on Varian Unity/Inova-400 NB (400 MHz) spectrometer or Bruker

Ascend™ 400 (400 MHz for $^{1}H$) spectrometer. $^{13}C$ NMR spectra were recorded on Varian Unity/Inova-400 NB (100 MHz) spectrometer or Bruker Ascend™ 400 (100 MHz for $^{13}C$) spectrometer. HPLC analyses were carried out with Waters 515 HPLC pumps and a 2487 dual wavelength absorbance detector connected to a PC with Empower workstation. Rotations were recorded on a JASCO-DIP-370 polarimeter. High-resolution mass spectra were obtained at a Waters ACQUITY UPLC with ESI Positive Mode.

**4.4.2. The Absolute Stereochemistry Discussion**

Electronic circular dichroism (ECD or CD) is a powerful spectroscopic method for solving stereochemical problems of chiral molecules.[14] By using quantum chemical calculations of time-dependent density functional theory (TD-DFT), ECD has become a rapid and reliable way to establish the absolute configuration of chiral compounds.[15] In this study, we employed ECD spectra and TD-DFT calculation to assign the absolute configuration of **4.28a**. The ECD spectra of **4.28a** in methanol at a concentration of 0.8-0.9 mg/mL were recorded in a 1mm path length quartz cuvette using a Jasco J-815 CD spectrometer (Jasco Inc., Japan).

The ECD spectra were calculated by the TD-DFT method, which has been proven to be reliable in predicting ECD spectra and assigning the absolute configuration of organic molecules. Calculations of the ECD spectra of 3D structure of *S*-**4.28a** (Figure 4.2) were carried out using the TD-M06/6-31+G** level with Gaussian 09.[16] Electronic excitation energies (nm) and rotational strengths ($\Delta\varepsilon$) were calculated for structures A. In order to cover the 200-400 nm range, 19 transitions were calculated. As shown in Figure 4.2, the simulated spectra is in good agreement with the experimental spectral data, and the *S* configuration could be reliably assigned to compound **4.28a**. The remaining configurations of acylated products were assumed by analogy.

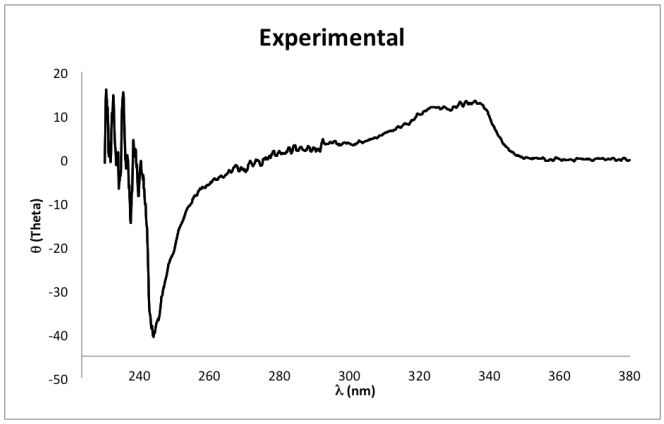


Experimental CD spectra of **4.28a**

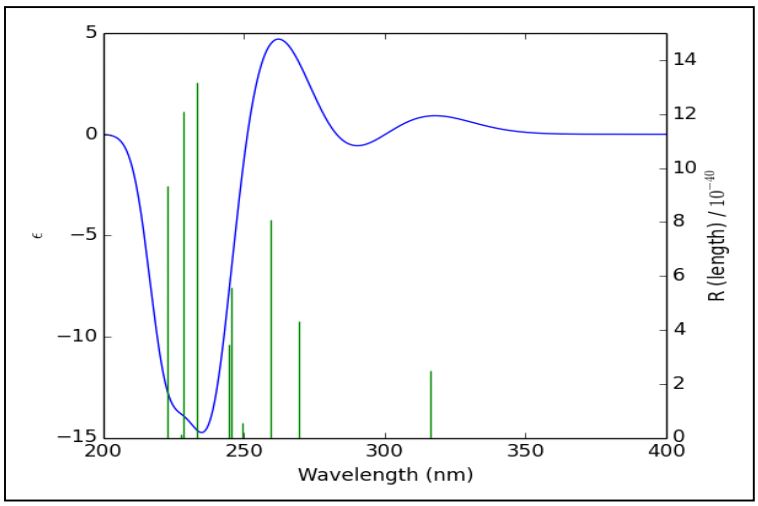


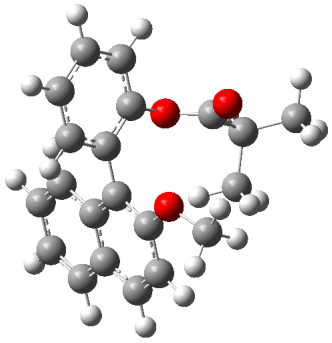

Simulated CD spectra of *S*-**4.28a**

Figure 4.2. TD-DFT Simulated Spectrum Calculated using B3LYP Method. (M06/6-31+G(d,p)optimization, the first 19 excited states were calculated. )

### 4.4.3. General Procedure for the Preparation of Biaryl Compounds

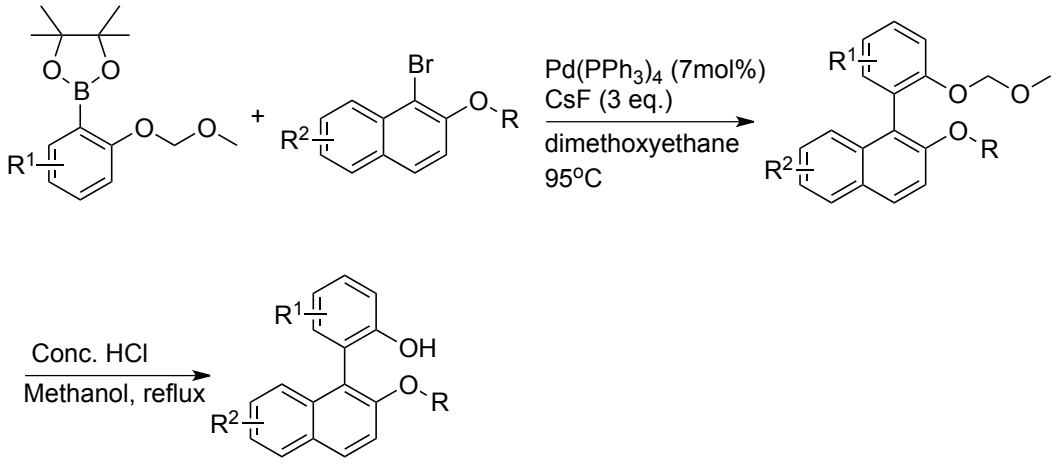


Scheme 4.13. Reaction Condition A[17]

Under an atmosphere of argon, degassed dimethoxyethane solution was added to a mixture of 1-bromo-2-methoxynaphthalene (1 equiv.), 2-[2-(methoxymethoxy)phenyl]-4,4,5,5-tetramethyl-1,3,2-dioxaborolane (1.1 equiv.), CsF (3 equiv.) and $Pd(PPh_3)_4$ (7 mol%). After being stirred for overnight at 95 °C, the resulting suspension was filtered through a pad of celite and washed with ethyl acetate. After evaporation *in vacuo*, the residue was purified by flash chromatography on silica gel eluting with ethyl acetate/hexane (5/95) to yield methoxymethyl (MOM) protected product (60-80 %yield). Concentrated hydrochloric acid was added to a solution of MOM protected compound in methanol. The reaction mixture was stirred overnight under reflux. After removal of the solvent, flash column chromatography with ethyl acetate/hexane (5/95) gave the desired product (70-80 %yield).

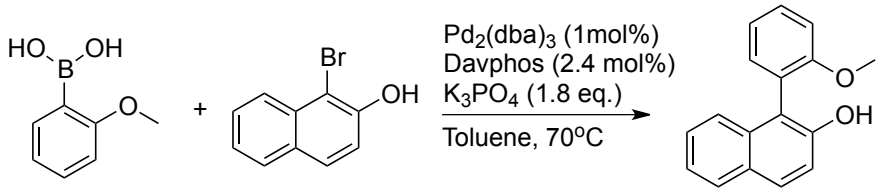


Scheme 4.14. Reaction Condition B[18]

Under an atmosphere of argon, degassed toluene solution was added to a mixture of 1-bromo-2-naphthol (1 equiv.), 2-methoxyphenylboronic acid (1.5 equiv.), 2-dicyclohexylphosphino-2'-(N,N'-dimethylamino)biphenyl (Davphos) (2.4 mol%), $Pd_2(dba)_3$ (1 mol%) and $K_3PO_4$ (1.8 eq.). After being stirred for overnight at 70 °C, the resulting suspension was filtered through a pad of celite and washed with ethyl acetate. After evaporation *in vacuo*, the residue was purified by flash chromatography on silica gel eluting with ethyl acetate/hexane (5/95) to yield product. (50-60 %yield).

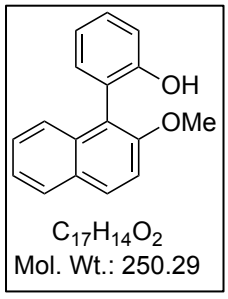


*rac*-**4.26a.** Condition A. $^1$H NMR ($CDCl_3$, 400 MHz) δ 3.92 (s, 3H), 4.97 (s, 1H), 7.1 (td, *J* = 7.6, 1.2 Hz, 1H), 7.14 (dd, *J* = 8, 1.2 Hz, 1H), 7.25 (dd, *J* = 7.6, 2 Hz, 1H), 7.38-7.44 (m, 4H), 7.51-7.54 (m, 1H), 7.87-7.89 (m, 1H), 7.99 (d, *J* = 9.2 Hz, 1H); $^{13}$C NMR ($CDCl_3$, 100 MHz) δ 56.8, 113.5, 116.0, 118.5, 120.5, 122.4, 124.1, 125.0, 127.1, 126.6, 126.8, 128.1, 129.4, 129.4, 130.5, 132.1, 133.7, 153.8, 154.5; ESI-HRMS: *m/z* calcd. for $(C_{17}H_{14}O_2Na)^+$ 273.0886; found 273.0894.

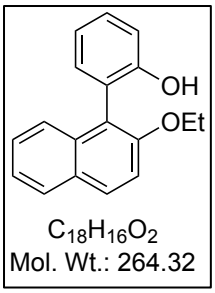


$C_{18}H_{16}O_2$
Mol. Wt.: 264.32

*rac*-**4.26b**. Condition A. $^1$H NMR ($CDCl_3$, 400 MHz) δ 1.3 (t, *J* = 7.2 Hz, 3H), 4.1-4.2 (m, 2H), 5.18 (s, 1H), 7.08 (td, *J* = 7.2, 1.2 Hz, 1H), 7.14 (dd, *J* = 8, 1.2 Hz, 1H), 7.26 (dd, *J* = 7.2, 2 Hz, 1H), 7.37-7.42 (m, 4H), 7.56-7.59 (m, 1H), 7.85-7.87 (m, 1H), 7.93 (d, *J* = 9.2 Hz, 1H); $^{13}$C NMR ($CDCl_3$, 100 MHz) δ 15, 65.7, 115.4, 116.2, 119.9, 120.4, 122.7, 124.2, 125.2, 126.9, 128.1, 129.3, 129.7, 130.3, 132.3, 133.8, 153.7, 153.9; ESI-HRMS *m/z* calcd. for $(C_{18}H_{17}O_2)^+$ 265.1229; found 265.1232.

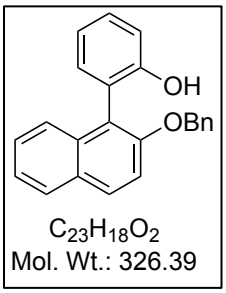


$C_{23}H_{18}O_2$
Mol. Wt.: 326.39

*rac*-**4.26c**. Condition A. $^1$H NMR ($CDCl_3$, 400 MHz) δ 4.96 (s, 1H), 5.12-5.19 (m, 2H), 7.07 (td, *J* = 7.2, 1.2 Hz, 1H), 7.13 (dd, *J* = 8, 1.2 Hz, 1H), 7.2-7.25 (m, 3H), 7.25-7.31 (m, 3H), 7.37-7.42 (m, 4H), 7.51-7.55 (m, 1H), 7.82-7.86 (m, 1H), 7.9 (d, *J* = 9.2 Hz, 1H); $^{13}$C NMR ($CDCl_3$, 100 MHz) δ 71.8, 116, 120.2, 120.5, 122.5, 124.4, 125.1, 127.04, 127.05, 127.8, 128.1, 128.5, 129.4, 129.8, 130.4, 132.1, 133.7, 136.8, 153.6, 153.8; ESI-HRMS *m/z* calcd. for $(C_{23}H_{18}O_2Na)^+$ 349.1205; found 349.1207.

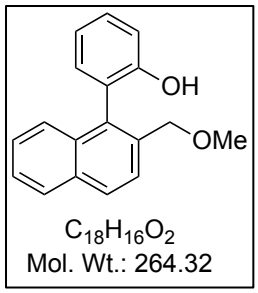


$C_{18}H_{16}O_2$
Mol. Wt.: 264.32

*rac*-**4.26d**. Condition A. $^1$H NMR ($CDCl_3$, 400 MHz) δ 3.33 (s, 3H), 4.34 (d, $J$ = 10.8 Hz, 1H), 4.38 (d, $J$ = 10.8 Hz, 1H), 5.44 (s, 1H), 7.05-7.14 (m, 3H), 7.38-7.45 (m, 3H), 7.48-7.52 (m, 1H), 7.67 (d, $J$ = 8.4 Hz, 1H), 7.9 (d, $J$ = 8.4 Hz, 1H), 7.95 (d, $J$ = 8.4 Hz, 1H); $^{13}$C NMR ($CDCl_3$, 100 MHz) δ 58.6, 73.3, 116.8, 120.7, 124.9, 126.2, 126.3, 126.61, 126.64, 128, 128.9, 129.7, 131.4, 132.9, 133, 133.5, 134.8, 153.9; ESI-HRMS *m/z* calcd. for $(C_{18}H_{16}O_2Na)^+$ 287.1048; found 287.1055.

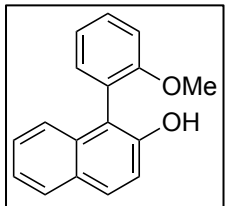


$C_{17}H_{14}O_2$
Mol. Wt.: 250.29

*rac*-**4.26e**. Condition B. $^1$H NMR ($CDCl_3$, 400 MHz) δ 3.78 (s, 3H), 5.32 (s, 1H), 7.15-7.21 (m, 2H), 7.29-7.4 (m, 5H), 7.51-7.55 (m, 1H), 7.83-7.85 (m, 2H); $^{13}$C NMR ($CDCl_3$, 100 MHz) δ 55.8, 111.9, 117.7, 117.8, 121.5, 122.5, 123.2, 124.8, 126.3, 128, 129.1, 129.5, 130.2, 133.4, 133.5, 150.6, 157.8; ESI-HRMS *m/z* calcd. for $(C_{17}H_{15}O_2)^+$ 251.1072; found 251.1077.

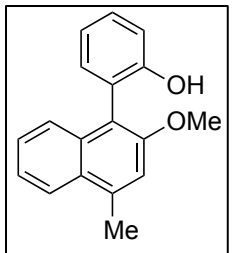


$C_{18}H_{16}O_2$
Mol. Wt.: 264.32

*rac*-**4.26f**. Condition A. $^1$H NMR ($CDCl_3$, 400 MHz) δ 2.26 (s, 3H), 4.06 (s, 3H), 4.65 (s, 1H), 6.81 (s, 1H), 7.03-7.14 (m, 3H), 7.35-7.44 (m, 4H), 8.27-8.3 (m, 1H); $^{13}$C NMR ($CDCl_3$, 100 MHz) δ 21.1, 55.8, 106.9, 115.4, 120.8, 122.2, 123.1, 124.7, 124.9, 125.3, 125.4, 127.4, 129.5, 131.7, 134.1, 136.4, 153.7, 155.8; ESI-HRMS *m/z* calcd. for $(C_{18}H_{17}O_2)^+$ 265.1229; found 265.1223.

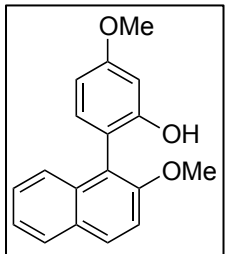


$C_{18}H_{16}O_3$
Mol. Wt.: 280.32

*rac*-**4.26g**. Condition A. $^1$H NMR ($CDCl_3$, 400 MHz) δ 3.87 (s, 3H), 3.9 (s, 3H), 5.01 (s, 1H), 6.67 (td, *J* = 8.4, 2.4 Hz, 2H), 7.11 (d, *J* = 8.4 Hz, 1H), 7.35-7.42 (m, 3H), 7.52-7.55 (m, 1H), 7.83-7.86 (m, 1H), 7.94 (d, *J* = 9.2 Hz, 1H); $^{13}$C NMR ($CDCl_3$, 100 MHz) δ 55.5, 57, 101.6, 107.1, 113.7, 114.8, 118.6, 124.2, 125.3, 127.2, 128.2, 129.7, 130.5, 132.8, 134.3, 154.8, 154.9, 160.9; ESI-HRMS *m/z* calcd. for $(C_{18}H_{17}O_3)^+$ 281.1178; found 281.1183.

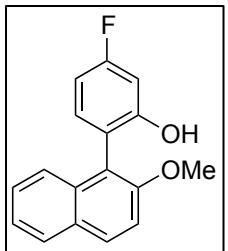


$C_{17}H_{13}FO_2$
Mol. Wt.: 268.28

*rac*-**4.26h**. Condition A. $^1$H NMR ($CDCl_3$, 400 MHz) δ 3.9 (s, 3H), 5.09 (s, 1H), 6.8 (td, *J* = 8.4, 2.8 Hz, 1H), 6.84 (dd, *J* = 10, 2.4 Hz, 1H), 7.16 (dd, *J* = 8.4, 6.8 Hz, 1H), 7.37-7.44 (m, 3H), 7.46-7.49 (m, 1H), 7.85-7.87 (m, 1H), 7.97 (d, *J* = 9.2 Hz, 1H); $^{13}$C NMR ($CDCl_3$, 100 MHz) δ 56.7, 103.6 (d, *J* = 25 Hz), 107.7 (d, *J* = 22 Hz), 113.4, 117.4, 118.3 (d, *J* = 4 Hz), 124.2, 124.7, 127.3, 128.2, 129.4, 130.8, 132.9 (d, *J* = 9 Hz), 133.8, 154.7, 155 (d, *J* = 12 Hz), 163.4 (d, *J* = 244 Hz); $^{19}$F NMR ($CDCl_3$, 376 MHz) δ -112.7; ESI-HRMS *m/z* calcd. for $(C_{17}H_{14}FO_2)^+$ 269.0978; found 269.0976.

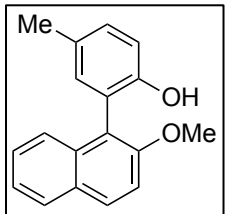


$C_{18}H_{16}O_2$
Mol. Wt.: 264.32

*rac*-**4.26i**. Condition A. $^1$H NMR ($CDCl_3$, 400 MHz) δ 2.35 (s, 3H), 3.91 (s, 3H), 4.8 (s, 1H), 7-7.03 (m, 2H), 7.17 (dd, *J* = 8.4, 2.4 Hz, 1H), 7.36-7.42 (m, 3H), 7.51-7.53 (m, 1H), 7.84-7.86 (m, 1H), 7.95 (d, *J* = 8.8 Hz, 1H); $^{13}$C NMR ($CDCl_3$, 100 MHz) δ 20.6, 56.8, 113.4, 115.8, 118.7, 122.1, 124, 125.1, 127, 128, 129.4, 129.6, 130, 130.4, 132.4, 133.8, 151.6, 154.4; ESI-HRMS *m/z* calcd. for $(C_{18}H_{17}O_2)^+$ 265.1229; found 265.1231.

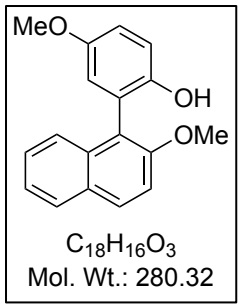


$C_{18}H_{16}O_3$
Mol. Wt.: 280.32

*rac*-**4.26j**. Condition A. $^1$H NMR ($CDCl_3$, 400 MHz) δ 3.78 (s, 3H), 3.91 (s, 3H), 4.72 (s, 1H), 6.79 (d, $J$ = 3.2 Hz, 1H), 6.95 (dd, $J$ = 8.8, 3.2 Hz, 1H), 7.04 (d, $J$ = 8.8 Hz, 1H), 7.37-7.43 (m, 3H), 7.55-7.57 (m, 1H), 7.84-7.87 (m, 1H), 7.95 (d, $J$ = 9.2 Hz, 1H); $^{13}$C NMR ($CDCl_3$, 100 MHz) δ 55.8, 56.8, 113.5, 115.1, 116.81, 116.84, 118.7, 123.1, 124.1, 125, 127.1, 128.1, 129.4, 130.5, 133.6, 147.9, 153.4, 154.3; ESI-HRMS *m/z* calcd. for $(C_{18}H_{17}O_3)^+$ 281.1178; found 281.1181.

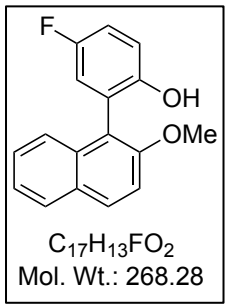


$C_{17}H_{13}FO_2$
Mol. Wt.: 268.28

*rac*-**4.26k**. Condition A. $^1$H NMR ($CDCl_3$, 400 MHz) δ 3.91 (s, 3H), 4.82 (s, 1H), 6.95 (dd, $J$ = 8.8, 2.8 Hz, 1H), 7.02-7.1 (m, 2H), 7.37-7.44 (m, 3H), 7.48-7.51 (m, 1H), 7.85-7.87 (m, 1H), 7.97 (d, $J$ = 9.2 Hz, 1H); $^{13}$C NMR ($CDCl_3$, 100 MHz) δ 56.8, 113.3, 115.8 (d, $J$ = 23 Hz), 116.9 (d, $J$ = 8 Hz), 117.5, 118.2 (d, $J$ = 23 Hz), 123.5 (d, $J$ = 8 Hz), 124.2, 124.6, 127.4, 128.2, 129.4, 130.9, 133.3, 149.9 (d, $J$ = 3 Hz), 154.4, 156.8 (d, $J$ = 236 Hz); $^{19}$F NMR ($CDCl_3$, 376 MHz) δ -124.5; ESI-HRMS *m/z* calcd. for $(C_{17}H_{14}FO_2)^+$ 269.0978; found 269.0976.

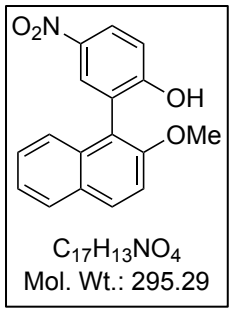


$C_{17}H_{13}NO_4$
Mol. Wt.: 295.29

*rac*-**4.26l**. Condition A. $^1$H NMR ($CDCl_3$, 400 MHz) δ 3.91 (s, 3H), 5.57 (s, 1H), 7.17 (d, *J* = 9.2 Hz, 1H), 7.36-7.46 (m, 4H), 7.87-7.9 (m, 1H), 8.03 (d, *J* = 8.8 Hz, 1H), 8.18 (d, *J* = 2.8 Hz, 1H), 8.28 (dd, *J* = 9.2, 2.8 Hz, 1H); $^{13}$C NMR ($CDCl_3$, 100 MHz) δ 56.6, 113, 115.1, 116.3, 123.1, 123.9, 124.5, 125.6, 127.9, 128.4, 128.5, 129.3, 131.8, 133.1, 141.6, 154.9, 159.5; ESI-HRMS *m/z* calcd. for $(C_{17}H_{14}NO_4)^+$ 296.0923; found 296.0926.

### 4.4.4. General Procedure for Dynamic Kinetic Resolution of Biaryl Compounds

To a mixture of racemic biaryl compounds (0.05 mmol), catalyst (15 mol%), Proton sponge® (0.06 mmol, Aldrich) and Molecular sieves 13X® (100mg, Aldrich), 2 mL dry $CHCl_3$ was added and heated to 40 °C. Isobutyric anhydride (0.06 mmol) was added at this temperature. After stirring for indicated time in Scheme 4.11, the reaction mixture was purified by column chromatography (hexane/ethyl acetate = 95/5) to afford the corresponding ester. The optical purity of the obtained product was determined by HPLC.

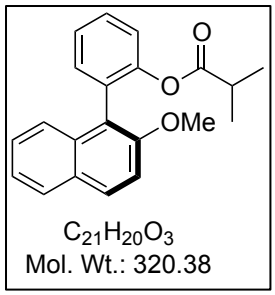


$C_{21}H_{20}O_3$
Mol. Wt.: 320.38

**4.28a** (80 %ee) HPLC (UV 254 nm, Chiralpak AD-3, *i*-PrOH/Hexane = 2/98, 0.5 mL/min), $t_1$ (minor) = 17.1 min, $t_2$ (major) = 22.3 min. $[\alpha]_D$ $^{22}$ 12.1 (*c* 0.66, $CH_2Cl_2$). $^1$H NMR ($CDCl_3$, 400 MHz) δ 0.66 (d, *J* = 6.8 Hz, 3H), 0.7 (d, *J* = 6.8 Hz, 3H), 2.3 (m, 1H), 3.86 (s, 3H), 7.28-7.31 (m, 1H), 7.34-7.43 (m, 6H), 7.48-7.52 (m, 1H), 7.81-7.83 (m, 1H), 7.9 (d, *J* = 9.2 Hz, 1H); $^{13}$C NMR ($CDCl_3$, 100 MHz) δ 18.2, 18.3, 33.8, 56.7, 113.4, 120.4, 122.8, 123.6, 125.2, 125.7, 126.4, 127.6, 128.6, 128.8, 129.4, 129.5, 132.5, 133.4, 149.3, 154.2, 174.7; ESI-HRMS: *m/z* calcd. for $(C_{21}H_{20}O_3Na)^+$ 343.1305; found 343.1302.

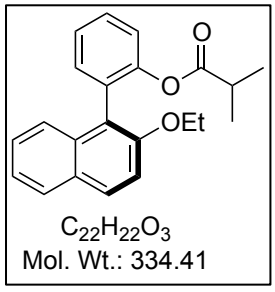


$C_{22}H_{22}O_3$
Mol. Wt.: 334.41

**4.28b** (77 %ee) HPLC (UV 220 nm, Chiralpak AD-3, *i*-PrOH/Hexane = 1/99, 0.5 mL/min), $t_1$ (minor) = 14.7 min, $t_2$ (major) = 20 min. $[\alpha]_D$ $^{23}$ 19.1 (*c* 0.69, $CH_2Cl_2$). $^1$H NMR ($CDCl_3$, 400 MHz) δ 0.63 (d, *J* = 6.8 Hz, 3H), 0.68 (d, *J* = 6.8 Hz, 3H), 1.24 (t, *J* = 6.8 Hz, 3H), 2.27 (m, *J* = 6.8 Hz, 1H), 4.04-4.12 (m, 2H), 7.27 (d, *J* = 8 Hz, 1H), 7.3-7.42 (m, 6H), 7.45-7.49 (m, 1H), 7.78-7.8 (m, 1H), 7.85 (d, *J* = 8.8 Hz, 1H); $^{13}$C NMR ($CDCl_3$, 100 MHz) δ 15, 18.2,

33.8, 65.4, 115.3, 121.3, 122.7, 123.6, 125.3, 125.5, 126.3, 127.6, 128.4, 129, 129.4, 129.5, 132.6, 133.5, 149.3, 153.6, 174.7; ESI-HRMS *m/z* calcd. for $(C_{22}H_{22}O_3Na)^+$ 357.1467; found 357.1460.

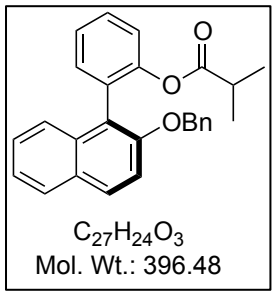


$C_{27}H_{24}O_3$
Mol. Wt.: 396.48

**4.28c** (67 %ee) HPLC (UV 220 nm, Chiralpak AD-3, *i*-PrOH/Hexane = 1/99, 0.5 mL/min), $t_1$ (minor) = 30.4 min, $t_2$ (major) = 40.3 min. $[\alpha]_D^{22}$ 9.5 (*c* 0.71, $CH_2Cl_2$). $^1$H NMR ($CDCl_3$, 400 MHz) δ 0.55 (d, *J* = 7.2 Hz, 3H), 0.63 (d, *J* = 7.2 Hz, 3H), 2.24 (m, *J* = 7.2 Hz, 1H), 5.1 (s, 2H), 7.2-7.34 (m, 9H), 7.35-7.38 (m, 2H), 7.4-7.43 (m, 1H), 7.45-7.5 (m, 1H), 7.75-7.78 (s, 1H), 7.8 (d, *J* = 8.8 Hz, 1H); $^{13}$C NMR ($CDCl_3$, 100 MHz) δ 18.3, 34, 71.7, 115.9, 121.9, 123, 124, 125.6, 125.9, 126.6, 127.1, 127.7, 127.8, 128.5, 128.8, 129.3, 129.6, 129.7, 132.8, 133.6, 137.7, 149.5, 153.5, 175; ESI-HRMS *m/z* calcd. for $(C_{27}H_{24}O_3Na)^+$ 419.1623; found 419.1633.

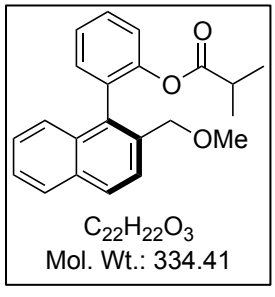


$C_{22}H_{22}O_3$
Mol. Wt.: 334.41

**4.28d** (11 %ee) HPLC (UV 220 nm, Chiralpak OD-3, *i*-PrOH/Hexane = 1/99, 0.5 mL/min), $t_1$ (major) = 13.4 min, $t_2$ (minor) = 16.1 min. $[\alpha]_D^{22}$ -6.7 (*c* 0.6, $CH_2Cl_2$). $^1$H NMR ($CDCl_3$, 400 MHz) δ 0.51 (d, *J* = 7.2 Hz, 3H), 0.55 (d, *J* = 6.8 Hz, 3H), 2.2 (m, *J* = 7.2, 6.8 Hz, 1H), 3.3 (s, 3H), 4.32 (s, 2H), 7.25 (dd, *J* = 8, 1.2 Hz, 1H), 7.33-7.39 (m, 4H), 7.42-7.46 (m, 1H),

7.5-7.54 (m, 1H), 7.68 (d, $J$ = 8.4 Hz, 1H), 7.84 (d, $J$ = 8 Hz, 1H), 7.88 (d, $J$ = 8.4 Hz, 1H); $^{13}$C NMR ($CDCl_3$, 100 MHz) δ 18, 18.1, 33.7, 58.3, 72.3, 122.9, 125.5, 125.6, 125.9, 126.1, 126.3, 127.7, 128.2, 129.1, 131.3, 131.9, 132.4, 132.7, 133, 134.5, 149.1, 174.9; ESI-HRMS *m/z* calcd. for $(C_{22}H_{22}O_3)^+$ 357.1467; found 357.1472.

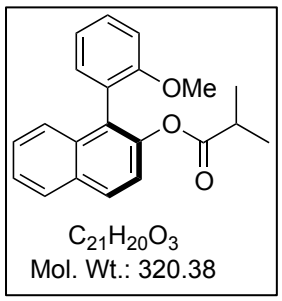


**4.28e** (23 %ee) HPLC (UV 220 nm, Chiralpak AD-H, *i*-PrOH/Hexane = 0.5/0.995, 0.5 mL/min), $t_1$ (minor) = 22.3 min, $t_2$ (major) = 29.1 min. $[\alpha]_D^{25}$ 5.5 (*c* 0.71, $CH_2Cl_2$). $^1$H NMR ($CDCl_3$, 400 MHz) δ 0.94 (d, $J$ = 6.8 Hz, 3H), 0.99 (d, $J$ = 6.8 Hz, 3H), 2.53 (m, $J$ = 6.8 Hz, 1H), 3.68 (s, 3H), 7.02-7.07 (m, 2H), 7.16-7.19 (m, 1H), 7.3 (d, $J$ = 8.8 Hz, 1H), 7.35-7.49 (m, 4H), 7.87-7.9 (m, 2H); $^{13}$C NMR ($CDCl_3$, 100 MHz) δ 18.7, 18.8, 34.2, 55.9, 111.2, 120.6, 121.8, 124.1, 125.5, 126.2, 126.4, 127.7, 128.2, 129, 129.6, 131.9, 132.2, 133.6, 146.1, 157.8; ESI-HRMS *m/z* calcd. for $(C_{21}H_{20}O_3Na)^+$ 343.1310; found 343.1315.

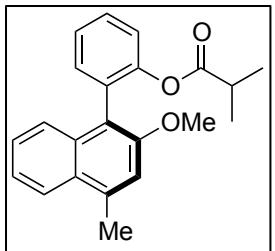


$C_{22}H_{22}O_3$
Mol. Wt.: 334.41

**4.28f** (25 %ee) HPLC (UV 220 nm, Whelk-(R,R), *i*-PrOH/Hexane = 1/99, 0.5 mL/min), $t_1$ (major) = 18.2 min, $t_2$ (minor) = 20.6 min. $[\alpha]_D^{22}$ -7.4 (*c* 0.69, $CH_2Cl_2$). $^1$H NMR ($CDCl_3$, 400 MHz) δ 0.58 (d, *J* = 6.8 Hz, 3H), 0.61 (d, *J* = 6.8 Hz, 3H), 2.22 (s, 3H), 2.23 (m, *J* = 6.8 Hz, 1H), 4.03 (s, 3H), 6.73 (s, 1H), 7.23 (dd, *J* = 8, 1.2 Hz, 1H), 7.27-7.3 (m, 2H), 7.32-7.4 (m, 3H), 7.47 (td, *J* = 7.6, 2 Hz, 1H), 8.21-8.23 (m, 1H); $^{13}$C NMR ($CDCl_3$, 100 MHz) δ 18.1, 18.2, 21, 33.8, 55.5, 106.4, 121.5, 122.9, 123.9, 124.1, 125.5, 125.6, 126, 126.5, 128.5, 132.4, 132.8, 133.6, 134.4, 149.5, 154.9, 175; ESI-HRMS *m/z* calcd. for $(C_{22}H_{22}O_3Na)^+$ 357.1467; found 357.1477.

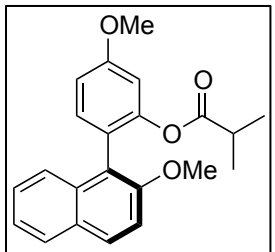


$C_{22}H_{22}O_4$
Mol. Wt.: 350.41

**4.28g** (72 %ee) HPLC (UV 220 nm, Chiralpak AD-3, *i*-PrOH/Hexane = 4/96, 0.5 mL/min), $t_1$ (minor) = 16.7 min, $t_2$ (major) = 20.7 min. $[\alpha]_D^{23}$ 4.7 (*c* 0.8, $CH_2Cl_2$). $^1$H NMR ($CDCl_3$, 400 MHz) δ 0.63 (d, *J* = 6.8 Hz, 3H), 0.66 (d, *J* = 6.8 Hz, 3H), 2.26 (m, *J* = 6.8 Hz, 1H), 3.84 (s, 3H), 3.89 (s, 3H), 6.83 (d, *J* = 2.8 Hz, 1H), 6.94 (dd, *J* = 8.8, 2.8 Hz, 1H), 7.26 (d, *J* = 8.4 Hz, 1H), 7.29-7.36 (m, 3H), 7.42-7.44 (m, 1H), 7.77-7.79 (m, 1H), 7.86 (d, *J* = 9.2 Hz, 1H);

$^{13}$C NMR ($CDCl_3$, 100 MHz) δ 18.21, 18.24, 33.8, 55.5, 56.7, 108.4, 111.9, 113.5, 120.2, 121.3, 123.5, 125.3, 126.4, 127.6, 128.9, 129.3, 132.8, 133.8, 150, 154.5, 159.8, 174.6; ESI-HRMS *m/z* calcd. for $(C_{22}H_{22}O_4Na)^+$ 373.1416; found 371.1423.

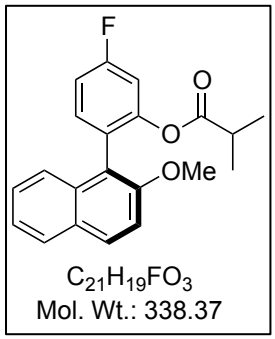


$C_{21}H_{19}FO_3$
Mol. Wt.: 338.37

**4.28h** (67 %ee) HPLC (UV 220 nm, Chiralpak AD-3, *i*-PrOH/Hexane = 1/99, 0.5 mL/min), $t_1$ (minor) = 15.8 min, $t_2$ (major) = 23.2 min. $[\alpha]_D^{23}$ 8.7 (*c* 0.76, $CH_2Cl_2$). $^1$H NMR ($CDCl_3$, 400 MHz) δ 0.63 (d, *J* = 6.8 Hz, 3H), 0.67 (d, *J* = 7.2 Hz, 3H), 2.27 (m, *J* = 7.2, 6.8 Hz, 1H), 3.84 (s, 3H), 7.05 (dd, *J* = 9.2, 2.8 Hz, 1H), 7.1 (td, *J* = 8.4, 2.4 Hz, 1H), 7.31-7.38 (m, 5H), 7.78-7.81 (m, 1H), 7.89 (d, *J* = 9.2 Hz, 1H); $^{13}$C NMR ($CDCl_3$, 100 MHz) δ 18.15, 18.17, 33.8, 56.6, 110.8 (d, *J* = 24 Hz), 112.9 (d, *J* = 21 Hz), 113.3, 119.3, 123.6, 124.9, 125.3 (d, *J* = 3 Hz), 126.6, 127.8, 128.8, 129.8, 133.2 (d, *J* = 9 Hz), 133.5, 149.9 (d, *J* = 11 Hz), 154.3, 162.2 (d, *J* = 246 Hz), 174.4; $^{19}$F NMR ($CDCl_3$, 376 MHz) δ -112.8; ESI-HRMS *m/z* calcd. for $(C_{21}H_{19}FO_3Na)^+$ 361.1216; found 361.1207.

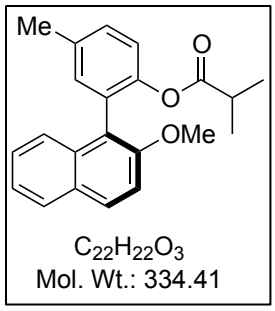


$C_{22}H_{22}O_3$
Mol. Wt.: 334.41

**4.28i** (78 %ee) HPLC (UV 220 nm, Whelk (R, R), *i*-PrOH/Hexane = 1/99, 0.5 mL/min), $t_1$ (major) = 22.9 min, $t_2$ (minor) = 26.6 min. $[\alpha]_D^{23}$ 36.2 (*c* 0.69, $CH_2Cl_2$). $^1$H NMR ($CDCl_3$, 400 MHz) δ 0.63 (d, *J* = 7.2 Hz, 3H), 0.67 (d, *J* = 6.8 Hz, 3H), 2.28 (m, *J* = 7.2, 6.8 Hz, 1H), 2.42 (s, 3H), 3.85 (s, 3H), 7.15 (d, *J* = 8.4 Hz, 1H), 7.17-7.18 (m, 1H), 7.26-7.37 (m, 4H), 7.41-7.44 (m, 1H), 7.78-7.81 (m, 1H), 7.87 (d, *J* = 9.2 Hz, 1H); $^{13}$C NMR ($CDCl_3$, 100 MHz) δ 18.26, 18.28, 21, 33.8, 56.7, 113.4, 120.5, 122.4, 123.5, 125.3, 126.4, 127.6, 128.9, 129, 129.3, 129.4, 132.9, 133.5, 135.2, 147, 154.2, 174.9; ESI-HRMS *m/z* calcd. for $(C_{22}H_{22}O_3Na)^+$ 357.1467; found 357.1475.

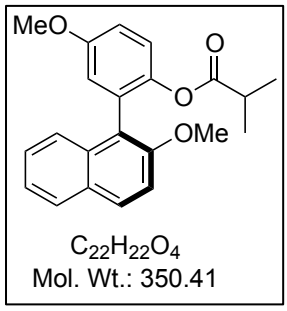


$C_{22}H_{22}O_4$
Mol. Wt.: 350.41

**4.28j** (75 %ee) HPLC (UV 220 nm, Chiralpak IA, *i*-PrOH/Hexane = 1/99, 0.5 mL/min), $t_1$ (minor) = 20.5 min, $t_2$ (major) = 27.7 min. $[\alpha]_D^{23}$ 28.3 (*c* 0.84, $CH_2Cl_2$). $^1$H NMR ($CDCl_3$, 400 MHz) δ 0.61 (d, *J* = 6.8 Hz, 3H), 0.65 (d, *J* = 6.8 Hz, 3H), 2.25 (m, *J* = 6.8 Hz, 1H), 3.82 (s, 3H), 3.85 (s, 3H), 6.9 (d, *J* = 2.8 Hz, 1H), 7 (dd, *J* = 8.8, 3.2 Hz, 1H), 7.17 (d, *J* = 8.8 Hz, 1H), 7.3-7.37 (m, 3H), 7.42-7.45 (m, 1H), 7.78-7.8 (m, 1H), 7.87 (d, *J* = 9.2Hz, 1H); $^{13}$C NMR

($CDCl_3$, 100 MHz) δ 18.2, 18.3, 33.8, 55.6, 56.8, 113.4, 114, 117.3, 120.3, 123.4, 123.6, 125.2, 126.5, 127.6, 128.8, 129.6, 130.2, 133.3, 142.9, 154.1, 157, 175.1; ESI-HRMS *m/z* calcd. for $(C_{22}H_{22}O_4Na)^+$ 373.1416; found 373.1414.

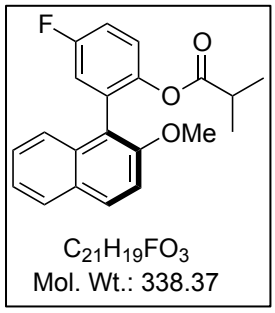


**4.28k** (75 %ee) HPLC (UV 220 nm, Chiralpak IA, *i*-PrOH/Hexane = 1/99, 0.4 mL/min), $t_1$ (minor) = 16.6 min, $t_2$ (major) = 22.5 min. $[\alpha]_D^{22}$ -0.4 (*c* 0.83, $CH_2Cl_2$). $^1H$ NMR ($CDCl_3$, 400 MHz) δ 0.61 (d, *J* = 6.8 Hz, 3H), 0.65 (d, *J* = 6.8 Hz, 3H), 2.25 (m, *J* = 6.8 Hz, 1H), 3.85 (s, 3H), 7.09 (dd, *J* = 8.8, 2.8 Hz, 1H), 7.13-7.23 (m, 2H), 7.31-7.4 (m, 4H), 7.79 (dd, *J* = 6.8, 1.6 Hz, 1H), 7.89 (d, *J* = 9.2 Hz, 1H); $^{13}C$ NMR ($CDCl_3$, 100 MHz) δ 18.16, 18.19, 33.7, 56.7, 113.2, 115.2 (d, *J* = 23 Hz), 119.07 (d, *J* = 17 Hz), 119.2, 123.7, 124 (d, *J* = 9 Hz), 124.8, 126.7, 127.8, 128.8, 130, 131.2 (d, *J* = 8 Hz), 133.1, 145.2 (d, *J* = 2 Hz), 154.1, 160 (d, *J* = 243 Hz), 174.8; $^{19}F$ NMR ($CDCl_3$, 376 MHz) δ -117.6; ESI-HRMS *m/z* calcd. for $(C_{21}H_{19}FO_3Na)^+$ 361.1216; found 361.1215.

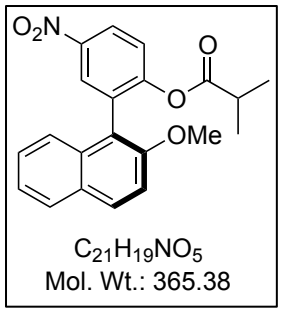


$C_{21}H_{19}NO_5$
Mol. Wt.: 365.38

**4.28l** (2 %ee) HPLC (UV 220 nm, Chiralpak AD-H, *i*-PrOH/Hexane = 5/95, 0.5 mL/min), $t_1$ (major) = 28.2 min, $t_2$ (minor) = 36 min. $[\alpha]_D^{23}$ 2.5 (*c* 0.9, $CH_2Cl_2$). $^1$H NMR ($CDCl_3$, 400 MHz) δ 0.66 (d, *J* = 7.2 Hz, 3H), 0.69 (d, *J* = 6.8 Hz, 3H), 2.3 (m, *J* = 7.2, 6.8 Hz, 1H), 3.85 (s, 3H), 7.27-7.3 (m, 1H), 7.33-7.4 (m, 3H), 7.44 (d, *J* = 9.2 Hz, 1H), 7.81-7.84 (m, 1H), 7.94 (d, *J* = 9.2 Hz, 1H), 8.29 (d, *J* = 2.8 Hz, 1H), 8.35 (dd, *J* = 8.8, 2.8 Hz, 1H); $^{13}$C NMR ($CDCl_3$, 100 MHz) δ 18.08, 18.1, 33.9, 56.5, 112.9, 117.6, 123.8, 123.9, 124, 124.2, 127.1, 128, 128.4, 128.7, 130.6, 131.1, 132.8, 145.4, 154.2, 154.4, 174; ESI-HRMS *m/z* calcd. for $(C_{21}H_{19}NO_5Na)^+$ 388.1161; found 388.1164.

**4.5. References**

1. Pellissier, H. Recent Developments in Dynamic Kinetic Resolution. *Tetrahedron* **2008**, *64*, 1563-1601.
2. Seeman, J. I. Effect of Conformational Change on Reactivity in Organic Chemistry. Evaluations, Applications, and Extensions of Curtin-Hammett/Winstein-Holness Kinetics. *Chem. Rev.* **1983**, *83*, 83-134.
3. Kitamura, M.; Tokunaga, M.; Noyori, R. Quantitative Expression of Dynamic Kinetic Resolution of Chirally Labile Enantiomers: Stereoselective Hydrogenation of 2-Substituted 3-oxo carboxylic Esters Catalyzed by BINAP-Ruthenium (II) Complexes. *J. Am. Chem. Soc.* **1993**, *115*, 144-152.

4. a) Pellissier, H. Dynamic Kinetic Resolution. *Tetrahedron* **2003**, 59, 8291-8327; b) Kim, M.-J.; Ahn, Y.; Park, J. Dynamic Kinetic Resolution and Asymmetric Transformations by Enzymes Coupled with Metal Catalysis. *Curr. Opin. Biol.* **2002**, *13*, 578-587; c) Faber, K. Non-Sequential Processes for the Transformation of A Racemate into A Single Stereoisomeric Product: Proposal for Stereochemical Classification. *Chem. Eur. J.* **2001**, *7*, 5004-5010; d) Steinreiber, J.; Faber, K.; Griengl, H. De-racemization of Enantiomers versus De-epimerization of Diastereomers-Classification of Dynamic Kinetic Asymmetric Transformations (DYKAT). *Chem. Eur. J.* **2008**, *14*, 8060-8072; e) Lee, J. H.; Han, K.; Kim, M. -J.; Park, J. Chemoenzymatic Dynamic Kinetic Resolution of Alcohols and Amines. *Eur. J. Org. Chem.* **2010**, 999-1015.
5. Kakiuchi, F.; Gendre, P. L.; Yamada, A.; Ohtaki, H.; Murai, S. Atropselective Alkylation of Biaryl Compounds by Means of Transition Metal-Catalyzed C-H/Olefin Coupling. *Tetrahedron: Asymm.* **2000**, *11*, 2647-2651.
6. Ros, A.; Estepa, B.; Ramírez-López, P.; Álvarez, E.; Fernández, R.; Lassaletta, J. M. Dynamic Kinetic Cross-Coupling Strategy for the Asymmetric Synthesis of Axially Chiral Heterobiaryls. *J. Am. Chem. Soc.* **2013**, *135*, 15730-15733.
7. Hazra, C. K.; Dherbassy, Q.; Wencel-Delord, J.; Colobert, F. Synthesis of Axially Chiral Biaryls through Sulfoxide-Directed Asymmetric Mild C-H Activation and Dynamic Kinetic Resolution. *Angew. Chem. Int. Ed.* **2014**, *53*, 13871-13875.
8. Zheng, J.; You, S. -L. Construction of Axial Chirality by Rhodium-Catalyzed Asymmetric Dehydrogenative Heck Coupling of Biaryl Compounds with Alkenes. *Angew. Chem. Int. Ed.* **2014**, *53*, 13244-13247.

9. Gustafson, J. L.; Lim, D.; Miller, S. J. Dynamic Kinetic Resolution of Biaryl Atropisomers via Peptide-Catalyzed Asymmetric Bromination. *Science* **2010**, *328*, 1251-1255.

10. Cozzi, P. G.; Emer, E.; Gualandi, A. Atroposelective Organocatalysis. *Angew. Chem. Int. Ed.* **2011**, *50*, 3847-3849.

11. a) Bringmann, G.; Breuning, M.; Tasler, S. The Lactone Concept: An Efficient Pathway to Axially Chiral Natural Products and Useful Reagents. *Synthesis* **1999**, 525-558; b) Bringmann, G.; Gulder, T.; Gulder, T. A. M.; Breuning, M. Atroposelective Total Synthesis of Axially Chiral Biaryl Natural Products. *Chem. Rev.* **2011**, *111*, 563-639; c) Bringmann, G.; Mortimer, A. J. P.; Keller, P. A.; Gresser, M. J.; Garner, J.; Breuning, M. Atroposelective Synthesis of Axially Chiral Biaryl Compounds. *Angew. Chem. Int. Ed.* **2005**, *44*, 5384-5427; d) Bringmann, G.; Menche, D. Stereoselective Total Synthesis of Axially Chiral Natural Products via Biaryl Lactones. *Acc. Chem. Res.* **2001**, *34*, 615-624.

12. We observed that isobutyrate substituted **4.28** underwent slow racemization after several months at room temperature and the racemization was faster in solvent.

13. Ashizawa, T.; Tanaka, S.; Yamada, T.; Catalytic *atropo*-Enantioselective Reduction of Biaryl Lactones to Axially Chiral Biaryl Compounds. *Org. Lett.* **2008**, *10*, 2521-2524.

14. a) Berova, N.; Bari, L. D.; Pescitelli, G. Application of Electronic Circular Dichroism in Configurational and Conformational Analysis of Organic Compounds. *Chem. Soc. Rev.* **2007**, *36*, 914-931; b) Nugroho, A. E.; Morita, H. Circular Dichroism Calculation for Natural Products. *J. Nat. Med.* **2014**, *68*, 1-10.

15. a) Chen, Y.-H.; Cheng, D.-J.; Zhang, J.; Wang, Y.; Liu, X.-Y.; Tan, B. Atroposelective Synthesis of Axially Chiral Biaryldiols via Organiccatalytic Arylation of 2-Naphthols. *J.*

*Am. Chem. Soc.* **2015**, *137*, 15062-15065; b) Li, L.; Wang, L.; Si, Y. Electronic Circular Dichroism Behavior of Chiral Phthiobuzone. *Acta Pharmaceutica Sinica B* **2014**, *4*, 167-171; c) Goerigk, L.; Grimme, S. Calculation of Electronic Circular Dichroism Spectra with Time-Dependent Double-Hybrid Density Functional Theory. *J. Phys. Chem. A* **2009**, *113*, 767-776; d) Abbate, S.; Lebon, F.; Longhi, G.; Morelli, C. F.; Ubiali, D.; Speranza, G. Vibrational and Electronic Circular Dichroism Spectroscopies and DFT Calculationa for the Assignment of the Absolute Configuration of Hydroxyl-Substituted 2-Tetralols. *RSC Adv.* **2012**, *2*, 10200-10208.

16. Frisch, M. J.; Trucks, G. W.; Schlegel, H. B.; Scuseria, G. E.; Robb, M. A.; Cheeseman, J. R.; Scalmani, G.; Barone, V.; Mennucci, B.; Petersson, G. A.; Nakatsuji, H.; Caricato, M.; Li, X.; Hratchian, H. P.; Izmaylov, A. F.; Bloino, J.; Zheng, G.; Sonnenberg, J. L.; Hada, M.; Ehara, M.; Toyota, K.; Fukuda, R.; Hasegawa, J.; Ishida, M.; Nakajima, T.; Honda, Y.; Kitao, O.; Nakai, H.; Vreven, T.; Montgomery, J. A., Jr.; Peralta, J. E.; Ogliaro, F.; Bearpark, M.; Heyd, J. J.; Brothers, E.; Kudin, K. N.; Staroverov, V. N.; Kobayashi, R.; Normand, J.; Raghavachari, K.; Rendell, A.; Burant, J. C.; Iyengar, S. S.; Tomasi, J.; Cossi, M.; Rega, N.; Millam, J. M.; Klene, M.; Knox, J. E.; Cross, J. B.; Bakken, V.; Adamo, C.; Jaramillo, J.; Gomperts, R.; Stratmann, R. E.; Yazyev, O.; Austin, A. J.; Cammi, R.; Pomelli, C.; Ochterski, J. W.; Martin, R. L.; Morokuma, K.; Zakrzewski, V. G.; Voth, G. A.; Salvador, P.; Dannenberg, J. J.; Dapprich, S.; Daniels, A. D.; Farkas, Ö.; Foresman, J. B.; Ortiz, J. V.; Cioslowski, J.; Fox, D. J. Gaussian 09, Revision E.01, Gaussian, Inc., Wallingford CT, **2009**.

17. Chausset-Boissarie, L.; Àrvai, R.; Cumming, G. R.; Besnard, C.; Kündig, E. P. Total Synthesis of (±)-Vertine with *Z*-Selective RCM as A Key Step. *Chem. Commun.* **2010**, *46*, 6264-6266.

18. Arseniyadis, S.; Mahesh, M.; McDaid, P.; Hampel, T.; Davey, S. G.; Spivey, A. C. Studies Towards the *N*-Acylative Kinetic Resolution of NOBIN. *Collect. Czech. Chem. Commun.* **2011**, *76*, 1239-1253.

# CHAPTER 5. ENANTIOSELECTIVE ALLYLIC AMINATION OF MORITA-BAYLIS-HILLMAN CARBONATES CATALYZED BY NOVEL CHIRAL 4-DIALKYLAMINOPYRDIDINE CATALYSTS

## 5.1. Introduction

The use of multifunctional Morita-Baylis-Hillman (MBH) adducts (Figure 5.1) for further transformations has attracted the attention of many research groups, due to the possibility of generating densely functionalized products in one step.[1] In the last decade, these efforts have resulted in great success being made in terms of rate, scope and enantioselectivity in transformation of MBH adducts.[2]

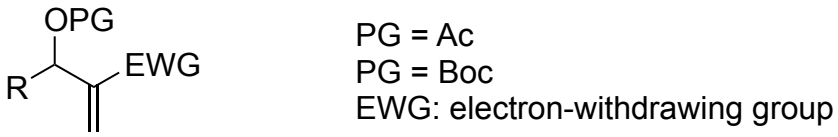


Figure 5.1. Protected Morita-Baylis-Hillman Adducts

After conversion of the alcohol to a leaving group such as an acetoxy (Ac) or a *tert*-butoxycarbonyl (Boc) group, two modes are generally recognized to control the regioselectivity at $\alpha$-position in the initial steps of MBH adducts transformation. One mode is that nucleophilic substitution takes place directly at the stereogenic allylic site (Scheme 5.1, Mode A). Trost and coworkers developed direct allylic substitution reaction using chiral palladium catalysts in the dynamic kinetic resolution of MBH acetates.[3] The other mode of selectivity can occur in an $S_N2$ fashion (Scheme 5.1, Mode B), Here the allylic alcohol is converted to a better leaving group, thereby increasing the electrophilic character at the allylic position of the MBH adduct. However, direct nucleophilic attack at the allylic position is disfavored at least partially due to the steric hindrance around this position. In fact, a series of nucleophiles react with these modified MBH

adducts in an $S_N2$' fashion favoring the nucleophilic substitution at the olefinic site.[4] MBH adducts which are activated by Lewis base organocatalysts prefer this way in most cases.

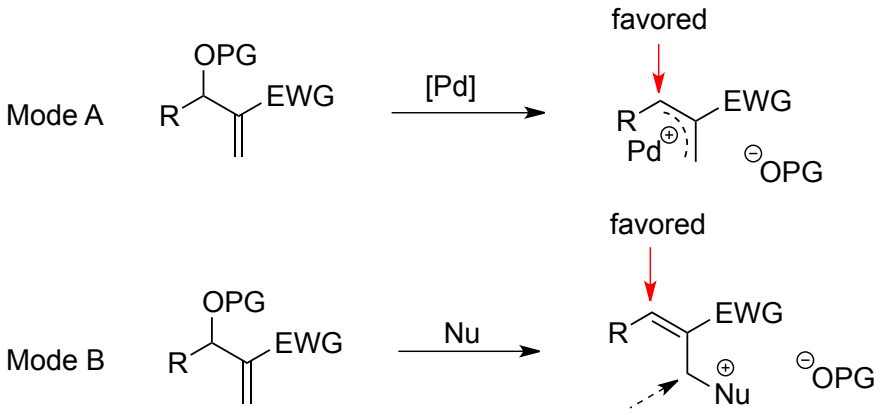


Scheme 5.1. Two Initialization Steps in MBH Adduct Transformation

Organocatalysis, with the advantages of being environmentally besign, metal-free and mild reaction conditions, has experienced a remarkable growth for the construction of carbo- and heterocycles. One dominant type of organocatalysts is Lewis base, which has long been applied in organic transformations to activate electrophiles. Lewis bases such as a tertiary phosphine or amine were employed in the activation of MBH adducts and achieved great success.[5] The mechanism proceeding with tertiary amine catalyzed nucleophilic substitution of MBH carbonates was proposed as Scheme 5.2. A tandem $S_N2$'-$S_N2$' sequence was involved.[6] Initial formation of a quaternary ammonium ion **5.3** through the tertiary amine addition to terminal site of the alkene conjugated to an electron-withdrawing group (EWG) in **5.1**, followed by elimination of the *tert*-butyl carbonate anion. After elimination of carbon dioxide, the *tert*-butoxy anion deprotonates the pronucleophile NuH. Then, the *in situ* formed nucleophile Nu attacks the olefinic bond of the cation intermediate **5.4** to afford the observed product **5.6** and eliminate the tertiary amine catalyst. In another situation, The quaternary ammonium ion intermediate **5.3** can

be further deprotonated by an extra or in situ generated base to give allylic amine ylide, like 1,3-dipole, which can undergo annulation reaction with an electrophile.

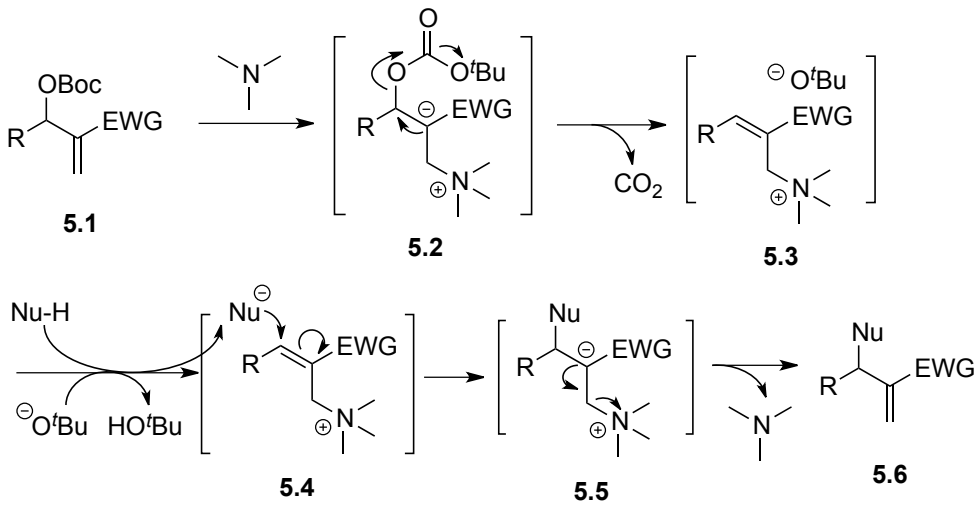


Scheme 5.2. Mechanism for Tertiary Amine Catalyzed Allylic Substitution of MBH Carbonates

The proper choice of the nucleophile, the leaving group and the catalyst are very critical for the desired regioselectivity of the reaction. If the nucleophilicity of the NuH is too strong, even without the assistance of the nucleophilic catalyst, direct addition of nucleophile to the electron deficient olefin will occur. In contrast, the nucleophilicity of the nucleophile must be stronger than catalyst in the second addition step. Thus a pronucleophile should be used in the first step and become a strong nucleophile after being deprotonated by *in situ* generated anion, which can add to the olefinic bond of the cation intermediate **5.4** and eliminate the catalyst.[6] In the asymmetric version of this process, since the Lewis base is incorporated into active intermediate **5.4**, a chiral Lewis base can potentially affect asymmetric induction in the subsequent steps.

A number of chiral tertiary amines and phosphines have been applied in the enantioselective allylic substitution of MBH adducts and achieved remarkable success. The

nucleophile could be carbon anion or heteroatom anions, like oxygen, nitrogen, *etc*. The multifunctional asymmetric allylic-substituted compounds have been synthesized using this approach. Among them, the enantioselective allylic amination of MBH adducts will produce asymmetric α-alkylidene β-amino carbonyl compounds, which are highly valuable building blocks in the synthesis of medicially relevant compounds as well as complex natural products. To access these valuable compounds, the aza-Morita-Baylis-Hillman (aza-MBH) reaction at first provided the direct synthetic approach.[7] However, the aza-MBH approach was limited by the reaction efficiency and substrate scope. In contrast, the asymmetric allylic substitution of MBH adducts with nitrogen nucleophiles is a much more efficient way to synthesize enantioenriched α-methylene-β-amino carbonyl compounds through carbon-nitrogen bond formation.

Kim and coworkers investigated the reaction of *p*-toluenesulfonamide ($TsNH_2$) and MBH acetate **5.7** in the presence of 0.5 equiv. chiral cinchona alkaloid derivative $(DHQD)_2PHAL$ **5.8** in aqueous THF.[8] The enantioselectivity of corresponding product reached up to 70 %ee, but the chemical yield was low due to the low reactivity of sulfonamide (Scheme 5.3).

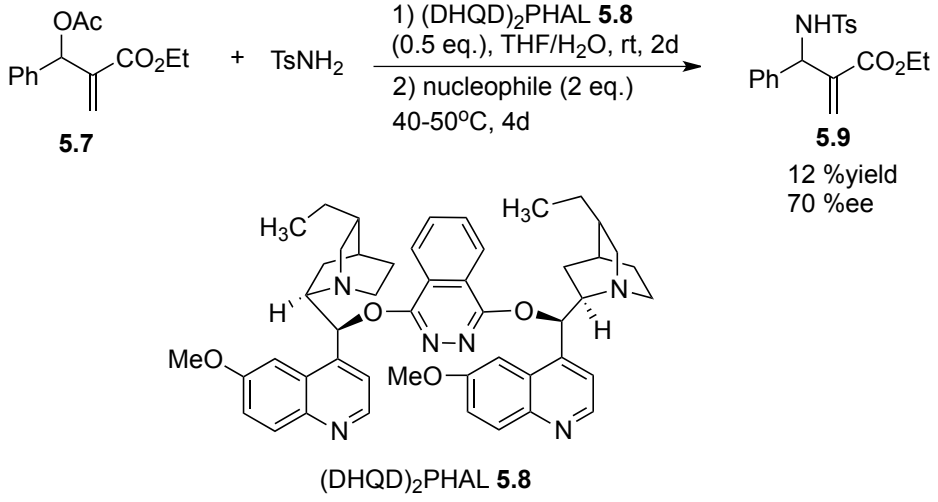


Scheme 5.3. Enantioselective Amination of MBH Acetates using $(DHQD)_2PHAL$

Lu and coworkers reported the TQO-catalyzed allylic amination of MBH carbonate **5.10**. A number of pronucleophiles, containing nitrogen, oxygen, and active carbon pronucleophiles have been tested. Among them, the amination products were obtained with moderate enantioselectivity and good yields (Scheme 5.4).[6]

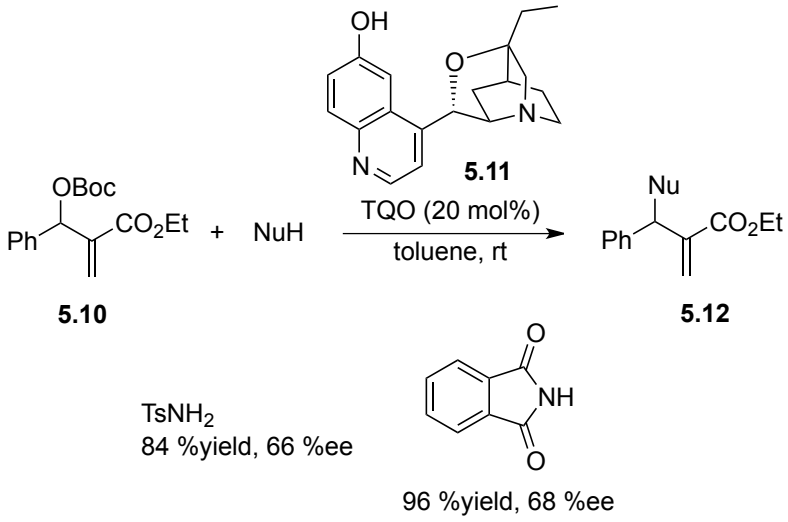


Scheme 5.4. TQO-Catalyzed Allylic Nucleophilic Substitution

To further improve the reaction efficiency of amination of MBH adducts, Chen group conducted this reaction with modified cinchona alkaloid catalyst $(DHQD)_2PYR$ **5.15**, which are more efficient to deliver α-methylene β-amino esters with good to excellent enantioselectivities and high yields (Scheme 5.5).[9] Naphthaline 1,8-dicarboximide **5.14** proved to be the most appropriate nitrogen source in this case.

They also investigated indole as pronucleophile in the allylic amination. The Friedel-Crafts reaction with indole compounds usually happens at the C3 position of indole. In the allylic amination study, they found that the *in situ* generated *tert*-butoxy anion could deprotonate the acidic N-H of an indole and resulting in nitrogen anion. This in turn reacted in an $S_N2$' fashion to attack olefin bond of ammonium salt intermediate. A diverse array of indole derivatives could be

tolerated under the catalysis of $(DHQD)_2PHAL$, affording the corresponding amination products with moderate to high enantioselectivities.[10]

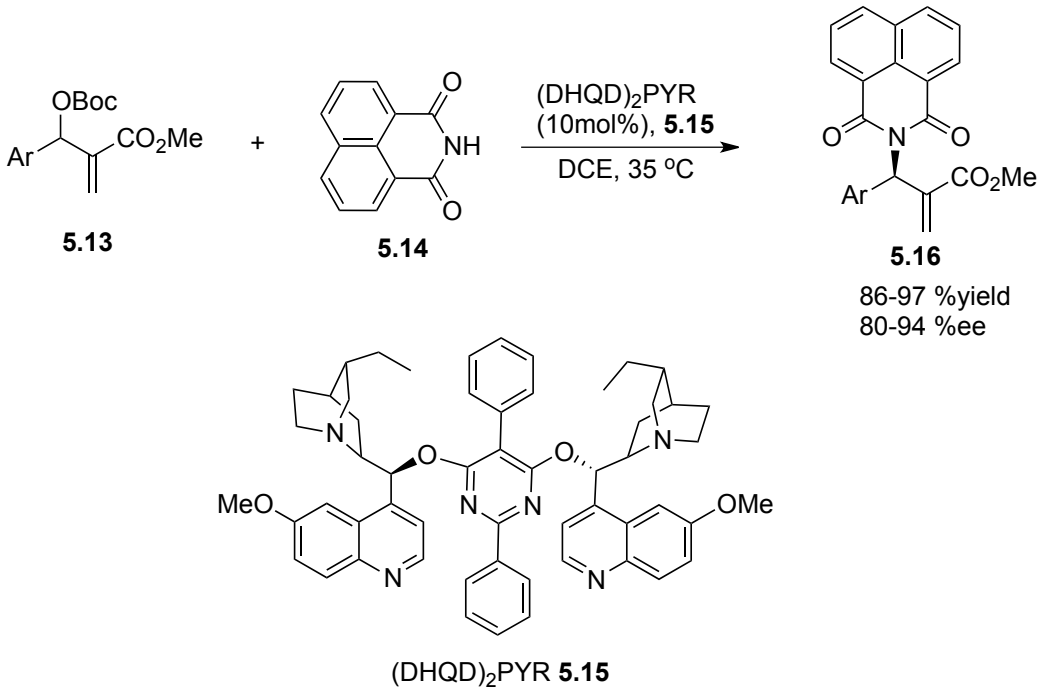


Scheme 5.5. Allylic Amination of MBH Carbonates with Naphthaline-1,8-Dicarboximide

Benzophenone imine, produced by condensation of benzophenone and ammonia, was utilized by Cheng and coworkers in the allylic amination of MBH carbonates. This method provided the most efficient way of producing unprotected α-methylene β-amino esters.[11] Benzophenone imine functioned as an ammonia surrogate. After reacting with MBH adduct, the benzophenone part can be recoveded by acidic hydrolysis and the primary β-amino ester were obtained as the hydrochloride salt. The reaction proceeded in good yields with excellent enantioselectivities (up to 99 %ee) for a wide range of MBH carbonates (Scheme 5.6).

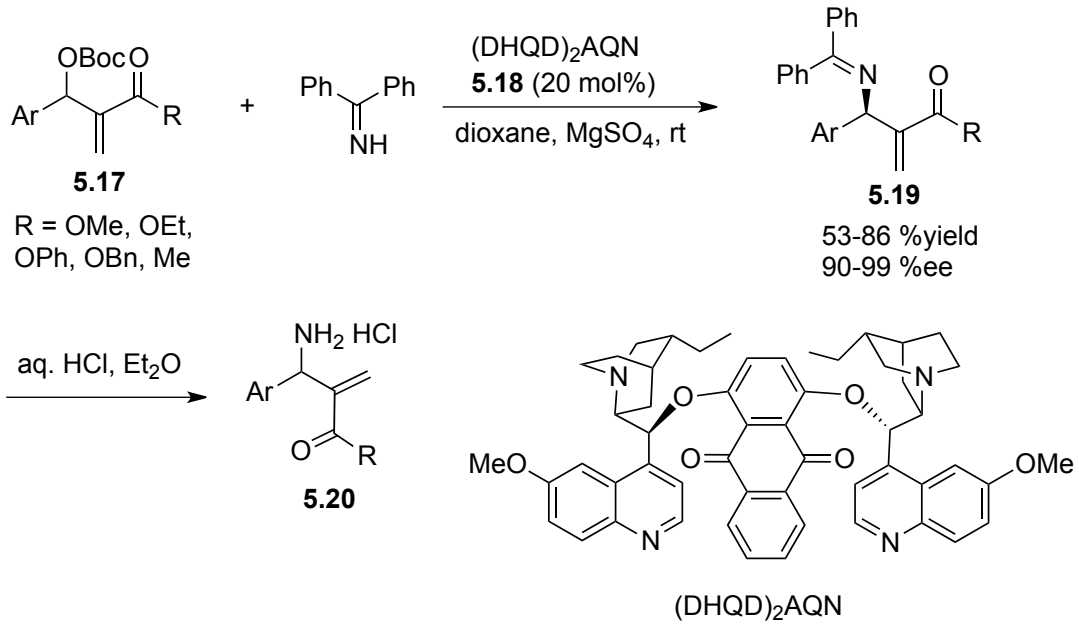


Scheme 5.6. Enantioselective Amination of MBH Carbonates with Ammonia Equivalent

Cinchona alkaloid derivatives have been widely used as efficient organocatalysts for asymmetric allylic amination of MBH adducts with various pronucleophiles and the substitution product scope was explored. High yields and enantioselectivities were achieved under mild reaction conditions with respect to a wide range of MBH adducts and various nitrogen pronucleophiles such as pyrrole derivatives, carbamates, tosyl carbamates and isatins.

Chiral tertiary phosphine were also explored in the allylic amination of MBH adducts. Hou group developed planar chiral cyclophane monophosphines for the reaction between MBH adducts and phthalimide and the corresponding allylic substituted product were obtained with good to moderate enantioselectivity.[12] To improve the allylic amination reaction efficiency by using phosphine catalyst, Shi group further developed chiral bifunctional phosphine organocatalyst containing Lewis basic phosphine site and Brønsted acidic thiourea site for the amination of MBH acetate derived from the methyl vinyl ketone or ethyl vinyl ketone. The reaction between phthalimide and MBH adducts afforded the amination product in up to 99 % yield and 90 %ee (Scheme 5.7).[13]

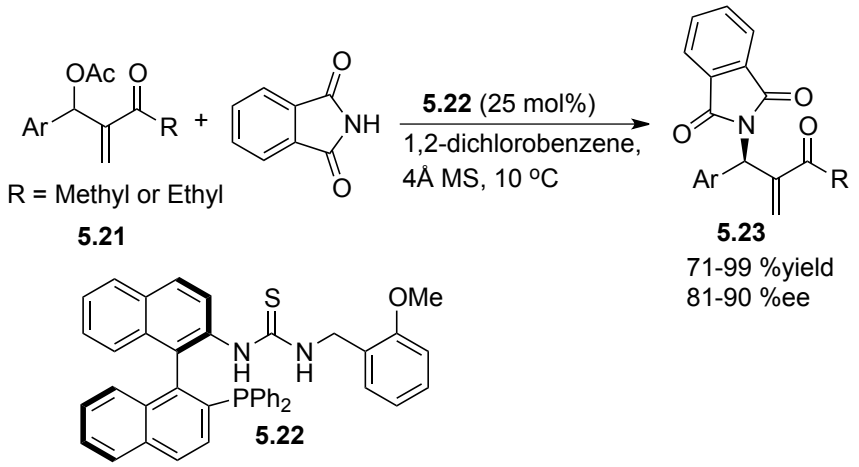


Scheme 5.7. Allylic Amination of MBH Acetates Catalyzed by Chiral Bifunctional Thiourea-Phosphane Organocatalysts

Cinchona alkaloid tertiary amine and phosphine have been identified as effective catalysts in the allylic amination of MBH adducts. Inspired by these elegant progress, and continuing our interest in fluxional pyridine type catalyst, we reasoned that our novel chiral 4-dialkylamino pyridine organocatalysts would be suitable for similar activation and provide the stereochemical control during the reaction process.

**5.2. Results and Discussion**

In the previous chapters, we have discussed the development of novel chiral DMAP catalysts that incorporate a fluxional group to control stereoselectivity in several types of kinetic resolutions. We are also interested in the application of the newly designed DMAP catalysts in other enantioselective transformations. To evaluate the nucleophilic characteristics of the new DMAP catalysts we have chosen the allylic amination of Morita-Baylis-Hillman (MBH) carbonates. Although there are a number of reports, which utilize chiral palladium complexes, chiral tertiary amines and phosphines for the transformation of MBH adducts, to the best of our knowledge, there is no example of using chiral DMAP for such a transformation.

### 5.2.1. Mechanism for DMAP Catalyzed Allylic Substitution of MBH Adducts

For the nucleophilic allylic amination of MBH adducts, a tandem $S_N2'$-$S_N2'$ mechanism with DMAP is illustrated in Scheme 5.8. The nucleophilic catalyst (DMAP) first adds to the MBH adduct in an $S_N2'$ fashion, followed by elimination of the *tert*-butyl carbonate anion. After elimination of carbon dioxide, the *tert*-butoxy anion deprotonates the pronucleophile. Then the *in situ* formed anionic nucleophile attacks the olefinic bond of the cation intermediate to afford the observed amination product.

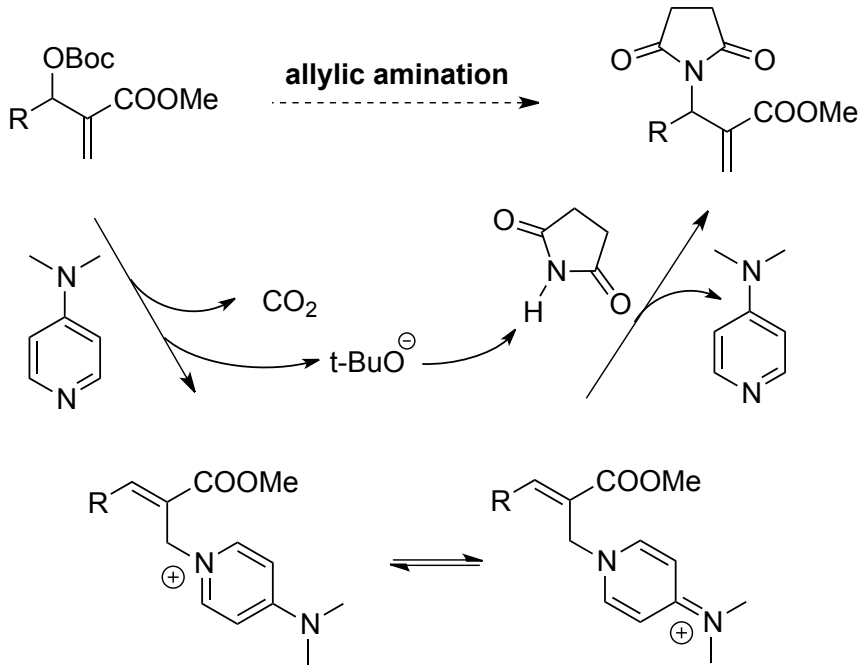


Scheme 5.8. Allylic Amination of MBH Carbonates Catalyzed by DMAP

### 5.2.2. Evaluation of Nitrogen Nucleophiles

We began our investigation by screening MBH carbonates **5.24a** with a variety of nitrogen nucleophiles **5.25** in toluene in the presence of 10 mol% **5.27** at room temperature to furnish the amination product. The results are summarized in Table 5.1.

Table 5.1. Screen Studies of Nitrogen Nucleophiles

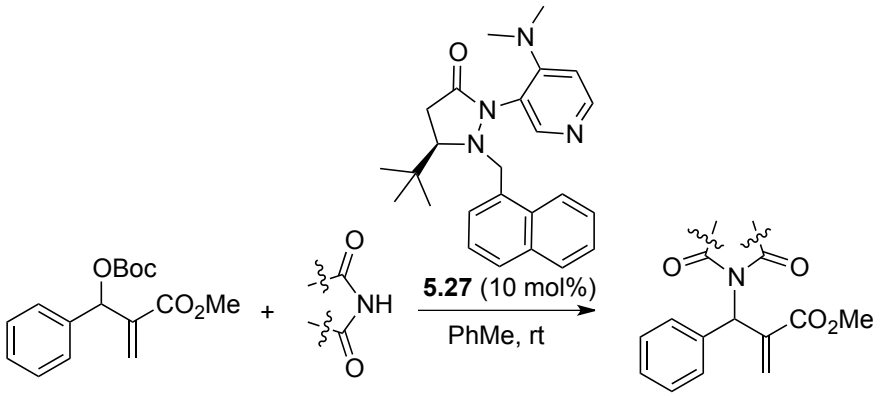


**5.24a** **5.25** **5.26**

| entry | Nitrogen Nu | Product | Time | Yield (%) | ee (%)[a-c] |
|---|---|---|---|---|---|
| 1 | 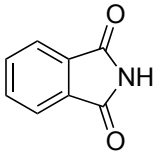 | **5.26a** | 24h | 76 | 31 |
| 2 | 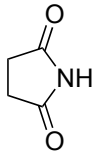 | **5.26b** | 24h | 75 | 39 |
| 3 | 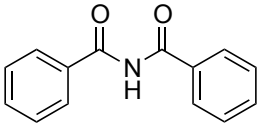 | **5.26c** | 36h | 26 | 3 |
| 4 | 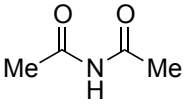 | **5.26d** | 7d | 16 | 11 |
| 5 | 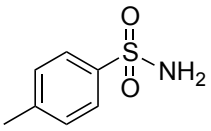 | **5.26e** | 3d | 17 | 25 |

[a]Reaction conditions: the reaction were performed with 1 equiv. of **5.24a**, 1.5 equiv. of **5.25** and 10 mol% of catalyst in toluene at room tem; [b]Isolated yield; [c]Determined by chiral HPLC analysis.

In general, better yield as well as enantioselectivity was obtained when cyclic imide pronucleophiles were used (Table 5.1, entries 1, 2). Succinimide was slightly better than phthalimide (compare entry 2 with 1). Both yield and enantioselectivity in reactions with acyclic

benzoylbenzamide and acetylacetamide were lower than cyclic nitrogen nucleophiles (entries 3, 4). Benzenesulfonamide as a nucleophile was better than acyclic pronucleophiles but inferior to cyclic imides (entry 5).

### 5.2.3. Evaluation of Solvents

A variety of solvents were screened for the reaction (Table 5.2). Four common solvents were investigated and reaction conducted in toluene showed the optimal result than other solvents.

Table 5.2. Solvent Evaluation for Allylic Substitution of MBH Carbonates

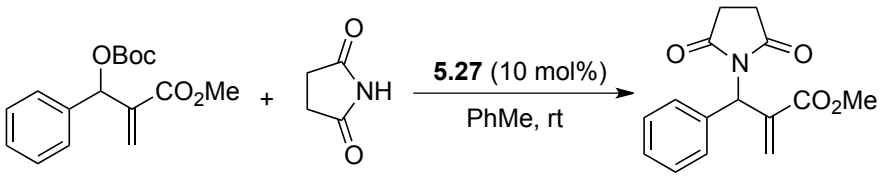


**5.24a** **5.25b** **5.26b**

| entry | Solvents | Time | Yield (%) | ee (%)[a-c] |
|---|---|---|---|---|
| 1 | THF | 24 | 62 | 35 |
| 2 | DCM | 24 | 80 | 17 |
| 3 | PhMe | 24 | 75 | 39 |
| 4 | MeOH | 48 | 45 | 29 |

[a,b,c] see Table 5.1.

### 5.2.4. Optimization of MBH Adducts

Next we examined MBH adducts with different leaving groups ($R^2$) and different electron withdrawing substituents ($R^1$) using succinimide as an aminating agent and **5.27** as the catalyst (Table 5.3). We found that the *tert*-butoxycarbonyl group (Boc) was optimal as a leaving group compared to an acetate or a benzoate (compare entry 1 with 2 and 3). The Boc group which produces a *tert*-butoxide anion *in situ*, generates the nucleophile from the pronucleophile more effectively, leading to the amination product in good yield (75%). Of the different electron

withdrawing groups evaluated, the methyl ester gave the product with the highest selectivity (compare entry 1 with 4, 5, and 6). In contrast, ethyl and benzyl esters as well as the methyl ketone gave adduct **5.26** in high yields but with only modest enantioselectivity (entries 4-6).

Table 5.3. Optimization Studies of MBH Carbonates

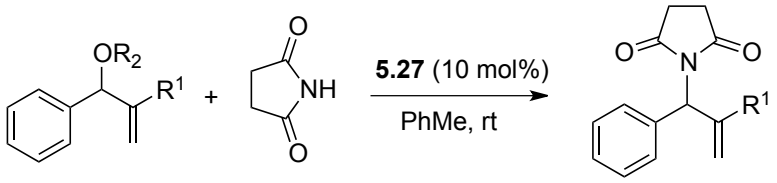


**5.24** **5.25b** **5.26**

| entry | $R^1$ | $R^2$ | Product | Time | Yield (%) | ee (%)[a-c] |
|---|---|---|---|---|---|---|
| 1 | $CO_2Me$ | Boc | **5.26b** | 24h | 75 | 39 |
| 2 | $CO_2Me$ | Ac | **5.26b** | 7d | 30 | 39 |
| 3 | $CO_2Me$ | 4-$NO_2$PhCO | **5.26b** | 6d | 9 | 33 |
| 4 | $CO_2Et$ | Boc | **5.26f** | 36h | 88 | 29 |
| 5 | $CO_2Bn$ | Boc | **5.26g** | 36h | 80 | 29 |
| 6 | COMe | Boc | **5.26h** | 36h | 90 | 27 |

[a,b,c] see Table 5.1.

### 5.2.5. Evaluation of Chiral DMAP Catalysts and Reaction Temperature

Based on the above results, reaction between MBH carbonates **5.24a** and succinimide **5.25b** was chosen as a model reaction. A number of chiral relay DMAP catalysts were examined next, and these results are summarized in Table 5.4. In general, all the DMAP catalysts examined in this study were able to catalyze the enantioselective amination of MBH carbonates and provided the product in yields ranging from 75-95% (entries 1-6). The catalysts examined in this study varied in the size of the fluxional group and the nature of the dialkylamino substituent on the pyridine ring (catalysts **5.27**-**5.31**). Generally, catalysts with a dimethylamino substituent at 4-pyridine gave higher selectivity (compare **5.27** with **5.28** and **5.30** with **5.31**). Interestingly,

catalyst **5.27** with a bulkier 1-naphthyl fluxional group was less effective than a smaller phenyl group (**5.30**) with respect to enantioselectivity. Catalyst **5.29** with a smaller chiral *i*-Pr group gave the product in lower selectivity as compared to **5.30** with a bigger *t*-Bu chiral group (33% vs 59%). Based on these results, catalyst **5.30** was chosen for further studies.

Table 5.4. Catalyst Optimization Studies

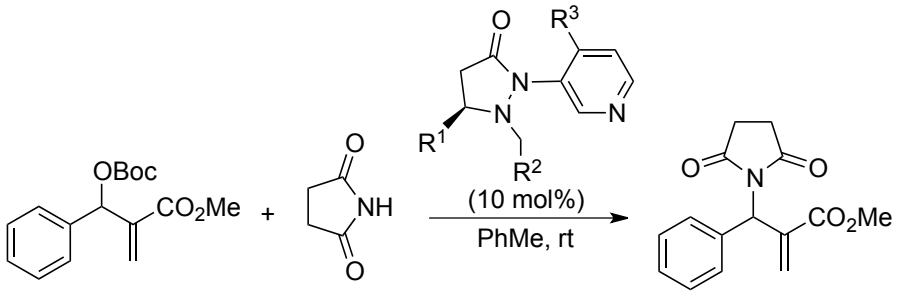


**5.24a** **5.25b** **5.26b**

| Catalysts | Time | Yield (%) | ee (%)[a-c] |
|---|---|---|---|
| **5.27** $R^1$ = *t*-Bu, $R^2$ = 1-naphthyl, $R^3$ = dimethylamino | 24h | 75 | 39 |
| **5.28** $R^1$ = *t*-Bu, $R^2$ = 1-naphthyl, $R^3$ = pyrrolidine | 40h | 95 | 29 |
| **5.29** $R^1$ = *i*-Pr, $R^2$ = phenyl, $R^3$ = dimethylamino | 48h | 95 | 33 |
| **5.30** $R^1$ = *t*-Bu, $R^2$ = phenyl, $R^3$ = dimethylamino | 40h | 85 | 59 |
| **5.31** $R^1$ = *t*-Bu, $R^2$ = phenyl, $R^3$ = pyrrolidine | 36h | 90 | 43 |

*a,b,c* see Table 5.1.

After identifying catalyst **5.30** that gave high yield and good selectivity, we evaluated the effect of reaction temperature and catalyst loading on the amination reaction. Results from these experiments are tabulated in Table 5.5. Reactions with 5, 10, and 25 mol% **5.30** gave the product with similar enantioselectivities and yields (entries 1-3). However, using 5 mol% catalyst, a relatively longer reaction time was required for good conversion (entry 3). Lowering the temperature to -10 °C led to improvement in enantioselectivity up to 67%, although the yield suffered slightly (62% vs 85%, entry 4).

Table 5.5. Temperature and Catalyst Loading Studies

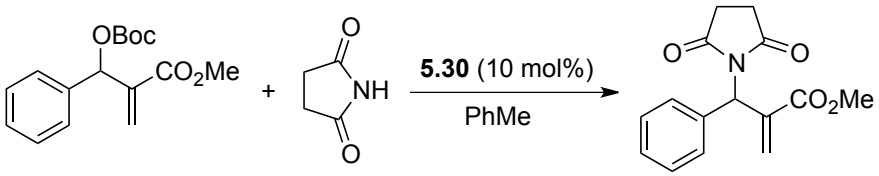


**5.24a** **5.25b** **5.26b**

| entry | Temp (°C) | Cat.loading (mol%) | Time | Yield (%) | ee (%)[a-c] |
|---|---|---|---|---|---|
| 1 | rt | 10 | 40h | 85 | 59 |
| 2 | rt | 25 | 48h | 88 | 57 |
| 3 | rt | 5 | 72h | 80 | 57 |
| 4 | -10 | 10 | 120h | 62 | 67 |

[a]Reaction conditions: the reaction were performed with 1 equiv. of **5.24a**, 1.5 equiv. of **5.25b** and **5.30** in toluene at given temp.
[b]Isolated yield. [c]Determined by chiral HPLC analysis.

### 5.2.6. Substrate Scope of the Asymmetric Allylic Amination of MBH Carbonates

Having established the optimal reaction conditions for the asymmetric allylic amination with succinimide, a variety of MBH carbonates were synthesized to study the substrate scope. Results from these experiments are shown in Table 5.6. MBH carbonates with electron-deficient aromatics were facile giving the products in excellent yield and good selectivity (entries 2 and 3). Reaction with an electron-rich aromatic proceeded with comparable enantioselectivity (entry 4). A MBH carbonate with disubstituted aromatic produced the product with good yield and the highest enantioselectivity observed in this series (entry 5, 72 %ee). A substrate containing an ortho substituent was less efficient, giving the product with low enantioselectivity (entry 6). Allylic amination of an alkyl substituted MBH substrate gave low yield and low enantioselectivity (entry 7). Several groups have developed a series of chiral organoamines or organophosphines as efficient organocatalysts for asymmetric substitutions of MBH adducts with various pronucleophiles. High yields and enantioselectivities were achieved with a wide range of

MBH adducts. [4,5a] Our results suggested that compared to cinchona alkaloid based tertiary amines or chiral tertiary phosphine catalysts, the chiral DMAP catalyst can also be used for the allylic amination of MBH carbonates. Although the selectivity is inferior, it opens a new insight into chiral DMAP catalysis, especially organocatalyst with fluxionality control.

Table 5.6. Substrate Scope of the Asymmetric Allylic Amination of MBH Carbonates

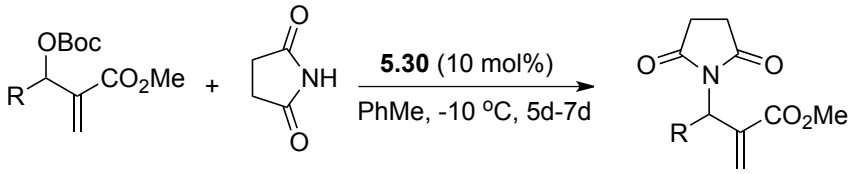


**5.24** **5.25b** **5.26**

| entry | R | Product | Yield (%) | ee (%)[a-c] |
|---|---|---|---|---|
| 1 | $C_6H_5$ | **5.26b** | 62 | 67 |
| 2 | 4-$NO_2C_6H_4$ | **5.26i** | 90 | 62 |
| 3 | 4-$CNC_6H_4$ | **5.26j** | 81 | 61 |
| 4 | 3-$MeOC_6H_4$ | **5.26k** | 70 | 63 |
| 5 | 3,5-$(MeO)_2C_6H_4$ | **5.26l** | 78 | 72 |
| 6 | 2-$BrC_6H_4$ | **5.26m** | 61 | 39 |
| 7 | *n*-$C_4H_9$ | **5.26n** | 27 | 16 |

[a]Reaction conditions: the reaction were performed with 1 equiv. of **5.24**, 1.5 equiv. of **5.25b** and 10 mol% of **5.30** in toluene at -10 °C. [b]Isolated yield. [c]Determined by chiral HPLC analysis.

### 5.2.7. Structural Analysis of Catalyst 5.30

The structure and absolute configuration of catalyst **5.30** was ascertained by single crystal X-ray analysis (Figure 5.2). The X-ray crystal structure unambiguously shows that the *tert*-butyl group could control the stereochemistry of the adjacent benzyl group because of the fluxionality of *N*-benzyl group. The steric repulsion between the fixed *tert*-butyl group and *N*-benzyl group lead to the opposite orientation and fluxional benzyl group looks like blocking the back as well

as the bottom of DMAP pyridine part, thus disfavoring attack from the back and the bottom, which facilitates enantiocontrol.

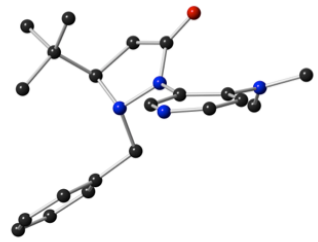

Figure 5.2. Single Crystal X-ray
Structure of Catalyst **5.30**

**5.3. Conclusion**

In conclusion, MBH adducts transformation have opened up new opportunities for construction of complex molecules. Our studies have shown that newly designed DMAP catalysts containing fluxional groups as a stereocontrol unit could also be effectively applied as a nucleophilic catalyst in asymmetric allylic aminations, which provide a novel tool to synthesize useful molecules. The catalyst preparation is highly tunable and up to 72% ee was achieved using catalyst **5.30** and a range of α-methylene β-amino esters were obtained with good yield and selectivities. Higher selectivity obtained with catalyst **5.30** with a bulky chiral C-5 substituent in comparison to reaction with **5.29** with a smaller C-5 substituent demonstrates that the 'chiral relay' concept is operative. Applying fluxionally chiral 4-dimethylamino pyridines in the enantioselective substitution of MBH adducts is less selective than asymmetric acylation. Further applications of chiral relay DMAP catalysts in asymmetric catalysis are in progress.

## 5.4. Experimental

### 5.4.1. General

All solvents were dried and degassed by standard methods and stored under nitrogen. Flash chromatography was performed using EM Science silica gel 60 (230-400 mesh). $^{1}$H NMR spectra were recorded on Varian Unity/Inova-400 NB (400 MHz) spectrometer. $^{13}$C NMR spectra were recorded on Varian Unity/Inova-400 NB (100 MHz) spectrometer. HPLC analyses were carried out with Waters 515 HPLC pumps and a 2487 dual wavelength absorbance detector connected to a PC with Empower workstation. Rotations were recorded on a JASCO-DIP-370 polarimeter. High resolution mass spectra were obtained at a Bruker Daltronics BioTOF HRMS spectrometer.

### 5.4.2. Experimental Details and Characterization

The Morita-Baylis-Hillman carbonates were prepared according to the literature reported.[14,15]

#### 5.4.2.1. General Procedure for the Allylic Nucleophilic Substitution of Morita–Baylis–Hillman Carbonates


Scheme 5.9. General Procedure for the Allylic Amination

Under an argon atmosphere, a solution of MBH carbonate (1 equiv.), succinimide (1.5 equiv.) and chiral DMAP catalyst (10 mol%) in toluene was stirred at the given temperature. Once the reaction was judged complete by TLC, the solvent was removed under reduced pressure, and the residue was chromatographed on silica gel (elution with ethyl acetate / hexane 1:5–1:2) to provide the product.

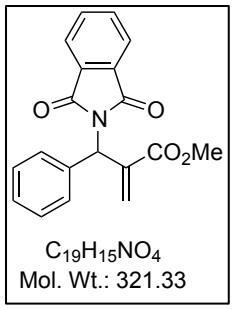


$C_{19}H_{15}NO_4$
Mol. Wt.: 321.33

**5.26a** Enantiomeric excess was determined by HPLC with a Chiralcel OD column (90:10 hexane:2-propanol, 0.5 mL/min, 254 nm); minor enantiomer $t_1$ = 19.2 min, major enantiomer $t_2$ = 42.6 min; $^1$H NMR ($CDCl_3$, 400 MHz) δ 3.67 (s, 3H), 5.6 (d, *J* = 1.6 Hz, 1H), 6.37 (s, 1H), 6.53 (d, *J* = 1.2 Hz, 1H), 7.27-7.34 (m, 3H), 7.41 (d, *J* = 7.2 Hz, 2H), 7.67-7.69 (m, 2H), 7.79-7.81 (m, 2H); $^{13}$C NMR ($CDCl_3$, 100 MHz) δ 52.4, 54.8, 123.6, 123.8, 128.3, 128.8, 129.9, 132, 134.3, 134.5, 137.2, 137.8, 166.3, 168.1; ESI-HRMS *m/z* calcd. for $(C_{19}H_{15}NO_4Na)^+$ 344.0893; found 344.0902.

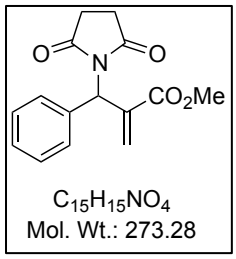


$C_{15}H_{15}NO_4$
Mol. Wt.: 273.28

**5.26b** Enantiomeric excess was determined by HPLC with a Chiralcel OD column (90:10 hexane:2-propanol, 0.5 mL/min, 254 nm); minor enantiomer $t_1$ = 33.4 min, major enantiomer $t_2$ = 50.4 min; $[\alpha]_D^{25}$ -121.1 (*c* 0.58, $CHCl_3$); $^1$H NMR ($CDCl_3$, 400 MHz) δ 2.65-2.66 (m, 4H), 3.7 (s, 3H); 5.45 (d, *J* = 2 Hz, 1H), 6.1 (t, *J* = 2 Hz, 1H), 6.45(d, *J* = 2 Hz, 1H), 6.45(d, *J* = 2 Hz, 1H), 7.27-7.37 (m, 5H); $^{13}$C NMR ($CDCl_3$, 100 MHz) δ 28.3, 52.3, 55.8, 128.5, 128.9, 129, 129.8, 136.8, 137.3, 166.2, 177.1; ESI-HRMS *m/z* calcd. for $(C_{15}H_{15}NO_4Na)^+$ 296.0893; found 296.0893.

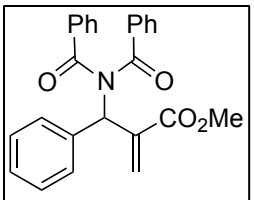


$C_{25}H_{21}NO_4$
Mol. Wt.: 399.44

**5.26c** Enantiomeric excess was determined by HPLC with a Chiralcel OD-3 column (97:3 hexane:2-propanol, 1.0 mL/min, 254 nm); minor enantiomer $t_1$ = 15.7 min, major enantiomer $t_2$ = 32.9 min; $^1$H NMR ($CDCl_3$, 400 MHz) δ 3.7 (s, 3H), 5.68 (d, *J* = 1.6 Hz, 1H), 6.52(m, 1H), 6.9 (s, 1H), 7.06(t, *J* = 7.6 Hz, 4H), 7.13-7.18 (m, 2H), 7.23-7.28(m, 1H), 7.32-7.36 (m, 2H), 7.55(d, *J* = 7.6 Hz, 2H); $^{13}$C NMR ($CDCl_3$, 100 MHz) δ 52.4, 61.8, 128.2, 128.3, 128.9, 129.1, 129.3, 129.7, 131.9, 137.6, 137.9, 139.3, 166.7, 173.7; ESI-HRMS *m/z* calcd. for $(C_{25}H_{21}NO_4Na)^+$ 422.1363; found 422.1362.

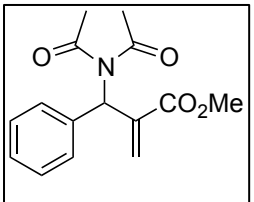


$C_{15}H_{17}NO_4$
Mol. Wt.: 275.30

**5.26d** Enantiomeric excess was determined by HPLC with a Chiralcel OD-3 column (98:2 hexane:2-propanol, 0.5 mL/min, 254 nm); minor enantiomer $t_1$ = 25.1 min, major enantiomer $t_2$ = 27.8 min; $^1$H NMR ($CDCl_3$, 400 MHz) δ 2.32 (s, 6H), 3.74 (s, 3H); 5.61 (d, *J* = 1.6 Hz, 1H), 6.26 (s, 1H), 6.49 (d, *J* = 1.6 Hz, 1H), 7.18-7.21(m, 2H), 7.25-7.35(m, 3H); $^{13}$C NMR ($CDCl_3$, 100 MHz) δ 27, 52.5, 60.7, 127.9, 128.1, 128.6, 128.8, 129.6, 137.2, 138.4, 166.9, 174.4; ESI-HRMS *m/z* calcd. for $(C_{15}H_{17}NO_4Na)^+$ 298.1050; found 298.1044.

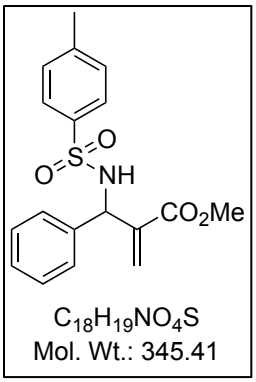


$C_{18}H_{19}NO_4S$
Mol. Wt.: 345.41

**5.26e** Enantiomeric excess was determined by HPLC with a Chiralcel OD-3 column (99:1 hexane:2-propanol, 0.7 mL/min, 254 nm); minor enantiomer $t_1$ = 112.4 min, major enantiomer $t_2$ = 117.1 min; $^1$H NMR ($CDCl_3$, 400 MHz) δ 2.38 (s, 3H), 3.57 (s, 3H), 5.28(d, *J* = 8.8 Hz, 1H), 5.64 (d, *J* = 8.8 Hz, 1H), 5.8 (s, 1H), 6.19 (s, 1H), 7.1-7.13 (m, 2H), 7.17-7.24 (m, 5H), 7.65 (d, *J* = 8.8 Hz, 2H); $^{13}$C NMR ($CDCl_3$, 100 MHz) δ 21.7, 52.2, 59.2, 126.6, 127.4, 127.9, 128.1, 128.8, 129.7, 137.8, 138.7, 138.8, 143.6, 166; ESI-HRMS *m/z* calcd. for $(C_{18}H_{19}SNO_4Na)^+$ 368.0927; found 368.0924.

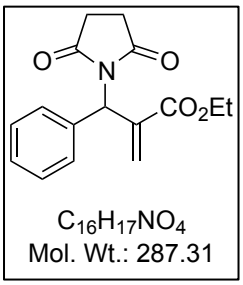


$C_{16}H_{17}NO_4$
Mol. Wt.: 287.31

**5.26f** Enantiomeric excess was determined by HPLC with a Chiralcel OD-3 column (90:10 hexane:2-propanol, 0.5 mL/min, 254 nm); minor enantiomer $t_1$ = 26.7 min, major enantiomer $t_2$ = 37.4 min; $^1$H NMR ($CDCl_3$, 400 MHz) δ 1.21 (t, *J* = 7.2 Hz, 3H), 2.65 (m, 4H), 4.10-4.2 (m, 2H), 5.41-5.42 (m, 1H), 6.1 (d, *J* = 1.6 Hz, 1H), 6.45 (m, 1H), 7.23-7.33 (m, 3H), 7.37 (d, *J* = 8 Hz, 1H); $^{13}$C NMR ($CDCl_3$, 100 MHz) δ 14.2, 28.3, 55.9, 61.2, 128.5, 128.9,

129.0, 129.5, 137, 137.6, 165.8, 177.1, 134, 136.6, 166.3, 177.2; ESI-HRMS *m/z* calcd. for $(C_{16}H_{17}NO_4Na)^+$ 310.1050; found 310.1055.

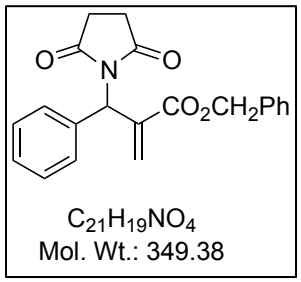


$C_{21}H_{19}NO_4$
Mol. Wt.: 349.38

**5.26g** Enantiomeric excess was determined by HPLC with a Chiralcel OD-3 column (95:5 hexane:2-propanol, 1.0 mL/min, 254 nm); minor enantiomer $t_1$ = 49.6 min, major enantiomer $t_2$ = 56.7 min; $^1$H NMR ($CDCl_3$, 400 MHz) δ 2.43 (s, 4H), 5.02 (d, *J* = 12 Hz, 1H), 5.29 (d, *J* = 12 Hz, 1H), 5.41 (d, *J* = 2 Hz, 1H), 6.08 (t, *J* = 2 Hz, 1H), 6.51 (d, *J* = 2 Hz, 1H), 7.27-7.38 (m, 10H); $^{13}$C NMR ($CDCl_3$, 100 MHz) δ 28.2, 55.9, 66.9, 128.5, 128.6, 128.8, 129, 129.1, 130.2, 135.8, 136.9, 137.5, 165.5, 177; ESI-HRMS *m/z* calcd. for $(C_{21}H_{19}NO_4Na)^+$ 372.1206; found 372.1198.

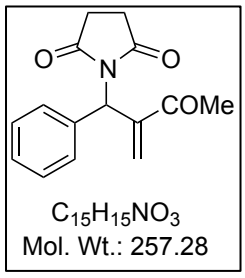


$C_{15}H_{15}NO_3$
Mol. Wt.: 257.28

**5.26h** Enantiomeric excess was determined by HPLC with a Chiralcel AD-3 column (96:4 hexane:2-propanol, 1.0 mL/min, 254 nm); minor enantiomer $t_1$ = 36.1 min, major enantiomer $t_2$ = 63.9 min; $^1$H NMR ($CDCl_3$, 400 MHz) δ 2.36 (s, 3H), 2.63 (m, 4H), 5.51 (d, *J* = 2 Hz, 1H), 6.06 (t, *J* = 1.6 Hz, 1H), 6.23 (d, *J* = 2 Hz, 1H), 7.23-7.33 (m, 5H); $^{13}$C NMR ($CDCl_3$,

100 MHz) δ 14.3, 28.3, 55.9, 61.2, 128.5, 128.9, 129, 129.5, 136.9, 137.6, 165.8, 177, 198.8; ESI-HRMS *m/z* calcd. for $(C_{15}H_{15}NO_3Na)^+$ 280.0944; found 280.0950.

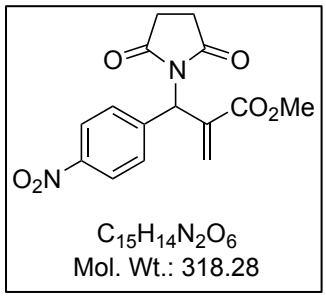


$C_{15}H_{14}N_2O_6$
Mol. Wt.: 318.28

**5.26i** Enantiomeric excess was determined by HPLC with a Chiralcel OD-3 column (70:30 hexane:2-propanol, 0.5 mL/min, 254 nm); minor enantiomer $t_1$ = 42.9 min, major enantiomer $t_2$ = 75.2 min; $[\alpha]_D^{25}$ -34.4 (*c* 0.77, $CHCl_3$); $^1$H NMR ($CDCl_3$, 400 MHz) δ 2.7-2.71 (m, 4H), 3.7 (s, 3H), 5.47 (d, *J* = 2 Hz, 1H), 6.24 (s, 1H), 6.5 (d, *J* = 2 Hz, 1H), 7.52 (d, *J* = 8.8 Hz, 2H), 8.18 (d, *J* = 8.8 Hz, 2H); $^{13}$C NMR ($CDCl_3$, 100 MHz) δ 28.3, 52.6, 54.8, 124.1, 129.9, 130.1, 136.1, 143.8, 147.9, 165.7, 176.8; ESI-HRMS *m/z* calcd. for $(C_{15}H_{14}N_2O_6Na)^+$ 341.0744; found 341.0749.

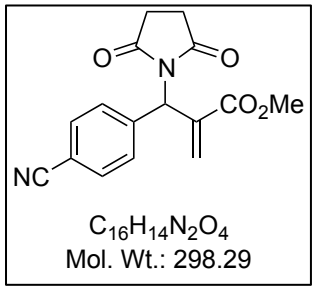


$C_{16}H_{14}N_2O_4$
Mol. Wt.: 298.29

**5.26j** Enantiomeric excess was determined by HPLC with a Chiralcel AD-3 column (95:5 hexane:2-propanol, 1.0 mL/min, 254 nm); minor enantiomer $t_1$ = 71.6 min, major enantiomer $t_2$ = 102.9 min; $[\alpha]_D^{25}$ -37.7 (*c* 1.03, $CHCl_3$); $^1$H NMR ($CDCl_3$, 400 MHz) δ 2.69-2.7 (m, 4H), 3.7 (s, 3H), 5.45 (d, *J* = 2 Hz, 1H), 6.18 (s, 1H), 6.5 (d, *J* = 2 Hz, 1H), 7.47 (d, *J* = 8 Hz, 1H), 7.6 (d, *J* =

8 Hz, 1H); $^{13}$C NMR ($CDCl_3$, 100 MHz) δ 28.3, 52.4, 55.1, 115.7, 115.9, 129.5, 131, 132.6, 132.7, 137.2, 161.5, 164, 166.1, 177; ESI-HRMS *m/z* calcd. for $(C_{16}H_{14}N_2O_4Na)^+$ 321.0846; found 321.0838.

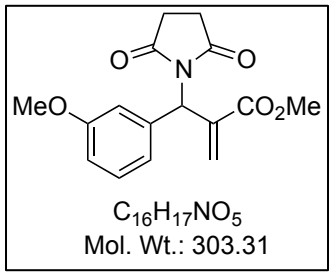


$C_{16}H_{17}NO_5$
Mol. Wt.: 303.31

**5.26k** Enantiomeric excess was determined by HPLC with a Chiralcel AD-3 column (95:5 hexane:2-propanol, 1.0 mL/min, 254 nm); minor enantiomer $t_1$ = 31.1 min, major enantiomer $t_2$ = 47.0 min; $[\alpha]_D^{25}$ -101.9 (*c* 1.22, $CHCl_3$); $^1$H NMR ($CDCl_3$, 400 MHz) δ 2.65-2.66 (m, 4H), 3.71 (s, 3H), 3.75 (s, 3H), 5.5 (d, *J* = 2 Hz, 1H), 6.07 (s, 1H), 6.46 (d, *J* = 2 Hz, 1H), 6.82 (dd, *J* = 8, 2.8 Hz, 1H), 6.92-6.96 (m, 2H), 7.23(t, *J* = 8 Hz, 1H); $^{13}$C NMR ($CDCl_3$, 100 MHz) δ 28.3, 52.4, 55.4, 55.8, 113.9, 114.7, 121.3, 129.91, 129.94, 137.1, 138.3, 160, 166.2, 177; ESI-HRMS *m/z* calcd. for $(C_{16}H_{17}NO_5Na)^+$ 326.0999; found 326.1002.

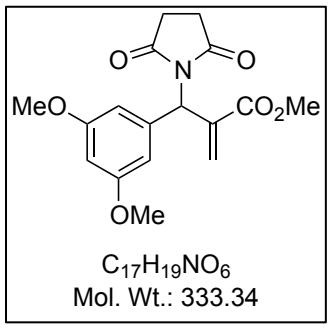


$C_{17}H_{19}NO_6$
Mol. Wt.: 333.34

**5.26l** Enantiomeric excess was determined by HPLC with a Chiralcel AD-3 column (95:5 hexane:2-propanol, 1.0 mL/min, 254 nm); minor enantiomer $t_1$ = 39.1 min, major enantiomer $t_2$ = 66.7 min; $[\alpha]_D^{25}$ -116.5 (*c* 1.02, $CHCl_3$); $^1$H NMR ($CDCl_3$, 400 MHz) δ 2.65-2.66 (m, 4H), 3.7

(s, 3H); 3.73 (s, 6H), 5.54(d, $J$ = 2.4 Hz, 1H), 6.01 (s, 1H), 6.37 (t, $J$ = 2.4 Hz, 1H), 6.45 (d, $J$ = 1.6 Hz, 1H), 6.53 (d, $J$ = 2.4 Hz, 2H); $^{13}$C NMR ($CDCl_3$, 100 MHz) δ 28.3, 52.3, 55.6, 55.9, 100.3, 107.1, 130, 137, 139.1, 161.1, 166.2, 177; ESI-HRMS *m/z* calcd. for $(C_{17}H_{19}NO_6Na)^+$ 356.1105; found 356.1110.

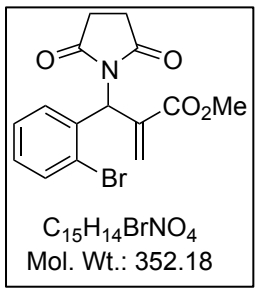

$C_{15}H_{14}BrNO_4$
Mol. Wt.: 352.18

**5.26m** Enantiomeric excess was determined by HPLC with a Chiralcel AD-3 column (95:5 hexane:2-propanol, 1.0 mL/min, 254 nm); minor enantiomer $t_1$ = 29.2 min, major enantiomer $t_2$ = 37.9 min; $[\alpha]_D^{25}$ -13.9 (*c* 1.27, $CHCl_3$); $^1$H NMR ($CDCl_3$, 400 MHz) δ 2.7 (m, 4H), 3.7 (s, 1H), 5.42 (d, $J$ = 1.6 Hz, 1H), 6.47 (s, 1H), 6.5 (d, $J$ = 1.6 Hz, 1H), 7.15 (td, $J$ = 8, 1.6 Hz, 1H), 7.26 (td, $J$ = 8, 1.2 Hz, 2H), 7.4 (dd, $J$ = 8, 1.6 Hz, 1H), 7.54 (dd, $J$ = 8, 1.2 Hz, 1H); $^{13}$C NMR ($CDCl_3$, 100 MHz) δ 28.3, 52.5, 55.5, 124.1, 127.7, 129.2, 130, 130.5, 133.3, 135.82, 135.84, 165.8, 176.8; ESI-HRMS *m/z* calcd. for $(C_{15}H_{14}BrNO_4Na)^+$ 373.9998; found 373.9971.

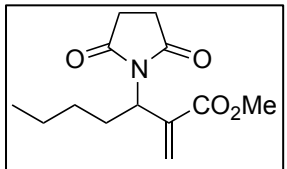

$C_{13}H_{19}NO_4$
Mol. Wt.: 253.29

**5.26n** Enantiomeric excess was determined by HPLC with a Chiralcel OD-3 column (95:5 hexane:2-propanol, 1.0 mL/min, 220 nm); minor enantiomer $t_1$ = 17.9 min, major

enantiomer $t_2$ = 26.1 min; $[\alpha]_D^{25}$ -15.8 (*c* 0.58, $CHCl_3$); $^1H$ NMR ($CDCl_3$, 400 MHz) δ 0.85 (t, *J* = 7.2 Hz, 3H), 1.13-1.35 (m, 4H), 1.82-1.89 (m, 1H), 2.09-2.18 (m, 1H), 2.63 (m, 4H), 3.7 (s, 3H), 5.04 (q, *J* = 4.4 Hz, 1H), 5.99(d, *J* = 1.6 Hz, 1H), 6.48(m, 1H); $^{13}C$ NMR ($CDCl_3$, 100 MHz) δ 14.1, 22.5, 28.2, 28.7, 29.1, 50.4, 52.3, 128.8, 136.8, 166.5, 177.1; ESI-HRMS *m/z* calcd. for $(C_{13}H_{19}NO_4Na)^+$ 276.1206; found 276.1204.

### 5.4.2.2. X-ray Analysis

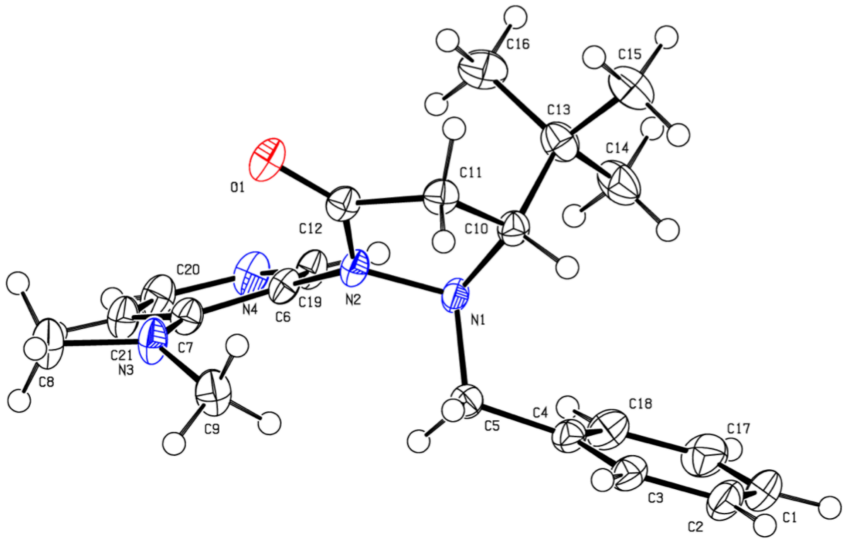


Figure 5.3. X-ray Structure Determination

Single crystal X-ray diffraction data of **5.30** was collected on a Bruker APEX-II CCD diffractometer. The crystal was kept at 99.99K during data collection. Cu radiation was used for the sample. Using Olex2, the structure was solved with the ShelXS structure solution program using Direct Methods and refined with the XL refinement package using Least Squares minimization. Basic information pertaining to crystal parameters and structure refinement is summarized in Table 5.7.

Table 5.7. Crystal Data and Structure Refinement

| | |
|---|---|
| Empirical formula | $C_{21}H_{28}N_4O$ |
| Formula weight | 352.47 |
| Temperature | 99.99K |
| Crystal system | trigonal |
| space group | $P3_2$ |
| *a*/Å | 13.2040(2) |
| *b*/Å | 13.2040(2) |
| *c*/Å | 11.5028(10) |
| $\alpha$, deg | 90 |
| $\beta$, deg | 90 |
| $\gamma$, deg | 120 |
| *V*, Å$^3$ | 1736.78(5) |
| *Z* | 3 |
| $d_{calcd}$, g.cm$^{-3}$ | 1.011 |
| $\mu$, mm$^{-1}$ | 0.501 |
| F(000) | 570.0 |
| Crystal size/mm$^3$ | 0.22 × 0.137 × 0.065 |
| Radiation | CuKa (l = 1.54178) |
| 2Θ range for data collection | 7.732 to 133.186 |
| Index ranges | -15 ≤ h ≤ 15, -15 ≤ k ≤ 15, -13 ≤ l ≤ 13 |
| Reflections collected | 18957 |
| Independent reflections | 3975 [$R_{int}$ = 0.0240, $R_{sigma}$ = 0.0162] |
| Data/restraints/parameters | 3975/1/241 |
| GOOF on $F^2$ | 1.056 |
| Final R indexes [I>=2σ (I)] | $R_1$ = 0.0226, $wR_2$ = 0.0579 |
| Final R indexes [all data] | $R_1$ = 0.0230, $wR_2$ = 0.0582 |
| Largest diff. peak/hole/e Å$^{-3}$ | 0.09/-0.13 |
| Flack parameter | 0.1(2) |

## 5.5. References


1. a) Basavaiah, D.; Rao, A. J.; Satyanarayana, T. Recent Advances in the Baylis-Hillman Reaction and Applications. *Chem. Rev.* **2003**, *103*, 811-892; b) Lee, K. Y.; Gowrisankar, S.; Kim, J. N. Baylis-Hillman Reaction of Chemical Transformations of Baylis-Hillman Adducts. *Bull. Korean Chem. Soc.* **2005**, *26*, 1481-1490; c) Cho, C.-W.; Kong, J.-R.; Krische, M. J. Phosphine-Catalyzed Regiospecific Allylic Amination and Dynamic Kinetic Resolution of Morita-Baylis Hillman Acetates. *Org. Lett.* **2004**, *6*, 1337-1339; d) Wei, Y.; Shi, M. Multifunctional Chiral Phosphine Organocatalysts in Catalytic Asymmetric Morita-Baylis-Hillman and Related Reactions. *Acc. Chem. Res.* **2010**, *43*, 1005-1018; e) Xu, S.; Zhu, S.; Shang, J.; Zhang, J.; Tang, Y.; Dou, J. Catalyst-Free Synthesis of Skipped Dienes from Phosphorus Ylides, Allylic Carbonates, and Aldehydes via a One-Pot $S_N2$' Allylation-Wittig Strategy. *J. Org. Chem.* **2014**, *79*, 3696-3703; f) Peng, C.; Joy, A. Baylis-Hillman Reaction as a Versatile Platform for the Synthesis of Diverse Functionalized Polymers by Chain and Step Polymerization. *Macromolecules* **2014**, *47*, 1258-1268; g) Xie, P.; Huang, Y. Morita-Baylis-Hillman Adduct Derivatives (MBHADs): Versatile Reactivity in Lewis Base-Promoted Annulation. *Org. Biomol. Chem.* **2015**, *13*, 8578-8595.
2. a) Trost, B. M.; Machacek, M. R.; Tsui, H. -C. Development of Aliphatic Alcohols as Nucleophiles for Palladium-Catalyzed DYKAT Reactions: Total Synthesis of (+)-Hippospongic Acid A. *J. Am. Chem. Soc.* **2005**, *127*, 7014-7024; b) Wang, D.; Yang, Y.-L.; Jiang, J.-J.; Shi, M. Chiral Phosphine-Catalyzed Asymmetric Allylic Alkylation of 3-Substituted Benzofuran-2(*3H*)-ones or Oxindoles with Morita-Baylis Hillman Carbonates. *Org. Biomol. Chem.* **2012**, *10*, 7158-7166; c) Peng, J.; Huang, X.; Cui, H.-L.; Chen, Y.-C.

Organocatalytic and Electrophilic Approach to Oxindoles with C3-Quaternary Stereocenters. *Org. Lett.* **2010**, *12*, 4260-4263; d) Chen, G. -Y.; Zhong, F.; Lu, Y. Asymmetric Allylic Alkylation of Isatin-Derived Morita-Baylis-Hillman Carbonates with Nitroalkanes. *Org. Lett.* **2012**, *14*, 3955-3957; e) Furukawa, T.; Nishimine, T.; Tokunaga, E.; Hasegawa, K.; Shiro, M.; Shibata, N. Orgaocatalyzed Regio- and Enantioselective Allylic Trofluoromethylation of Morita-Baylis-Hillman Adducts Using Ruppert-Prakash Reagent. *Org. Lett.* **2011**, *13*, 3972-3975.

3. Trost, B. M.; Thiel, O. R.; Tsui, H. -C. DYKAT of Baylis-Hillman Adducts: Concise Total Synthesis of Furaquinocin E. *J. Am. Chem. Soc.* **2002**, *124*, 11616-11617.
4. Liu, T. -Y.; Xie, M.; Chen, Y. -C. Organocatalytic Asymmetric Transformations of Modified Morita-Baylis-Hillman Adducts. *Chem. Soc. Rev.* **2012**, *41*, 4101-4112.
5. a) Wei, Y.; Shi, M. Recent Advances in Organocatalytic Asymmetric Morita-Baylis-Hillman/aza-Morita-Baylis-Hillman Reactions. *Chem. Rev.* **2013**, *113*, 6659-6690; b) Xiao, Y.; Sun, Z.; Guo, H.; Kwon, O. Chiral Phosphines in Nucleophilic Organocatalysis. *Beilstein J. Org. Chem.* **2014**, *10*, 2089-2121.
6. Y. Du, X. Han, X. Lu, Alkaloids-Catalyzed Regio- and Enantioselective Allylic Nucleophilic Substitution of *tert*-Butyl Carbonates of the Morita-Baylis-Hillman Products. *Tetrahedron Lett.* **2004**, *45*, 4967-4971.
7. a) Langer, P. New Strategies for the Development of An Asymmetric Version of the Baylis-Hillman Reaction. *Angew. Chem. Int. Ed.* **2000**, *39*, 3049-3052; b) Ma, G. -N.; Jiang, J. -J.; Shi, M.; Wei, Y. Recent Extensions of the Morita-Baylis-Hillman Reaction. *Chem. Commun.* **2009**, 5496-5514; c) Declerck, V.; Martinez, J.; Lamaty, F. Aza-Baylis-Hillman Reaction. *Chem. Rev.* **2009**, *109*, 1-48; d) Basavaiah, D.; Reddy, B. S.; Badsara,

S. S. Recent Contributions from the Baylis-Hillman Reaction to Organic Chemistry. *Chem. Rev.* **2010**, *110*, 5447-5674.

8. Kim, J. N.; Lee, H. J.; Gong, J. H. Synthesis of Enantiomerically Enriched Baylis-Hillman Alcohols from Their Acetates: Combination of Kinetic Resolution During the Salt Formation with $(DHQD)_2PHAL$ and Following Asymmetric Induction during Hydrolysis with $NaHCO_3$ as A Water Surrogate. *Tetrahedron Lett.* **2002**, *43*, 9141-9146.
9. Zhang, S. -J.; Cui, H. -L.; Jiang, K.; Li, R.; Ding, Z. -Y.; Chen, Y. -C. Enantioselective Allylic Amination of Morita-Baylis-Hillman Carbonates Catalyzed by Modified Cinchona Alkaloids. *Eur. J. Org. Chem.* **2009**, 5804-5809.
10. Cui, H. -L.; Feng, X.; Peng, J.; Lei, J.; Jiang, K.; Chen, Y. -C. Chemoselective Asymmetric N-Allylic Alkylation of Indoles with Morita-Baylis-Hillman Carbonates. *Angew. Chem. Int. Ed.* **2009**, *48*, 5737-5740.
11. Lin, A.; Mao, H.; Zhu, X.; Ge, H.; Tan, R.; Zhu, C.; Cheng, Y. Organocatalytic Enantioselective Amination of Morita-Baylis-Hillman Carbonates with Masked Ammonia: A Facile Method for the Synthesis of Unprotected α-Methylene-β-Amino Esters. *Chem. Eur. J.* **2011**, *17*, 13676-13679.
12. Zhang, T. -Z.; Dai, L. -X.; Hou, X. -L. Enantioselective allylic Substitution of Morita-Baylis-Hillman Adducts Catalyzed by Planar Chiral [2.2]paracyclophane Monophosphines. *Tetrahedron: Asymm.* **2007**, *18*, 1990-1994.
13. Deng, H. -P.; Wei, Y.; Shi, M. Chiral Bifunctional Thiourea-Phosphane Organocatalysts in Asymmetric Allylic Amination of Morita-Baylis-Hillman Acetates. *Eur. J. Org. Chem.* **2011**, *2011*, 1956-1960.
14. Hoffmann, H. M. R.; Rabe, J. DABCO-Catalyzed Coupling of Aldehydes with Activated Double Bonds. 4. Stereoselective Synthesis of Trisubstituted Olefins and Terpenoid

Building Blocks via 2-(Hydroxyalkyl)-2-propenoic Esters. *J. Org. Chem.* **1985**, *50*, 3849-3859.

15. Feng, J.; Lu, X.; Kong, A.; Han, X. A Highly Regio- and Stereo-selective [3+2] Annulation of Allylic Compounds and 2-Substituted 1,1-Dicyanoalkenes Through a Catalytic Carbon-phosphorus Ylide Reaction. *Tetrahedron* **2007**, *63*, 6035-6041.

# CHAPTER 6. CONCLUSION AND OUTLOOK

We have developed synthetic methodology of fluxionally chiral 4-dialkylamino pyridine catalysts that is amenable for scale up and diversity can be introduced in the fluxional group, C5 substituent on the pyrolidinone as well as the pyridine 4-substituent without much difficulty. Different catalysts were synthesized with $R^1$, $R^2$ and $R^3$ substituents for reaction evaluation.

The novel fluxionally chiral DMAP molecules serve as an effective acylation catalyst for the kinetic resolution of racemic *sec*-alcohols, and especially biaryl compounds. A number of secondary alcohol racemates were resolved with moderate to good selectivities (*s* factor up to 37), which are comparable to other chiral pyridine catalysts in the kinetic resolution of secondary alcohols. Biaryl substrates were resolved with good to high selectivities with up to 51 by using this catalyst system. To the best of our knowledge, the selectivities obtained for kinetic resolution of biaryl compounds are better than previously reported asymmetric acylation catalysts.

The novel fluxionally chiral 4-dialkylamino pyridine molecules served as an effective acylation catalyst for the dynamic kinetic resolution of biaryl compounds. The equilibrium between the atropoisomers of the biaryl substrates was demonstrated from chiral HPLC analysis and the temperature was found to be a key point in controlling the stereochemical outcome of acylative dynamic kinetic resolution. The efficiency of novel chiral DMAP catalyst in dynamic kinetic resolution declined compared to simple kinetic resolution under high temperature. Good yields and enantioselectivities were obtained for configurationally stable biaryl product. The best enantioselectivity was achieved with 80 %ee. Our present protocol provides a new approach for the preparation of optically active biaryl compounds.

Finally, MBH adducts transformation have opened up new opportunities for construction of complex molecules. Our studies have shown that newly designed DMAP catalysts containing fluxional groups as a stereocontrol unit could also be effectively applied as a nucleophilic catalyst in asymmetric allylic aminations, which provide a novel tool to synthesize useful molecules. The catalyst preparation is highly tunable and up to 72 %ee was achieved for the product and a range of α-methylene β-amino esters were obtained with good yield and selectivities.

Fluxional organocatalysts can be used in enantioselective processes and transfer stereochemical information and enantioselectivity can be affected by changing fluxional groups. Further applications of chiral relay DMAP catalysts in asymmetric catalysis are in progress. In this type of fluxional chiral catalyst, the role of chiral axis C-N bond between pyridine ring and pyrazolidinone ring in the reaction process and the conformational change of the transition state during the reaction will be investigated by computational studies.

Future study of chiral relay project will focus on applying chiral template with fluxional chirality as a platform for novel catalyst design. Different kinds of catalytic center could be utilized to connect with chiral template with fluxional group, such as imidazole, thiourea, phosphine, etc. More and more new catalysts could be developed by using this platform for stereocontrol in a variety of asymmetric transformations including the exploration of new reaction types.